BOOK OF ABSTRACTS

Proceedings of the

19th International Colloquium on Mechanical Fatigue of Metals

ICMFM XIX

International Colloquium - **MECHANICAL FATIGUE OF METALS**
05-07 September 2018 **| FEUP, Porto, Portugal**

Title. **Proceedings of the 19th International Colloquium on Mechanical Fatigue of Metals. Book of Abstracts.**

Editors. **Abílio Manuel Pinho DE JESUS, José António Fonseca de Oliveira CORREIA, Ana Maria Azevedo NEVES, Rui Artur Bártolo CALÇADA, António Augusto FERNANDES**

ISBN. **978-972-752-237-8**

2018, Universidade do Porto – Faculdade de Engenharia

Preface

Fatigue represents one of the most important types of damage experienced by materials and structures during normal service. Today metallic alloys are still the most important materials applied in the majority of components and structures allowing important service loads; therefore the study of the different aspects of metals fatigue attracts permanent attention of scientists, engineers and designers. The International Colloquium on Mechanical Fatigue of Metals (ICMFM) has been organized periodically aiming a fruitful discussion of the most recent advances in the field. This international colloquium is intended to facilitate and encourage the exchange of knowledge and experiences among the different communities involved in both fundamental and applied research in this field of fatigue of metals, looking the problem of fatigue from a multiscale viewpoint, exploring analytical and numerical approaches, without losing the applications perspective.

The First International Colloquium on Mechanical Fatigue of Metals was organized in Brno, Czech Republic in 1968. Afterwards, regular Colloquia on Mechanical Fatigue of Metals started in 1972 also in Brno and were originally limited to participants form the countries of the former "Eastern Block". They continued until the 12th Colloquium in 1994 (Miskolc, Hungary) every two years. After a break twelve years long, the Colloquia restarted in 2006 (Ternopil, Ukraine), followed by the ones in 2008 (Varna, Bulgaria), 2010 (Opole, Poland), 2012 (Brno, Czech Republic), 2014 (Verbania, Italy) and 2016 (Gijón, Spain). The current edition (nineteenth) of the colloquium, organized between 5th and 7th of September 2018 at the Faculty of Engineering of the University of Porto, Portugal, gathers more than 130 participants from more than 20 nationalities demonstrating the vitality of the ICMFM.

This book gathers the abstracts of the works presented in the colloquium. In general, the abstracts were organized into eighteenth chapters, according to the main topics of the symposia/sessions foreseen in the programme of the colloquium.

The Organizing Committee of the 19th ICMFM deeply acknowledges all authors that contributed to the success of this event, with their exciting presentations. The members of the Advisory and Scientific Committees are also fully acknowledged for their support to the colloquium. Special thanks are also addressed to the Symposia Organizers, Plenary Speakers, Chairmen of the Sessions for their dedication, knowledge and energy brought to this event. Sponsors are also

fully acknowledged for their important contributions. Finally, a word of appreciation for the Organizing Committee members as well as students and other FEUP/INEGI/IC and Abreu staff for their tireless support.

The editors of the Proceedings of the 19th International Colloquium on Mechanical Fatigue of Metals (Book of Abstracts),

Abílio Manuel Pinho de Jesus, José António Fonseca de Oliveira Correia, Ana Maria Azevedo Neves, Rui Artur Bártolo Calçada, António Augusto Fernandes

Organization

Local Organizing Committee

Co-Chairs:
Abílio de Jesus (University of Porto, Portugal)
António A. Fernandes (University of Porto, Portugal)
José António Correia (University of Porto, Portugal)
Rui Calçada (University of Porto, Portugal)

Members:
Abílio de Jesus (University of Porto, Portugal)
Alfonso Fernández-Canteli (University of Oviedo, Spain)
Ana M. A. Neves (University of Porto, Portugal)
António A. Fernandes (University of Porto, Portugal)
Bruno Pedrosa (University of Coimbra, Portugal)
Carlos Rebelo (University of Coimbra, Portugal)
Cláudio Horas (University of Porto, Portugal)
Constança Rigueiro (University of Coimbra, Portugal)
Grzegorz Lesiuk (Wroclaw University of Technology, Poland)
Guilherme Alencar (University of Porto, Portugal)
Isabel Valente (University of Minho, Portugal)
José António Correia (University of Porto, Portugal)
José Miguel Castro (University of Porto, Portugal)
José Xavier (University of Trás-os-Montes e Alto Douro, Portugal)
Linamaria Gallegos-Mayorga (University of Brest, France)
Luís Simões-da-Silva (University of Coimbra, Portugal)
María Jesús Lamela Rey (University of Oviedo, Spain)
Mariana Rodrigues (University of Porto, Portugal)
Marco Parente (University of Porto, Portugal)
Miguel Muñiz-Calvente (University of Oviedo, Spain)
Mohammad R. Shah Mohammadi (University of Coimbra, Portugal)
Patricia Raposo (University of Porto, Portugal)
Paulo Tavares (INEGI, University of Porto, Portugal)
Pedro Moreira (INEGI, University of Porto, Portugal)
Renato Natal Jorge (University of Porto, Portugal)
Rui Calçada (University of Porto, Portugal)
Sergio Blasón (University of Oviedo, Spain)
Sergio O. Tavares (University of Porto, Portugal)
Slobodanka Jovasevic (University of Coimbra, Portugal)
Stéphane Sire (University of Brest, France)

International Advisory Scientific Committee

Abílio M.P. De Jesus (University of Porto, Portugal)
Alfonso Fernández-Canteli (University of Oviedo, Spain)
Alfredo Navarro (University of Seville, Spain)
André Pineau (MINES ParisTech, France)
Andrei Georgievich Kotousov (University of Adelaide, Australia)
Dariusz Rozumek (Opole University of Technology, Poland)
Filippo Berto (NTNU, Norway)
Gianni Nicoletto (University of Parma, Italy)
Gilbert Henaff (ISAE-ENSMA, France)
Gregory Glinka (University of Waterloo, Canada)
Iris Alvarez-Armas (National University of Rosario, Argentina)
Jaroslav Polák (Academy of Sciences of the Czech Republic, Czech Republic)
José Domínguez-Abascal (University of Seville, Spain)
Jose Méndez (ENSMA, France)
Luca Susmel (University of Sheffield, UK)
Ludvík Kunz (Academy of Sciences of the Czech Republic, Czech Republic)
Majid Reza Ayatollahi (Iran University of Science & Technology, Tehran, Iran)
Manuel de Freitas (University of Lisbon, Portugal)
Martina Zimmermann (Technical University of Dresden, Germany)
Mario Guagliano (Politecnico di Milano, Italy)
Michael Vormwald (Darmstadt University of Technology, Germany)
Neil James (Plymouth University, UK)
Paulo Tavares de Castro (University of Porto, Portugal)
Stefanie Stanzl-Tschegg (BOKU, Austria)
Stefano Beretta (Politecnico di Milano, Italy)
Tim Topper (University of Waterloo, Canada)
Valery Shlyannikov (Russian Academy of Sciences, Kazan, Russia)
Yukitaka Murakami (Kyushu University, Japan)
Zhe-Feng Zhang (Institute of Metal Research Chinese Academy of Sciences, China)

International Scientific Committee

Abílio M.P. De Jesus (University of Porto, Portugal)
Ahmad Kamal Ariffin (National University of Malaysia, Malaysia)
Alfonso Fernández-Canteli (University of Oviedo, Spain)
Aleksandar Sedmak (University of Belgrade, Serbia)
Alexandre Velhinho (New University of Lisbon, Portugal)
Alfredo Navarro (University of Seville, Spain)
Alfredo Ribeiro (University of Trás-os-Montes e Alto Douro, Portugal)
Ana M. A. Neves (University of Porto, Portugal)
Anna Rakoczy (Transportation Technology Center, USA)
André Pineau (MINES ParisTech, France)
Andrea Carpinteri (Università di Parma, Italy)
Andrei Georgievich Kotousov (University of Adelaide, Australia)
António A. Fernandes (University of Porto, Portugal)
Antonio Martín-Meizoso (University of Navarra, Spain)
Anthony Ingraffea (Cornell University, USA)
Attilio Arcari (U.S. Naval Research Lab, USA)
Benno Hoffmeister (RWTH Aachen University, Germany)
Boulent Iman (University of Surrey, UK)
Carlo Castiglioni (Polytechnic of Milan, Italy)
Carlos Rebelo (University of Coimbra, Portugal)
Cesar Azevedo (University of São Paulo, Brazil)
Chao Jiang (Hunan University, China)
Chris Rodopoulos (Monash University, Australia)
Cristina Rodríguez González (University of Oviedo, Spain)
Constança Rigueiro (University of Coimbra, Portugal)
Dariusz Rozumek (Opole University of Technology, Poland)
David McDowell (Georgia Institute of Technology, USA)
David Taylor (Trinity College, Ireland)
Dianyin Hu (Beihang University, China)
Egor Moskvichev (KSC/KRASN, Russia)
Elzbieta Pieczyska (Polish Academy of Sciences, Poland)
Emilio Martínez-Pañeda (University of Cambridge, UK)
Emmanuel Gdoutos (Democritus University of Thrace, Greece)
Etienne Pessard (Arts et Metiers ParisTech, Paris, France)
Fernando Antunes (University of Coimbra, Portugal)
Filipe Samuel Silva (University of Minho, Portugal)
Filippo Berto (NTNU, Norway)
Francesco Iacoviello (U. of Cassino e del Lazio Meridionale, Italy)
Francesco Morelli (University of Pisa, Italy)
Franck Morel (Arts et Métiers ParisTech, France)
Gang Chen (Tianjin University, China)
Gilbert Henaff (ISAE-ENSMA, France)
Gregory Glinka (University of Waterloo, Canada)
Grzegorz Lesiuk (Wroclaw University of Technology, Poland)
Hermes Carvalho (Federal University of Minas Gerais, Brazil)
Hérnan Pinto Arancet (Pontific Catholic University of Valparaíso, Chile)
Inés Fernández Pariente (University of Oviedo, Spain)
Isabel Valente (University of Minho, Portugal)
Iris Alvarez-Armas (National University of Rosario, Argentina)
Javier Belzunce (University of Oviedo, Spain)
Jaime Pinho de Castro (Pontific Catholic University of Rio de Janeiro, Brazil)
Jaroslav Polák (Academy of Sciences of the Czech Republic, Czech Republic)
Jeong Kyun Hong (Joining JK Research LLC, Ireland)
Jesús Toribio (University of Salamanca, Spain)
John Leander (KTH Royal Institute of Technology, Sweden)
José A.F.O. Correia (University of Porto, Portugal)
José Domingos Costa (University of Coimbra, Portugal)
José Domínguez-Abascal (University of Seville, Spain)
José Guilherme Silva (State University of Rio de Janeiro, Brazil)
José Martins Ferreira (University of Coimbra, Portugal)
José Méndez (ENSMA, France)
José Miguel Castro (University of Porto, Portugal)
José Xavier (University of Trás-os-Montes and Alto Douro, Portugal)
Leslie Banks-Sills (Tel Aviv University, Israel)
Linamaria Gallegos-Mayorga (University of Brest, France)
Luca Susmel (University of Sheffield, UK)
Ludvík Kunz (Academy of Sciences of the Czech Republic, Czech Republic)
Luís Borrego (Polytechnic Institute of Coimbra, Portugal)
Luis Reis (University of Lisbon, Portugal)
Luis Simões da Silva (University of Coimbra, Portugal)
Majid Ayatollahi (Iran University of Science & Technology, Iran)
Manuel de Freitas (University of Lisbon, Portugal)
Manuel López Aenlle (University of Oviedo, Spain)
Marco Meggiolaro (Pontific Catholic University of Rio de Janeiro, Brazil)
Marco Parente (University of Porto, Portugal)
Marcus Feldmann (RWTH Aachen University, Germany)
María Jesús Lamela Rey (University of Oviedo, Spain)
María Nogal (Trinity College Dublin, University of Dublin, Ireland)
Mario Guagliano (Politecnico di Milano, Italy)
Manuel Fonte (Escola Superior Náutica Infante D. Henrique, Portugal)
Martina Zimmermann (Technical University of Dresden, Germany)
Massimo Rossetto (Politecnico di Torino, Italy)
Matthew Hebdon (Virginia Tech, USA)
Meinhard Kuna (University of Freiberg, Germany)
Michael Vormwald (Darmstadt University of Technology, Germany)

Table of contents

Invited Speakers

Prof. Andrei Kotousov

University of Adelaide

Australia

Effects of 3D stress states near the crack front on fracture and fatigue

Andrei Kotousov is the current President of the Australian Fracture Group (https://www.australianfracturegroup.org/). He has actively promoted fracture research in Australia and internationally through a wide international collaborative network and various appointments, most notably as Vice-Chairman of the National Committee on Applied Mechanics (2009-14), which organises a vibrant biennial conference series (ACAM) with a fracture theme, and as Chair of the International Conference on Structural Integrity and Failure (SIF) in 2014 and 2016. He is serving on the Editorial Board of several journals devoted to Fracture Research, notably the Fatigue and Fracture of Engineering Materials and Structures, for which he also served as Guest Editor for a special issue devoted to selected papers from ACAM 7, and Materials & Design.

Dr. Kotousov made significant contributions to 3D Fracture Mechanics publishing more than 100 journal and conference articles in this area. Other research areas include geo-mechanics and Structural Health Monitoring. He often leads and participates in large structural failure investigations. Andrei provided an expert advice to many national and international companies and authorities including Siemens Ltd (Germany) and HDI-Gerling Insurance Company, Charles Taylor Adjusting (Australia) Pty Ltd, its principal, Munich Reinsurance Company (UK General Branch) and the Office of the State Coroner of South Australia.

Prof. Manuel Freitas

Instituto Superior Técnico, Lisboa

Portugal

Very High Cycle Fatigue under Multiaxial Loading Conditions

Manuel Freitas is a Professor (retired) of Mechanical Design and Structural Materials at Instituto Superior Técnico, Technical University of Lisbon. Researcher at IDMEC, Instituto de Engenharia Mecânica on the Center for Mechanical Design. He completed the Mechanical Engineer degree at Instituto Superior Técnico, Technical University of Lisbon (1972) and a PhD degree in Mechanical Sciences at Université de Technologie de Compiegne, France (1982). He was Assistant Professor (1983-1987), Associate Professor (1987-1997) and Full Professor (1998-2013) at Instituto Superior Técnico, Technical University of Lisbon and Visiting Professor at École Centrale de Paris, France (1991). Served as Head of Mechanical Engineering Department (2003-2007), Scientific Coordinator of the Research Institute of Materials Science and Engineering (2002-2007) and Vice President of the School Council of Instituto Superior Técnico (2009-2013).

His major research interests include the mechanical behavior of materials under multiaxial loading conditions, namely multiaxial fatigue and fracture of metallic materials and mixed mode delamination of composite materials and applications of these concepts to mechanical engineering design.

Professor Manuel Freitas supervised 10 PhD students and was the Coordinator of the Engineering Design and Advanced Manufacturing joint doctoral program, between Instituto Superior Técnico ofoTechnical University if Lisbon, Faculty of Engineering of University of Porto and School of Engineering of University of Minho; was the editor of two books on Mechanics of Composite Materials and Multiaxial Fatigue and Fracture; has published more than 100 papers in international scientific journals.

Prof. Gianni Nicoletto

University of Parma

Italy

High performance metal parts produced by additive manufacturing: the fatigue challenge

Gianni Nicoletto is currently full professor at the Department of Engineering and Architecture of the University of Parma, Italy. He was born in Trento, Italy, in 1954. He received his Laurea in Mechanical Engineering at the University of Bologna, Italy, in 1979 and a MSc degree in Mechanical Engineering at Virginia Tech (USA) in 1981. He was assistant professor at the Faculty of Engineering, University of Bologna, Italy, between 1983 and 1992. Between 1993 and 1999 he was associate professor at the Faculty of Engineering, University of Parma, Italy. Since 2000 he is full professor at the Faculty of Engineering, University of Parma, Italy, where he taught the courses on Machine design, Mechanics of Materials, Fatigue and Fracture of Metallic Materials, Structural Integrity and Composite Materials. He received the Doctor h.c. in Materials Engineering by the University of Žilina (Slovakia) in 2006. In 2006 he was co-founder of the academic spin off company TP Engineering srl, becoming president and scientific director since then. The company currently employs 15 engineers; is active in computer-aided-engineering, product innovation and advanced engineering materials; its clients are primary automotive companies, automotive part production companies, and equipment manufacturing companies. Since 2013 he is scientific consultant of the metal additive manufacturing company BEAM-IT. He is currently national coordinator of the AIAS Working Group on Design for additive and lean manufacturing. He has published over than 150 peer-reviewed contributions in international journals in the following topics: Mechanics of materials, Fatigue and fracture of metallic materials, Composite materials, Fatigue design, Experimental mechanics, Additive manufacturing, Finite element method, Automotive engineering. His current activity in metal additive manufacturing is focused on: i) fatigue and fracture characterization of AM materials and components; ii) development of structural design methods for AM parts; iii) development of know—how about AM and transfer to industry and academia.

Luca Susmel

University of Sheffield

United Kingdom

Static and fatigue behaviour of aluminium-to-steel thin welded joints

Since 1998 Luca has focussed his attention mainly on problems related to the static and fatigue assessment of engineering materials and components. In particular, by working both in Italy (University of Padova, University of Ferrara, University of Udine) and in Ireland (Trinity College, Dublin), he has devised several novel engineering methods suitable for designing components (experiencing stress concentration phenomena of any kind) against fatigue as well as against static failures. According to his modus operandi, Luca has performed both theoretical and experimental investigations and all the design methods he has formalised so far have always been validated through a systematic experimental work. Luca has an outstanding and unique expertise in designing notched and welded components against constant and variable amplitude multiaxial fatigue.

The work done in the above research areas has led to more than 150 scientific papers in the period 1999-2018 (of which 124 publications in international peer-reviewed scientific journals) as well as to a book devoted to the multiaxial fatigue assessment (Susmel, L., Multiaxial Notch Fatigue: from nominal to local stress-strain quantities. Woodhead & CRC, Cambridge, UK, ISBN: 1 84569 582 8, March 2009). His scientific papers have attracted significant interest from the international scientific community, evidenced by an h-index of 27 with about 2100 citations in total according to Scopus (h-index of 31 with about 3100 citations according to Google Scholar). He is a member of the Editorial Boards of the two leading international journals in the fatigue and fracture field, namely “International Journal of Fatigue” and “Fatigue & Fracture of Engineering Materials & Structures”. Luca is also the Associate Editor of “Frattura ed Integrità Strutturale: The International Journal of the Italian Group of Fracture” (ISSN 1971-8993). Luca is the Editor-in-Chief of “Theoretical and Applied Fracture Mechanics” (published by Elsevier) which is the top journal in the fracture mechanics field (Impact Factor=2.659).

Luca has developed a software specifically designed to perform the fatigue assessment of plain/notched/welded components subjected to both constant and variable amplitude uniaxial/multiaxial fatigue loading (Copyright document N. 007849-D007048, released by SIAE – Società Italiana degli Autori ed Editori, www.siae.it).

Fatigue crack growth – experimental, theoretical and numerical approach

A-FCG-ICMFM

Organized by:

Grzegorz Lesiuk, Poland

José A. F. O. Correia, Portugal

Abílio M. P. de Jesus, Portugal

Filippo Berto, Norway

Wei Huang, China

Rui Calçada, Portugal

Crack Propagation Under Cyclic Bending in Welded Specimens After Heat Treatment

D. Rozumek[a*], J. Lewandowski[a], G. Lesiuk[b], J.A.F.O. Correia[c]

[a] *Department of Mechanics and Machine Design, Opole University of Technology, Opole, Poland*
[b] *Department of Mechanics, Material Science and Engineering, Wrocław University of Science and Technology, Wrocław, Poland*
[c] *INEGI/Faculty of Engineering, University of Porto, Porto, Portugal*
**Corresponding author: d.rozumek@po.opole.pl*

Keywords: Crack propagation; Welding; Bending; Notches; Heat treatment.

ABSTRACT

This paper presents the results of the fatigue crack propagation obtained for welded specimens made of S355 steel subjected to bending for different forms of heat treatment.

Shapes and dimensions of the test specimens with welds are presented in Fig. 1. The initial material of test specimens was drawn bar with Ø30 mm diameter, which was used for making two types of components of the specimens, being fixed together by fillet welded joints on both sides (concave and convex welds).

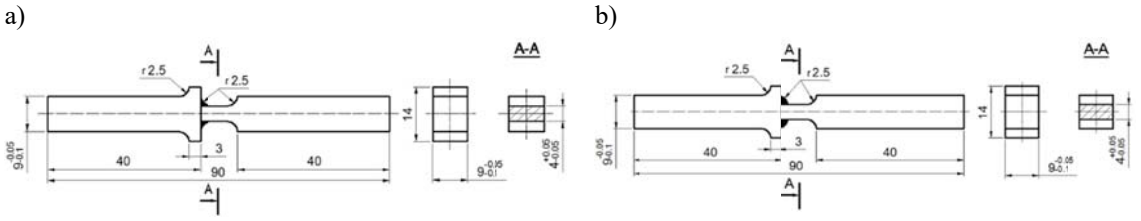

Fig. 1. Shapes and dimensions of specimens with: a) concave welds, b) convex welds, dimensions in mm.

Hand-made welds were made based on the TIG method using the inert gas shielding (Argon) for protection. In addition, during welding, the welding wire marked with the W-42-2-W2Sil symbol according to the EN ISO 636 was used. Pre-selection of specimens were carried out before the experimental tests. All tested specimens were subject to non-destructive testing by using magnetic particle test method under UV light [1]. These tests allowed eliminating welded specimens, on the surface of which defects (mainly cracks) that could influence the final result of the experimental research were revealed. Experimental tests were performed on welded specimens without heat treatment (raw - after welding) and on specimens after heat treatment. The heat treatment was carried out by subjecting the specimens to relief annealing at 630˚C during 2 hours. The tests were performed on the fatigue test stand MZGS – 100 [2]. During the tests the force was controlled (in the considered case, the moment amplitude was controlled) works under loading frequency equal to 28.4 Hz. The theoretical stress concentration factor in the specimen under bending is of $K_t = 1.38$. Unilaterally restrained specimens were subjected to cyclic bending with the constant load ratio $R = M_{min} / M_{max} = -1$, and amplitude of moment, M_a, equal to 9.2 N·m, which corresponded to the nominal amplitude of normal stress for the net section of $\sigma_a = 383$ MPa (solid specimen). Fatigue crack growth on the specimen surface was observed with the optical method. The fatigue crack increments were measured with the micrometre located in the portable

microscope with magnification of 20 times and accuracy up to 0.01 mm. At the same time, a number of loading cycles, N, was recorded.

During laboratory tests, initiation and fatigue cracks growth from one side of the specimen (from top or bottom) were observed, and after a certain period of propagation, the crack growth occurred also on the other side specimen. Fig. 2 presents the fatigue crack length versus number of cycles for the obtained results of experimental tests on the specimens. In Fig. 2 can be observed that the longest fatigue life indicate specimens made of solid material without heat treatment.

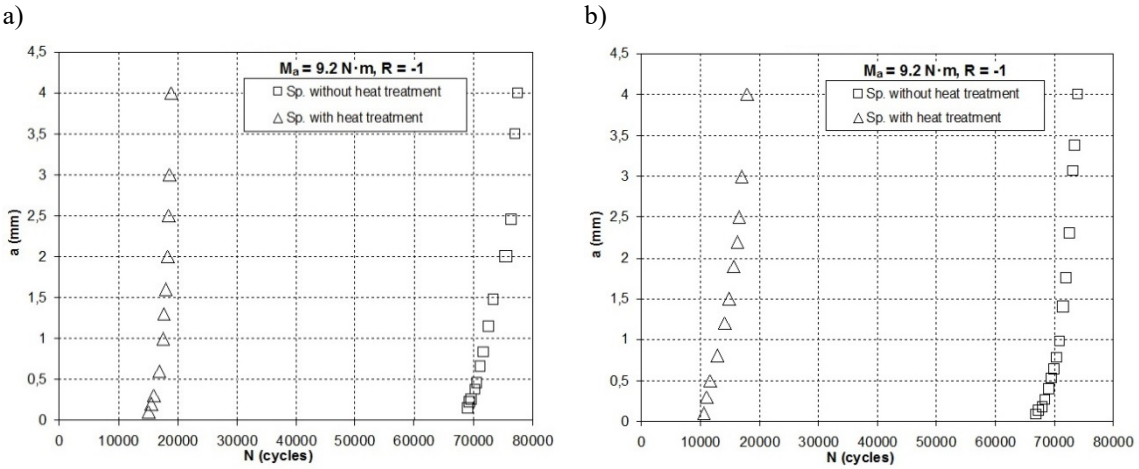

Fig. 2. Crack length vs. number of cycles under bending for test specimens with: a) concave welds, b) convex welds.

In specimens with concave welds (Fig. 2a) subjected to relief annealing, the fatigue crack initiation took place at 15100 cycles, and the specimens were damaged at 19000 cycles. Specimens without heat treatment showed the highest fatigue life, in which the crack initiation occurred at 69000 cycles, and their damaged at 77500 cycles. Similar behaviour, shown in Fig. 2b, is also observed in specimens with convex welds. In specimens subjected to relief annealing, the fatigue crack initiation occurred at 10500 cycles, and the specimens were damaged at 18000 cycles. Specimens without heat treatment also showed the highest fatigue life, in which the crack initiation occurred at 67000 cycles, and their damaged at 74000 cycles. Significant decrease in fatigue life of specimens after heat treatment was caused by structural changes occurring in the tested material as a result of heat treatment. In the specimens without heat treatment there was a martensite and bainite microstructure, and after the heat treatment the microstructure of bainite and sorbitol (which occurs in the heat affected zone - HAZ) was observed. The main crack growth was outside the weld and primary HAZ in the area of the specimen with a spheroidite structure, enriched with cementite.

REFERENCES

[1] Lewandowski, J., Rozumek, D.: Cracks growth in S355 steel under cyclic bending with fillet welded joint. Theoretical and Applied Fracture Mechanics 86, 342-350 (2016).
[2] Rozumek, D., Macha, E.: J-integral in the description of fatigue crack growth rate induced by different ratios of torsion to bending loading in AlCu4Mg1. Materialwissenschaft und Werkstofftechnik 40(10), 743-749 (2009).

Effect of Heat Treatment on the Fatigue Crack Growth Rate in 42CrMo4 Steel

M. Duda[a*], G. Lesiuk[a], D. Pyka[a], M. Szata[b]

[a] *Faculty of Mechanical Engineering, Department of Mechanics, Materials Science and Engineering, Wrocław University of Science and Technology, Wrocław, Poland*
[b] *Faculty of Technology and Natural Sciences, Wrocław University of Science and Technology, Wrocław, Poland*
**Corresponding author: monika.duda@pwr.edu.pl*

Keywords: 42CrMo4; Fatigue crack growth; Heat treatment; Microstructure.

ABSTRACT

Research on influence of mechanical parameters and microstructural characteristics on fatigue behaviour of the material is carried under multiple approaches. One of them is modification of the material through heat treatment in order to obtain specific microstructure [1] and mechanical properties. Additionally due to increasing usage of numerical modelling and simulation there is strong need to develop efficient and easily applicable numerical method of fatigue crack growth rate (FCGR) investigation. There were proposed various methods of modelling FCG in different modes [2, 3].

In this paper there are presented experimental results of investigation on FCGR of 42CrMo4 steel after different heat treatments as well as results obtained from numerical simulations of each differently heat treated sample. The initial results are presented in Fig. 1.

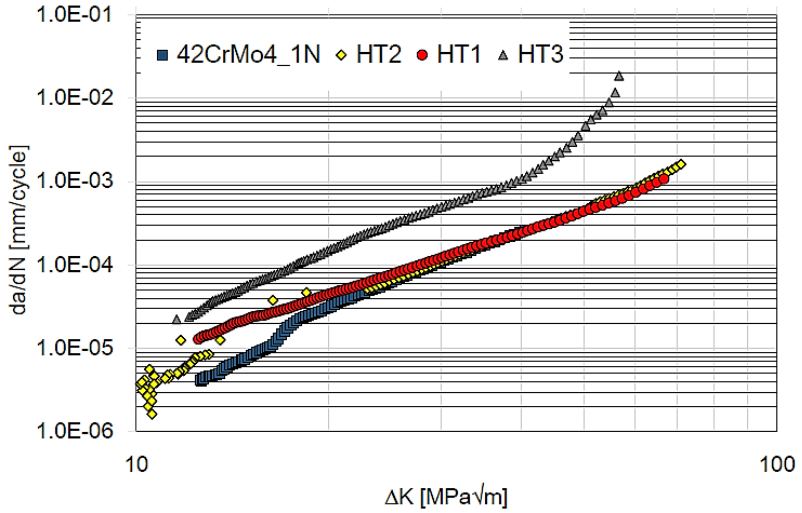

Fig. 1. Kinetic Fatigue Fracture Diagram (KFFD) for 42CrMo4 steel with various configuration of heat treatment (R=0.1) [1].

REFERENCES

[1] Lesiuk, G., Duda, M.M., Correia, J., Jesus, A.M.P., Calçada, R.: Fatigue crack growth of 42CrMo4 and 41Cr4 steels under different heat treatment conditions. International Journal of Structural Integrity 9(3), 326-336 (2018).
[2] Kucharski, P., Lesiuk, G., Szata, M.: Description of fatigue crack growth in steel structural components using energy approach - Influence of the microstructure on the FCGR. AIP Conference Proceedings 1780, 050003 (2016).
[3] Lesiuk, G., Kucharski, P., Correia, J.A.F.O., De Jesus, A.M.P., Rebelo, C., Simões da Silva, L.: Mixed Mode (I+II) Fatigue Crack Growth of Long Term Operating Bridge Steel. Procedia Engineering 160, 262-269 (2016).

Characterization of Fatigue and Damage Behavior of Extruded Chip Profiles of AW6060 Aluminum Alloy

A. Koch[a*], P. Wittke[a], F. Kolpak[b], A. E. Tekkaya[b], F. Walther[a]

[a]*Department of Materials Test Engineering (WPT), TU Dortmund University, 44227 Dortmund, Germany*
[b]*Institute of Forming Technology and Lightweight Components (IUL), TU Dortmund University, 44227 Dortmund, Germany*
**Corresponding author: alexander3.koch@tu-dortmund.de*

Keywords: Hot extrusion; Fatigue development; Aluminum chips; Computed tomography; Alternating current potential drop.

ABSTRACT

Due to a great potential for resource saving, the direct recycling of aluminum chips by means of hot extrusion is a promising alternative to the energy-intensive remelting process. Profiles extruded from aluminum machining chips, normally considered as scrap, have shown inferior quasi-static mechanical properties when compared to extruded cast material in past investigations [1]. Concerning the cyclic behavior of chip-based extruded material, only a few studies are available.

For the production of chip-based aluminum profiles the geometrically determined chips, machined from aluminum AW6060 blocks, were cold compacted to billets with a relative density of 0.78 and a diameter of $d_b = 66$ mm to improve the mechanical properties of the resulting profiles. In order to homogenize the material, the billets were heat-treated for 8 h at 550 °C [1]. Finally, the chip-based billets were extruded to profiles with a diameter of $d_p = 12$ mm with a hydraulic extrusion press at 450 °C, allowing a welding of the chips at temperatures below the melting temperature. In the current work, cast-based and chip-based specimens of flat-face die profiles with an extrusion ratio of 30.25, defined as the quotient between the cross-sectional areas of the billet and the profile, have been compared in quasi-static and cyclic tests.

For the characterization of the fatigue behavior, continuous load increase tests as well as constant amplitude tests [2] were carried out on a servohydraulic fatigue testing system (Instron 8872, F_{max} = 10 kN). To measure the plastic strain amplitude, an extensometer ($l_0 = 10$ mm) was used. Additionally, deformation-induced changes in electrical potential and temperature were determined using the ACPD (alternating current potential drop) method and thermocouples, respectively. Exemplary results for a load increase test for a chip-based specimen are shown in Fig. 1a. The change in AC potential ΔU_{AC} decreases until $N < 10^4$ cycles. After a short plateau phase, the progression is exponential and shows a similar trend to the progression of plastic strain amplitude $\varepsilon_{a,p}$. At about $N = 9.5 \cdot 10^4$ cycles there is a significant change in the slope. The change in temperature ΔT shows values nearby zero for $N < 8 \cdot 10^4$ cycles, followed by a linear increase and an exponential increase after about $N = 12 \cdot 10^4$ cycles until failure.

All specimens were analyzed by means of computed tomography (CT) scans before the mechanical tests in order to detect defects in the micro- and macro-structure such as pores or voids resulting from insufficient welding of the chips. In addition, metallographic investigations, like barker etching technique, were used to detect grain boundaries and weld seams.

The comparison of the quasi-static and cyclic properties of cast- and chip-based specimens is shown in Table 1. The results show that both, the quasi-static and the cyclic properties of chip-based specimens are significantly inferior when compared to conventional extruded cast-based specimens. This is due to

weld seams occurring between the chips during the extrusion process. Parameters such as shear stress, pressure and local strain in the chips during the extrusion are critical for a satisfactory welding process [3].

The pressure and local strain in the chips during the extrusion are considered insufficient at a certain diameter of the profile to break down superficial oxide layers, resulting in a delamination phenomenon directly connected to a critical extrusion ratio. This is observable by means of optical microscopic analyses, as the delamination can clearly be recognized at the critical diameter (Fig. 1b).

For the chip-based specimens, a significantly different damage behavior compared to the cast-based specimens could be determined, which was investigated by CT analyses. Through an intermittent experimental strategy, in which CT investigations of the crack progress were performed after certain number of cycles in constant amplitude tests, an initiation of two independent cracks in different planes was observed. These two cracks, initially propagating perpendicular to the load direction along the weld seams, change propagation in load direction and finally merge into a crack parallel to the load direction along the weld seams (Fig. 1c). In accordance with the results of the intermittent test the change of slope of the AC potential clearly indicates the initiation of a second crack for the load increase test (Fig. 1a).

Table 1. Quasi-static and cyclic properties of cast-based and chip-based specimens.

	Yield strength [MPa]	Ultimate tensile strength [MPa]	Elongation at break [10^{-2}]	Number of cycles to failure (σ_a = 120 MPa)	Fatigue strength ($N_f = 2 \cdot 10^6$) [MPa]
Cast-based	45.9 ± 0.5	140.5 ± 1.7	26.6 ± 2.9	47,487	90
Chip-based	54.1 ± 5.4	133.3 ± 5.8	18.2 ± 0.6	24,180	65

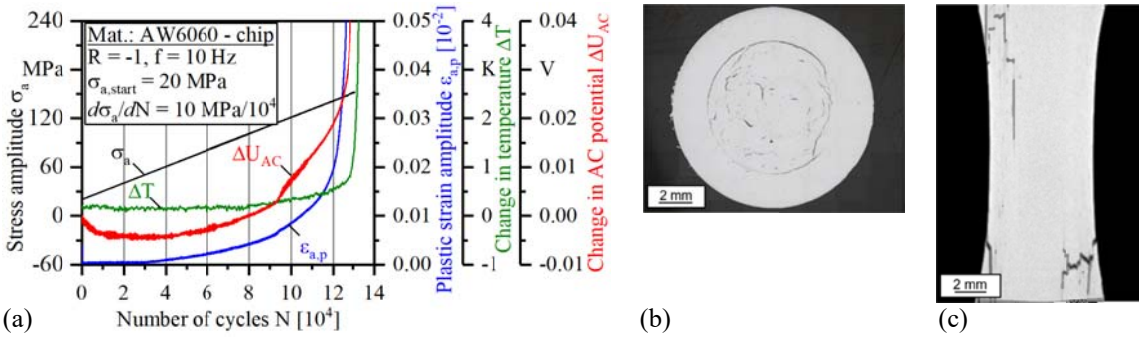

Fig. 1. (a) Plastic strain amplitude, change in temperature and change in AC potential in continuous load increase test for chip-based specimen; (b) optical micrograph for chip-based extruded profile, cross-section; (c) CT image of intermittent tested chip-based specimen in constant amplitude test ($N = 0.98 \cdot N_f$), longitudinal section.

REFERENCES

[1] Tekkaya, A.E., Schikorra, M., Becker, D., Biermann, D., Hammer, N., Pantke, K.: Hot profile extrusion of AA-6060 aluminum chips. Journal of Materials Processing Technology 209, 3343-3350 (2009).

[2] Walther, F.: Microstructure-oriented fatigue assessment of construction materials and joints using short-time load-increase procedure. Materials Testing 56, 519-527 (2014).

[3] Donati, L., Tomesani, L.: The prediction of seam welds quality in aluminum extrusion. Journal of Materials Processing Technology 153-154, 366-373 (2004).

ACKNOWLEDGMENTS

The authors thank the German Research Foundation (DFG) for its financial support within the research project “Analysis and extension of the limits of application in metal forming based recycling of aluminum chips” (WA 1672/16, TE 508/60).

Micro-Notch Size Effect on Small Fatigue Crack Propagation of Nickel-Based Superalloy GH4169

J. Wang[a], R. Wang[a], Y. Wang[b], Y.Ye[b], X. Zhang[a], S. Tu[a*]

[a]*Key Laboratory of Pressure Systems and Safety, Ministry of Education, School of Mechanical and Power Engineering, East China University of Science and Technology, Shanghai 200237, P.R. China*

[b]*National Quality Supervision and Test Center of Pressure Piping Components National Quality Supervision and Test Center of Pressure Piping Components (NPCTC), Nanjing, 211100, P.R. China*

**Corresponding author: sttu@ecust.edu.cn*

Keywords: Micro-notch effect; Fatigue; Small crack propagation; Replica.

ABSTRACT

In the past years, the disasters caused by fatigue has aroused consensus, and the safety life design methods have been widely used in the service time design for structures under fatigue load. However, most of those design methods considered the structures integrated with no defects, such as cavities and micro-cracks. Nevertheless the cracks would initiate and propagate from these defects which might limit the fatigue life largely. Indeed, many structural parts such as aircraft wings were servicing with many defects. Their safety was mainly determined by the crack propagation law and the critical crack size.

Since the 20th century, many crack propagation models have been put forwards. Insides, the most famous models are Paris law [1] and its derivative models. Considering the stress ratio effect, and the crack closure effect, Walker [2], Forman [3] and Newman [4] had modified the Pairs law. These laws are appropriate for long cracks. But for short cracks, they apparently to possess higher crack propagation rate than long cracks at the same stress intensity factor, which should be paid more attention.

This study investigated the micro defects effect and exposed the crack propagation regular of both small and long cracks on Nickel-based superalloy GH4169. Deng [5], Ye [6] and Qing [7] have studied the grain size effect on small fatigue crack propagation with this kind of material. The crack detection method used in this study was almost the same as their works. Micro-notches were first machined on each specimen. Replica way was applied to acquire crack length.

In this study, fatigue tests with different micro-notch sizes at room temperature and 650°C were carried out. The crack initiation life and crack propagation rate were record on the replicas. The stress intensity factor was calculated with Newman's method and the micro-structure analysis was observed with optical microscope, electron microscope and electron backscatter diffraction (EBSD) method. Several conclusions were listed as follows:

(i) The initiation life, total fatigue life and the crack propagation rate were largely influenced by the length and the depth of the micro-notch. While the width of the crack showed little effect. Finite element method was carried out to calculate the stress concentration of different notch size, which showed some relationship between crack initiation.

(ii) The relationship between crack propagation rate with different micro-notch size at room temperature and stress intensity factor range was exhibited in Fig.1. Affected by micro-structure, the small crack propagation rate expressed huge volatility. Ye has proposed for both small and long cracks with the size of plastic zone, which was modified here considering the micro-notch size effect.

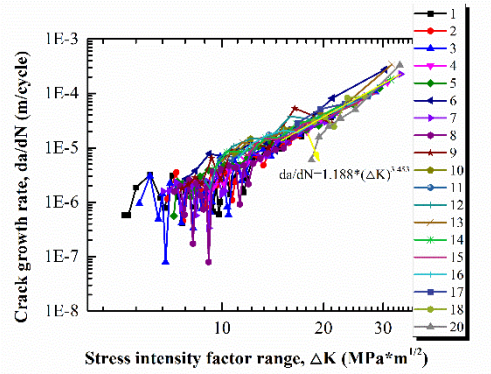

Fig. 1**.** The crack propagation rate with different micro-notch size at room temperature along with stress intensity factor range.

(iii) Micro-structure effect was clear discussed. Large angle grain boundary showed large resistance to small crack propagation. The size and distribution of grain boundary angle were affected by many aspects. Here, a distribution function was introduced to the crack propagation model for small cracks to characterize grain boundary effect.

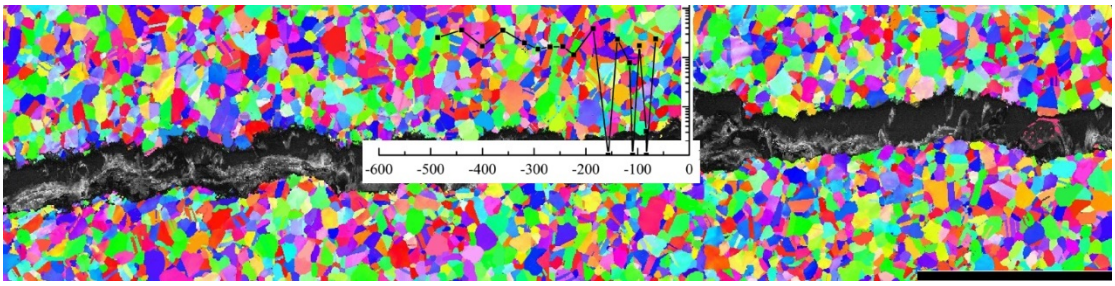

Fig. 2**.** EBSD result for micro-structure effect on small crack propagation.

REFERENCES

[1] Paris, P., Erdogan, F.: A critical analysis of crack propagation laws. Journal of Basic Engineering 85 (4), 528–534 (1963).

[2] Walker, K.: The Effect of Stress Ratio During Crack Propagation and Fatigue for 2024-T3 and 7075-T6 Aluminium, Effects of Environment and Complex Load History on Fatigue Life: STP 462, ASTM Special Technical Publication, 1–14 (1970).

[3] Forman, R.G.: Study of fatigue crack initiation from flaws using fracture mechanics theory. Engineering Fracture Mechanics 4 (2), 333–345 (1972).

[4] Newman, J.C.: An empirical stress-intensity factor equation for the surface crack. Engineering Fracture Mechanics 15(1–2), 185-192 (1981).

[5] Deng, G.J., Tu, S.T., Wang, Q.Q., et al.: Small fatigue crack growth mechanisms of 304 stainless steel under different stress levels. International Journal of Fatigue 64(7), 14–21 (2014).

[6] Ye, S., Zhang, X.C., Gong, J.G., et al.: Multi-scale fatigue crack propagation in 304 stainless steel: experiments and modelling. Fatigue & Fracture of Engineering Materials & Structures 40(11), 1928-1941 (2017).
[7] Qin, C.H., Zhang, X.C., et al.: Grain size effect on multi-scale fatigue crack growth behaviour of Inconel alloy GH4169. Engineering Fracture Mechanics 142, 140–153 (2015).

ACKNOWLEDGMENTS

The authors would like to acknowledge gratefully for the financial support through National Natural Science Foundations of China (51371082, 51322510) and 111 project. The author X.C. Zhang is also grateful for the support by Shanghai Pujiang Program, Young Scholar of the Yangtze River Scholars Program, and Shanghai Technology Innovation Program of SHEITC (CXY-2015-001).

Low Cycle Fatigue Life Test and Research on a Prefabricated HA Defective Disk

A. Zhengyu Zhu[a,b], B. Haijun Xuan[a,b*], C. Yushen Zou[a,b]

[a] *High-Speed Rotating Machinery Laboratory, College of Energy Engineering, Zhejiang University, China*
[b] *Collaborative Innovation Center for Advanced Aero-engine, China*
**Corresponding author: marine@zju.edu.cn*

Keywords: Aircraft engines; Disks; Low cycle fatigue; Crack growth; Implantation process; Fracture analysis; Titanium hard alpha; Simulation analysis.

ABSTRACT

Titanium HA (hard alpha) inclusions may be introduced during the production of titanium alloys, especially during the melting process. The existence of inclusions undermines the continuity of the titanium alloy matrix. Stress concentration, initiation of fatigue cracks, acceleration of crack propagation, reduction of material quality and service reliability are caused by the presence of inclusions. Therefore, a TC4 material disk was designed to study the influence of disk on the fatigue properties of the disk when it contains HA defects in this paper. HA defects are artificially implanted into the blank and formed after forging, and their position and shape are detected by ultrasonic wave. Then the low cycle fatigue test was carried out for the titanium alloy disk with HA defects, the crack initiation and propagation characteristics of the HA defect and the effect on the fatigue life of the disk are researched as well. Comparing the simulation with the experiment, the results show that the crack propagation rate calculated by the simulation analysis is in good agreement with the experimental results.

Mathematical Representation of Fatigue Crack Growth Models in Steel Using Dimensional Analysis – Theory and Experiment

M. Szata[a*], G. Lesiuk[b]

[a] *Faculty of Technology and Natural Sciences, Wrocław University of Science and Technology, 27 Wybrzeże Wyspiańskiego st., 50-370 Wrocław, Poland*
[b] *Department of Mechanics, Material Science and Engineering, Wrocław University of Science and Technology, Smoluchowskiego 25, 50-370 Wrocław, Poland*
**Corresponding author: Mieczyslaw.Szata@pwr.edu.pl*

Keywords: Crack propagation; Fatigue; Mean stress effect; Dimensional Analysis; Kinetic fatigue fracture diagrams.

ABSTRACT

Typically, for cyclic crack growth resistance there are constructed the kinetic fatigue fracture diagrams (KFFD). The main way (a classic one) of describing the fatigue fracture kinetics is the force approach – promoted in standard ASTM E647 [1]. The rate of a crack growth is described as a function of stress intensity factor. This function based on experimental data is power law - type form in relation to ΔK (stress intensity range $\Delta K=K_{max}-K_{min}$) or its maximal value in cycle K_{Imax}. However, in this case a mean stress (R-ratio) effect is reflected in shifting of the da/dN-ΔK curves. Another group of quantities, suitable for description of fatigue crack growth process, is a group based on strain energy density parameters associated with the existing hysteresis loops. The role of energy parameter in FCGR process can be found with Dimensional Analysis approach and their geometrical methods. In this case, the Universal Graph [2] method was used for estimation of the kinetic equation based on energy dissipated in one cycle of loading. This non-classical method reduces the dimensional dependences to some functions at the dimensionless fiber. It should be underlined that it does not break a symmetry among incoming arguments [3]. The main algorithm of this method is summarized as follows [2]:

- identify all dimensional basis related to the main process,
- treat one of the physical quantity as a main parameter; in this case this quantity should appear in each product,
- construct the hyper-plane for each basis.

The physical variables and its dimension have been presented in Table 1. Finally, after transformation and returning to initial physical quantities, a new "*crack driving force*" as the energy parameter can be expressed as:

$$\Delta H = \frac{W_c}{B\left(1-\frac{K_{\mathrm{Im}ax}^2}{K_{fc}^2}\right)} \tag{1}$$

Where; W_c-energy dissipated in each cycle of loading, B – specimen thickness, K_{fc} – fatigue cyclic stress intensity factor. In course of the experiment, two types of fatigue fracture kinetics have been recorded. In the first one, the range of changes in the stress intensity factor ΔK appears, which characterizes the intensity of cyclic strain in the crack tip, and in the second one, ΔS quantity appears, corresponding to the

searched dissipation energy of strain recorded in the form of a hysteresis loop. As a new crack driving force was used ΔS parameter:

$$\Delta S = \frac{W_c^{(1)}}{1-\frac{K_{Imax}^2}{K_{fc}^2}} \tag{2}$$

Table 1. Involved dimensional analysis variables in FCGR process.

Symbol	Variable	Description	Physical Dimensions	F	L
Y	W_c	Strain energy density	[F]	1	0
A	ΔH	Energy parameter as a "crack driving force"	$[FL^{-1}]$	1	-1
B	B	Thickness	[L]	0	1
C	K_{fc}^2	Critical stress intensity factor raised to the power of two	$[F^2L^{-3}]$	2	-3
D	K_{Imax}^2	Maximal value of stress intensity factor raised to the power of two	$[F^2L^{-3}]$	2	-2

For test were used CT-specimens (W=48mm, t=18mm) prepared in accordance with ASTM E647 [1]. The energy kinetic fatigue fracture diagram is presented in Fig.1

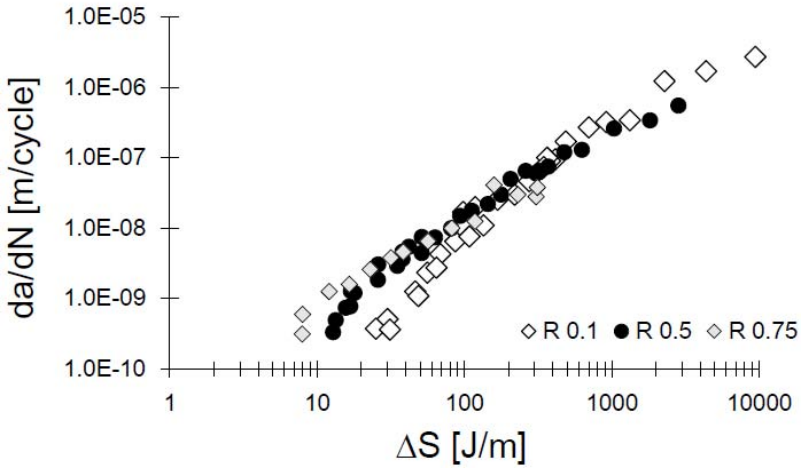

Fig. 1. Kinetic fatigue fracture diagram for 41Cr4 steel (Q+T condition) based on energy parameter ΔS.

REFERENCES

[1] ASTM E647-15a: Standard test method for measurement of fatigue crack growth rates. ASTM International.

[2] Rybaczuk, M.: Geometrical methods of dimensional analysis in problems of mechanics. Scientific Papers of the Institute of Materials Science and Applied Mechanics of the Technical University of Wroclaw, Wroclaw (1993) (in Polish).

[3] Kasprzak, W., Lysik, B., Rybaczuk, M.: Measurement, Dimensions, Invariant Models and Fractals. Publishing House, "Spolom", Lviv, Ukraine (2004).

ACKNOWLEDGEMENTS

The experimental works have been supported by the Wroclaw University of Technology, Faculty of Technology and Natural Sciences.

Fatigue Crack Growth in Long Term Operated 19th/20th Century Steel Members Under Mixed Mode Loading (I+II, I+III)

G. Lesiuk[a*], D. Rozumek[b], M. Duda[a], M. Smolnicki[a], Z. Marciniak[b], J.A.F.O. Correia[c], A.M.P. De Jesus[c], H. Krechkovska[d]

[a] *Department of Mechanics, Material Science and Engineering, Wrocław University of Science and Technology, Smoluchowskiego 25, 50-370 Wrocław, Poland*
[b] *Department of Mechanics and Machine Design, Opole University of Technology, Mikolajczyka 5, 45-271 Opole, Poland*
[c] *INEGI/Faculty of Engineering, University of Porto, Rua Dr. Roberto Frias, 4200-465 Porto, Portugal*
[d] *National Academy of Sciences of Ukraine, Karpenko Physico-Mechanical Institute, Naukova 5 str., Lviv, 79060, Ukraine*
**Corresponding author: Grzegorz.Lesiuk@pwr.edu.pl*

Keywords: Crack propagation; Puddle iron; Old mild steel; Mixed mode fatigue fracture; Degradation.

ABSTRACT

The maintenance of the old steel structures is one of the main challenges in engineering practice – mainly due to the lack of the experimental data performed for existing old steel structures erected at the turn of the 19th and 20th centuries. In this paper the fatigue crack growth behavior in structural components from the old 19th (and early 20th) centuries structures (e.g. bridges) has been investigated. The delivered material for investigation was extracted from a beam made from puddled iron and mild rimmed steel, commonly used 100 years ago. It has been confirmed in author's experimental works that the fatigue crack growth rate in this ancient type of steel is higher than in its modern equivalent. One of the fundamental engineering tasks is the problem of the extension of the precritical fatigue crack growth in such a type of steel Material for investigation was gained from the railway old riveted, metallic bridge (1899-1902) located in Kluczbork (Poland, rail line 143 – 67.749km). The general view of the girder structure is shown in Fig. 1.

Fig. 1. General view of the structural element from Kluczbork bridge.

The paper presents the results of an experimental investigation of the crack path and description of fatigue crack growth in plane specimens made of old mild steel (Fig.1) as well puddle iron [1] under tension and shear state and bending with torsion state. Specimens with rectangular cross-sections [2] and stress concentrator in the form of external one-sided sharp notch were used. The tests were performed under the load ratios R = 0, 0.1. The tests were performed under the different slot inclinations (mode I+II) and different ratios of torsion to bending moments (mode I+III). The results of the experimental tests have been described using ΔK stress intensity factor range.

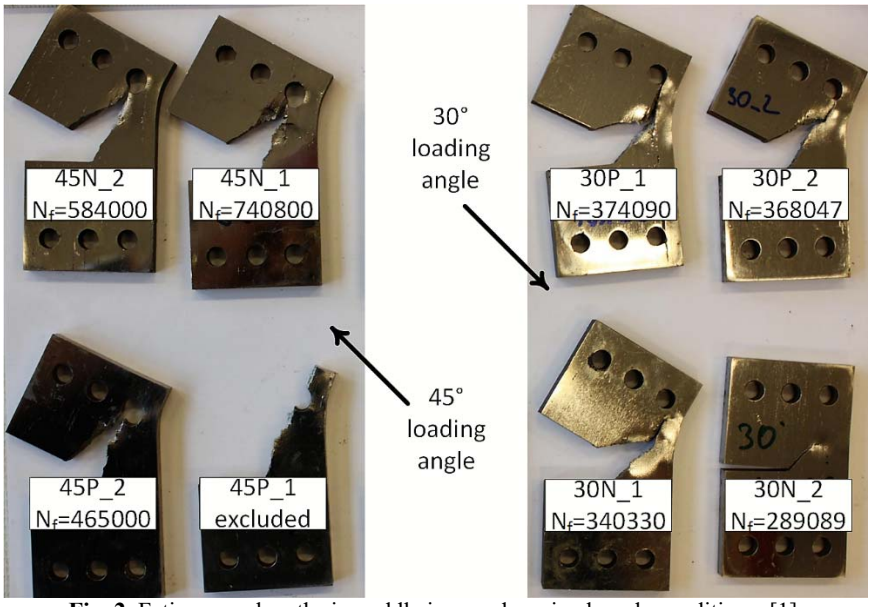

Fig. 2. Fatigue crack paths in puddle iron under mixed mode conditions, [1].

The obtained results for puddle iron [1] have shown the inadequacy of classical mixed-mode load theories for the prediction of the crack initiation angle. For old mild steel, the existing criteria are suitable for the prediction of crack imitation angle in analytical models as well numerical simulations. However, the puddle iron (Fig. 2) shows a tendency to the brittleness in TL direction. It seems that, for puddle iron, a new criterion of the mixed-mode loading should be formulated in terms of material anisotropy. A noticeable is a fact that under mixed mode condition I+II the fatigue lifetime (for both materials) increase with the ratio K_{II}/K_I.

REFERENCES

[1] Lesiuk, G., Kucharski, P., Correia, J. A., De Jesus, A. M. P., Rebelo, C., da Silva, L. S.: Mixed mode (I+ II) fatigue crack growth in puddle iron. Engineering Fracture Mechanics 185, 175-192 (2017).
[2] Rozumek, D., Marciniak, Z., Lesiuk, G., Correia, J. A. F. O.: Mixed mode I/II/III fatigue crack growth in S355 steel. Procedia Structural Integrity 5, 896-903 (2017).

ACKNOWLEDGMENTS

The experimental works have been supported by the Wroclaw University of Science and Technology – project no 401/0029/17

Mixed Mode Fatigue Crack Paths in S355 Steel in Terms of Fractal Geometry and Fractography Analysis

P. Kotowski[a], G. Lesiuk[a*], D. Rozumek[b], Z. Marciniak[b], J.A.F.O. Correia[c], Abilio M.P. De Jesus[c]

[a] *Department of Mechanics, Materials Science and Engineering, Wrocław University of Science and Technology, Smoluchowskiego 25, 50-370 Wrocław, Poland*
[b] *Department of Mechanics and Machine Design, Opole University of Technology, Mikolajczyka 5, 45-271 Opole, Poland*
[c] *INEGI/Faculty of Engineering, University of Porto, Rua Dr. Roberto Frias, 4200-465 Porto, Portugal*
**Corresponding author: Grzegorz.Lesiuk@pwr.edu.pl*

Keywords: Mixed mode fracture; Fatigue; Fractography; Fractal geometry; Roughness parameters.

ABSTRACT

The paper presents the results of an experimental investigation of the crack path and description of fatigue crack surface in plane specimens made of S355 steel under tension shear state (mode I+II) and bending with torsion (mode I+III). The tests were performed under different slot inclinations (mode I+II, specimen shown in Fig. 1a) and different ratios of torsion to bending moments (mode I+III, specimen shown in Fig. 1b) for the load ratios R = 0.1, 0 respectively. The results of the experimental tests have been described using ΔK stress intensity factor range.

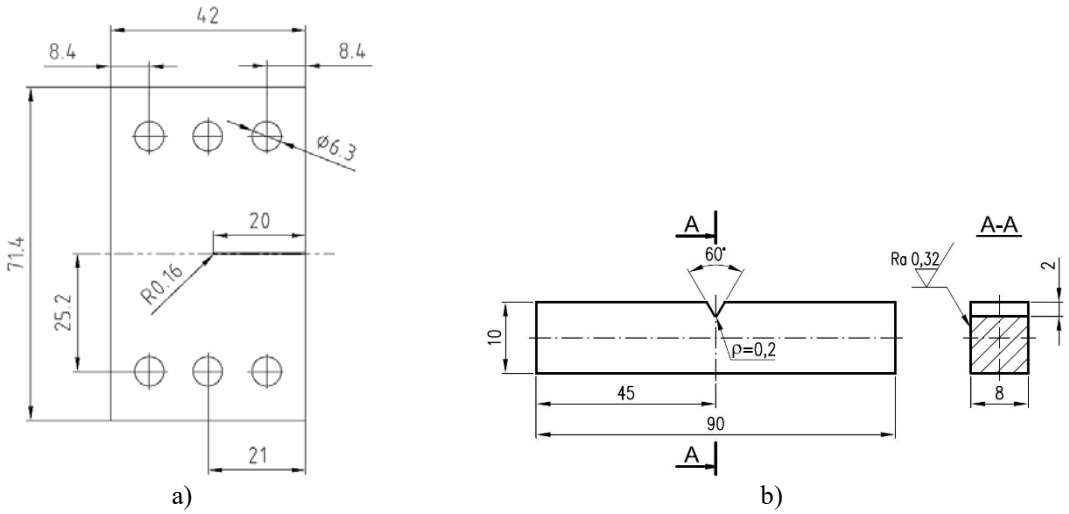

Fig. 1. Shape and dimensions of specimen for a) mode I+II, b) mode I+III, dimensions in mm [1].

After experiments, the fatigue crack paths were numerically determined and compared with experimental crack paths. The stress intensity factors were calculated using numerical approach (BEM – boundary element method) in FRANC2D and FRANC3D software. The mixity ratio K_{II}/K_I or K_{III}/K_I plays an important role in crack initiation angle – Fig. 2. After fatigue crack growth rate tests, the fracture surface of specimens were investigated using fractal geometry [2, 3] as well roughness parameters.

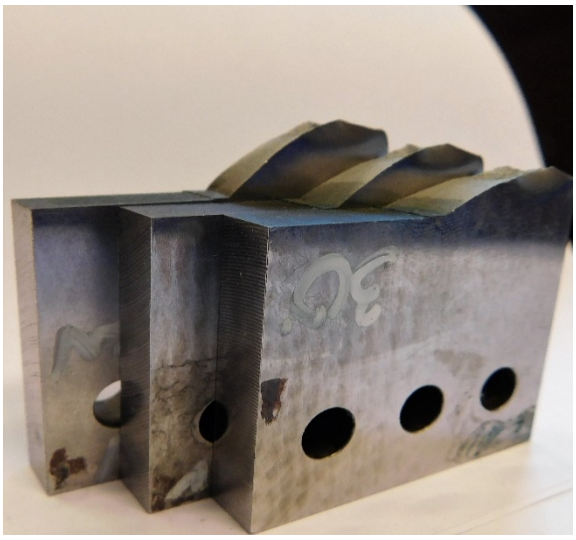

Fig. 2. Typical fatigue crack paths obtained for different slot inclinations (30°, 45°, 60°).

Box-counting fractal dimension was determined for the obtained fracture surface. In this study, the indirect method was applied and the dimension was determined for the vertical profile of the surface. The image of the profile, seen through the microscope coupled with a camera, was recorded in a computer, where numerical processing was performed. For calculation of the same fractal dimension, the FD3 program has been used. The essential element of the method is optimisation concerning microscopic magnification (scale of a length), resolution of the recorded image and selection of the grey level threshold at binarization. This method allows determination of the fractal dimension with an absolute accuracy of 0.05 in non-dimensional units. A complete method of determination of the fractal dimension for fracture surfaces of ferrous alloys was described in [3].

REFERENCES

[1] Rozumek, D., Marciniak, Z., Lesiuk, G., &Correia, J. A. F. O.: Mixed mode I/II/III fatigue crack growth in S355 steel. Procedia Structural Integrity 5, 896-903 (2017).
[2] Mandelbrot, B. B.: The fractal geometry of nature, Vol. 173. New York: WH freeman (1983).
[3] Kotowski, P.: Fractal dimension of metallic fracture surface. International Journal of Fracture 141 (1-2), 269-286 (2006).

Short and Long Crack Growth of Aluminium Cast Alloys

M. Leitner[a*], R. Aigner[a], S. Pomberger[a], M. Stoschka[a],
C. Garb[b], S. Pusterhofer[b]

[a] *Christian Doppler Laboratory for Manufacturing Process based Component Design, Chair of Mechanical Engineering, Montanuniversität Leoben, Austria*
[b] *Chair of Mechanical Engineering, Montanuniversität Leoben, Austria*
**Corresponding author: martin.leitner@unileoben.ac.at*

Keywords: Crack growth; Aluminium cast, Crack closure; Resistance curve; Microstructural effects.

ABSTRACT

This paper deals with an experimental characterization of the short and long crack growth behaviour of aluminium AlSi cast alloys. The work includes four different material types exhibiting a variation of the alloy specification, heat treatment, eutectic modifier as well as the cast component, where the specimens for the fracture mechanical tests are extracted from, see Table 1. Preliminary studies [1, 2] revealed that these cast process parameters can significantly affect the fatigue strength; hence, this paper continuatively focuses on the crack growth characteristics as presented in [3, 4].

Table 1. Overview of investigated aluminium cast materials.

Alloy specification	Heat treatment	Eutectic modifier	Cast component
EN AC-45500	T6	Strontium (Sr)	Cylinder head (ch)
EN AC-45500	T6	Sodium (Na)	Cylinder head (ch)
EN AC-46200	T5	Strontium (Sr)	Cylinder head (ch)
EN AC-46200	T6	Strontium (Sr)	Crank case (cc)

The experiments cover both the short and long crack fatigue regime. Within the short crack growth special attention is laid on the effective threshold of the stress intensity factor range $\Delta K_{th,eff}$ [5] as well as the increasing influence of crack closure phenomena [6], such as plasticity- and roughness-induced crack closure effects [7], during crack propagation. A compression pre-cracking method to generate near-threshold fatigue-crack-growth-rate data [8] is applied to evaluate the resistance (R-) curve [9] of the investigated AlSi cast materials. To describe the course of the fatigue crack threshold ΔK_{th} starting from the effective value $\Delta K_{th,eff}$ at a crack extension of $\Delta a=0$ up to the long crack growth threshold $\Delta K_{th,lc}$, the empirical approach as presented in [10] is utilized, see Eq. (1).

$$\Delta K_{th} = \Delta K_{th,eff} + (\Delta K_{th,lc} - \Delta K_{th,eff}) \cdot (1 - e^{(-\Delta a/l_R)}) \quad (1)$$

Further on, if the crack extends and the long crack growth threshold $\Delta K_{th,lc}$ is reached, the common crack propagation law introduced by Paris and Erdogan [11] is employed. Fig. 1 (left) depicts the experimental crack growth results for three single-edge-notched-bending samples made of EN AC-45500-T6 Sr (ch). All fracture mechanical tests are conducted at a load stress ratio of $R=-1$. A subsequent evaluation of the R-curve in Fig. 1 (right) shows that the effective threshold values in the short crack regime match well, but major differences regarding the influence of the crack closure effects and the final long crack growth threshold can be observed. In [12] it is presented that microstructural characteristics significantly affect the fatigue crack growth of aluminium cast alloys. Hence, further experiments with optical in-situ crack growth detection according to the procedure given in [13] are conducted.

The results of the in-situ optical analysis show that the microstructure, such as eutectic phases (Fig. 2, left) or shrinkage pores (Fig. 2, right), influence not only the crack growth rate, but additionally the crack path, whereat both need to be considered to properly assess the lifetime in the short and long crack fatigue regime of cast aluminium alloys.

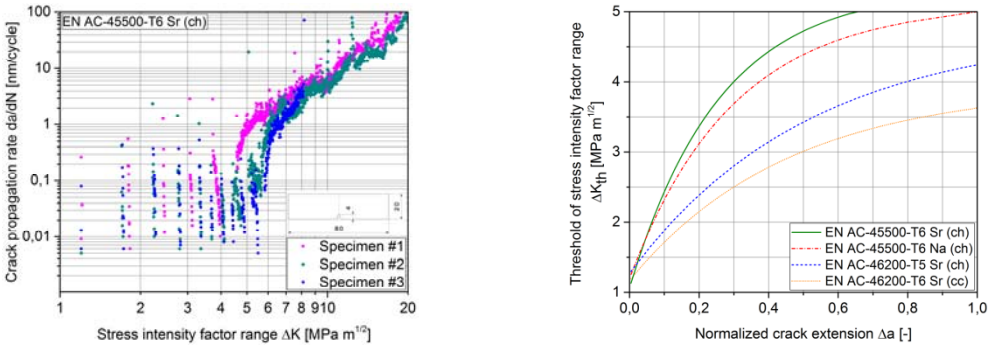

Fig. 1. Experimental crack growth results for EN AC-45500-T6 Sr (ch) (left) and evaluation of the fatigue crack resistance curve for the different test series (right).

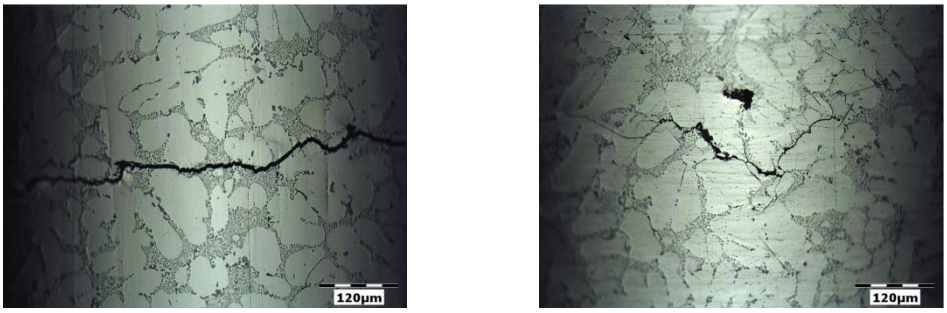

Fig. 2. In-situ optical detection of microstructural effects on the long crack growth behaviour of AlSi cast alloys.

REFERENCES

[1] Garb, C., Leitner, M., Grün, F.: Fatigue strength assessment of AlSi7Cu0.5Mg T6W castings supported by computed tomography microporosity analysis. Procedia Engineering 160, 53-60 (2016.)

[2] Leitner, M., Garb, C., Remes, H., Stoschka, M.: Microporosity and statistical size effect on the fatigue strength of cast aluminium alloys EN AC-45500 and 46200. Materials Science & Engineering A 707, 567-575 (2017).

[3] Casellas, D., Pérez, R., Prado, J.M.: Fatigue variability in Al–Si cast alloys. Materials Science and Eng. A 398, 171-179 (2005).

[4] Spangenberger, A.G. et al.: Microstructural mechanisms and advanced characterization of long and small fatigue crack growth in cast A356-T61 aluminum alloys. International Journal of Fatigue 97, 202-213 (2017).

[5] Pippan, R.: The effective threshold of fatigue crack propagation in aluminium alloys. Philosoph. Mag. A 77:4, 861-873 (1998).

[6] Pippan, R., Hohenwarter, A.: Fatigue crack closure: a review of the physical phenomena. Fatigue Fract Eng 40, 471-495 (2017).

[7] Kim, J.H., Lee, S.B.: Behavior of plasticity-induced crack closure and roughness-induced crack closure in aluminum alloy. International Journal of Fatigue 23, 247-251 (2001).

[8] Newman, Jr., J.C., Yamada, Y.: Compression precracking methods to generate near-threshold fatigue-crack-growth-rate data. International Journal of Fatigue 32, 879-885 (2010).

[9] Pippan, R., Plöchl, L., Stüwe, H.P.: Resistance curves for the threshold of fatigue crack propagation. Proceedings of ECF 10 – Structural Integrity, 1441-1449 (1994)

[10] Maierhofer, J., Gänser, H.-P., Pippan, R.: Modified Kitagawa–Takahashi diagram accounting for finite notch depths. International Journal of Fatigue 70, 503-509 (2015).

[11] Paris, P., Erdogan, F.: A Critical Analysis of Crack Propagation Laws. J. Basic Engineering 85 (1963).

[12] Lados, D.A. et al.: Microstructural mechanisms controlling fatigue crack growth in Al–Si–Mg cast alloys. Materials Science and Engineering A 468-470, 237–245 (2007)

[13] Huter, P. et al.: Comparison of microstructural crack paths between hypo-eutectic Al–Si–Cu and Al–Si–Mg cast alloys in high plasticity regimes under rotating bending. Materials Science & Engineering A 618, 578-585 (2014).

The Role of Crack Closure Parameter in Modelling of Fatigue Crack Growth in Terms of Energy Approach

G. Lesiuk[a]

[b] *Department of Mechanics, Materials Science and Engineering, Wrocław University of Science and Technology, Smoluchowskiego 25, 50-370 Wrocław, Poland*
**Corresponding author: Grzegorz.Lesiuk@pwr.edu.pl*

Keywords: Crack propagation; Fatigue; Mean stress effect; Crack closure model; Energy approach.

ABSTRACT

Since the publication of the Elber's work [1], the problem of crack closure effect is a major topic in fatigue fracture mechanics and fatigue crack growth in terms of a mean load influence. As it is well known from experimental practice, the R-ratio (K_{min}/K_{max}) strongly influences the unification process of description of the fatigue crack growth rate in a force driven approach. In many works, it has been proved that the stress R-ratio effect is negligible if we consider ΔK_{eff} as a crack driving force parameter in Kinetic Fatigue Fracture Diagram (KFFD):

$$\Delta K_{eff} = K_{\max} - K_{op}. \tag{1}$$

However, in several papers (e.g. Xiong et al. [2]) it was demonstrated that the ΔK_{eff} does not always consolidate experimental data in a one line. Therefore, the energy approach [3, 4] seems to be predestined for description of FCGR data without mean stress effect. In this case, a noticeable fact is that energy models work well in "Paris regime" region. In near threshold region a significant data scatter is observed – Fig. 1.

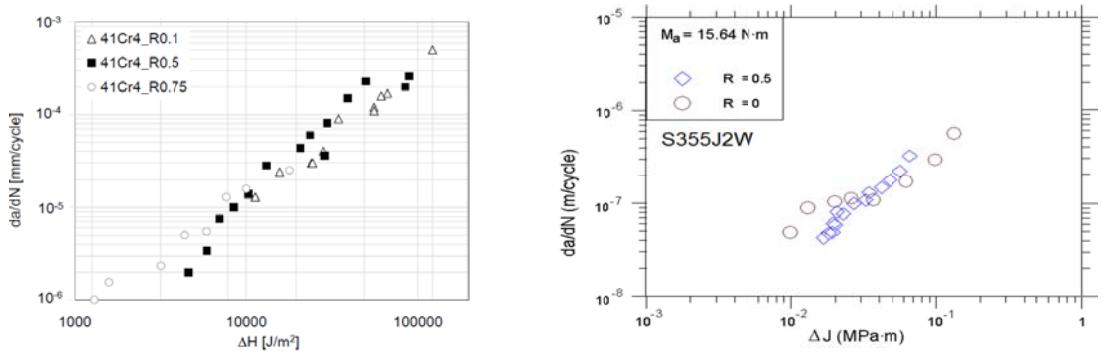

a) b)

Fig. 1. Kinetic fatigue fracture diagram for 41Cr4 steel based on energy ΔH parameter (a) and S355J2W steel based on ΔJ parameter (b) [5].

According to energy model considerations and crack closure phenomenon, the corrections of crack closure parameters are required in near threshold region. A general algorithm of closure point (closure load) identification consists in:

- Registration of the signals F-COD at desired load cycles,

- Decomposition of the F-COD line for linear and nonlinear parts by fitting the linear dependence (two constants A_0 and A_1) and second order polynomial function (three constants B_0, B_1, B_2),
- Optimization of the values of the B_0, B_1, B_2 due to minimizing residual sum of squares (RSS) deviation from linear coincidence.

Based on existing models, as well experimental data, crack closure corrections in near threshold region has been performed. The experimental results for 42CrMo4 steel (for different R-ratios) are presented in Fig. 2.

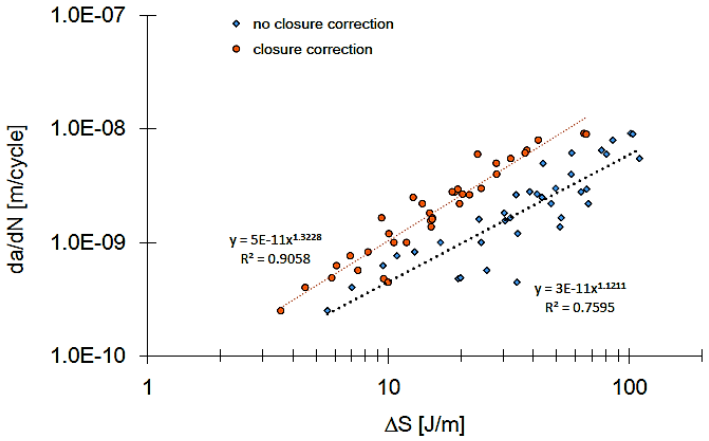

Fig. 2. Near threshold *da/dN-ΔS* region for 41Cr4 steel (tempered in 200°C, R=0.1, 0.5, 0.75) before and after closure corrections

As a conclusion, it is postulated to reformulate the energy models for near threshold region. It is demonstrated that the crack closure effect plays an important role in this region. A noticeable is decreasing of experimental data scatter for results with closure corrections. It is worth to underline that the new U-crack closure function will be required for energy approach. The simple analytical corrections regarding to crack closure effect can be successful used for energy models in near threshold region.

REFERENCES

[1] Elber, W.: Fatigue crack closure under cyclic tension. Engineering Fracture Mechanics 2, 37-45 (1970).

[2] Xiong, Y., Katsuta J., Kawano K., Sakiyama T.: Examination of fatigue crack driving force parameter. Fatigue & Fracture of Engineering Materials & Structures 31, 754–765 (2008).

[3] Szata, M., Lesiuk, G.: Algorithms for the estimation of fatigue crack growth using energy method. Archives of Civil and Mechanical Engineering 9(1), 119-134 (2009).

[4] Rozumek, D.: J-integral in the description of elasto-plastic crack growth kinetics curve. Archive of Mechanical Engineering 53(3), 211-225 (2006).

[5] Lesiuk, G., Szata, M., Rozumek, D., Marciniak, Z., Correia, J.A.F.O., De Jesus, A.M.P.: Energy description of fatigue crack growth process-theoretical and experimental approach. Procedia Structural Integrity 5, 904-911 (2017).

High Temperature Fatigue Behaviour of Secondary AlSi7Cu3Mg Alloys

A. De Mori[a*], G. Timelli[a], F. Berto[b]

[a]*Department of Management and Engineering, University of Padova, 36100 Vicenza, Italy*
[b]*Department of Engineering Design and Materials, Norwegian University of Science and Technology, 7491 Trondheim, Norway*
**Corresponding author: alessandro.demori@phd.unipd.it*

Keywords: Al–Si alloy; Microstructure; High temperature fatigue; Hardness; Ageing.

ABSTRACT

Due to excellent castability, low weight, corrosion resistance and good mechanical properties, Aluminium-Silicon based foundry alloys are widely used for several automotive parts such as engine blocks and cylinder heads. It is well-known how these industrial components are applied at extreme and complicated working conditions since they reach temperatures up to 300 °C, far beyond the limit for existing Al-Si casting grades; technological changes in engine materials are required [1-3].

Nowadays aluminium recycling is becoming increasingly important since it saves about 95% of the energy required for primary aluminium production, thus resulting in significant savings and reduction of greenhouse gases emissions. As a result, secondary aluminium alloys present lower cost than primary ones, but also small amounts of elements and impurities which can negatively affect the final mechanical properties [4-5].

Most of research activities paid attention about mechanical properties at room temperature. On the contrary, information regarding high temperature fatigue behaviour of the aforementioned alloys is very limited, despite their use and diffusion.

The aim of this work is to characterise the high temperature fatigue behaviour of secondary AlSi7Cu3Mg foundry alloys.

The experimental alloy was melt in a resistance-heated furnace at 760 °C and the chemical composition, performed with an optical emission spectrometry, is shown in Table 1. Castings were produced by using the *reference die* proposed in the document CEN/TR 16748:2014 [6].

Table 1. Chemical composition of the investigated AlSi7Cu3Mg alloy (wt%).

Alloy	Si	Fe	Cu	Mn	Mg	Zn	Cr	Ni	Ti	Sr	Al
AlSi7Cu3Mg	6.7	0.42	3.56	0.29	0.32	0.05	0.013	0.009	0.100	0.0001	bal.

Specimens were then heat-treated in an air-circulating furnace. The solution treatment was performed at 485 °C for 24 h, followed by water quench at room temperature. Material hardness was tested at room temperature after different ageing times at 180 °C. Furthermore, specimens for fatigue testing were artificially aged at 180 °C for 8 h, corresponding to a T7 heat treatment.

Fatigue tests were carried out under load control with a stress ratio R = 0.01. As-cast specimens were tested at room temperature while the heat-treated ones were characterized both at room and elevated temperatures, i.e. 200 and 300 °C. After testing, microstructural investigations were carried out by optical microscopy. Some microstructural features, such as the secondary dendrite arms spacing (SDAS) of α-Al phase, the roundness of eutectic Si particles, were quantitatively evaluated by using an image analyser.

Fig. 1 shows typical as-cast and T7 heat-treated microstructures observed in the specimens tested at room temperature. The morphology of eutectic Si particles changes from unmodified, typical of the as-cast state, to a globular shape after heat treatment. The performed heat treatment leads both to a complete dissolution of Cu-containing phases and to the precipitation of finely dispersed particles throughout the α-Al matrix.

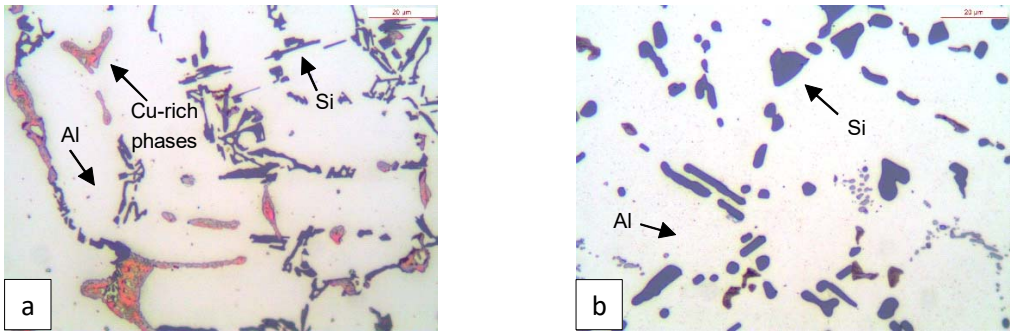

Fig. 1. Typical microstructure of secondary AlSi7Cu3Mg alloy in (a) as-cast and (b) heat-treated conditions.

Fatigue results of heat-treated AlSi7Cu3Mg alloy are reported in Fig. 2. In general, higher stress amplitudes correspond to lower number of cycles before failure. The fatigue resistance progressively decreases when passing from room to high temperatures. While the fatigue behaviour at 200 °C is comparable to that at room temperature, the fatigue properties significantly decrease at 300 °C due to the coarsening of strengthening precipitates.

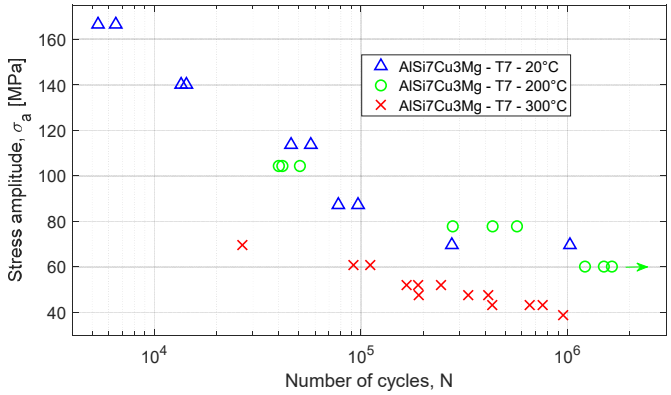

Fig. 2. Fatigue results of heat-treated AlSi7Cu3Mg alloy at different testing temperatures.

REFERENCES

[1] Huter, P., Renhart, P., Oberfrank, S., Schwab, M., Grun, F., Stauder, B.: High- and low-cycle fatigue influence of silicon, copper, strontium and iron on hypo-eutectic Al-Si-Cu and Al-Si-Mg cast alloys used in cylinder heads. International Journal of Fatigue 82, 588–601 (2016).

[2] Yang, Y., Zhong, S.-Y., Chen, Z., Wang, M., Ma, N., Wang, H.: Effect of Cr content and heat-treatment on the high temperature strength of eutectic Al–Si alloys. Journal of Alloys and Compounds 647, 63–69 (2015).

[3] Shaha, S.K., Czerwinski, F., Kasprzak, W., Friedman, J., Chen, D.L.: Ageing characteristics and high-temperature tensile properties of Al–Si–Cu–Mg alloys with micro-additions of Mo and Mn. Materials Science & Engineering A 684, 726–736 (2017).

[4] Cui, J., Roven, H.: Recycling of automotive aluminum. Transactions of Nonferrous Metals Society of China 20, 2057–2063 (2010).

[5] Camicia, G., Timelli, G.: Grain refinement of gravity die cast secondary AlSi7Cu3Mg alloys for automotive cylinder heads. Transactions of Nonferrous Metals Society of China 26, 1211–1221 (2016).

[6] CEN/TR 16748:2014, Aluminium and aluminium alloys – Mechanical potential of Al-Si alloys for high pressure, low pressure and gravity die casting.

Mixed Mode Fatigue Crack Growth in Rail Steel

G. Lesiuk*[a], M. Smolnicki[a], M. Duda[a], R. Mech[a], J.A.F.O. Correia[b], A. M.P. De Jesus[b]

[a] *Department of Mechanics, Materials Science and Engineering, Wrocław University of Science and Technology, Smoluchowskiego 25, 50-370 Wrocław, Poland*
[b] *INEGI/Faculty of Engineering, University of Porto, Rua Dr. Roberto Frias, 4200-465 Porto, Portugal*
**Corresponding author: grzegorz.lesiuk@pwr.edu.pl*

Keywords: Rail steel; Mixed mode fatigue crack growth; CTS specimen; Crack paths; SIF calculation.

ABSTRACT

The paper presents the results of an experimental investigation of the mixed mode (I+II) fatigue crack growth. It is well known that crack growth phenomenon in railheads requires a complex analysis of forces, such as the crack tip opening and sliding displacements, under repeated rolling contact. From the service point of view, the mixed mode fracture failure of rails is one of the main mechanism of cracking. As an example, it can be demonstrated in Fig. 1.

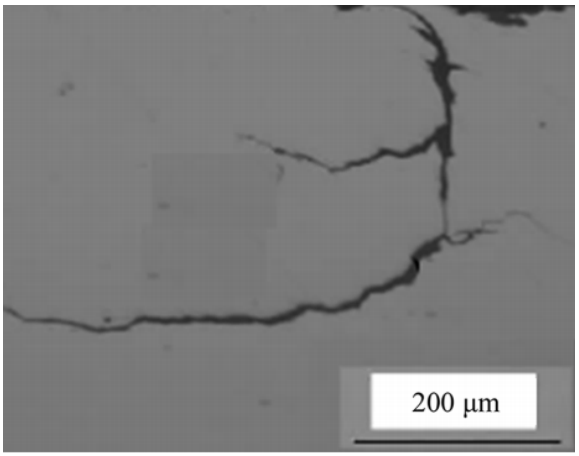

Fig.1. Experimental crack path in Datong– Qinhuangdao line rail [1].

For fatigue crack growth predictions, FEM methodology has been involved based on experimental observations of fatigue crack growth behaviour under mixed mode conditions. For fatigue fracture tests, the CTS (Compact Tension Shear) specimens were involved (Fig. 2a) using additional fixture for uniaxial testing machine (Fig. 2b). In order to obtain the kinetic fatigue fracture diagrams in terms of mixed-mode loading conditions, the experimental measurements were arranged in accordance to the Richard conception [2]. For comparison of the tested results the typical fatigue crack growth rate for pure mode I was performed in accordance with the ASTM E647 [3] using the CT specimen (W=50, t=8mm) and ΔK decreasing test (f=10Hz, R=0.1). The crack length was monitored using optical and compliance method (pure mode I). For the mixed-mode loading conditions CTS were involved. Due to the material limitations, the main dimensions were equal: W=42 mm, t=8mm. The initial notch with pre-crack (mode I condition) satisfied the CTS – Richard [2] suggestions for the normalized crack length: a/W=0.52÷0.55. The tests were performed for different elastic mixity parameter range:

$$M_e = \frac{2}{\pi} a \tan\left(\frac{K_I}{K_{II}}\right). \quad (1)$$

The value of the dimensionless parameter M_e=0 corresponds to pure shear state (mode II) and the value M_e=1 means that the specimen is loaded under pure mode I

a)

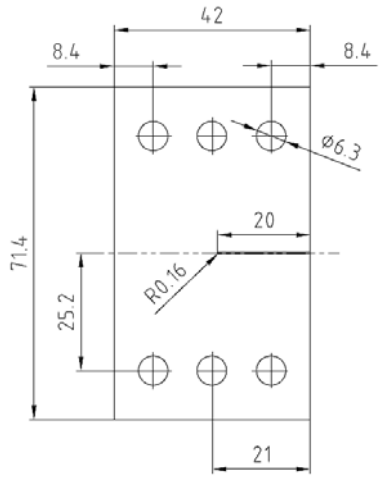

b)

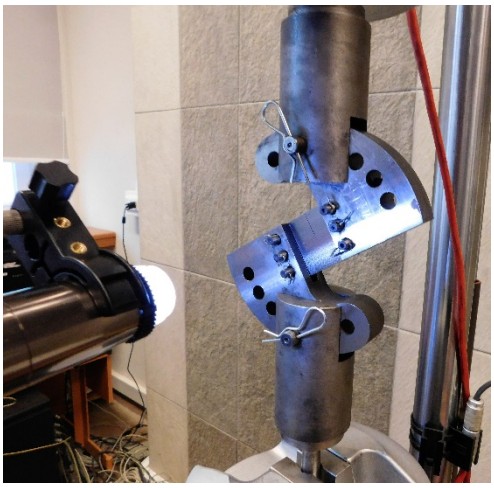

Fig. 2. Mixed mode fatigue load test a) CTS specimen and dimensions, b) general view on the measurement stand under mixed mode load configuration

The obtained experimental results of fatigue crack growth under mixed mode condition I+II indicate that the fatigue lifetime increase with the decreasing value of elastic mixity parameter Me. The existing criteria (MTS, SED, MERR) predict correctly the initial fatigue crack bifurcation angle for mode condition I+II. The fatigue crack growth process under mixed mode condition I+II can be described by new proposed equivalent stress intensity factor ΔK_{eq}.

REFERENCES

[1] Guo, H.M., Wang, W.J., Liu, T.F. et al: Analysis of damage behavior of heavy-haul railway rails. China Mech Eng 25(2):269–270 (2014) (in Chinese).
[2] Richard, H.A.: Bruchvorhersagen bei überlagerter normal- und Schub Beanspruchung von Rissen. VDI Forschungsheft 631, 1-60 (1985) (in German).
[3] ASTME647-15a, Standard test methods for fatigue crack growth rate, ASTM International.

ACKNOWLEDGEMENTS

Numerical calculations were carried out using resources provided by Wroclaw Centre for Networking and Supercomputing (http://wcss.pl), Grant No. 447.

The publication has been prepared as a part of the Support Programme of the Partnership between Higher Education and Science and Business Activity Sector financed by City of Wroclaw.

Stress Concentration Factor Predictions for Offshore Tubular KT-Joints Based on Parametric Equations and Simplified Numerical Analysis

Shaghayegh Yaghoubi[a,b], António Mourão[b]*, José A.F.O. Correia[b], Paulo Mendes[b], José Miguel Castro[b], Abílio M.P. de Jesus[b], Rui Calçada[b]

[a] *Maritime Department, Amirkabir University of Technology, Tehran, Iran*
[b] *Faculty of Engineering, University of Porto, Portugal*
**Corresponding author: up201306134@fe.up.pt*

Keywords: Stress concentration factor; Tubular KT-joints; Finite element analysis; SCF parametric equations.

ABSTRACT

Taken as a promising basis to achieve the EU energy goals for 2020 and 2050 in regard to sustainable energy sources, offshore wind farms allow for an increased electric production due to the higher wind speeds and an "unrestrained" amount of available space [1].

However, offshore wind farms present a disadvantage when compared with onshore wind turbine structures since they are constantly subjected to other environmental loads besides wind, leading to increased fatigue damage accumulation around welded joints [1].

When dealing with tubular joints offshore standards, the DNVGL code offer a fatigue analysis based on hot-spot stresses, for this reason the stress concentration factors (SCF) become of extreme relevance.

Several approaches for determining SCF are proposed in literature where parametric equations from several authors using geometrical parameters and depending on the type of loading are used with aims to calculate SCF around the weld fillet. Another possibility can be made using a finite element analysis (FEA) where the stress concentration factor can be obtained as a relation between hot-spot stresses and nominal stresses, the first can be achieved either by linear or quadratic extrapolation.

In this paper, a comparison between a FEA model and parametric equations proposed by Efthymiou according to DNVGL standard [2], and Lloyd's register [3] for calculating the SCF, is proposed. For this analysis a KT-type joint of an operating jacket-type offshore platform is considered (see Fig. 1).

In the definition of the finite element model, it was used the program ANSYS R19.0® to simulate the conditions and boundaries around the tubular joint and in the tubular joint itself. The choice of elements type for the analysis depends on the geometry of the joint and the purpose for which the results of the analysis will be used. The 3D numerical model was built using solid finite elements and a linear-elastic stresses analysis was used. The mechanical properties used in the numerical analysis of the KT-joint under consideration are the following: density equal to 7.850E-6 kg/mm^3; modulus of elasticity equal to 210000 N/mm^2; and shear modulus equal to 80770 N/mm^2. The S420 steel was used in the offshore structure. The loads to be considered in the FE analysis of the KT-joint under consideration can be seen in ref. [4].

A comparison and discussion of the stress concentration factors results between the Lloyd's register KT joint equations, DNVGL parametric equations and FE analysis are presented (Table 1). For the axial

loading case between the FE model-DNV and between the FE model-Lloyd, the SCF chord in brace A is way more conservative for the finite element model but for the other brace locations where the SCF is located, the SCF is conservative for the analytical solutions. SCF saddle for brace B calculated using FE analysis is way too conservative and is unrealistic. It can be verified that the values of SCF in general from the analytical parametric equations are more conservative when compared with finite element analysis. However, the finite element analysis leads to better results for the values of stress concentration factor for chord-brace A, chord-brace C, and for Chord in axial force, in-plane bending and out-of-plane loading cases, respectively. The parameters that have caused influence in evaluation of SCF beside the non-dimensional geometric parameters in finite element study are: boundary condition at brace and chord ends with their respective length; type of mesh element; and, the mesh refinement around the intersection of the braces and the chord.

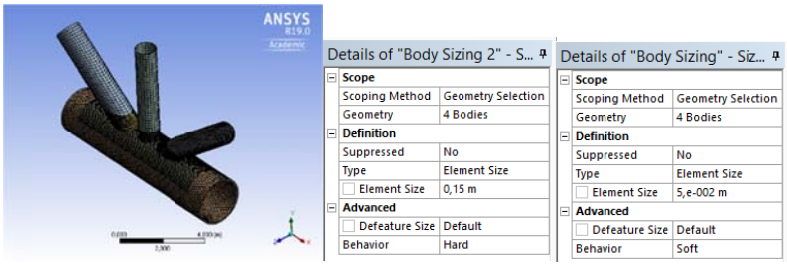

Fig. 1. Solid FE model with the designed meshing refinement.

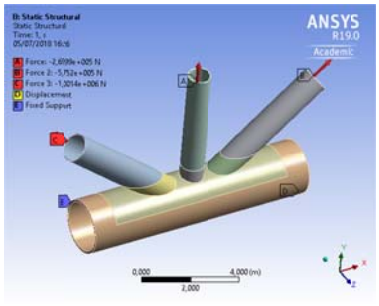

Fig. 2. Solid model with the representation of the axial forces.

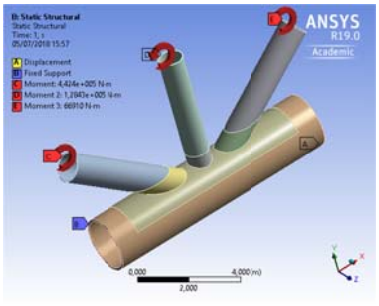

Fig. 3. Solid model with the representation of the in-plane bending moment.

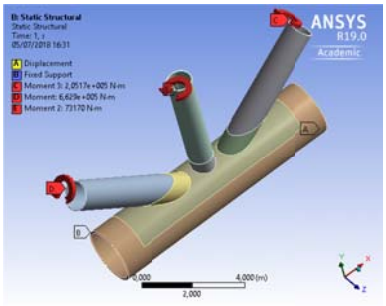

Fig. 4. Solid model with the representation of the out-of-plane bending moments.

Table 1. Stress concentration factors for axial loading from the Lloyd and DNVGL parametric equations and FE analysis.

Comparision	**SCF AS/AC**				
	DNV	**Lloyd**		**FEA**	
Chord		**Crown**	**Saddle**		
A (5110)	1.601	1.773	1.733	3.624	
B (5116)	2.949	1.598	0.935	0.341	
C (5112)	1.369	1.117	1.047	0.444	
Brace	**DNV**	**Crown**	**Saddle**	**Crown**	**Saddle**
A (5110)	1.823	1.861	1.596	1.171	1.649
B (5116)	3.409	1.480	0.217	1.688	8.863
C (5112)	1.786	1.861	1.250	0.970	1.488

REFERENCES

[1] Charkrabarti, S.K.: Handbook of Offshore Engineering - Volume I, Elsevier, USA (2005).
[2] DNV GL Group. DNVGL-RP-0005:2014-06: Fatigue design of offshore steel structures (2014).
[3] UK Health and Safety Executive: Stress concentration factors for simple tubular joints- assessment of existing and development of new parametric formulae, OTH 354, Lloyd's Register of Shipping, London, UK (1997).
[4] Mendes, P.: Stress concentration factor evaluation in offshore tubular KT joints for fatigue design. MSc Thesis, Civil Engineering, Faculty of Engineering, University of Porto, Porto, Portugal (2018).

Effect of the Stress Ratio on the Prediction of Fatigue Crack Growth in 42CrMo4 Steel

M. Escalero[a*], S. Blasón[b], H. Zabala[a], M. Muñiz-Calvente[b]

[a] *Structural Reliability Department, Mechanics Area, IK4-Ikerlan Research Center. Jose M. Arizmendiarreta Ibilbidea, 2, 20500 Arrasate-Mondragón, Spain.*
[b] *Department of Construction and Manufacturing Engineering, University of Oviedo. C\ Pedro Puig Adam, s/n, 33204 Gijón, Spain.*
**Corresponding author: mescalero@ikerlan.es*

Keywords: Fatigue crack growth; Stress ratio effect; 42CrMo4; Walker; NASGRO.

ABSTRACT

One of the predominant failure mechanisms of pitch bearings for blades of wind turbines is the in-service cracking of the outer ring (Fig. 1a) [1]. This ring, usually made of 42CrMo4 steel, is subjected to wind and inertial loads transmitted through the rolling elements and to the tightening preload exerted by the bolts. In fact, [2] states that, during the operation of the wind turbine, a defect may initiate at the edge of one of the holes drilled for mounting the bolts. First of all, this defect grows as a surface crack and afterwards it evolves to a through-crack, in a section subjected to variable amplitude mode-I stresses in the hoop direction [2]. A rainflow analysis of the critical stresses in a real practical example showed that the stress ratio (R) ranges from 0.1 to 0.6 in the load spectrum.

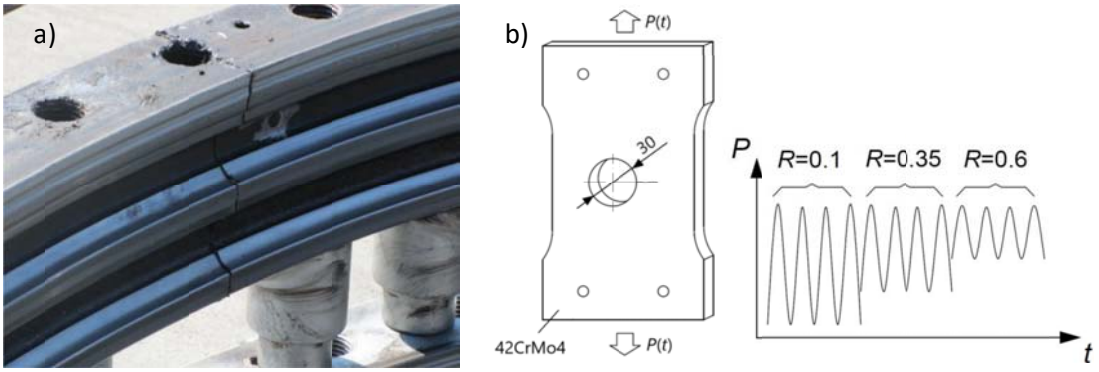

Fig. 1. a) Real bearing ring broken during operation. Courtesy of RBB Engineering [1]; b) schematic representation of the structural detail and the loads studied in this work.

For the sake of simplicity, in this work the growth of a hole-edge through-crack was studied in the structural detail depicted in Figure 1b. It shares certain characteristics with the real application, such as, material, 42CrMo4, and loading mode, mode-I. The applied force is cyclic, oscillating sinusoidally with ratios of 0.1, 0.35 and 0.6. Assuming linear elastic behavior at the crack tip, crack growth rate may be described as a function of stress intensity factor range, using one of the many crack growth laws available in the literature that relate both variables considering the well-known stress ratio effect [3]. It follows that when performing crack growth predictions neither the choice of the crack growth law nor the determination of the fitting coefficients is trivial.

In this study, three different tasks were carried out. In first place, crack growth curves were characterized according to ASTM E647 at the aforementioned three stress ratios, using standardized

Compact Tension specimens. Walker and NASGRO equations were fitted to the experimental fatigue crack growth rate (FCGR) data and the fitting coefficients were determined using different datasets. Secondly, crack growth was predicted in the presented structural detail (Fig. 1b), according to a methodology based on BS 7910:2013, resorting to previously mentioned crack growth laws and different fitted coefficients. Last but not least, 88 mm-wide and 6 mm-thick plates with a 30 mm diameter hole were tested under a maximum force of 50 kN and different stress ratios (namely; 0.1, 0.35 and 0.6). That maximum force was chosen so that the maximum stress at the net section did not exceed 40% of the yield strength.

Results (Fig. 2) show that ΔK-based crack growth laws are appropriate for describing FCGR in 42CrMo4 steel, without resorting to energy methods, at least below the stress levels applied here. Walker equation proved to be more accurate than NASGRO for describing FCGR at stress ratios between 0.1 and 0.6 in Region II. Regarding Walker equation, the number of cycles at predicted critical crack length was estimated with errors lower than 5% by characterizing crack growth curves at extreme values of R (0.1 and 0.6) and using those datasets to determine fitting coefficients at any stress ratio. For that law, it was not worth characterizing FCGR at intermediate Rs, not even to predict crack growth at those stress ratios. Regarding NASGRO equation, determining crack growth coefficients at R=0.1 and using them at other stress ratios resulted in unacceptable estimations of crack growth, with errors up to 40%, approximately. Also with this law, it was not worth characterizing FCGR at intermediate Rs, because using coefficients derived at extreme Rs yielded very similar results (differences in error below 7%).

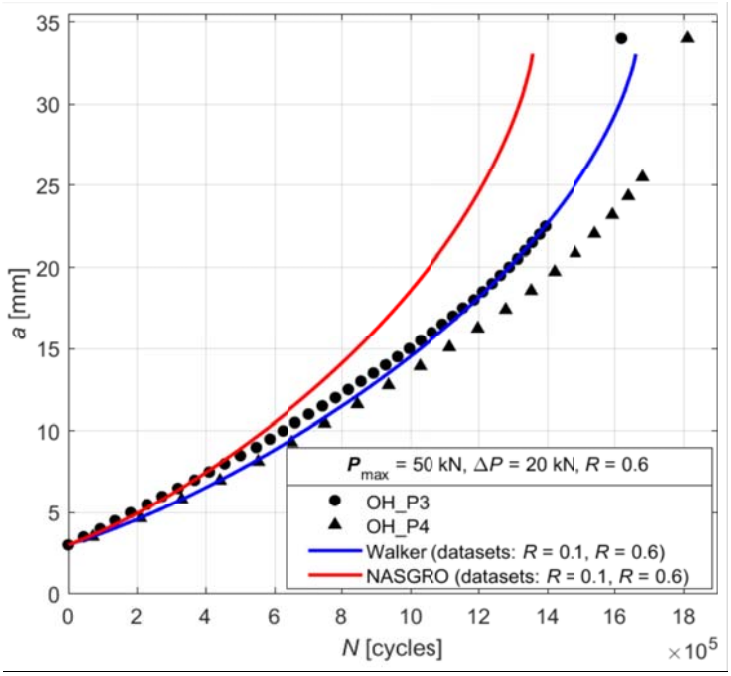

Fig. 2. Experimental and predicted crack growth at R=0.6. The coefficients of both Walker and NASGRO were determined using crack growth curves at extreme values of R (namely 0.1 and 0.6).

REFERENCES

[1] Budny, R.: Improving pitch bearing reliability. Available: http://www.rbbengineering.com/wp-content/uploads/2016/03/RBB-Pitch-Bearing-Reliability-Presentation.pdf. [Accessed: 05-Jan-2017] (2016).

[2] Escalero, M. et al.: Study of alternatives and experimental validation for predictions of hole-edge fatigue crack growth in 42CrMo4 steel. Eng. Struct. Under Rev. (2018).

[3] Blasón, S., et al.: Proposal of a fatigue crack propagation model taking into account crack closure effects using a modified CCS crack growth model. Procedia Struct. Integr. 1, 110–117 (2016).

Fatigue Fracture Process of Puddle Iron

G. Lesiuk[a*], J.A.F.O. Correia[b], G. Pękalski[a], M.Duda[a], A.M.P. De Jesus[b], J. Rabiega[c], R. Calcada[b]

[a]*Department of Mechanics, Material Science and Engineering, Faculty of Mechanical Engineering, Wrocław University of Science and Technology, Smoluchowskiego 25, 50-370 Wrocław, Poland*
[b]*INEGI/Faculty of Engineering, University of Porto, Rua Dr. Roberto Frias, 4200-465 Porto, Portugal*
[c]*Department of Bridges and Railways, Faculty of Civil Engineering, Wrocław University of Science and Technology, Smoluchowskiego 25, 50-370 Wrocław, Poland*
**Corresponding author: Grzegorz.Lesiuk@pwr.edu.pl*

Keywords: Fatigue fracture; Mixed mode loading; Puddle iron; Crack closure; Crack paths; SIF calculation.

ABSTRACT

The structural components from structures such as bridge members are subjected to a long operating period of time. The problem of fatigue cracks is more interesting in existing bridge structures with existing cracks. In case of the structures erected at the turn of the 19th and 20th century, the cracks are natural elements of the old steel metallic structures. The uniaxial fatigue crack growth description relation led us often to significant errors in predicting of a residual lifetime. As a good example, it can be a residual lifetime of the riveted joints in such a type of structures. On the other hand, the 19th century structures were erected from the puddled iron or low carbon mild rimmed steel. The obtained results from several ancient railway metallic bridges (from Poland and Portugal) have shown the presence of microstructural degradation processes in puddled iron. The kinetic fatigue fracture diagrams (KFFD) have been obtained for post-operated steel. The problem of crack closure has been involved in fatigue crack growth process during the experiments and its understanding is fundamental for the analysis of stress ratio *R* effects on KFFD. An experimental and numerical approach has been involved for the evaluation of the crack closure/opening forces based on the hysteresis loop deformation. The implemented algorithm in the numerical environment gives promising results in description of the kinetics of fatigue crack growth of the old metallic materials with consideration of crack closure effect. In this paper some examples of degenerated microstructures have been presented. In order to fill a lack in experimental data in the literature, the results of a mixed-mode (I+II) fatigue crack growth have been presented and discussed on the background of existing fracture mechanics models. All the results have been implemented to the Abaqus environment.

For mixed mode fatigue fracture test the CTS (Compact Tension Shear) specimens were involved (Fig. 1a) using additional fixture for uniaxial testing machine (Fig. 1b).

a) b)

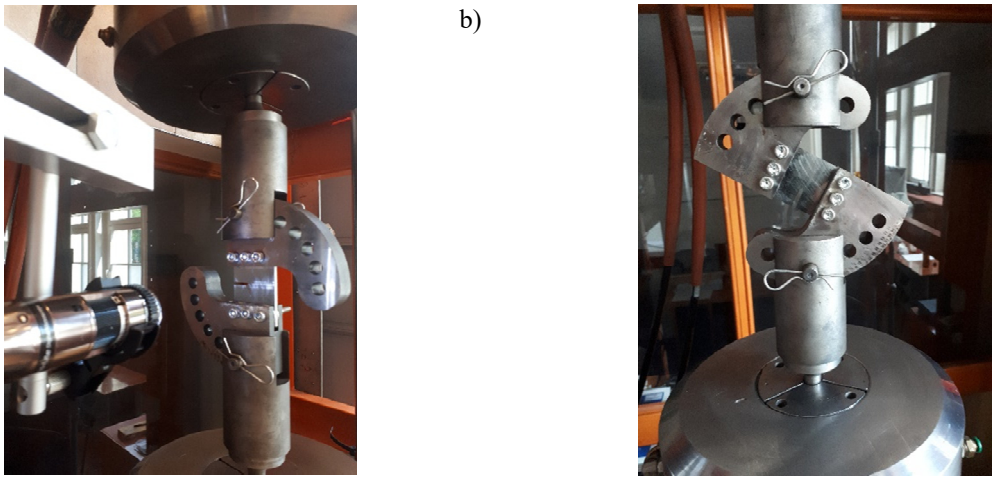

Fig. 1. Mixed mode load test a) CTS specimen tested in mode I, b) CTS specimen tested in mixed mode state (I+II)

The initial stress intensity factors were calculated using For CTS specimen the closed form solutions of SIFs presented by Richard [1]:

$$K_I = \frac{F\sqrt{\pi a}\cos\theta}{Wt(1-a/W)}\sqrt{\frac{0.26+2.65(a/W-a)}{1+0.55(a/W-a)-0.08(a/W-a)^2}}, \tag{1}$$

$$K_{II} = \frac{F\sqrt{\pi a}\sin\theta}{Wt(1-a/W)}\sqrt{\frac{-0.23+1.4(a/W-a)}{1-0.67(a/W-a)+2.08(a/W-a)^2}}. \tag{2}$$

Where: F – applied force, a – crack length, W – specimen width, Θ – load angle.

Based on fracture surface analysis for specimen tested under mixed mode conditions, a noticeable is typical fracture surface shaped by numbers of nonmetallic inclusions with large areas of fracture caused by initial sliding mode of fatigue crack growth (noticeable is influence of the K_{II} in the initial fatigue crack path). As the crack growth, the sliding mode is decreased, where the typical fatigue fracture area is presented. Fracture surface is similar to the mode I crack propagation type due to increasing K_I/K_{II} with growing crack.

REFERENCES

[1] Richard, H.A.: Bruchvorhersagen bei Überlagerter Normal und Schubbeanspruchung von Rissen, VDI Forschungsheft 631, 1-60 (1985).

ACKNOWLEDGMENTS

The experimental works have been supported by the Wroclaw University of Science and Technology – project no 401/0029/17.

Influence of Microstructural Inhomogeneities on the Fatigue Crack Growth Behavior Under Very Low Amplitudes for Two Different Aluminum Alloys

T. Kirsten[a], M. Kuczyk[b]*, M. Wicke[c], A. Brückner-Foit[c], F. Bülbül[d], H.-J. Christ[d], M. Zimmermann[a]

[a] *Institute for Materials Science, Technical University of Dresden, Germany*
[b] *Fraunhofer Institute for Material and Beam Technology, Dresden, Germany*
[c] *Institute for Materials Engineering, University of Kassel, Germany*
[d] *Institute for Materials Engineering, University of Siegen, Germany*
**Corresponding author: martin.kuczyk@iws.fraunhofer.de*

Keywords: Ultrasonic fatigue testing; Very high cycle fatigue; Long crack growth behaviour; EBSD; Microstructural barriers.

ABSTRACT

The fatigue behaviour of metallic materials at very high cycles ($N > 10^7$) is subject of a great variety of scientific papers. However, fatigue crack growth in the VHCF regime is far less intensively investigated. Previous studies showed that fatigue cracks can grow even at amplitudes well below the classical fatigue limit. Aim of the present study is to analyse the fatigue crack growth at very low amplitudes near the threshold regime and to gain insight into the barrier function of microstructural inhomogeneities such as grain boundaries and precipitates.

Two different aluminium alloys in different heat treatment conditions were investigated: the precipitation hardening alloy EN AW 6082 in peak-aged (pa) and overaged (oa) condition and the work hardening alloy EN AW 5083 in soft annealed condition.

Tests were performed at an ultrasonic fatigue testing system with a resonance frequency of about 20 kHz and a load ratio of R = -1. In order to investigate the crack growth behaviour in the threshold regime, the thresholds were determined by means of the load-shedding method for all three material conditions. The results, averaged out of three measurements each, are shown in Table 1.

Table 1. Fatigue crack growth threshold values ΔK for the aluminium alloys EN AW 6082 and EN AW 5083.

EN AW 6082 pa	EN AW 6082 oa	EN AW 5083
1.46 MPa√m	1.35 MPa√m	1.57 MPa√m

Subsequently, tests were performed under constant stress intensity factors ΔK. The load amplitude was continuously adapted after optical measurements of the crack length throughout the entire test. Due to the changes of the crack growth rate over the crack length (Fig. 1), the crack growth behaviour is influenced by the microstructure. Crack growth retardation is mainly caused by primary precipitates, which can be found in both alloys. Especially the fine distributed ferritic precipitates are causing the crack to decelerate. Grain boundaries can affect the behaviour as well, but for the alloy EN AW 6082 the effect is less pronounced due to the bigger grain size of 2000 µm in rolling direction and 50-100 µm perpendicular to it. This might be as well the reason for the smaller average crack growth rate for the alloy EN AW 5083.

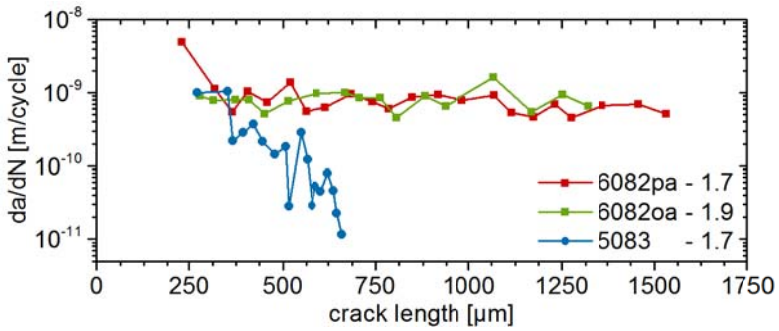

Fig. 1. Fatigue crack growth behaviour under constant ΔK values for the three investigated material conditions.

Electron backscatter diffraction (EBSD) images were taken in order to investigate the effect of grain boundaries on the crack growth. By determining the slip systems with the highest Schmid factor and comparing their orientation in the grain with the crack path, the crack propagation mode can be defined. Independent of the alloy and material condition, the predominant crack propagation is mode I, as it is known for the behaviour of long cracks. In case of the alloy EN AW 5083 there are also some regions were the crack propagates in a shear controlled mode, as can be seen in Fig. 2. Due to the smaller average grain size the influence of grain boundaries becomes bigger. Some regions of shear controlled crack propagation could be found for alloy EN AW 6082 as well, but rarely and limited to only a few grains.

Furthermore the EBSD analysis is used to gain insight into the formation of the plastic zone in front of the crack tip. Recent results from flat samples have already shown that the plastic zone is very small compared to the microstructural features (grain size, precipitates). In case of shear dominated crack growth there is only one plastically influenced region in front of the crack tip. [1]

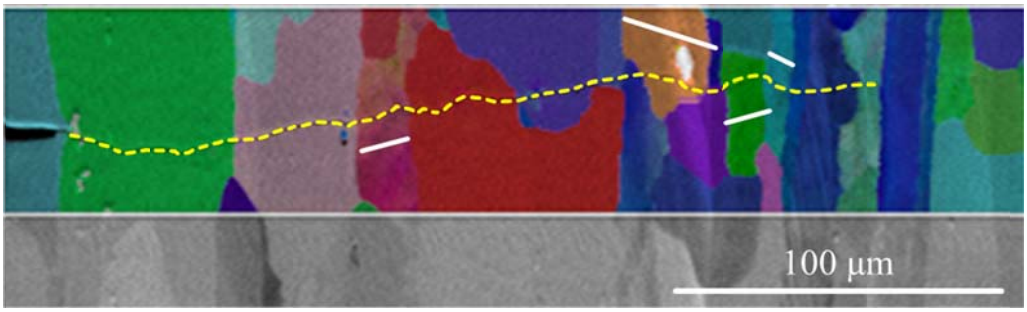

Fig. 2. EBSD analysis of aluminium alloy EN AW 5083, under constant ΔK value (1.7 MPa√m). Regions of shear controlled crack growth indicated by white lines.

REFERENCES

[1] Stein, T., Wicke, M., Brückner-Foit, A., Kirsten, T., Zimmermann, M., Bülbül, F., Christ, H.-J..: Crack growth behavior in an aluminum alloy under very low stress amplitudes. Journal of Materials Research 23(32), 1–8 (2017).

Towards Quantitative Explanation of Effective Thresholds of Mode III Fatigue Crack Propagation in Metals

T. Vojtek[a,b*], S. Žák[a], J. Pokluda[a,c]

[a]*Central European Institute of Technology (CEITEC), Brno University of Technology, Technická 10, 616 00 Brno, Czech Republic*
[b]*CEITEC IPM, Institute of Physics of Materials, Academy of Sciences of the Czech Republic, Žižkova 22, 616 62 Brno, Czech Republic*
[c]*Faculty of Mechanical Engineering, Brno University of Technology, Technická 2, 616 69 Brno, Czech Republic*
**Corresponding author: tomas.vojtek@ceitec.vutbr.cz*

Keywords: Effective threshold; Mode III; Local growth mode; Tortuous crack front; Metals.

ABSTRACT

This work is focused on quantitative interpretation of the mode III effective thresholds measured for long fatigue crack propagation in various metallic materials. Although fatigue cracks have been investigated by many researches since several decades, there are still many open questions. For instance, fatigue crack growth threshold value and the related mechanism of resistance to crack propagation are still not explained in a satisfactory way [1, 2].

Resistance to fatigue crack propagation should be divided into the intrinsic and the extrinsic component [3]. Intrinsic (effective) threshold for mode I was shown to be a very useful parameter, since it depends only on the Young's modulus and magnitude of the Burgers' vector of the metal [4, 5]. It does not depend on microstructural factors such as hardening or grain size. This makes it a universal and predictable parameter for most metallic materials. On the other hand, the extrinsic component (crack tip shielding), mostly represented by crack closure, is not so well predictable and the experimental values vary for different microstructures, the stress ratio and other conditions, especially in the near-threshold region.

Under shear-mode loading the extrinsic component is even more significant and less predictable than under mode I loading due to friction between fracture surfaces [6]. Therefore, once the effective threshold is known, the extrinsic component can be determined quantitatively by simple subtraction, which allows it to be studied separately. Measurement of effective thresholds using high stress ratio $R > 0.7$ is not possible to use for mode II and mode III loading (the crack does not open). Therefore, the effective thresholds were measured for various metallic materials using a special method with open precracks generated by cyclic compressive loading [7]. Relationships taking into account shear modulus and magnitude of the Burgers' vector were proposed for prediction of the mode II effective thresholds. The relationships are based on the dominancy of mode I or mode II local growth mechanism and take into account a characteristic crack deflection angle. Typical values of this angle for various types of metallic materials were introduced. The resulting threshold values correlated well with those obtained experimentally [8].

The crack growth mechanism based on cyclic motion of dislocations works similarly for mode I and mode II cracks. In the case of the remote mode III cracks, however, no straightforward local mode III growth mechanism exists [9]. It was suggested that the macroscopic mode III crack propagation is realized by microscopic local mode II advances of the crack, starting at the asperities of the crack front.

Local mode II stress intensity factors were determined for such a serrated crack front loaded by remote mode III. The results showed that the ratio of experimentally obtained mode II and mode III effective thresholds could be fully explained by the local mode II stress intensity factors at the serrated crack front, taking into account the average in-plane asperity angles measured on fracture surfaces. It

indicates that the remote mode III crack propagation is controlled by the local mode II component, for which the threshold can be predicted. Since the ratio of experimentally obtained mode II and mode III effective thresholds was nearly equal for all tested metallic materials, a relationship for prediction of the effective threshold can be formulated also for mode III.

REFERENCES

[1] Chowdhury, P., Sehitoglu, H.: Mechanisms of fatigue crack growth – a critical digest of theoretical developments. Fatigue Fract. Engng. Mater. Struct., 1–23 (2016).

[2] Zerbst, U., Vormwald, M., Pippan, R., Gänser, H.-P., Sarrazin-Baudoux, C., Madia, M.: About the fatigue crack propagation threshold of metals as a design criterion – A review. Eng. Fract. Mech. 153, 190–243 (2016).

[3] Ritchie, R.O.: Mechanisms of fatigue crack propagation in metals, ceramics and composites: Role of crack tip shielding. Materials Science and Engineering: A103, 15-28 (1988).

[4] Hertzberg, R.W.: On the calculation of closure-free fatigue-crack propagation data in monolithic metal-alloys. Mater. Sci. Eng. A190, 25-32 (1995).

[5] Liaw, P.K., Lea, T.R., Logsdon, W.A.: Near-threshold fatigue crack growth behavior in metals. Acta Metallurgica 31, 1581–1587 (1983).

[6] Tschegg, E. K., Stanzl, S. E.: The significance of sliding mode crack closure on mode III fatigue crack growth. Basic questions in fatigue, ASTM STP 924. vol. 1, pp. 214–232. ASTM, West Conshohocken (1988).

[7] Vojtek, T., Pokluda, J., Hohenwarter, A., Pippan, R.: Progress in Understanding of Intrinsic Resistance to Shear-mode Fatigue Crack Growth in Metallic Materials. Int J Fatigue 89, 36–42 (2016).

[8] Vojtek, T., Pippan, R., Hohenwarter, A., Pokluda, J.: Prediction of effective mode II fatigue crack growth threshold for metallic materials. Eng Fract Mech 174, 117–126 (2017).

[9] Vojtek, T., Hohenwarter, A., Pippan, R., Pokluda, J.: Experimental Evidence of a Common Local Mode II Growth Mechanism of Fatigue Cracks Loaded in Modes II, III and II+III in Niobium and Titanium. Int J Fatigue 92, 470–477 (2016).

ACKNOWLEDGMENTS

This work was financially supported by the Czech Science Foundation (GA CR) in the frame of the Project No. 17-15716Y and by the Ministry of Education, Youth and Sports of the Czech Republic under the project CEITEC 2020 (LQ1601).

Development of Methods for Early Damage Assessment

A. Kotousov[a*], J. Vidler[a], J. Hughes[a], C.T. Ng[a]

[a] School of Mechanical Engineering, *The University of Adelaide, Australia*
**Corresponding author: Andrei.kotousov@adelaide.edu.au*

Keywords: Early damage; Third-order elastic constants; Rayleigh waves; Fatigue.

ABSTRACT

Over the past two decades an introduction of advanced manufacturing techniques and better defect control have resulted into a substantial improvement of the quality of structural materials as well as to a significant prolongation of the early stages of damage. The early stages of damage might not associated with micro-defects, and can be governed by different microscopic mechanisms. For example, in fatigue cross slip of screw dislocations, mutual annihilation of dislocations, random glide of dislocations or slip asymmetry lead to the accumulation of irreversible plastic strain during cycling. This plastic strain largely controls the crack initiation stage and the overall lifetime of the structure, specifically, in the high-cycle fatigue regime.

Previous research has demonstrated that the third-order elastic constants (or so-called Murnaghan constants [1]), which in undamaged material are normally associated with the anharmonicity of lattice, are sensitive to the localised micro-plasticity and microscopic changes within the grain structure. Therefore, the progressive measurement of these constants can be utilised for the assessment of the early stages of damage [2]. This concept was recently tested and demonstrated for metals, concrete and composites subjected to fatigue, creep and radiation damage [3].

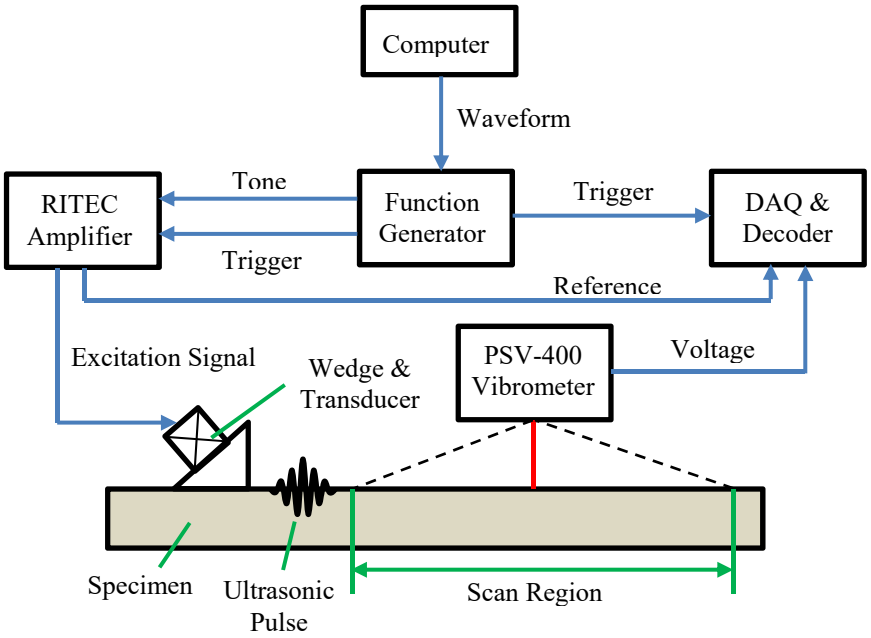

Fig. 1. Experimental schematic.

The third-order constants cannot be obtained from common stress-strain diagrams and need an application of more sophisticated experimental techniques. There are currently two techniques, which both utilise high-frequency ultrasonic waves for the evaluation of the third-order elastic constants. The first technique is based on the acoustoelastic effect, and it is based on the measurement of the change of the phase or group velocities under different levels of the applied stresses. The second technique requires the excitation of a strong ultrasonic pulse of bulk, Rayleigh or Lamb waves, which is capable to produce a noticeable non-linear response, e.g. the generation of the second-order harmonic wave. The experimental rig, which was utilised in the current work, for excitation and sensing of ultrasonic pulses is shown in Fig.1 [4].

The presentation briefly describes the progress towards the development of experimental methods for early damage assessment. It also describes the development of the new damage theory, which apart from the classical damage mechanics, is focusing on early damage.

REFERENCES

[1] Murnaghan, F.D.: Finite Deformations of an Elastic Solid. American J. Mathematics 52, 235-260 (1937)
[2] Mohabuth M., Kotousov A., Ng C.T.: Effect of uniaxial stress on the propagation of higher-order Lamb wave modes. Int. J. Nonlinear Mech. 86, 104-111 (2016).
[3] Matlack K.H., Kim, J.-Y., Jacobs L. J., Qu J.: Review of Second Harmonic Generation Measurement Techniques for Material State Determination in Metals. J. Nondestruct. Eval. 34, Article 273 (2015)
[4] Hughes, J.M., Howie, J., Vidler, J, Mohabuthy, M.: Non-contact measurement of nonlinear Rayleigh waves using the scanning laser vibrometer. ACAM9 Conference proceedings, 358-363 (2017).

Probabilistic Fatigue & Fracture Approaches Applied to Materials and Structures

B-PFFA-ICMFM

Organized by:

Alfonso Férnandez-Canteli, Spain

Antonio Martín-Meizoso, Spain

Abílio M. P. de Jesus, Portugal

José A. F. O. Correia, Portugal

Filippo Berto, Norway

Miguel Calvente, Spain

Shun-Peng Zhu, China

Dianyin Hu, China

Probability Distribution Type for the Accumulated Damage from Miner's Rule in Fatigue Design

J. Hoole[a*], P. Sartor[a], J.D. Booker[b], J.E. Cooper[a], X.V. Gogouvitis[c], R.K. Schmidt[d]

[a] *Department of Aerospace Engineering, University of Bristol, United Kingdom*
[b] *Department of Mechanical Engineering, University of Bristol, United Kingdom*
[c] *Safran Landing Systems, Gloucester, United Kingdom*
[d] *Safran Landing Systems, Ajax, Canada*
**Corresponding author: jh12317@bristol.ac.uk*

Keywords: Fatigue analysis; Monte Carlo Simulation; Skewed distribution; Accumulated damage; Miner's rule.

ABSTRACT

Within the sphere of fatigue design, many metallic components are designed against fatigue failure using 'traditional' analysis approaches based upon stress-life (S-N) curves and Miner's rule. This approach is known as the safe-life fatigue analysis process and is currently used for safety-critical aerospace structural components [1], along with components from many other industrial sectors. The component 'safe-life' represents the number of duty cycles after which the component must be removed from service. However, the safe-life fatigue analysis process contains many sources of variability due to the statistical nature of fatigue parameters and the assumptions made within the analysis process. To ensure that components retain their structural integrity in-service, conservatism in the form of safety factors is used to account for this variability. Conservatism can result in components being 'over-sized', increasing component weight and life cycle cost, thereby compromising the performance of the overall structure. Conservatism can also lead to the potential component life not being fully exploited due to earlier retirement from service. Research being conducted by the authors aims to develop a novel probabilistic approach that computes the probability of fatigue failure associated with a component safe-life. This probability of failure could be used to challenge the conservatism required within the safe-life fatigue analysis process, potentially leading to more efficient components with longer predicted safe-life values, which are still safe and reliable in-service.

A probabilistic approach, as opposed to a deterministic one, characterises the variability in the inputs to the safe-life fatigue analysis process (e.g. S-N data sets, loading, etc.) using probability distributions [2]. Probabilistic methods such as Monte Carlo Simulations could be used to propagate the variability through the safe-life fatigue analysis process to produce a probability distribution of the process output, which can either be the component safe-life or the accumulated fatigue damage calculated using Miner's rule. The output probability distribution is then used to compute the probability of fatigue failure for the component. Previous work regarding the development of a probabilistic approach for safe-life fatigue analysis has focused on characterising the distribution of the component safe-life and directly computing the probability of failure, without characterising the distribution of the accumulated fatigue damage from Miner's rule [2, 3]. The limited literature that has characterised the probability distribution of the accumulated damage has only considered the variability present within the S-N data used to generate S-N curves [4, 5].

In this paper, the probability distribution type that best characterises the variability in the

damage, when accounting for the variability within S-N data, loading and component geometry, will be identified. As the accuracy of the probability of failure value from the probabilistic approach is dependent on the accuracy of the accumulated fatigue damage distribution, it is crucial that the most accurate probability distribution type is selected. In order to generate and characterise the probability distribution of the accumulated fatigue damage from Miner's rule, a Monte Carlo Simulation will be applied to a safe-life fatigue analysis case study that employs a stress-life approach. S-N data from the Engineering Sciences Data Unit (ESDU) [6] will be used to represent the typical variability present in S-N data sets. Initial studies conducted by the authors have shown that even for a simple case study, the distribution of accumulated fatigue damage and Log_{10} values of accumulated fatigue damage cannot be accurately characterised using the Normal, Log-Normal and Weibull distributions that are commonly used when performing probabilistic fatigue analysis, as shown in **Fig. 1**. As a result, more complex and 'skewed' probability distribution types, such as: skew-Normal, 3-parameter Log-Normal and 3-parameter Weibull may need to be considered. Commonly used distribution types also demonstrate non-realistic threshold values, which represent the limits of the distribution. For example, a Normal distribution permits negative values, which would not provide a realistic representation of the accumulated fatigue damage values. Therefore, the selection and fitting of the more complex and skewed distribution types to the accumulated fatigue damage from Miner's rule will be presented within this paper.

Fig. 1. The 'skewed' probability distribution histogram shape of Log_{10} values of accumulated fatigue damage from a

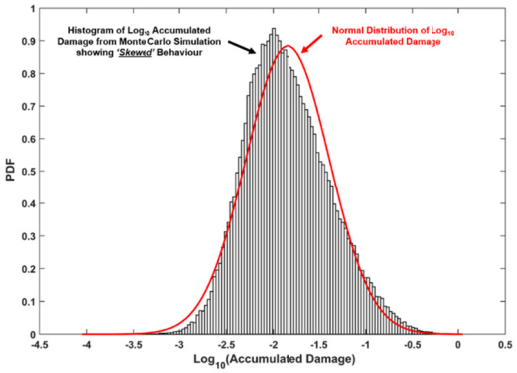

Monte Carlo Simulation of a simple initial case study that accounted for variability within the S-N data, loading and component geometry. A Normal distribution of the Log_{10} accumulated fatigue damage is shown for comparison.

REFERENCES

[1] Braga, D. F. O, et al.: Advanced design for lightweight structures: Review and prospects, Progress in Aerospace Sciences 69, 29-39 (2014).

[2] Ocampo, J, et al.: Development of a Probabilistic Linear Damage Methodology for Small Aircraft, Journal of Aircraft 48(6), 2090-2106 (2011).

[3] Watson, C, et al.: A Comparison of the Deterministic and Probabilistic Aspects of the ASME III Fatigue Evaluation Procedures, In: Proceedings of the ASME 2014 Pressure Vessels & Piping Conference, Anaheim, USA, (2014).

[4] Paolino, D. S., Cavatorta, M. P.: On the application of the stochastic approach in predicting fatigue reliability using Miner's damage rule, Fatigue and Fracture of Engineering Materials &Structures 37, 107-117 (2013).

[5] Rathod, V., et al.: Probabilistic Modeling of Fatigue Damage Accumulation for Reliability Prediction, International Journal of Quality, Statistics and Reliability 2011, Article ID 718901, 10 pages (2011).

[6] Endurance of high-strength steels data item, ESDU 04019a, Engineering Sciences Data Unit, United Kingdom, 42, 43 (2004).

ACKNOWLEDGMENTS

This paper presents work performed as part of the Aerospace Technology Institute (ATI) funded "Large Landing Gear of the Future" project in collaboration with Safran Landing Systems.

The Interactive Method Reliable and Reproducible S-N-Curve for Systems

K. Block[a*]

[a]*Fobatec GmbH, Dortmund, former Technical University of Dortmund, Germany*
**Corresponding author: klaus.block@tu-dortmund.de*

Keywords: S-N-Curve; Statistically evaluated; Systems; Quality conformance tests.

ABSTRACT

The Interactive Method is a method to determine the fatigue resistance up to the fatigue limit resistance of materials and systems. By a relatively small number of tests the fatigue limit resistance can be defined as a quantile each with a necessary confidence level. Already after a few tests with different load levels, a prognosis for the final result can be determined.

A new mathematical function was chosen to describe the complete S-N-Curve:

$$\Delta S = \Delta S_D + (S_1 - \Delta S_D).\, a^{(lgN)^b} \qquad (1)$$

with

$\Delta S = f(N)$	amplitude of the fatigue load bearing capacity;
a, b	positive non dimensional values, with a < 1,0
N	number of cycles
ΔS_D	amplitude of the fatigue limit bearing capacity
S_1	statically load bearing capacity

After 4 tests with different load levels a first approximation of the S-N-Curve as a mean value and an estimation of a x-quantile value is possible. During the following tests period tests and calculations are alternating (Interaction between calculation are tests). For the final results at least 20 tests are necessary to get reliable and reproducible values for the statistically evaluated quantile of the S-N-Curve (Fig. 1).

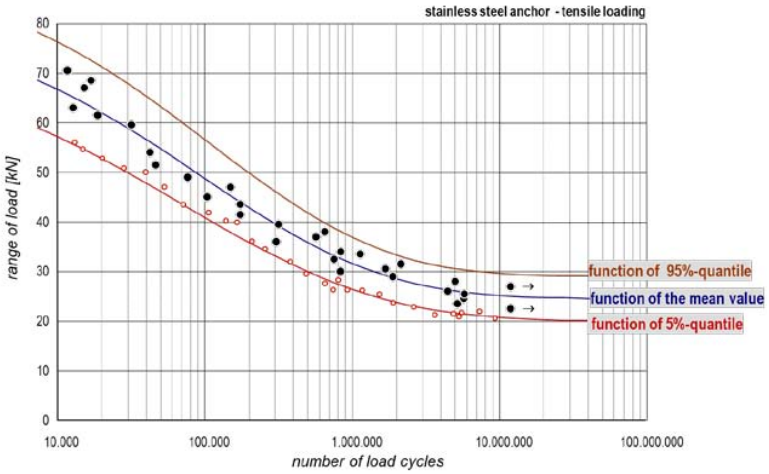

Fig. 1. Final results of the S-N-Curve.

This method had been checked and proofed by a Monte-Carlo-Simulation. The Result of this check is shown in Fig. 2.

After every test between the 4th test and the final test all relevant values can be calculated. These values show the development of e.g. the mean value or/and the quantile value for a chosen number of cycles.

Many metal fastener systems for civil engineering have been successfully tested with this method, anchors and anchor channels in concrete and reinforcing steel [3]. This method is also described in a European Approval Document [1]. It was first published already in [2].

The individual failure is influenced by the range of load and the different materials. Principally different positions of a fastener fail. That means that the material fatigue behaviour cannot be transferred to the fatigue behaviour of a system. A test series can be presented, which shows, that the concrete strength can enlarge the fatigue resistance of a steel fastener more that 30% [4].

Finally, for every product, which is in practical use, the quality has to be checked in certain time distances. Based on the Interactive Method only three tests with different load levels are necessary for this check.

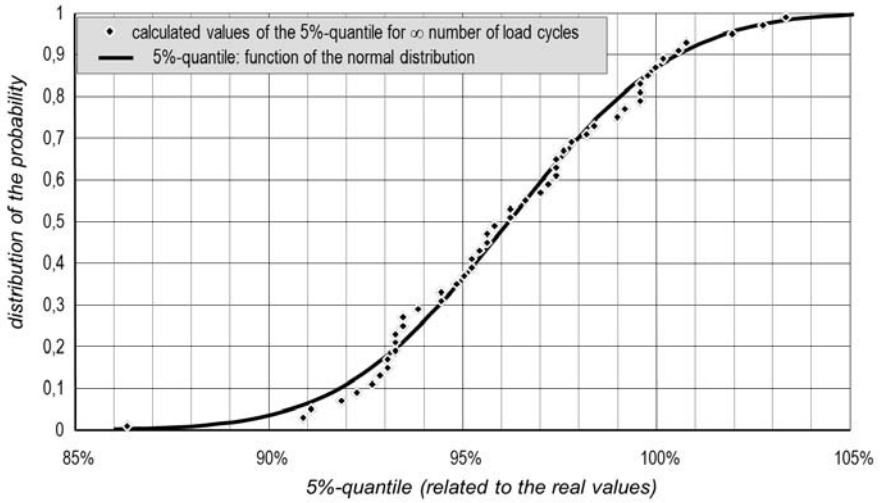

Fig. 2. Results of Monte-Carlo-Simulation.

REFERENCES

[1] EOTA, EAD DP 14-33-0250-06.01, Post–installed fasteners in concrete under fatigue cyclic loading (2018).

[2] Block, K.; Dreier, F.: Die Ermüdungsfestigkeit zuverlässig und Kostengünstig ermitteln – Das Interaktive Verfahren, Materialprüfung 40 (1998).

[3] Maurer, R., Block, K.; et. al.: Fatigue strength of reinforcing steel – determination by using the Interactive Procedure, fib Symposium 2011, Prague (2011).

[4] Block, K.; Dreier, F.; Bigalke, D.: Fatigue Bearing Capacity of Anchors Exposed to Shear Loading, Beton- und Stahlbetonbau 2007, Special Edition (2007).

Extending the Weibull Probabilistic Model to Include LCF Assessment

S. Blasón[a*], M. Muniz-Calvente[a], J.A.F.O. Correia[b], A.M.P. De Jesus[b], E. Castillo[c,d], A. Fernández-Canteli[a]

[a] *Dept. of Construction and Manufacturing Engineering, University of Oviedo. C/Pedro Puig Adam, s/n, 33204 Gijón, Spain*
[b] *INEGI, Facuty of Engineering University of Porto, Rua 4200-465 Porto, Portugal*
[c] *Real Academia de Ciencias Exactas, Físicas y Naturales, Valverde 24, 8004 Madrid, Spain*
[d] *Real Academia de Ingeniería de España, don Pedro 10, 28005 Madrid, Spain*
**Corresponding author: blasonsergio@uniovi.es*

Keywords: S-N probabilistic field; LCF region; Generalized fatigue parameter.

ABSTRACT

In this work the generalized parameter range $\Delta GP = E\cdot[\sigma_{max}\ (d\varepsilon/d\sigma)_{max} - \sigma_{min}\ (d\varepsilon/d\sigma)_{min}]$ is proposed as the reference "driving force" in the probabilistic fatigue model of Castillo-Canteli [1] as a plausible alternative to the conventional $\Delta\sigma = \sigma_{max} - \sigma_{min}$ parameter. As a result, extension of that model to the LCF case is feasible once the limitations evidenced in its basic version of the aforementioned model are overcome. In particular, the upper bound dictated by the ultimate stress is now preserved and the limiting number of cycles (denoted B parameter in the model) unambiguously interpreted as the minimum number of cycles to achieve failure in the LCF region. The strain gradients are calculated from the monotonic stress-strain diagram of the material, in this case defined by a convenient, though arbitrary, analytical expression. The experimental fatigue results from [2] are transformed according to the new generalized parameter to assess the ΔGP-N field using the basic Weibull model. The conventional $\Delta\sigma - N$ field, showing the expected typical sigmoidal shape, can be recovered from the ΔGP-N field. The approach, far from representing a simple data fitting, based on empirical models [3], allows the probabilistic prediction of LCF failures in practical design while including the scale effect thus ensuring transferability of the experimental program results to component design.

REFERENCES

[1] Castillo, E., Fernández Canteli A.: A unified statistical methodology for modeling fatigue damage. Springer (2009).

[2] Correia, J.A.F.O, Calvente, M., Blasón, S., Lesiuk, G., Brás, I.M.C., De Jesus, A.M.P., Moreira, P.M.G.P., Fernández-Canteli, A.: Fatigue Life Response of P355NL1 Steel under Uniaxial Loading Using Kohout-Věchet Model. Procedia Engineering 160, 109-116 (2016).

[3] Kohout, J., Vechět, S.: A new function for fatigue curves characterization and its multiple merits. Int. J. of Fatigue 23, 175-183 (2001).

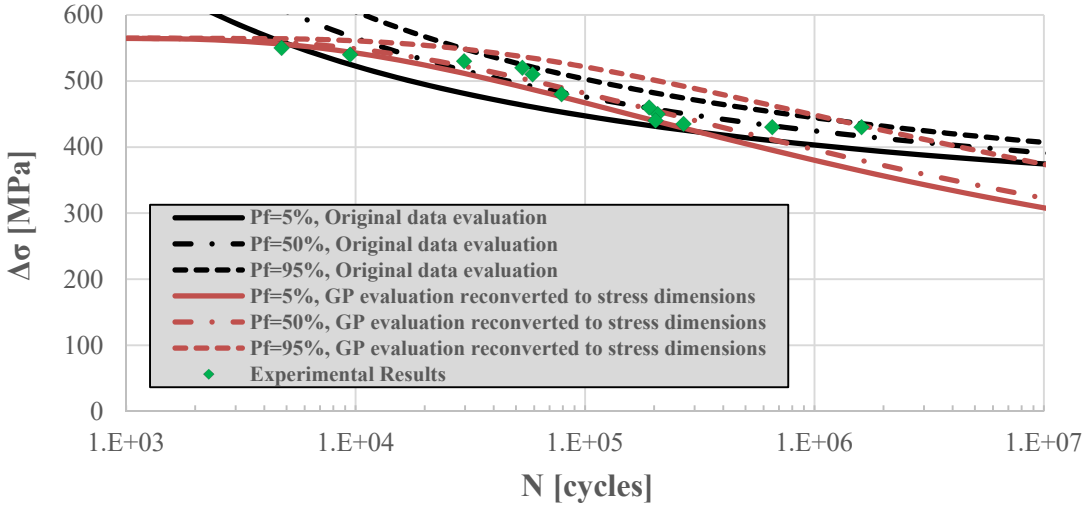

Fig. 1**.** Superposition of the probabilistic fatigue Δσ-N and ΔGP-N fields using the LCF model proposed.

Updating the Failure Probability of Miter Gates Based on Observation of Water Levels

T. Van Dang[a*], Q. Anh Mai[a], P.G. Morato[a], P. Rigo[a]

[a]*Department of ArGEnCo/ANAST – University of Liege, Belgium*
**Corresponding author: thuongdv@tlu.edu.vn*

Keywords: Fatigue; Miter gate; Probability of failure; Updating failure probability; Inspection.

ABSTRACT

Hydraulic steel structures, especially lock gates play a significant role in keeping navigation traffic uninterrupted. After a few decades of operation, many of the welded joints may suffer various degrees of deterioration, primarily due to fatigue. To economically combining crack inspection with a scheduled maintenance of the movable parts of the gate, it is valuable to predict inspection time of the welded joints using the historical operations of the gate, i.e. the variation of water levels. Updating failure probability of welded joint is mature in offshore industry, but it is rarely applied for inland navigation lock gates where low cycle fatigue usually happens. The scope of this paper is to predict the optimum inspection time of a welded joint using the observed water levels of the operational history. The procedure of the present methodology can be found in **Fig.** 1**.**

Stresses are calculated for each observed water level by using analytical formulas or finite element method. Each lockage corresponds to a stress cycle. Since water levels in front and behind the gate are not always the same for every lockage due to seasonal flows of the river, the different stress-ranges occurring during the year are represented by an equivalent stress-range value. This equivalent stress-range is used to calculate failure probabilities. Failure probability of the welded joint is first calculated using a limit state function based on Miner's rule (S-N model) [1] because this cumulative fatigue damage principle is used in the design stage. The S-N curve is taken from EN 1993-1-9. To incorporate the crack inspection results into assessing failure probability, a fracture mechanics (FM) model is used for crack propagation. The most widely used model is the Paris-Erdogan law [2], Eq. (1).

$$\frac{da}{dN} = C(\Delta K)^m = \mathrm{C}(Y\Delta\sigma\sqrt{\pi a})^m \quad (1)$$

where N is the number of cycles, da/dN is the rate of crack growth, C and m are material parameters, Y is geometry function, Δσ is the equivalent stress range and ΔK is the amplitude of the stress intensity factor.

The FM model is calibrated to reach identical failure probabilities as obtained from the S-N model analysis. The calibration algorithm is carried out by a least-squares fitting in cumulative failure probability space (Pc), as shown in Eq. (2).

$$\min \sum_{t=1}^{T} \left(Pc_{SN}(t) - Pc_{FM}(t; x_1 \dots x_N)\right)^2 \quad (2)$$

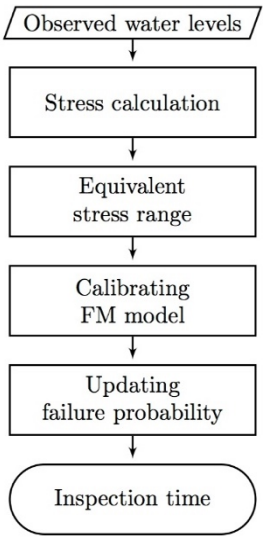

Fig. **1**. Updating procedure.

where $Pc_{SN}(t)$ is the cumulative failure probability at time t, evaluated using the S-N model; $Pc_{FM}(t; x_1 \dots x_N)$ is the cumulative failure probability at time t, evaluated using FM model with a set of parameters $(x_1 \dots x_N)$ representing initial crack size, C, uncertainty of stress range. T is the service life of the considered structures.

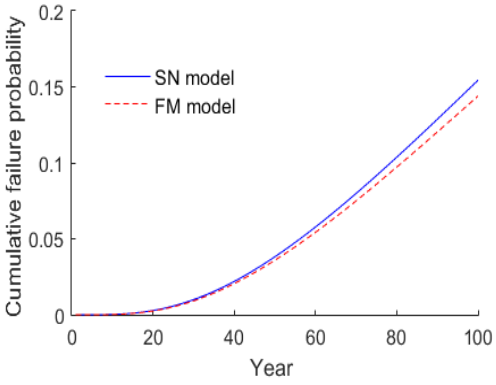

Fig. 2. Calibrated result.

The probability of detection (POD) is used as a metric for quantifying the performance of non-destructive testing. POD curves describe the probability that a certain crack size is detected during inspection. In the present paper the POD curves are assumed to be represented by the Log-Odds-Log scale model [2]:

$$\text{POD(a)} = \frac{\alpha a^{\gamma}}{1+\alpha a^{\gamma}} \qquad (3)$$

where a (mm) is the crack depth and α, γ are regression parameters. To see the effects of POD on the predicted inspection time, three cases of inspection labelled A ($\alpha = 0.3$ mm^{-1}, $\gamma = 3.0$), B ($\alpha = 0.085$ mm^{-1}, $\gamma = 3.0$) and C ($\alpha = 0.035$ mm^{-1}, $\gamma = 3.0$) are used [3].

The simulation method is used to update the failure probability (P_f), considering POD and repair policies. It is assumed that all detected cracks are repaired. For the case where crack detected and not repaired, as suggested in [5], it should not be considered in the simulation method as an unrealistically large number of samples is required for updating. The maximum allowable annual probability of failure $P_f = 1.4\text{x}10^{-3}$ (equivalent to a target reliability index after 50 years is 1.5 in EN1990) and 90% probability of detection in three inspection techniques are used.

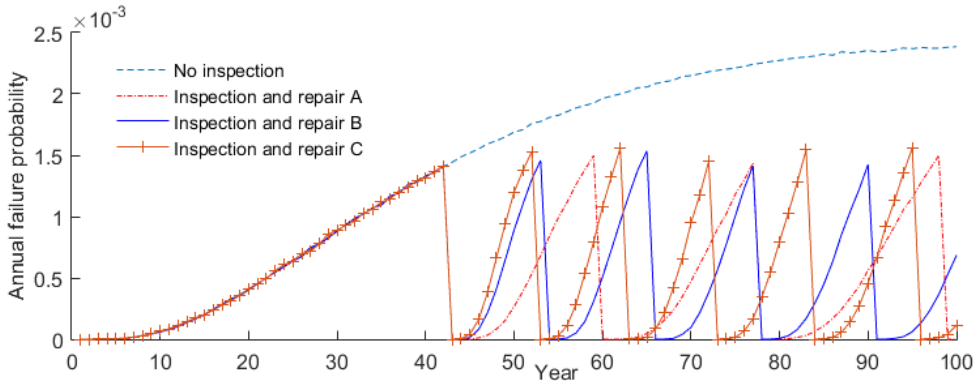

Fig. 3. The updating annual failure probability with 90% POD in three inspection techniques.

The result showed that after about 40 years in service, crack inspection should be done to allow the gate keeping the safety level defined in EN1990 (see **Fig.** 3.). The crack inspection quality significantly affects the predicted future inspection time. Since the scheduled maintenance of the movable parts is unavoidable, crack inspection should be planned in the design stage to reduce the investment cost.

REFERENCES

[1] Miner, M. A.: Cumulative damage in fatigue. Am. Soc. Mech. Eng. - J. Appl. Mech. 12, 159–164 (1945).

[2] Paris, P., Erdogan, F.: A Critical Analysis of Crack Propagation Laws. J. Basic Eng. 85 (4) (1963).

[3] Berens, A.P., Hovey, P.: Evaluation of NDE reliability characterization. Dayt. Air Force Wright-Aeronautical Lab. Wright-Patterson Air Force Base, vol. I (1981).

[4] Kulkarni, S.S., Achenbach, J.D.: Optimization of inspection schedule for a surface-breaking crack subject to

fatigue loading. Probabilistic Eng. Mech. 22 (4), 301–312 (2007).
[5] Mai, A.Q., Sørensen, J.D., Rigo, P.: Updating failure probability of a welded joint in offshore wind turbine substructures. OMAE2016-54232, 1–10 (2016).

ACKNOWLEDGMENTS

This research is funded by the Wallonie-Bruxelles International (WBI).

Structural Integrity of Steel and Composite Bridges

C-ISSIBRIDGES-ICMFM

Organized by:

Abílio M. P. de Jesus, Portugal

Carlos Rebelo, Portugal

Hermes de Carvalho, Brazil

José A. F. O. Correia, Portugal

Khaled M. Mahmoud, USA

Luís Simões da Silva, Portugal

Matthew Hebdon, USA

Rui Calçada, Portugal

Peter Collin, Sweden

Laser Peening as a Preventive Maintenance Against Fatigue Crack Initiation in Steel Structures in the Field

Y. Sano[a*], Y. Sakino[b]

[a] *ImPACT Program, Japan Science and Technology Agency, Japan*
[b] *Kindai University Faculty of Engineering, Japan*
**Corresponding author: yuji.sano@jst.go.jp*

Keywords: Residual stress; Fatigue; Field application; Palmtop laser.

ABSTRACT

Joining and welding are essential to construct large steel structures such as bridges. However, they inevitably introduce geometrical/material discontinuity or tensile residual stresses around the joints, which reduces the fatigue life and strength of the structures. Laser peening (or laser sock peening) can improve the residual stresses from tensile to compressive by irradiating laser pulses to the structures covered with water [1, 2]. Studies on the effects of laser peening have revealed that the fatigue properties of various materials could be dramatically improved [3, 4].

To use laser peening for steel structures in the field, the authors tried to reduce laser pulse energy down to 20 mJ, considering the downsizing of laser system [5]. As a result, compressive residual stresses were successfully introduced on HT780 (780 MPa grade high-strength steel) plates as shown in Fig. 1. Surface residual stresses attained in all conditions are on the same level around the yield strength, while the penetration depth of the effect largely depends on the conditions and increases with increasing the laser pulse energy. Fatigue experiments with HT780 welded specimens were performed to confirm the effects of laser peening on large steel structures such as bridges. Typical results are shown in Fig. 2. The fatigue lives were prolonged by laser peening at least 25 times even if the 20 mJ pulse energy was used.

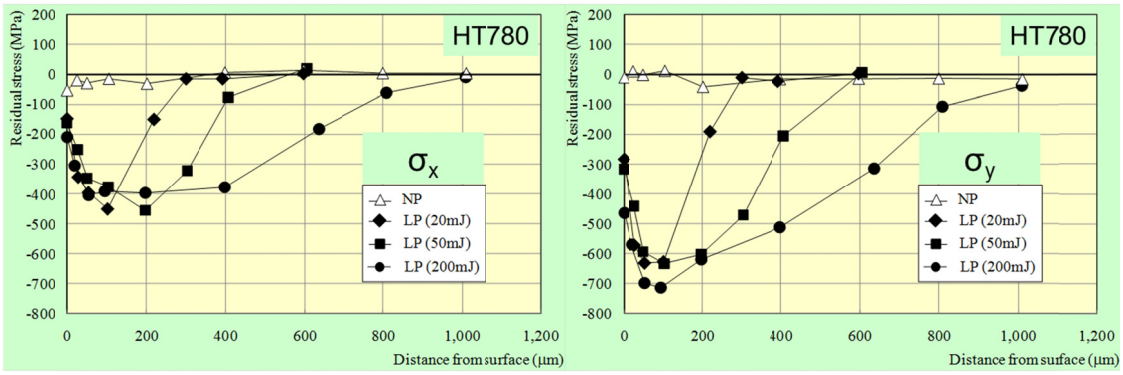

Fig. 1. Residual stress in-depth profile of HT780 with and without laser peening.

On the other hand, a palmtop-sized ultra-compact power laser was recently developed in the Institute for Molecular Science (IMS) [6] under the framework of Japanese national program, ImPACT (Impulsing PAradigm Change through Disruptive Technologies Program) [7]. Trial operation of the laser recorded a stable pulse energy of 35 mJ which is enough intense for laser peening of steel structures. The laser can be used in all positions and easily handled by a multi-axes robotic arm, which could open the door to

actual applications of laser peening in the maintenance of aged infrastructures such as bridges in the field as shown in Fig. 3.

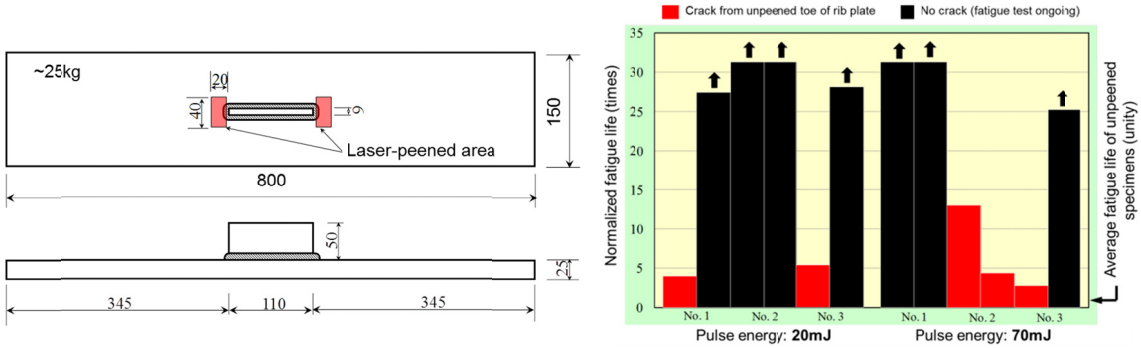

Fig. 2. HT780 welded specimen (left) and fatigue test result (right).

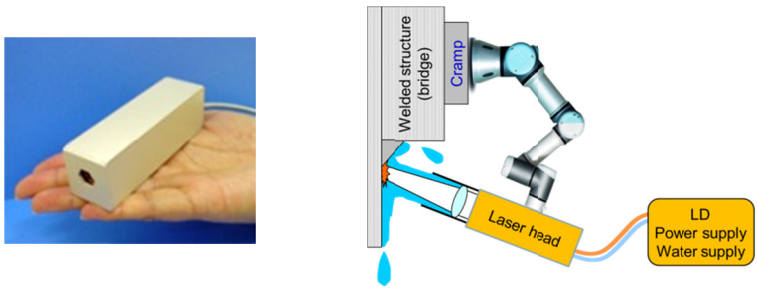

Fig. 3. Mock-up of a palmtop laser (right) and concept to apply laser peening to a field structure (right).

The effects of laser peening with low energy laser pulses on residual stresses and fatigue properties, the status of the palmtop laser development and concept of actual applications to infrastructures in the field will be presented.

REFERENCES

[1] Sano, Y., Mukai, N., Okazaki, K., Obata, M.: Residual stress improvement in metal surface by underwater laser irradiation. Nucl. Instrum. Methods Phys. Res. B 121, 432-436 (1997).

[2] Sano, Y., Yoda, M., Mukai, N., Obata, M., Kanno, M., Shima, S.: Residual stress improvement mechanism on metal material by underwater laser irradiation. J. Atomic Energy Soc. Japan. 42, 567-573 (2000).

[3] Sano, Y., Obata, M., Kubo, T., Mukai, N., Yoda, M., Masaki, K., Ochi, Y.: Retardation of crack initiation and growth in austenitic stainless steels by laser peening without protective coating. Mater. Sci. Eng. A 417, 334-340 (2006).

[4] Sano, Y., Masaki, K., Gushi, T., Sano, T.: Improvement in fatigue performance of friction stir welded A6061-T6 aluminum alloy by laser peening without coating. Mater. Des. 36, 809-814 (2012).

[5] Sakino, Y., Yoshikawa, K., Sano, Y., Sumiya, R., Kim, Y.-C.: A basic study for application of laser peening to large-scale steel structure. Quarterly J. Japan Weld. Soc. 41, 231-237 (2013).

[6] Zheng, L., Kausas, A., Taira, T.: Drastic thermal effects reduction through distributed face cooling in a high power giant-pulse tiny laser. Opt. Mater. Exp. 7, 3214-3221 (2017).

[7] ImPACT Homepage, http://www.jst.go.jp/impact/en/program/03.html.

Development of Efficient Approach for Fatigue Cracking Assessment of Riveted Details

C. Silva Horas[a*], A.M.P. de Jesus[b], Rui Calçada[a]

[a]*CONSTRUCT-LESE, University of Porto, Faculty of Engineering, Rua Dr. Roberto Frias, 4200-465 Porto, Portugal*
[b]*INEGI, University of Porto, Faculty of Engineering, Rua Dr. Roberto Frias, 4200-465 Porto, Portugal*
**Corresponding author: claudio.silva.horas@fe.up.pt*

Keywords: Bridges; Modal superposition; Crack propagation; Crack initiation.

ABSTRACT

The growing number of existing bridges that are close to or over the end of their planned service life represents an imminent economic burden. Since the replacement of these structures would have unacceptable costs, it has been established as major priority the development of analysis tools and strategies aiming at extending their safe operation. Among the structural phenomena which may jeopardize the safety of metallic bridges, the fatigue cracking is a critical source of damage and shall be carefully analysed.

The fatigue assessment of structural components of large bridges is a complex task which is highly conditioned by geometrical and loading issues. The numerical assessment of local phenomena related with cyclic acting loadings leads to a complex multi-scale numerical problem which hinders or makes unfeasible an accurate fatigue damage assessment using classic approaches (refer to Fig. 1).

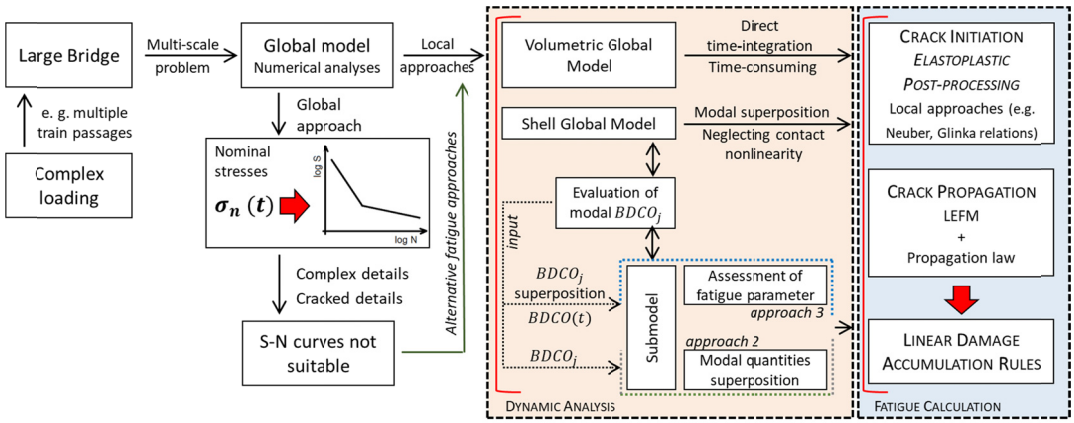

Fig. 1. General workflow for the numerical analysis of fatigue issues in large bridges

As outlined in Fig. 1, the most important standards and guidelines propose global S-N approaches which do not allow an adequate fatigue local analysis of complex details, new or existing ones, typically found in railway bridges. Therefore, considering the structural complexity of large bridges and the importance of fatigue phenomena, it is necessary to find computationally efficient solutions to evaluate the progression of local damages under dynamic loadings. The aim of the present paper is to propose effective approaches based on the modal superposition technique and submodelling principles to compute local fatigue quantities essential to evaluate fatigue cracking in the presence of local geometric, material or contact nonlinearities. Such approaches intent to be an alternative to the direct time-integration using algorithms such as the Hilber-Hughes-Taylor (*HHT*), which require the calculation of thousands of load steps leading to unsustainable computational times when local exhaustive analyses are required [1,2].

Considering the presented framework, a simple case-study was idealised aiming to validate the proposed approaches and the accuracy of the obtained results for riveted joints with local nonlinearities. A simply supported steel beam with a 10m span and a HEB 700 cross-section, cracked and strengthened at mid-span by a riveted patch, was idealised and submitted to different dynamic loadings characterized by magnitude, p, and velocity, v. Three methodologies based on Fig. 1) were adopted: i) approach 1, consisting on the analysis of a volumetric global model using the HHT algorithm; ii) approach 2, based on the superposition of modal quantities; and iii) approach 3, grounded on the determination of displacement fields around the detail using the modal superposition technique. Both approaches 2 and 3 consider a submodelling process based on a global shell model and a local submodel of the critical detail.

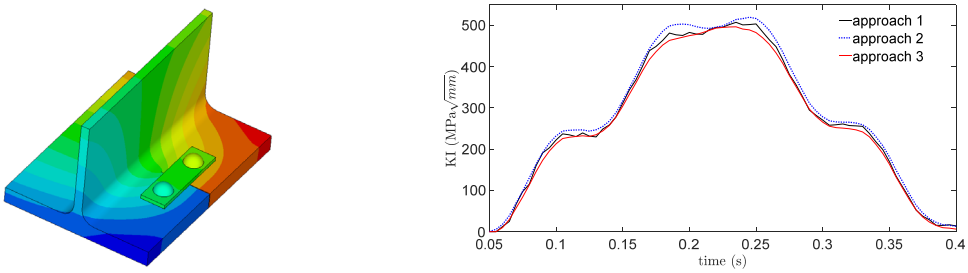

a) volumetric submodel of the cracked flange

b) stress intensity factor time-history, $K_I(t)$

Fig. 2. Comparison of the obtained results considering local nonlinearities (p=100kN, v=100km/h)

Concerning approach 2, the modal displacement fields obtained from the shell global model at the submodel boundaries, $BDCO_j$, were inputted into the submodel (Fig. 2 a)) to calculate the required modal quantities for fatigue analysis. For approach 3, $BDCO_j$ were evaluated and superimposed to compute $BDCO(t)$. Then, for each time instant, $BDCO$s were inputted into the submodel and the necessary local fatigue quantities assessed. Overall, both approaches allowed obtaining accurate results. Although, approach 2 was found applicable only if at the point where the modal quantities are assessed, the influence of initial stress/strain states or contact nonlinearities is negligible (e. g. Fig. 2 b)). In terms of computational efficiency, in average, to compute comparable results, approach 1 took 7h05m, approach 2 required 2s and approach 3 took 2h30m. Regarding approach 3, it should be highlighted that a process of network parallel computing combined with shared memory multiprocessing was adopted to potentiate the computational efficiency. Therefore, considering the achieved results, it can be said that the proposed approaches may be implemented to perform accurate and effective local fatigue analyses of riveted details.

REFERENCES

[1] Horas, C.S., Correia, J.A.F.O., De Jesus, A.M.P., Kripakaran, P., Calçada, R.: Application of the modal superposition technique combined with analytical elastoplastic approaches to assess the fatigue crack initiation on structural components. Eng. Fract. Mech. 185, 271–283 (2017).

[2] Horas, C.S., Alencar, G., De Jesus, A.M.P. Calçada, R.: Development of an efficient approach for fatigue crack initiation and propagation analysis of bridge critical details using the modal superposition technique. Eng. Fail. Anal. 89, 118–137 (2018).

ACKNOWLEDGMENTS

This work was financially supported by: Project POCI-01-0145-FEDER-007457 – CONSTRUCT – Institute of R&D In Structures and Construction funded by FEDER funds through COMPETE2020 - Programa Operacional Competitividade e Internacionalização (POCI); Project POCI-01-0145-FEDER-030103- funded by FEDER funds through COMPETE2020 - POCI – and by national funds through FCT - Fundação para a Ciência e a Tecnologia; PD/BD/114101/2015.

Numerical Analysis of a Repair Measure of an Old Metallic Bridge Detail Subjected to Out-of-Plane Loading

J. Kwad[a,b*], G. Alencar[c], J. Correia[c,d], A. de Jesus[d], R. Calçada[c], P. Kripakaran[a]

[a] *College of Engineering, Mathematics and Physical Sciences Vibration Engineering Section, University of Exeter, UK.*
[b] *Civil Engineering Department, University of Anbar, Iraq.*
[c] *CONSTRUCT-LESE, Faculty of Engineering (FEUP), University of Porto, Portugal.*
[d] *INEGI, Faculty of Engineering (FEUP), University of Porto, Portugal.*
**Corresponding author: jeek201@exeter.ac.uk.*

Keywords: Distortion-induced fatigue; Fatigue; Steel bridges; Retrofit.

ABSTRACT

Distortion-induced fatigue damage from out-of-plane deformation in web gaps of bridge connection details is examined. This type of fatigue damage often forms at the end of vertical stiffeners or connection plates for floor beams in the web gap region, or in the weld of lateral gusset plates to the girder web [1]. Out-of-plane distortion is well-known as a key cause of localized fatigue cracking in bridges. [2] Connor & Fisher have calculated that nearly 90% of all fatigue cracking is caused by either secondary stress at areas of fatigue sensitivity or distortion that is out-of-plane. The goal of this study was to develop and evaluate the performance of retrofit techniques for existing steel bridges that have already sustained damage due to distortion-induced fatigue, or are anticipated to experience distortion-induced fatigue cracking within their design life.

In this study, a retrofit solution for a connection in an old bascule steel bridge located in Exeter (UK) is investigated. The so-called cut-back retrofit as proposed by [3] is used based on a geometric improvement of the transverse stiffener with web gaps in order to reduce stresses in the external transverse stiffeners, which are subjected to tension due to distortion created by vehicle's traffic. A numerical assessment was carried out through finite element sub models of the critical connections, considering conventional local approaches such as the hot-spot stress method and the notch stress method [4]. Results show that small cut-back of 20 mm was sufficient to contribute to a significant reduction of the out-of-plane stresses for both methods (Fig. 1). Further investigations are under development, which includes the calibration of the sub model for static moving load based on measurements of nominal and local strains in order to perform fatigue life estimations of the connection considering roadway traffic according to current European standards [5] in two conditions: (i) as-built and (ii) with improved geometry.

REFERENCES

[1] Connor, R.J., Fisher, J.W. Identifying Effective and Ineffective Retrofits for Distortion Fatigue Cracking in Steel Bridges Using Field Instrumentation. J. Bridg. Eng. 11, 745–752 (2006).
[2] Fisher, J.W., Roy, S.: Fatigue damage in steel bridges and extending their life. Advanced Steel Construction 11(3), 250–268 (2015).
[3] Connor, R.J., Lloyd, J.B.: Maintenance Actions to Address Fatigue Cracking in Steel Bridge Structures. West Lafayette (2017).
[4] Hobbacher, A.F.: Recommendations for Fatigue Design of Welded Joints and Components. International Institute

of Welding (IIW) (2016).
[5] EN 1991-2. Eurocode 1: Actions on structures - Part 2: Traffic loads on bridges. Brussels, Belgium: CEN (2003).
[6] Kwad, J., Alencar, G., Correia, J., Jesus, A., Calçada, R., Kripakaran, P.: Fatigue assessment of an existing steel bridge by finite element modelling and field measurements. Journal of Physics: Conference Series 843(0), 12038 (2017).

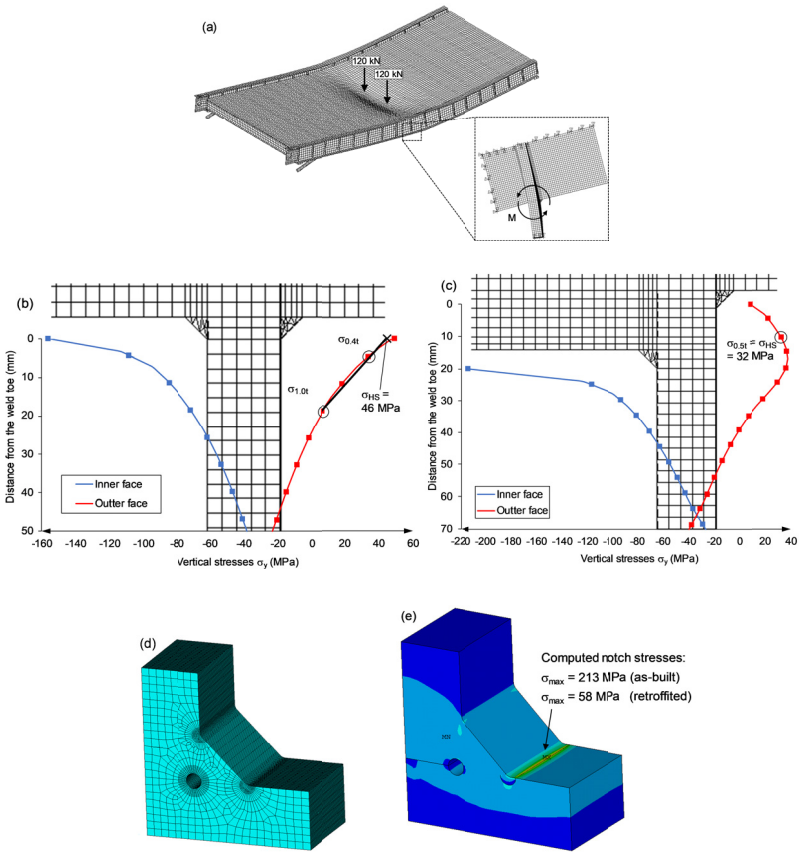

Fig.1. Deformed shape of the bridge's finite element model subjected to the maximum value of truck axle (240 kN) permitted for a British Fatigue Load Model, (b),(c) comparison between the hot-spot stress estimations for the as-built and the retrofitted condition and (d) sub-model used for the notch stress computation and(e) comparison between the notch stress for the as-built and the retrofitted condition [6].

ACKNOWLEDGMENTS

The first author would like to acknowledge the financial support of The Higher Committee for Education Development in Iraq (HCED IRAQ) scholarship reference D11000218, and the second author would like to acknowledge the final support of the National Council for Scientific and Technological Development, CNPq, Brazil, scholarship reference 203662/2014-8. The authors would also like to acknowledge the Vibration Engineering Section (VES) at the University of Exeter for providing the national instrument equipment used in this investigation and the on-site support given by VES research team. The authors would also like to thank the Bridges and Structures team at Devon County Council (UK) for sharing data and providing access to the Bascule Bridge.

Fatigue Critical Detail Analysis of the Hercílio Luz Bridge Based on Local Strain Approach and Linear Damage Rule

Zhongxiang Liu[a], José Correia[b], Hermes Carvalho[c], Matthew Hebdon[d], António Mourão[b*], Abílio M.P. de Jesus[b], Rui Calçada[b], Filippo Berto[e]

[a]*Southeast University, Nanjing, P. R. China*
[b]*Faculty of Engineering, University of Porto, Portugal*
[c]*Federal University of Minas Gerais, Belo Horizonte, Minas Gerais, Brazil*
[d]*Department of Civil & Environmental Engineering, Virginia Tech, Blacksburg, USA.*
[e]*NTNU, Department of Engineering Design and Materials, Trondheim, Norway*
**Corresponding author: up201306134@fe.up.pt*

Keywords: Global-local fatigue analysis; Riveted bridge; Life prediction; Local approaches.

ABSTRACT

Increasing traffic demands (i.e. load intensity and operational life) on ancient riveted metallic bridges and the fact that these bridges were not explicitly designed against fatigue make the fatigue performance assessment and fatigue life prediction of riveted bridges a concern. This paper presents a global-local fatigue analysis methodology that integrates beam-to-solid sub-modelling, elastoplastic of material in local region and local fatigue life prediction approach. The proposed beam-to-solid sub-modelling can recognize accuracy local stress/strain information accompanying with the global structural effect on the fatigue response of local riveted joints. The fatigue life is predicted based on cumulative linear damage rule, local strains and number of cycles with consideration of traffic data, where the relation between the fatigue life and local strain is derived according to the Basquin and Manson-Coffin law. Besides, the elastoplastic of material is considered. The proposed methodology for fatigue life prediction is implemented in a case study of an ancient riveted bridge [1].

A systematic global-local analysis methodology for fatigue performance assessment and remaining life prediction of ancient riveted bridges is presented, where beam-to-solid sub-modelling and the life prediction based on a local approach are integrated [1,2].

Fig. 1 shows each step for utilizing the methodology for fatigue assessment exactly. To effectively verify the proposed methodology, a case study was conducted. The case study selected to validate the proposed methodology was the Hercílio Luz Bridge (HLB), located between the Santa Catarina Island and the mainland of Brazil, which is an eye-bar chain suspension bridge built in 1926 [3,4].

Strain ranges and number of cycles causing by single truck across the bridge are obtained by using the rain-flow counting. The annual damage index can be derived incomprehension with the damage index due to single truck and traffic statistical results, where the average daily volume being 6000 is adopted according to research by Rossigali et al. [5]. Assuming that failure occurs when the cumulative damage exceeds 1, fatigue lives of concerned joint based on the strain states around the rivet holes are determined, as listed in Table 1. The predicted lives of the regions around the riveted hole are longer than 50 years expect for the region around the Hole 15, indicating that in the gusset plate are much more prone to fatigue failure and needs to be strengthened for insufficiency.

Thus, it can concluded that the methodology for fatigue evaluation based on the fatigue strain damage parameter and the Palmgren-Miner rule using the effect of the global model as well as the local model for the critical detail proved to be quite efficient. Thus, the methodology can be extended to other

fatigue damage variables, based on stress, strain and energy, under uniaxial and multiaxial loading conditions.

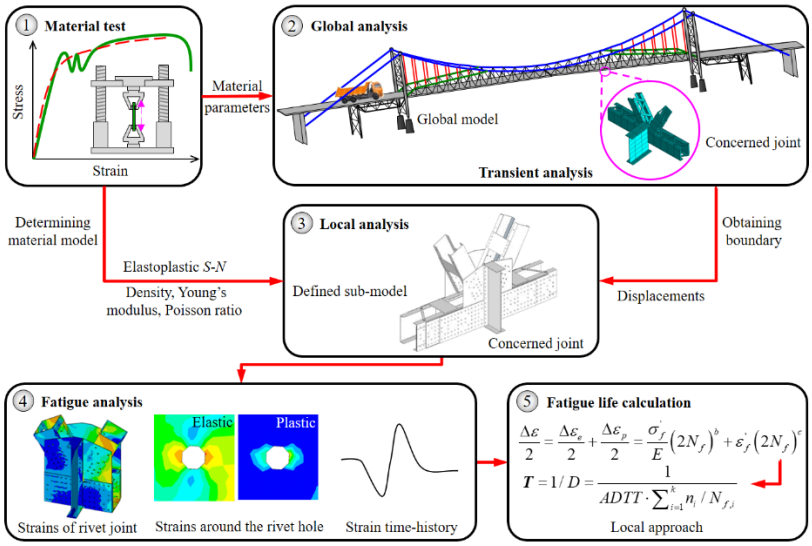

Fig. 1. Flow chart of the proposed global-local fatigue analysis.

Table 2. Fatigue life prediction.

Critical region	$\sum_{i=1}^{k}\frac{n_i}{N_{f,i}}$	*ADTT*	Fatigue life (year)
Hole 1	8.526×10^{-9}	2.19×10^{6}	53.6
Hole 12	6.730×10^{-9}		67.8
Hole 13	7.878×10^{-9}		58.0
Hole 15	9.858×10^{-9}		46.3

ACKNOWLEDGMENTS

Support from the Portuguese Science Foundation (FCT) under the post-doctoral grant No. SFRH/BPD/107825/2015 and the Scientific Research Foundation of Graduate School of Southeast University under grant No. YBJJ1818 is gratefully acknowledged. This work was also financially supported in part by the Federal University of Minas Gerais and Teixeira Duarte SA. Special thanks are given to Prof. Tong Guo at Southeast University, China, for his professional guidance and valuable discussion in the research process.

REFERENCES

[1] Liu, Z., Correia, J., Carvalho, H., Mourão, A., de Jesus, A., Calçada, R., Berto, F.: Global-local fatigue assessment of an ancient riveted metallic bridge based on sub-modelling of the critical detail. Fatigue & Fracture of Engineering Materials & Structures (2018) (in press).
[2] Leite, R.C.G., de Jesus, A.M.P., Correia, J., Raposo, P, Jorge, R.N., Parente, M.P., Calçada, R.: A methodology for a global-local fatigue analysis of ancient riveted metallic bridges. International Journal of Structural Integrity 9(3), 355-380 (2018).
[3] Liu, Z., Hebdon, M.H., Correia, J.A.F.O., et al.: Fatigue assessment of critical connections in a historic eye-bar suspension bridge. J Perform Constr. Facil. 2018 (in press).
[4] Carvalho, H., Fakury, R.H., Vilela, P.M.L.: Structural integrity assessment and rehabilitating of Hercílio Luz bridge. Frattura ed Integrità Strutturale 11(42), 93-104 (2017).
[5] Rossigali, C.E., Pfeil, M.S., Battista, R.C., Sagrilo, L.V.: Towards actual Brazilian traffic load models for short span highway bridges. Revista IBRACON de Estruturas e Materiais 8(2), 124-139 (2015).

Fatigue Damage Factor Calibration for Long-Span Cable-Stayed Bridge Decks

J. Oliveira Pedro[a], C. Baptista[b], M. Duval[c], A. Nussbaumer[d*]

[a]*Instituto Superior Tecnico, Lisbon, Portugal*
[b]*GRID International, Lisbon, Portugal*
[c]*Losinger Marazzi SA, Lausanne, Switzerland*
[d]*RESSLab, EPFL, Lausanne, Switzerland*
**Corresponding author: alain.nussbaumer@epfl.ch*

Keywords: Steel-concrete deck; Lambda factor; Fatigue load model; Influence line.

ABSTRACT

Fatigue safety verification is an important part in the steel highway and railway bridge design. The part 2 of the Eurocode 3 (EN1993-2) proposes a simple and fast fatigue verification procedure. It consists in determining the value of the maximum stress range at the location of a specific detail based on the passage of a fatigue load model (FLM3), a standard heavy vehicle with 4 axles of 120 kN each. This stress range is multiplied by a λ-factor, called damage equivalent factor that represents the damaging effects of the real traffic. This resulting action effect is used in the fatigue verification against the resistance expressed in terms of stress range of the fatigue detail. The λ-factor is function of a critical length, related to the static system and influence line shape. The method is appealing to design engineers, however the λ-factor has limits and is not defined in the EN1993-2 for some cases or lengths over 80 m. This is in particular the case for cable-stayed bridges, where a combination of two internal forces in the deck: bending and compression (induced by the stays) is a characteristic of this bridge system. It is not clear which one best describes the maximum and minimum stresses. Furthermore, such long span bridges also have multiple truck lanes and may combine road and railway traffic, another case not addressed by the current standard.

To address the above problems, the Vasco da Gama bridge is taken as the study case. Its main characteristics are two lateral spans of 204.5m and a central span of 420m for a total of 829m. The model considers two towers and six piers (three in each side span), which prevents excessive bending in the towers. The whole deck is supported by 64 stays in a semi-harp shape. The towers and the piers are in concrete and the deck is a composite steel-concrete deck, with two longitudinal I-shape steel girders, transversal steel girders and precast concrete slab panels with a thickness of 0.25m. The stress influence lines were determined as a combination of both bending and compression influence lines. Thus, one can define the stress range in one element, at a specific location, under a mobile load. To determine new λ-factor for critical lengths for the stays, the method consisted of calculating a stress range with a fatigue load model (FLM3). Then, a "real traffic" was randomly generated as a combination of the 5 Heavy Vehicles (HV) from FLM4 and light vehicles as described in [1, 2], shown to be a good approximation of real traffic fatigue effects, see Fig. 1. The traffic composition is defined and also the distance between vehicles and used on the different influence lines. Using an S-N curve with two slopes as in EN1993-1-9, the total damage and an equivalent stress range at 2 x 10^6 cycles are determined. The ratio between these two stresses gives the damage equivalent factor:

$$\lambda = \frac{\Delta\sigma_{E,2}}{\Delta\sigma(Q_{FLM3})} \quad (1)$$

The results of the λ-factor computed for different critical lengths are shown in Fig. 2. All results were adapted to get λ-factor values for the same case as the standard, that is 500'000 HV/y in the slow lane, and an average HV weight of 480 kN. In order to do so, the EN1993-2 formula for partial factor λ2 was used as a first approximation to scale the results from the different studies; thus the absolute values obtained are estimates but the trends shown are correct. Also shown in the figure are the original

computations made for establishing the current EN lambda formula, from Heft 711, 1995 [3], as well as simulations made by Maddah [1]. Our proposition for the "mid-span case" is to use a constant value for critical lengths above 80m. For stays, both steel and cable constructional details are present, thus computations using 2 different S-N curves where carried out: 1) m = 3; 5; and cut-off, and 2) m = 4;6; no cut-off, respectively.

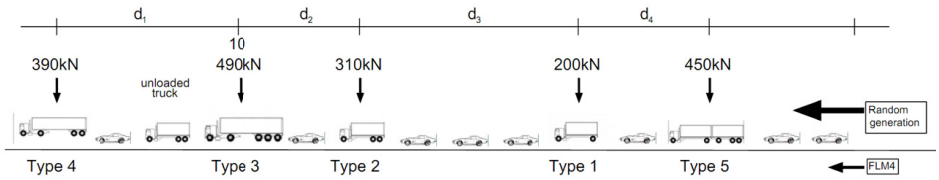

Fig. 1. Traffic generation using FLM4.

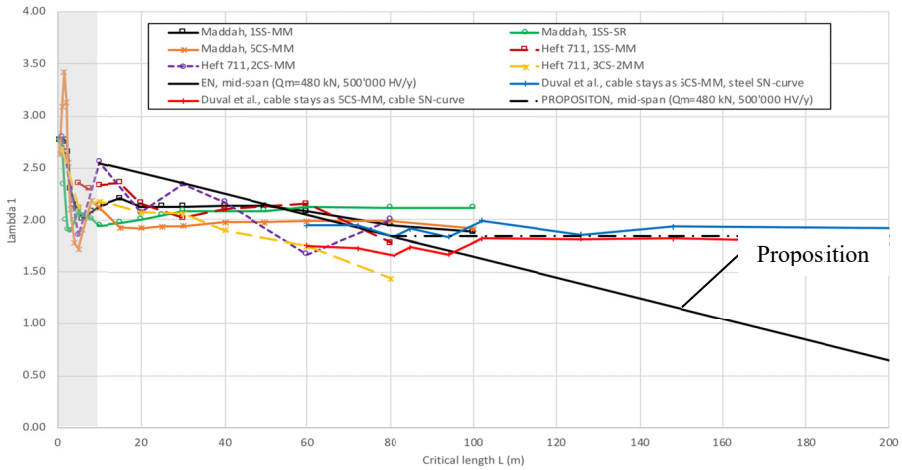

Fig. 2. Comparison of λ-factor, EN1993-2 "mid-span case", for different stays, previous studies [1, 3] and proposition.

From this study, the following conclusions were drawn:

- For the stays and girders, the influence line of the bending moments can be used for determining the critical length (with the maximum variation of the moments to determine the stress range)
- The damage equivalence factor shows a constant trend for lengths higher than 80 m
- The different shapes (slopes) of the S-N curves could be accounted for with a partial factor λ_5
- For combinations of road and railway traffic, a simultaneity coefficient of 1.2 on the added damage sums from highway and railway (i.e. $D_{railway+road} = 1.2 \cdot [D_{railway} + D_{road}]$) was shown to be valid for the long influence lines, over 200 m, analyzed.

REFERENCES

[1] Maddah, N.: Fatigue Life Assessment of Roadway Bridges based on Actual Traffic Loads. PhD thesis no 5575, Ecole Polytechnique Fédérale de Lausanne, Lausanne (2013).
[2] Baptista, C.: Multiaxial and variable amplitude fatigue in steel bridges. PhD thesis n° 7044, EPFL/IST, EPFL, Switzerland (2016).
[3] Sedlacek, G., Merzenich, G.: Hintergrundbericht zum Eurocode 1 - Teil 3.2: Verkehrslasten auf Straßenbrücken. Report n° 711. Bundesministerium für Verkehr, Germany (1995).

ACKNOWLEDGMENTS

The comments and help of Martin Garcia and Pierre Lorne during this work were appreciated and are acknowledged.

S-N Curves for Variable Amplitude Based on Experiments and a Probabilistic Initiation-Propagation Model

C. Baptista[a], A. Nussbaumer[b*], A. Reis[c]

[a]*GRID International, Lisbon, Portugal*
[b]*RESSLab, EPFL, Lausanne, Switzerland*
[c]*Instituto Superior Técnico, Lisbon, Portugal*
**Corresponding author: alain.nussbaumer@epfl.ch*

Keywords: Flange tip attachments; Fatigue behaviour; Fracture mechanics; Initiation-propagation model; Double slope S-N curve.

ABSTRACT

Steel bridges have become slender and lighter with the generalisation of welded connections, increasing the relevance of fatigue phenomena and, as a result, fatigue design has become a leading ultimate limit state verification. During their life, constructional details may experience up to $200 \cdot 10^6$ cycles due to traffic loads. While the majority of these stress ranges are below the Constant Amplitude Fatigue Limit (CAFL), some few high stress cycles can trigger the start of fatigue damage and lead the remaining load spectra to become damaging. The damage process due to stress ranges below the CAFL, depends on the load spectra, and design provisions based on a double slope S-N curve, originating from Haibach's model and used in the Eurocodes, have shown to be unsafe under some conditions [1]. The behaviour under spectra loading is thus of major importance for the fatigue design of steel bridges.

This paper, extracted from [2], focuses on the fatigue behaviour of welded joints under variable amplitude loads. Fatigue tests have been conducted under constant and variable amplitudes on a typical bridge detail, often used previously by Gurney, see Fig. 1, with results up to $70 \cdot 10^6$ cycles, both under constant (R = 0.5) and variable amplitude ("stalactitical" bloc load sequence, R = 0.5 to 0.1).

The damaging character of stress cycles with amplitudes below the CAFL was investigated with experimental crack growth curves, obtained using the Alternative Current Potential Drop method (ACPD), which showed the detrimental effect of stress ranges below the conventional CAFL.

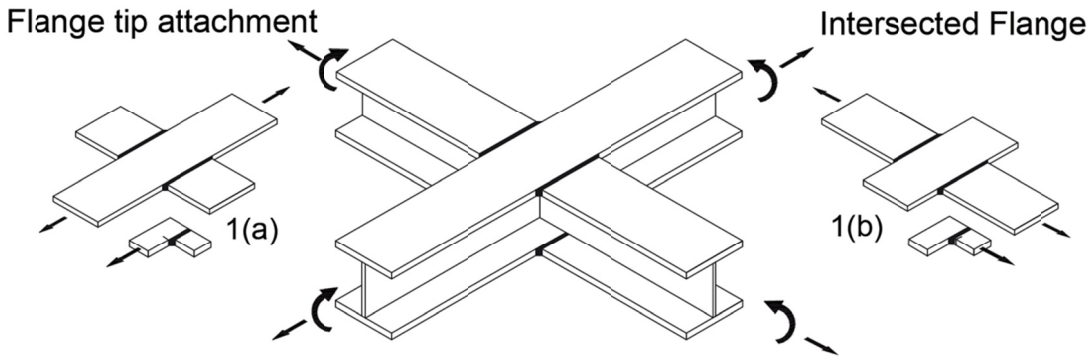

Fig. 1. Typical bridge deck detail and the 2 specimen configurations tested, with further distinction between (a) Flange tip attachment and (b) Intersected Flange.

A two-step model with initiation-propagation was established to estimate the experimental fatigue lives. It uses a local notch strain approach to model initiation life, accounting for local repeated yielding [3]. Local elasto-plastic strains are considered by Neuber's notch rule and material cyclic strain-stress curve is modelled with the Ramberg-Osgood relation. A classical fracture mechanics crack propagation

model based on Paris Law is used for crack propagation. The model is applied to different load spectra, with due account for the sequential threshold drop effects and initiation life. Total fatigue life (N_{total}) is divided in crack initiation (N_i) and propagation (N_p). The model was implemented in a probabilistic Monte Carlo framework to include the random nature of the main parameters on simulations to characterise the shape of the S-N curve under constant and variable amplitude loads. The results of the simulations show that load spectra shape can be correlated with the S-N curves, namely the 2nd slope value, denominated k, below the CAFL. A Type II Generalised Extreme Value distribution is fitted to the histogram of all simulated k values. Fig. 2 shows an example of the variable amplitude S-N curves for a linear spectra shape factor (ν =1). The 2nd slope value depends both on the notch case and the load spectra and for load spectra characterised by a Weibull frequency distribution, it can be reasonably estimated by $k=m+2/\nu$, where ν is the Weibull shape parameter.

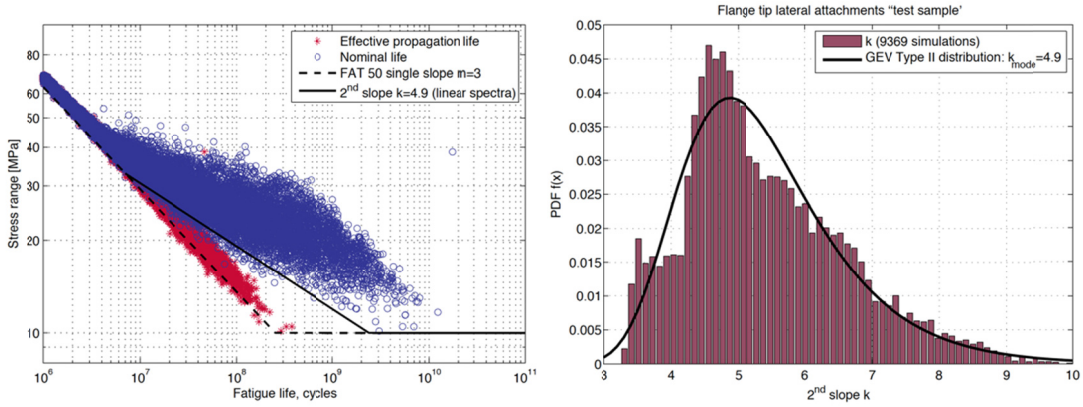

Fig. 2. Example of variable amplitude S-N curves simulations, linear spectra shape factor, 2nd slope value k = 4.9.

REFERENCES

[1] Gurney, T.: Cumulative damage of welded joints. Woodhead Publishing Limited, Cambridge, England (2006).

[2] Baptista, C.: Multiaxial and variable amplitude fatigue in steel bridges. PhD thesis n° 7044, EPFL/IST, EPFL, Switzerland (2016).

[3] Chattopadhyay, A., Glinka, G., El-Zein, M. et al.: Stress analysis and fatigue of welded structures, Welding in the World 55(7-8), 2-21 (2011).

ACKNOWLEDGMENTS

The work presented here was carried out at within the « IST-EPFL Doctorate Joint Initiative », with a grant from the Portuguese SNF (FCT), n° SFRH / BD / 75203 / 2010 and a sponsorship of GRID-Consulting Engineers SA, Lisbon. The experimental work presented in this paper was conducted at the Structural Laboratory of the Civil Engineering Department at the Swiss Federal Institute of Technology at Lausanne (EPFL). Special thanks are due to S. Demierre, G. Rouge, Frederique Dubugnon, Gilles Guignet and Armin Krkic for their technical assistance during laboratory testing. Special acknowledgments are due to Prof. Nitschke-Pagel for performing the residual stress measurements at IFS Braunschweig University in Germany.

Fatigue Resistance of Single Shear Preloaded Bolted Connections – Experimental Tests on Standard and Resin Injected Bolts

B. Pedrosa[a*], J.A.F.O. Correia[a,b], C. Rebelo[a], A. Jesus[b], M. Veljkovic[c], L. Simões da Silva[a]

[a] *Department of Civil Engineering, University of Coimbra, Rua Luis Reis Santos, 3030-788 Coimbra, Portugal*
[b] *Faculty of Engineering, University of Porto, Rua Dr. Roberto Frias, 4200-465 Porto, Portugal*
[c] *Faculty of Civil Engineering and Geosciences, Delft University of Technology, Delft, Netherlands.*
**Corresponding author: bruno.pedrosa@uc.pt*

Keywords: Fatigue assessment, Injected bolts, Strengthening operations.

ABSTRACT

Maintenance and safety assurance of old riveted bridges designed in the period which steel has become an economically viable material for bridge construction, i.e., between the end of the 19th and the beginning of the 20th century, deserve special attention. These structures are prone to present high levels of structural degradation due to their long service life [1]. Repairing and strengthening operations of old riveted steel bridges may use alternative fastening techniques, such as rivets, welding, high strength friction grip bolts, fitted bolts and resin-injected bolts. The mechanical performance of resin-injected bolts have been demonstrated essentially based on quasi-static or creep tests [2]–[4], which strengthen the importance to assess its fatigue strength [5]. Injection bolts can be produced from standard bolts adapting them for the resin injection process as mentioned in Annex K of EN 1090-2 [6] and illustrated in Fig. 1.

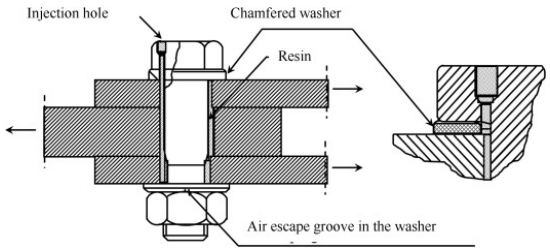

Fig. 1. Injection bolt in a double lap joint.

Specimens are composed of steel plates manufactured with new steel S355 and plates composed of puddled iron extracted from structural elements of a centenary Portuguese bridge named Eiffel bridge. A total of 24 specimens were tested including two types of bolts – resin injected and standard bolts – and four distinct stress amplitudes – low cycle, high cycle and two levels for medium cycle fatigue regimes. Two M24 bolts of high strength class 10.9 were used and preload was determined as $0.7 f_{ub} A_s$. Since this experimental study aims to reproduce a rehabilitation campaign in an old steel bridge, no special treatment was given to the plate surfaces. The adhesive used for injection bolts was the epoxy based resin Sikadur®-52. Specimens were tested on a WALTERBAI Servohydraulic Universal Testing Machine rated to 600 kN under load control with a stress R-ratio equal to 0.1. The test frequency was set to 5 Hz. Fatigue experimental results are presented in Figure 2 in the form of S-N curves. Run-outs are identified with an arrow. In what concerns the comparison between the obtained data and the design recommendation on EC3-1-9 [7], it is clear that detail 90 does not represent a safe design criterion. The mechanical heterogeneities that characterize old steel material influenced the fatigue strength of the

studied detail. A statistical approach was implemented based on ASTM E739-91 [8] and the lower boundary of the 95% confident band was defined. It is clear that the influence of resin was not evident for the tested specimens. Fatigue results were also compared with Taras and Greiner proposal [9] for one shear riveted joints with old steel materials. It is a safe design criterion. In order to adapt this proposal to bolted connections, authors suggest to adopt the same slope and a detail category of 90 MPa.

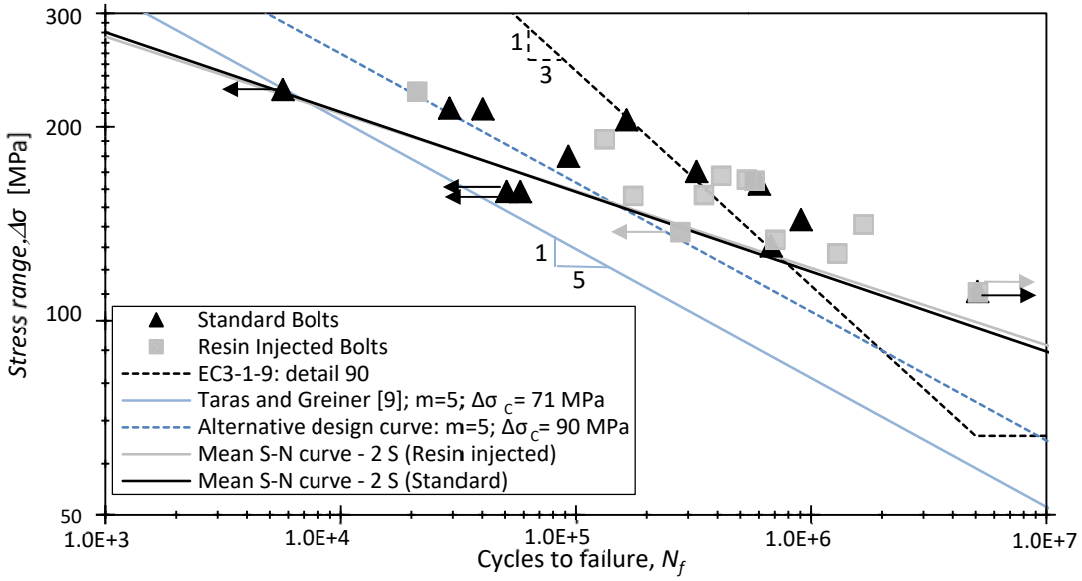

Fig. 2. S-N fatigue data from single shear preloaded bolted connections

REFERENCES

[1] Akesson, B.: Fatigue life of riveted railway bridges, 1st ed., London, UK (1994).

[2] European Convention for Constructional Steelwork (ECCS): European Recommendations for Bolted Connections with Injection Bolts. Publication No. 79 (1994).

[3] Mattes, J.: Substituição de Rebites por Parafusos Injetados com Resina, M.Sc. Thesis, IST/UTL, Lisboa (2007).

[4] Gresnigt, A.M., Sedlacek, G., Paschen, M.: Injection Bolts to Repair Old Bridges. pp. 349-360, (http://www.epicuro.co.uk/uploads/349.pdf) (August 2018).

[5] Correia, J., Pedrosa, B., Raposo, P., De Jesus, A., Gervásio, H., Rebelo, C., Calçada, R., Simões da Silva, L.: Fatigue strength evaluation of resin-injected bolted connections using statistical analysis. Engineering 3(6), 795–805 (2017).

[6] European Committee for Standardization (CEN): EN 1090-2: Execution of steel structures and aluminium structures - Part 2 (2008).

[7] European Committee for Standardization (CEN): EN 1993-1-9: Eurocode 3: Design of steel structures – Part 1-9: Fatigue (2005).

[8] American Society for Testing and Materials (ASTM): ASTM E739-91: Standard Practice for Statistical Analysis of Linear or Linearized Stress-Life (S-N) and Strain-Life (ε-N) Fatigue Data (2012).

[9] Taras, A., Greiner, R.: Statistical Background to the Proposed Fatigue Class Catalogue for Riveted Components. Report: Contribution to WG6.1 – Assessment of Existing Steel Structures, ECCS TC6, Spring Meeting – Lausanne – March 22-23 (2010).

ACKNOWLEDGMENTS

The authors acknowledge the Portuguese Science Foundation (FCT) for the financial support through the post-doctoral grant SFRH/BPD/107825/2015. The authors grate-fully acknowledge the funding of PROLIFE - Prolonging Life Time of Old Steel and Steel-Concrete Bridges (RFSR-CT-2015-00025) by Research Fund for Coal and Steel (RFCS).

Evaluation of Distortion-Induced Fatigue Cracking of Highway Bridge Critical Details Considering Road Surface Deterioration Effects

G. Alencar[a*], J.G.S. da Silva[b], A. de Jesus[c], R. Calçada[a]

[a] *CONSTRUCT, Faculty of Engineering of University of Porto, Rua Dr. Roberto Frias, 4200-465, Porto, Portugal.*
[b] *FEN/UERJ, State University of Rio de Janeiro, Rua São Francisco Xavier, Rio de Janeiro, Brazil.*
[c] *LAETA-INEGI, Faculty of Engineering of University of Porto, Rua Dr. Roberto Frias, 4200-465, Porto, Portugal.*
**Corresponding author: guilherme.alencar@fe.up.pt*

Keywords: Distortion-induced fatigue; Road-roughness condition; HSS method; Highway bridges.

ABSTRACT

According to an estimation [1], nearly 90% of all fatigue cracking is the result of out-of-plane distortion secondary stresses at fatigue-sensitive details (Fig. 1b). In this study, numerical analyses on a distortion-induced fatigue critical detail of a composite steel-concrete highway bridge (Fig. 1) were performed considering the hot-spot S-N approach and the nominal S-N approach [2]. Both global 2D and 3D model and local refined solid models were developed in ANSYS. Dynamic analyses were performed through the mode superposition method [3] taking into account the vehicle-bridge dynamic interaction [4]. The main goal was to perform a more realistic fatigue life evaluation considering pavement deterioration effects, also supported by a local stress approach in order to demonstrate the peculiarities of such analysis (Fig. 2). Therefore, it was adopted deterioration model of the pavement (RRC_t) found in [5,6], Eq. (1), which depends on: i) the type of fatigue vehicle by means of the equivalent 18-kips AASHTO single axle load (CESAL); ii) the initial road-roughness condition in terms of the International Road-roughness Index (IRI_0); iii) the time t in years; iv) an environmental coefficient, η, which varies from 0.01 to 0.7; and v) the Structural number (SNC) of the bridge pavement layer.

$$RRC_t = 6.1972\times10^{-9}\cdot\exp\{[1.04^{\eta t}.[IRI_0 + 263(1+SNC)^{-5}(CESAL)_t]]/0.42808\} + 2\times10^{-6} \quad (1)$$

Multiple numerical simulations were performed throughout all the bridge's life-cycle considering a common linear damage limited by a value of 0.5 to reach failure, in order to perform fatigue life estimations thus comparing the different fatigue strength approaches and numerical models. Besides the capacity to identify the most prone location to fatigue crack initiation, also confirmed by experimental observation in real cracked bridges [1], the results (see Table 1) have shown very non-conservative results obtained for the traditional nominal S-N approach when compared to the HSS method, which is an indication of the greater suitability of the latter to investigate the fatigue behaviour of complex welded joints subjected to complex out-of-plane loading.

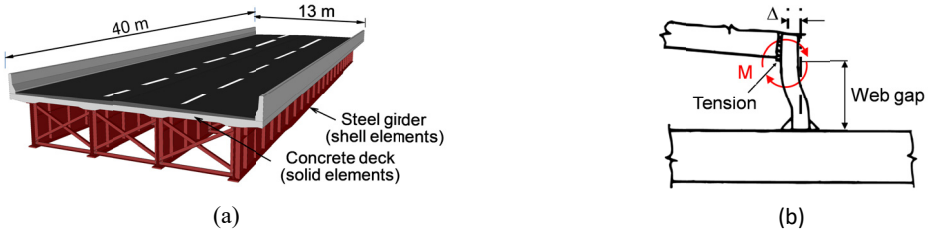

Fig. 1. (a) investigated highway bridge [7], (b) distortion-induced loading mechanism in web gaps.

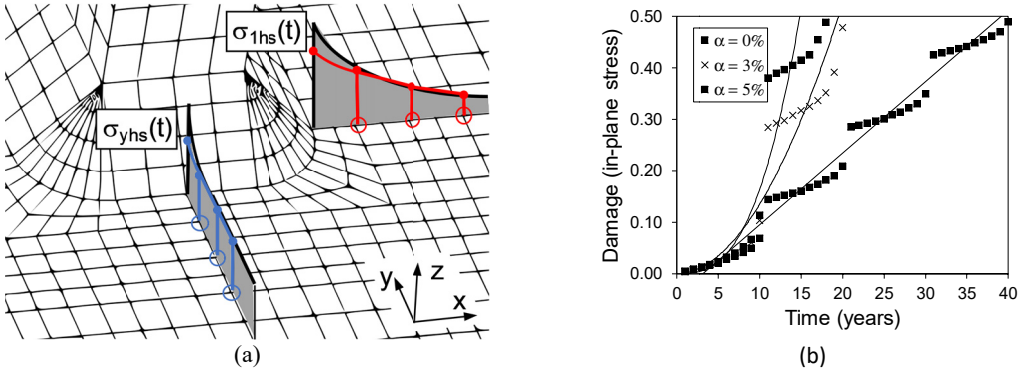

Fig. 2. (a) in-plane [$\sigma_{1hs}(t)$] and out-of-plane [$\sigma_{yhs}(t)$] transient hot-spot stresses, (b) example of damage accumulation pattern for the Hot-spot S-N approach [$\sigma_{1hs}(t)$] considering different traffic growth rates (α).

Table 1. Fatigue life estimations of the investigated bridge critical detail ($\gamma_{Mf} = 1.35$) in years [7].

Evaluation approach	FE numerical model	S-N Curve	Stress dir.	Traffic growth (α)		
				0%	3%	5%
Nominal S-N approach	2D Bridge beam model	FAT 80	In-plane σ_x	>>100	61	47
Nominal S-N approach	3D Bridge global model	FAT 80	In-plane σ_x	>>100	88	60
Hot-spot S-N approach	3D detail local model	FAT 100	In-plane σ_{1hs}	106	38	34
Hot-spot S-N approach	3D detail local model	FAT 100	Out-of-plane σ_{yhs}	41	20	19

REFERENCES

[1] Fisher, J.W., Roy, S.: Fatigue damage in steel bridges and extending their life. Adv. Steel Constr. 11, 250–68 (2015).

[2] EN 1993-1-9. Eurocode 3: Design of steel structures - Part 1-9: Fatigue Fatigue strength of steel structures, European Comitte for Standardization, Brussels (2005).

[3] Albuquerque, C., De Castro, P.M.S.T., Calçada, R.: Efficient crack analysis of dynamically loaded structures using a modal superposition of stress intensity factors. Eng. Fract. Mech. 93, 75–91 (2012).

[4] da Silva, J.G.S.: Dynamical performance of highway bridge decks with irregular pavement surface. Comput. Struct. 82, 871–881 (2004).

[5] Paterson, W., Attoh-Okine, B.: Summary models of paved road deterioration based on HDM-III. Transp Res Rec, 99–105 (1992).

[6] Zhang, W., Cai, C.S.: Fatigue Reliability Assessment for Existing Bridges Considering Vehicle Speed and Road Surface Conditions. J. Bridg. Eng. 17, 443–453 (2012).

[7] Alencar, G., de Jesus, A.M.P., Calçada, R.A.B., Silva, J.G.S.D.: Fatigue life evaluation of a composite steel-concrete roadway bridge through the hot-spot stress method considering progressive pavement deterioration. Eng. Struct. 166, 46–61 (2018).

ACKNOWLEDGMENTS

The authors gratefully acknowledge the financial support for this research work provided by the Brazilian Science Foundation's CNPq (doctoral scholarship process 203662/2014-8), CAPES and FAPERJ. Authors acknowledge the Portuguese Foundation for Science and Technology for the funding, particularly through the Project POCI-01-0145-FEDER-007457 - CONSTRUCT - Institute of R&D in Structures and Construction funded by FEDER funds through COMPETE2020 - Programa Operacional Competitividade e Internacionalização (POCI).

Risk Analysis and Safety of Large Structures and Components

Symposium D-RAS-ICMFM

Organized by:

Aleksandar Sedmak, Serbia

José A. F. O. Correia, Portugal

Vladimir Moskvichev, Russia

Abílio M. P. de Jesus, Portugal

Andrei Kotousov, Australia

Grzegorz Lesiuk, Poland

John Leander, Sweden

Matthew Hebdon, USA

Miguel Muñiz-Calvente, Spain

Rui Calçada, Portugal

&

Structural Integrity of Renewable Energy and Oceanic Structures

Symposium H-SIOS-ICMFM

Organized by:

Carlos Rebelo, Portugal

José António Correia, Portugal

José Miguel Castro, Portugal

Maria Nogal, Ireland

Sudath Siriwardane, Norway

Tiago Ferradosa, Portugal

Nicholas Fantuzzi, Italy

Fatigue Resistance Models of Structural for RBI-Maintenance

S. Belodedenko[a], G. Bilichenko[a], A. Baglay[a], A. Grechany[a]

[a] *Mechanical Engineering Department, National Metallurgical Academy of Ukraine, Ukraine*
**Corresponding author: sergeibelo@gmail.com*

Keywords: Risk; Overload; Damage; Lifetime; Safety index.

ABSTRACT

Structural whose failure is related with significant consequences can be designed with a large margin of safety. As a result of this, they have a long, but unfortunately an indefinite (uncertainty), period of operation. The advanced strategy by technical conditions to which belongs RBI (risk based inspection)-maintenance, does not assume the decommissioning of a subject through a fixed period. After a specified period, technical condition check is provided, after which a decision is taken on further operation of the facility. This period, according to the ALARP principle, depending on the probability and severity of the failure is no less 1 year.

This does not mean that in the period between inspections, one should forget about monitoring the state of the structure. The evaluation of the technical condition is carried out by checking the diagnostic parameters which react for the action of damaging processes. However, control of damages is still difficult to implement by direct (physical) methods. In practice, this is done through load monitoring. This indirect method needs regular, not periodic, registration. It is difficult to organize such a procedure. Therefore, the principle of Standardized Load Histories is used, due to which it is possible to refuse continuous monitoring, but to control the accumulation of damages [1].

With the correct application of diagnostic algorithms, the forecast reliability indicators are adequate to the actual ones. The required level of safety is observed. Its decrease, as a rule, is due to the appearance of rare overloads. Then the loading process can be modeled as block, consisting of the main background process with damage per cycle d_b and overloads with damage d_{ol}. This approach requires the availability of extended data on fatigue resistance. This article is devoted to their consideration.

In order to quickly determine the damage d through the durability of N as $d = 1 / N$, instead of the traditional *S-N* curve, the lifetime general equation (LGE) should be used, where the main factors are the arguments - amplitude stress σ_a, average cycle stress σ_m or cycle asymmetry coefficient R, theoretical coefficient of stress concentration α_σ:

$$lgN = b_0 - mlg\sigma_a - b_R R - b_\alpha \alpha_\sigma + b_{RR} R^2 - b_{\alpha\alpha}\alpha^2 + b_{m\alpha}\alpha_\sigma \cdot lg\sigma_a \ , \quad (1)$$

where $b_i\ b_{ii}\ b_{ij}$ - sensitivity coefficients to the effect of factors, m - rate of *S-N*-curve slope or sensitivity to fatigue stress amplitude.

For fixed values of R and α_σ, the LGE are transformed into *S-N*-curves; for fixed values of N and α_σ from LGE, analogues of limiting amplitudes are obtained; from the fixed values of σ_a and σ_m, R, the effective stress concentration coefficients are calculated from the function $N\ (\alpha_\sigma)$.

The second basic relationship, combining the results of fatigue tests, is the equation for the dispersion of durability. It is represented by the linearized function of the lifetime logarithm S_{lgN} standard deviation from its median value $\overline{lgN}$:

$$S_{lgN} = \mathrm{B} + k\left(\overline{lgN} - lgN_A\right). \tag{2}$$

The parameters of the equation *B, k,* lgN_A are determined experimentally when obtaining a fatigue reference curve, which precedes the experiments to obtain the LGE. This dependence is necessary for the search the lifetime distribution function (LDF), which is involved in risk assessment.

The third model is the accumulated damage function a_0:

$$a_0 = a_{ol} + \Delta a_b + \Delta a_R \quad , \tag{3}$$

where $a_{ol}=a_0(X_{ol})$ – basic function of accumulated damage;

Δa_b– correction of the base function from the influence of the factor $X_b=d_b10^7$;

Δa_R – correction of the base function from the influence of the asymmetry of the cycle R.

The main factor that affects the accumulation of damage during overloads is its relative value $X_{ol} = d_{ol} / d_b$. The basic function has non-monotonic behavior and can be represented as:

$$a_{ol} = lg\left[10^p X_{ol}^{-m_1} exp\left(-\frac{X_{ol}}{X_0}\right) + 10^A X_{ol}^{m_2}\left(1 - exp\left(-\frac{X_{ol}}{X_0}\right)\right)\right]. \tag{4}$$

The parameters of the equation *p, A,* X_0, m_1, m_2 are partially determined experimentally, partially selected by recommendations.

The combination of three models of fatigue resistance allows not only to locate accurately the LDF, but also to solve the problem of very high cycle fatigue [2]. For this region it is difficult to establish experimentally the limits of endurance. The idea of using block-program tests for this is not new. Due to it there are accelerated fatigue tests. In this aspect, the function Δa_b is actual. Knowing its behavior at $X_b < 1$, we can estimate the lifetime at very small amplitudes of the baseline process.

REFERENCES

[1] Będkowski, W.: Assessment of the fatigue life of machine components under service loading – a review of selected problems. Journal of theoretical and applied mechanics 52(2), 443–458 (2014).
[2] Arcari, A., et al.: Variable amplitude fatigue life in VHCF and probabilistic life predictions. Procedia Engineering 114, 574 – 582 (2015).

Comparison of the Structural Reliability of Corroded X52 Steel Pipeline Using Different Monte-Carlo Techniques

Mohamed El Amine Ben Seghier[a*], Joelton Barbosa[a,c], José A.F.O Correia[b], Abílio De Jesus[b]

[a] *Laboratory of Petroleum Equipment's Reliability and Materials, University M'hamed Bougara of Boumerdes Boumerdes, Algeria E-mail: benseghier.ma@univ-boumerdes.dz*
[b] *INEGI, Faculty of Engineering, University of Porto, Rua Dr. Roberto Frias, 4200-465 Porto, Portugal. E-mail: jacorreia@inegi.up.pt; ajesus@fe.up.pt*
[c] *Federal University of Rio Grande do Norte, Natal, Brazil. E-mail: joeltonfb@gmail.com*
**Corresponding author: benseghier.ma@univ-boumerdes.dz*

Keywords: Oil pipeline; Corrosion; Failure probability; Monte Carlo technique.

ABSTRACT

The reliability levels of corroded oil pipeline are an important matter to the owners and the environment due to the catastrophic consequence, which could happened from the rupture or the leak of these pipelines. Recently, a different method are developed to estimate the failure probability in engineering problems based on the Crude Monte-Carlo technique to improve this simple technique. In this paper, a comparison between different methods based on Monte-Carlo technique are carried out to investigate the structural reliability of a corroded pipeline carrying oil made in X52 steel. Both external and internal corrosion defects obtained from periodic inspection are included in the calculation. The aim of this study is to find the most efficient and robust method with the less computational cost for evaluating the failure probability of corroded pipelines.

An Enhanced Sequential Optimization and Reliability Assessment Strategy and its Application in Uncertainty-Based Multidisciplinary Design and Optimization

Debiao Meng[a*], Yan Li[a], Qing Ai[b, c], Hua Zhang[d]

[a] *School of Mechanical and Electrical Engineering, University of Electronic Science and Technology of China, China*
[b] *Department of Civil Engineering, Shanghai Jiao Tong University, Shanghai, China*
[c] *College of Civil Engineering, Tongji University, Shanghai, China*
[d] *Shanghai Institute of Satellite Engineering, China*
**Corresponding author: dbmeng@uestc.edu.cn*

Keywords: Sequential optimization and reliability assessment; Shifting vector; Reliability index; Uncertainty-based multidisciplinary design and optimization; Solar array drive assembly.

ABSTRACT

With the development of concurrent engineering, Uncertainty-based Multidisciplinary Design and Optimization (UMDO) has been widely utilized to obtain high reliability and safety for complex systems [1-3]. In general, there is a three-level optimization structure in UMDO. The original design space is explored in the outer loop. The multidisciplinary coupling analysis is performed in the inner loop. Between outer and inner loop, reliability evaluation is conducted.

The Sequential Optimization and Reliability Assessment (SORA) strategy is a powerful method which can decouple the above three-level optimization problem into sequential cycles of deterministic Multidisciplinary Design and Optimization (MDO) problems with modified constraints and probability analysis [4-6]. In each cycle, the probability analysis follows the solution of deterministic MDO. After solving the deterministic MDO, the reliability index is obtained by uncertainty analysis. According to the Performance Measure Approach (PMA), then, the shifting vectors can be constructed based on the reliability index to convert uncertainty constraints into equivalent deterministic constraints. During this process, PMA can find the minimum performance function value while target reliability index can also be satisfied. However, the performance functions in MDO problems are generally high nonlinear. In this situation, it is different for the shifting vector obtained by PMA to give right moving direction of limit state constraints, which is shown in Fig. 1.

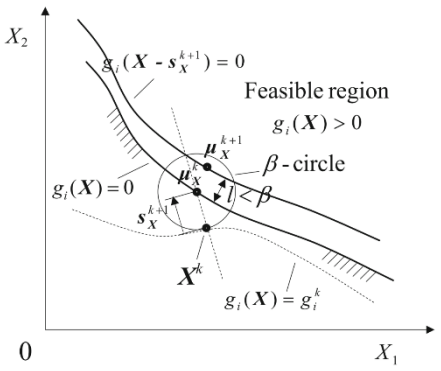

Fig. 1**.** The SORA and shifting vector in highly-nonlinear performance function [4].

To deal with the above challenge, a modified shifting vector (MSV) method is proposed and developed in this study. Based on MSV, the enhance SORA strategy is utilized to decouple UMDO and improve the design efficiency. Shifted limited state function is involved to search most probable point and derive MSV to deterministic optimization model for the next cycle, instead of the specific performance function. In order to illustrate the effectiveness of the proposed method, a UMDO problem of solar array drive assembly is solved here, which is illustrated in Fig. 2. The uncertainties in material properties and the multidisciplinary interactions between structure and thermology are considered here. The UMDO process is illustrated in Fig. 2.

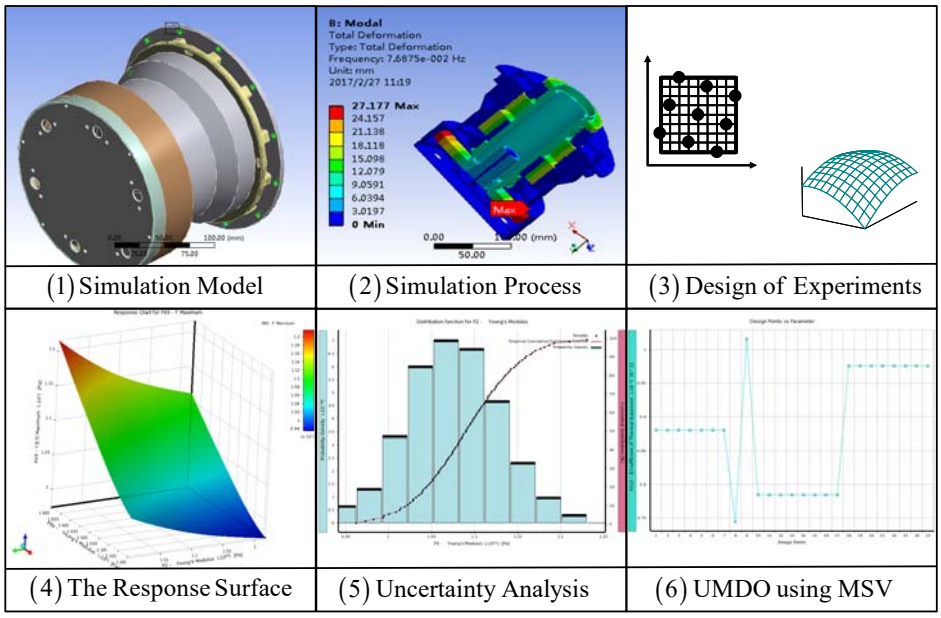

Fig. 2. The SORA and shifting vector in highly-nonlinear performance function.

REFERENCES

[1] Meng, D., Zhang, H., Huang, T.: A concurrent reliability optimization procedure in the earlier design phases of complex engineering systems under epistemic uncertainties. Advances in Mechanical Engineering 8(10), 1-8 (2016).
[2] Meng, D., Li, Y., Huang, H.Z., Wang, Z., Liu, Y.: Reliability-based multidisciplinary design optimization using subset simulation analysis and its application in the hydraulic transmission mechanism design. Journal of Mechanical Design 137(5), 051402-1-9 (2015).
[3] Meng, D., Huang, H.Z., Wang, Z., Xiao, N.C., Zhang, X.: Mean-value first-order saddlepoint approximation based collaborative optimization for multidisciplinary problems under aleatory uncertainty. Journal of Mechanical Science and Technology 28(10), 3925-3935 (2014).
[4] Chen, Z., Qiu, H., Gao, L., Li, P.: An optimal shifting vector approach for efficient probabilistic design. Structural and Multidisciplinary Optimization 47(6), 905-920 (2013).
[5] Li, X., Qiu, H., Xu, F., Gao, L.: A new optimal shifting vector method using reliability index for reliability-based design optimization. In: Proceedings of the 7th Asia-Pacific International Symposium on Advanced Reliability and Maintenance Modeling, pp. 265-272. McGraw-Hill Education Press, Seoul, Korea (2016).
[6] Wang, X., Wang, R., Wang, L., Chen, X., Geng, X.: An efficient single-loop strategy for reliability-based multidisciplinary design optimization under non-probabilistic set theory. Aerospace Science and Technology 73, 148-163 (2018).

ACKNOWLEDGMENTS

The supports from the National Natural Science Foundation of China (Grant No. 51605080), the China Postdoctoral Science Foundation (Grant No. 2015M580780), and the China Postdoctoral Science Special Foundation (Grant No. 2017T100685) are gratefully acknowledged.

Computational-Experimental Approaches for Fatigue Reliability Assessment of Turbine Blisks

Shun-Peng Zhu[a]*, Qiang Liu[a], Weiwen Peng[a], Xian-Cheng Zhang[b]

[a] *Institute of Reliability Engineering, School of Mechanical and Electrical Engineering, University of Electronic Science and Technology of China, Chengdu 611731, China*

[b] *Key Laboratory of Pressure Systems and Safety, Ministry of Education, School of Mechanical and Power Engineering, East China University of Science and Technology, Shanghai 200237, China*

**Corresponding author: zspeng2007@uestc.edu.cn*

Keywords: Fatigue; reliability; uncertainty; sensitivity analysis; turbine blisk

ABSTRACT

In the present study, a computational-experimental framework is developed for fatigue reliability assessment of turbine blisks, which is shown in Fig. 1. Within the framework, the over speed testing is innovatively combined with stochastic finite element (FE) analysis for quantifying the uncertainty in the experimental data, material properties and loads. In detail, two schemes are elaborated in the framework based on probabilistic S-N curves and stochastic FE simulation by coupling with sampling techniques [1,2]. The stochastic FE simulation incorporates the Chaboche constitutive model with Fatemi-Socie [3,4] criterion for fatigue behaviour modelling and life prediction. Moreover, experimental deformation and numerical FE analysis are conducted according to the full-scale over speed tests of a turbine blisk under increased step-stress loadings. The probabilistic S-N curves and probabilistic $\log\omega$-$\log N_f$ curves are shown in Fig. 2 and Fig. 3, from which the PDF of fatigue life N_{f0} of the turbine blisk under the normal working condition can be obtained. Reliability sensitivity analysis is performed to provide an importance ranking of random variables [5,6], which are shown in Fig. 4 and Fig. 5. Results indicate that stochastic FE analysis-based scheme provides more conservative predictions than the probabilistic S-N curves-based one.

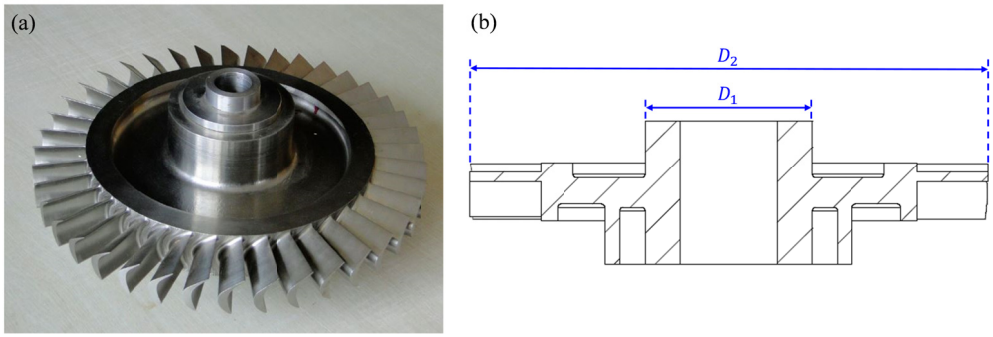

Fig. 1. Structural sketch of the turbine blisk (a) specimen and (b) sectional drawing.

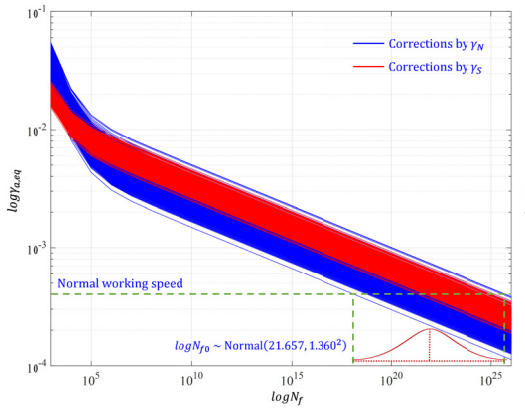

Fig. 2. Probabilistic *S-N* curves.

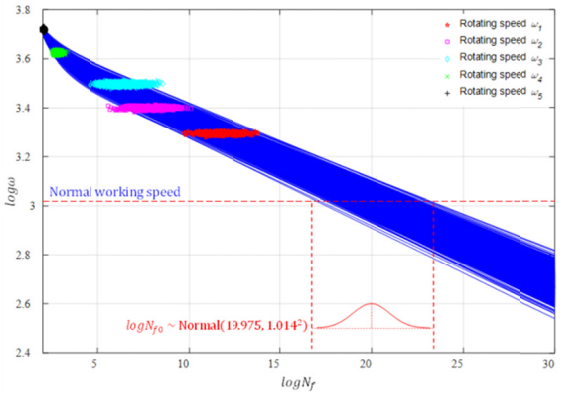

Fig. 3. Probabilistic $\log \omega$-$\log N_f$ curves.

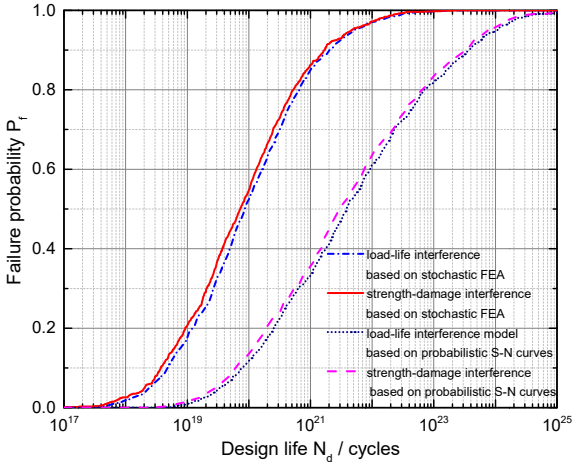

Fig. 4. Failure probability P_f vs. design life N_d.

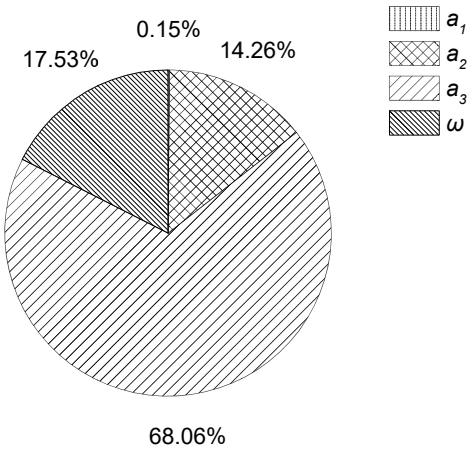

Fig. 5. Reliability sensitivity factors of random variables.

REFERENCES

[1] ASME BPVDC III-Div. 1., ASME boiler & pressure vessel design code – III Div. 1 – rules for construction of nuclear facility components (2005).

[2] Langer, B.: Design of pressure vessels for low-cycle fatigue. Journal of Basic Engineering 84(3), 389-399 (1962).

[3] Fatemi, A., Socie, D.F.: A Critical plane to multiaxial fatigue damage including out-of-phase loading. Fatigue and Fracture of Engineering Materials and Structures 11, 149-165 (1988).

[4] Yu, Z.Y., Zhu, S.P., Liu, Q., et al.: Multiaxial fatigue damage parameter and life prediction without any additional material constants. Materials 10(8), 923 (2017).

[5] Melchers, R.E., Ahammed, M.: A fast approximate method for parameter sensitivity estimation in Monte Carlo structural reliability. Computers and Structures 82, 55-61 (2004).

[6] Huang, X., Zhang, Y.: Reliability sensitivity analysis for rack-and-pinion steering linkages. Journal of Mechanical Design 132(7), 071012 (2010).

ACKNOWLEDGMENTS

Financial supports of the National Natural Science Foundation of China (No. 11672070 and 11302044), the China Postdoctoral Science Foundation Funded Project (No. 2015M582549 and 2017T100697), the Fundamental Research Funds for the Central Universities (No. ZYGX2016J208) and the Open Project Program of Key Laboratory of Deep Earth Science and Engineering (Sichuan University), Ministry of Education (No. DUSE201701) are acknowledged.

Data Truncation on the Extrapolation of Loads for Fatigue Analysis of Offshore Wind Turbine Towers

Rui Teixeira[a*], Maria Nogal[a], Alan O'Connor[a]

[a] *Department of Civil, Structural and Environmental Engineering, Trinity college Dublin, Ireland*
**Corresponding author: rteixeir@tcd.ie*

Keywords: Renewable energy; Offshore Wind Energy; Statistical Extrapolation; Fatigue analysis.

ABSTRACT

Design of offshore wind turbine (OWT) towers to structural fatigue is an effort demanding procedure. The current design practices recommend the definition of load distributions, extrapolation of loads and cycles to be used with the widely known linear damage summation rule [1,2].

In the particular case of the tower component fatigue design, its calculation for wind turbines, as a cumulative event, means that the designer needs to simulate and replicate the damage suffered by the wind turbine during its design life time (T).

Due to computational limitations, most of the times it is not feasible to replicate the OWT tower lifetime to its extent and the reliability assessment of these components is limited. Statistical techniques are applied to approximate the loads experienced by the turbine during its T full extent by using a shorter a lifetime (t) where the OWT operation is fully addressed.

Probabilistic limitations in the current fatigue design of wind turbine components with low S-N curve slope (m) were identified in reference [3].

Long term loads and their number of cycles are obtained with statistical extrapolation of a truncated set of data. Below the reference threshold, the loads are multiplied for T and accounted without any statistical background.

If approximation of the tail region is not accurate the loads can be over or underestimated. Similarly the process of extrapolation can have high influence in the cumulated fatigue damage ($\sum D_{SH}$) even if a high number of computational simulations is performed (e.g. not adequate selection of threshold value in Fig. 1). This has direct implication on the estimated cumulated damage and may produce erroneous results.

The current paper proposes then to identify the probabilistic limitations and characterize uncertainty in the calculation of OWT tower fatigue design life. Uncertainty is addressed by comparing different sets of data with a long-term reference simulation. The techniques used to truncate the data are discussed and the amount of statistical variation introduced by the statistical models compared with a reference 1 year simulation of operation.

The tower component, manufactured in steel, has some specificities of its own. Therefore, a comprehensive discussion on extrapolation of loads is presented in regard of these type of components, which are characterized by their low S-N slope.

Results show that OWT estimated T is highly dependent on t used for approximate T, on the truncation method and on the statistical model used.

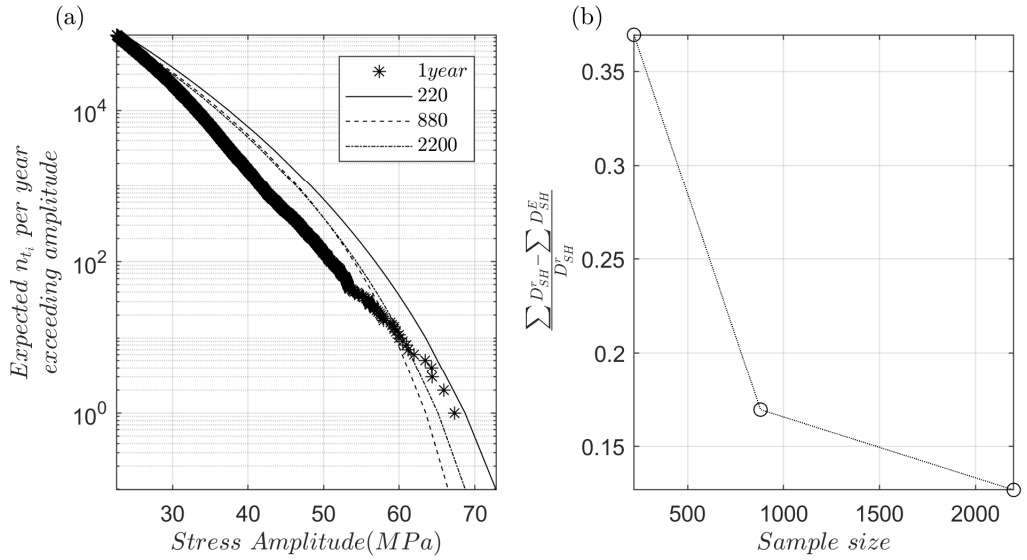

Fig. 1**.** (a) Comparison of fit of statistical models depending on the sample sizes and approximation o to the tail of a real one year distribution. (b) Error in the calculated cumulated damage ($\sum D_{SH}$) for different fits of the tail.

REFERENCES

[1] IEC: Wind turbines part 1: Design requirements. Technical Report 61400-1, International Electrotechnical Commission, Geneva, Switzerland (2005).
[2] IEC: Wind turbines part 3: Design requirements for offshore wind turbines. Technical Report 61400-3, International Electrotechnical Commission, Geneva, Switzerland (2009).
[3] Moriarty, P.J., Holley, W., Butter, C.P.: Extrapolation of extreme and fatigue loads using probabilistic methods. National Renewable Energy Laboratory (2004).

ACKNOWLEDGMENTS

This project has received funding from the European Union Horizon 2020 research and innovation programme under the Marie Skłodowska-Curie grant agreement No. 642453.

Fatigue Analysis for an Offshore Jacket-Type Platform Using Simplified and Local Approaches

António Mourão[a]*, José A.F.O. Correia[a], José Miguel Castro[a], Carlos Rebelo[b], Abílio M.P. de Jesus[a], Nicholas Fantuzzi[c], Rui Calçada[a]

[a] *Faculty of Engineering, University of Porto, Portugal*
[b] *Faculty of Sciences and Technology, University of Coimbra, Portugal*
[c] *Department of Civil, Chemical, Environmental and Materials Engineering, University of Bologna, Italy*
**Corresponding author: up201306134@fe.up.pt*

Keywords: Fatigue analysis; offshore platform; SCF parametric equations; Local approaches.

ABSTRACT

Fatigue cumulative damage in offshore structures is caused by external environmental loads. The fatigue analysis for these structures is made using design codes, namely, DNVGL-RP-0005:2014-06 [1], GD-09-2013 [2], EN 1993-1-9 [3], BS5400 [4], guide for fatigue assessment of offshore structures proposed by American Bureau of Shipping [5], recommendations for fatigue design of welded joints and components suggested by IIW [6], among others.

The environmental loading conditions for the North Sea are based on the wave measurements using recorders kept at the sea surface and practice recommendations proposed by DNVGL [7]. In this way, the fatigue analysis can be done based on Palmgren-Miner rule using global S-N curves and simplified fatigue approach using the two-parameter Weibull distribution for the stresses.

In this paper, a fatigue analysis for an offshore jacket-type platform using simplified and local approaches is proposed. A comparison between the simplified fatigue approach proposed by the DNVGL and a fatigue local approach is made. The last is based on Neuber rule and Ramberg-Osgood description with aims to determine the local stress and strain ranges (see ref. [8]). Additionally, the Coffin-Manson strain-based curve is used to evaluate the fatigue damage [8].

The case-study used in this research work is an offshore jacket-type structure (see Figure 1) located in the North Sea, off the west coast of Norway. The platform sets on a sea bed 115.67m below the sea surface. The structure has 4 frames in the North-South direction and 2 perpendicularly. At mudline the structure has 80 x 60 m square meters and $80\times24m^2$ at topside, reviling the massive size of the metallic structure made from S420 structural steel, with an approximate number of 140 meters of height. For the fatigue analysis, the critical KT-type joint is composed by 6 secondary elements, 3 from the plane XZ and other 3 from YZ (see Figure 2). The tubular elements of the offshore platform are of S420 steel. However, for the fatigue analysis using the local approach was used the S355 steel by the unavailability of material data in the literature regarding fatigue results for S420 steel [9].

From this research, it is possible to conclude that all fall within safety limits imposed by the DNVGL standard. It is also possible to conclude that hot-spot stress-based approach does in fact achieve a more conservative depiction of fatigue damage of the structure when compared with nominal stresses (see ref. [8]). Additionally, it is also possible to ascertain that a fatigue analysis based on local strain fatigue damage parameter portrays a higher level of fatigue damage when compared with others approaches.

Since fatigue is a phenomenon of the material and the local approach is the only one to take material properties into consideration, as expected it presents a more conservative fatigue damage evaluation.

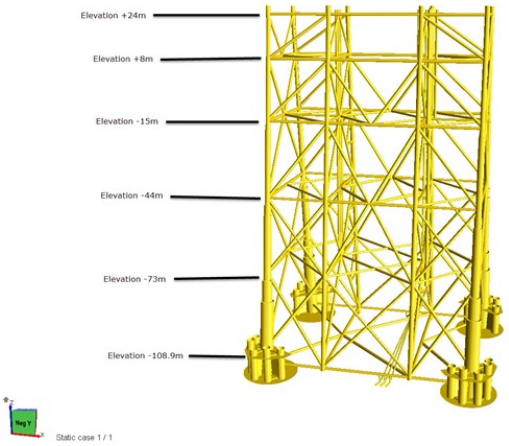

Fig. 1. Case study of an offshore jacket-type platform.

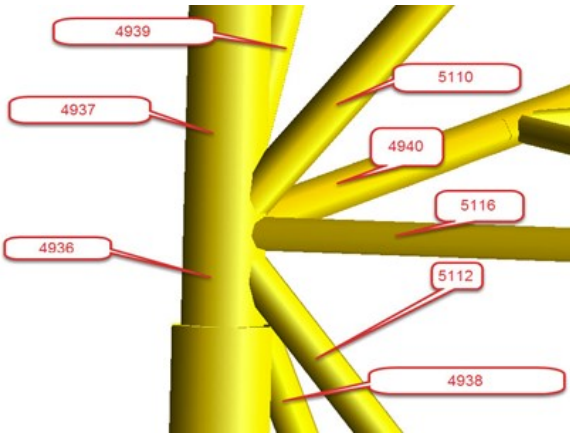

Fig. 2. Numbered elements of the critical joint (JT-RA-6).

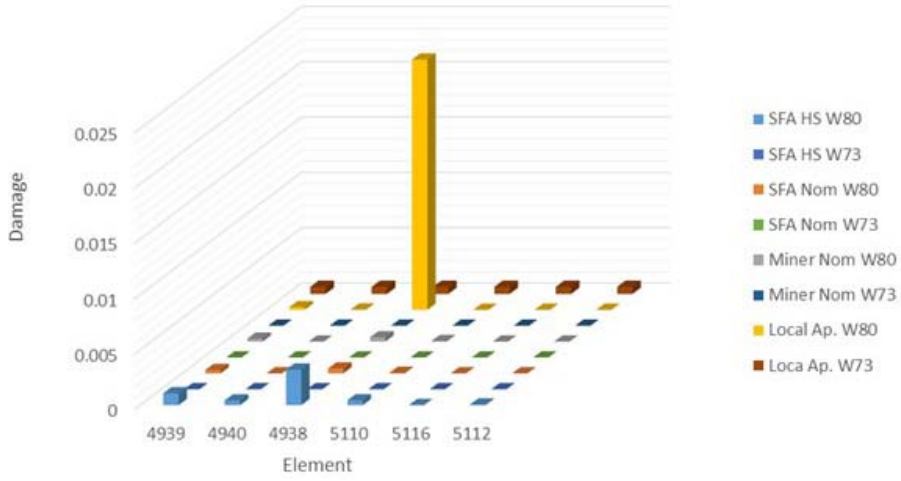

Fig. 3. Fatigue damage evaluation per element of the critical joint for simplified and local approaches.

REFERENCES

[1] DNV GL Group. DNVGL-RP-0005:2014-06: Fatigue design of offshore steel structures (2014).
[2] China Classification Society. GD-09-2013: Guidelines for fatigue strength assessment of offshore engineering structures (2013).
[3] CEN-TC 250. EN 1993-1-9: Eurocode 3, Design of steel structures – Part 1-9: Fatigue. European Committee for Standardization, Brussels (2003).
[4] British Standards Institution. BS7910:2005: Guidance on Methods for Assessing the Acceptability of Flaws in Metallic Structures (2005).
[5] American Bureau of Shipping. Guide for fatigue assessment of offshore structures; 2003, updated 2014.
[6] International Institute of Welding: Recommendations for Fatigue Design of Welded Joints and Components. Doc. XIII-2151r4-07/XV-1254r4-07; Paris, France, October 2008.
[7] DNV GL Group. DNVGL-RP-C205:2014: Environmental conditions and environmental loads; 2014.
[8] Mourão, A.: Fatigue analysis of a jacket-type offshore platform based on local approaches, MSc Thesis, 193 pages, Civil Engineering, Faculty of Engineering, University of Porto, Porto, Portugal (2018).
[9] Correia, J.A.F.O., de Jesus, A.M.P., Fernández-Canteli, A., Calçada, R.A.B.: Modelling probabilistic fatigue crack propagation rates for a mild structural steel. Frattura ed Integrita Strutturale 31, 80-96 (2015).

Structural Integrity and Lifing Solutions

Symposium E-FSI-ICMFM

Organized by:

Xiancheng Zhang, China

Shun-Peng Zhu, China

Dianyin Hu, China

Filippo Berto, Norway

Haijun Xuan, China

Zhiyong Huang, China

Wei Huang, China

Abílio M. P. de Jesus, Portugal

Crystal Plastic Finite Element Analysis of Creep-Fatigue Interaction of GH720Li Nickel-Based Superalloy

Dianyin Hu[a,b,c*], Jianxing Mao[a], Qihang Ma[a], Rongqiao Wang[a,b,c]

[a] *School of Energy and Power Engineering, Beihang University, Beijing 100191, China*
[b] *Collaborative Innovation Center of Advanced Aero-Engine, Beijing 100191, China*
[c] *Beijing Key Laboratory of Aero-Engine Structure and Strength, Beijing 100191, China*
**Corresponding author: hdy@buaa.edu.cn (D.Y. Hu)*

Keywords: Creep-fatigue; Crystal plasticity mechanics; Nickel-based superalloy; Finite element analysis.

ABSTRACT

The creep-fatigue failure of the nickel-based superalloy under high temperature is mainly due to the cracking of grain boundaries, of which the failure life is usually related to the grain size. In this study, the grain size effect on the creep-fatigue life of nickel-based superalloy GH720Li was analyzed by using crystal plastic finite element analysis method (CP-FEM), involving anisotropic crystal plasticity theory and representative volume element.

In order to characterize the plastic strain acceleration under creep-fatigue loading, improved nonlinear isotropic hardening rule and the kinematic hardening rule are employed to describe the plastic strengthening characteristics of individual crystal. Simulation results reveal that stress concentration is generated by the mechanical properties mismatch and non-uniform distributed constraints among grains, leading to the dependence of creep-fatigue failure on grain size in GH720Li.

Creep-fatigue experiments are conducted at an elevated temperature of 650°C with different grain sizes to verify the CP-FEM. The life prediction model is modified by the character of microstructural inhomogeneity in material, exhibiting a good agreement with obtained experimental data. Scanning electron microscopy observation illustrates a prominent correlation between grain boundary damage length and grain size, which is consistent with the simulated local stress-strain distribution. Thus, the CP-FEM can reflect the local deformation and damage in the grain scale, contributing to an effective solution for creep-fatigue damage in GH720Li superalloy.

Prediction of Fatigue Crack Initiation and the Life Time

Haohui Xin[a*], Milan Veljkovic[a]

[a] Faculty of *Civil Engineering and Geosciences, Delft University of Technology, Netherlands*
**Corresponding author: H.Xin@tudelft.nl*

Keywords: Fatigue crack initiation; Fatigue life time prediction; Smith, Watson, and Topper (SWT) damage model; Extended finite element approach.

ABSTRACT

The assessment of fatigue crack initiation and propagation behaviour of steel material is essential to predict fatigue behaviour of structural connections. Conventional finite element method (FEM) required mesh refinement to capture the singular asymptotic fields in the neighbourhood of the crack tip, the mesh must be updated continuously to match the discontinuity as the crack growth progresses. The extended finite element approach (XFEM) alleviates above shortcomings by enriching the displacement vector. As shown in Eq.(1), the enrichment functions included the near-tip asymptotic functions and a discontinuous function.

$$\mathrm{u} = \sum_{i=1}^{n} N_i(x)\left[u_i + H(x)a_i + \sum_{\alpha=1}^{4} F_\alpha(x) b_i^\alpha\right] \tag{1}$$

where $N_i(x)$ is general shape functions, u_i is general nodal displacement vector, the nodal enriched degree of freedom a_i and associated jump function $H(x)$ is used to represent the jump in displacement across the crack surfaces, the nodal enriched degree of freedom b_i and associated asymptotic crack-tip function $F_\alpha(\mathrm{x})$ is used to capture the singularity around the crack tip, n is total node number in the model.

XFEM-based cohesive segments method and phantom nodes is used to predict the fatigue crack initiation and propagation of structure steel. As illustrated in Fig.1, phantom nodes are superposed on the original real nodes aiming to represent the discontinuity of the cracked elements. When the fatigue crack initiation criterion is not reached, the element is intact and each phantom node is completely constrained to its corresponding real node. When the fatigue crack initiation criterion is fulfilled, the element is "cracked" and the element splits in two parts. Each part is formed by a combination of real and phantom nodes depending on the orientation of the crack. In this paper, a user-defined fatigue damage initiation subroutine (UDMGINI) based on Smith, Watson, and Topper (SWT) damage model is implemented in ABAQUS software package to predict the fatigue crack initiation. A crack is established or the crack length of an existing crack is extended when the fatigue crack initiation criterion *f*, see Eq.(2), reached the value 1.0, within a given tolerance. After the fatigue crack initiation criterion is achieved, the damage evolution law similar to surface based cohesive behaviour is used to predict fatigue crack propagation. The power law (Eq. 3) is employed to consider a mixed mode crack propagation.

$$f = 1.0 + \frac{1}{2}\sigma_{n,\max}\Delta\varepsilon_1 - \frac{\sigma_f'^2}{E}(2N)^{2b} - \sigma_f'\varepsilon_f'(2N)^{b+c} \tag{2}$$

$$\frac{G_{eq}}{G_{eq}^c} = \left(\frac{G_I}{G_I^c}\right)^n + \left(\frac{G_{II}}{G_{II}^c}\right)^n + \left(\frac{G_{III}}{G_{IIII}^c}\right)^n \tag{3}$$

where: $\sigma_{n,max}$ is maximum normal stress on the principal strain range plane, $\Delta\varepsilon_1$ is principal strain range, N is number of loading cycles, G and G^C represented fracture energy release rate and critical fracture energy release rate, respectively. σ_f', ε_f', b and c are material dependent parameters related to the fatigue behaviour.

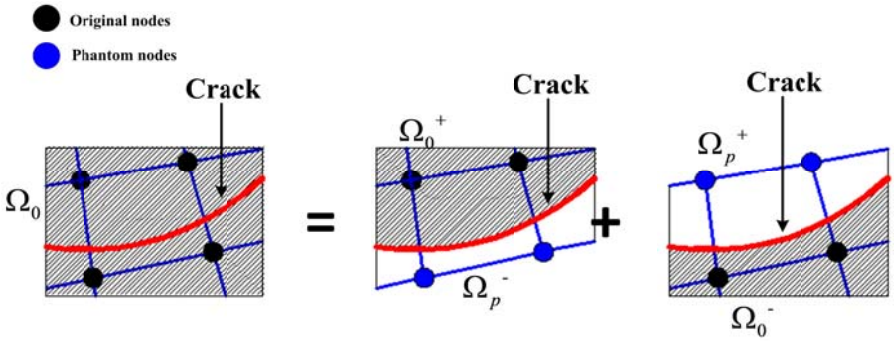

Fig. 1. The schematic of the phantom node method.

As is shown in Fig. 2, the simulation results are validated by comparing with results from experiments. Very successful prediction of the fatigue behaviour of coupon specimens made of S355 mild steel and S690 high strength steel is achieved. A typical failure mode of the coupon specimen is shown in Fig.3. The fatigue crack initiated near the fillet arches due to local stress concentration, and propagated towards centre line gradually, when the net section becomes insufficient to bear previous load the specimen raptures.

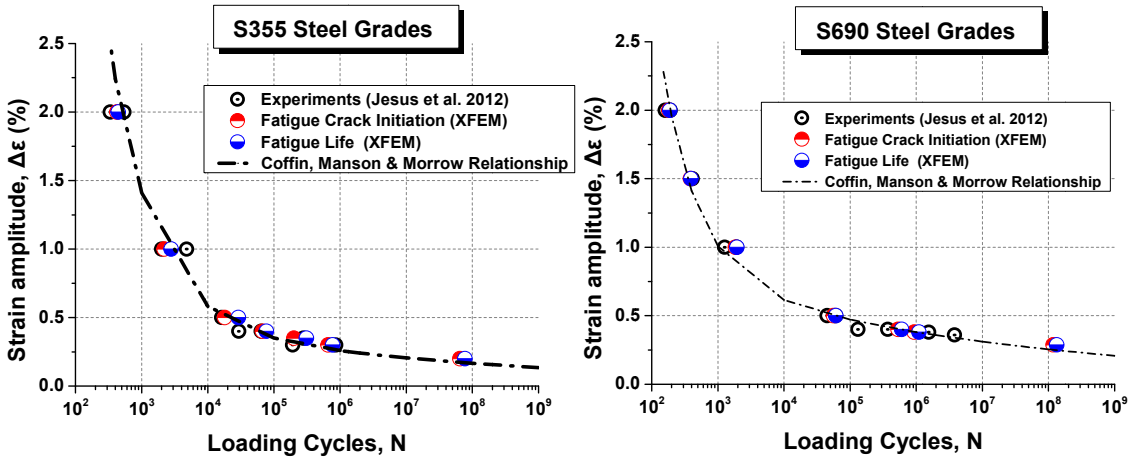

Fig. 2. Fatigue life time comparison between numerical and experimental results.

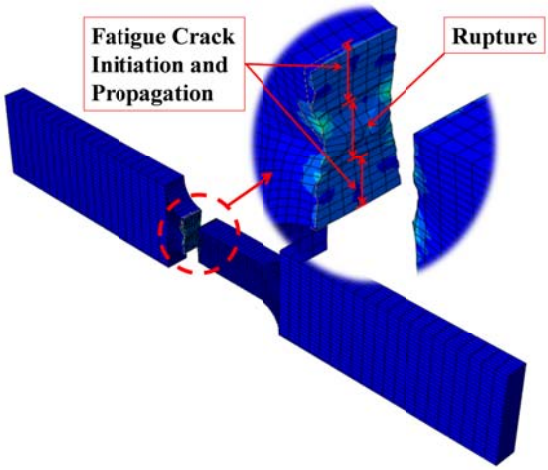

Fig. 3. A critical cross section of the coupon specimen prior the fracture.

Experimental Investigation on Low Cycle Fatigue and Creep-Fatigue Behaviour of MAR-M247 at 900°C

I. Šulák[a*], K. Obrtlík[a]

[a] *Institute of Physics of Materials, Academy of Sciences of the Czech Republic, Žižkova 22, 616 62 Brno, Czech Republic*
**Corresponding author: sulak@ipm.cz*

Keywords: Nickel-based superalloy; High temperature low cycle fatigue; Creep-fatigue interaction; Dislocation structure; Damage evaluation.

ABSTRACT

The daily routine of high-temperature facilities involves complex stress-strain loading where creep, fatigue and environmental damage take place. During start-ups and shut-downs periods, critical components often undergo repeated elastic-plastic loading resulting in a low cycle fatigue (LCF). However, the main part of the service is characterized by steady state conditions where creep is involved. LCF tests and creep-fatigue tests with tensile and compressive strain dwells (both in each cycle) were carried out under total strain control with the symmetrical waveform in polycrystalline nickel-based superalloy MAR-M247 at 900°C in air. Fatigue life curves in the representation of stress amplitude, total strain amplitude and plastic strain amplitude versus the number of cycles to failure were assessed and are shown in Fig. 1. Additional data of creep-fatigue interaction tests with only tensile dwells were to improve discussion of obtained results. Dwell sensitivity, manifesting itself in a reduction of fatigue life compared to continuous cycling, was observed both in the total strain amplitude representation and in the Basquin representation. The Coffin-Manson plastic strain representation shows an insignificant effect of dwells at the highest strain amplitude while a slight increase of fatigue life appears in medium and low total strain amplitude domain. Data obtained from stress relaxation curves were used to assess the fraction of creep damage. Generalized damage accumulation rule combining pure fatigue and pure creep data were used to evaluate damage due to fatigue-creep-environment interaction and it is represented by Eq. 1,

$$N_f(\varepsilon_{apef})/n_f(\varepsilon_{apef}) + \sum_n \sum_i (t_{ni+1} - t_{ni})/t_r((\sigma_{ni+1} - \sigma_{ni})/2) + D_{(tdi)} = 1. \quad (1)$$

The importance of the interaction increases with the test duration. The dwell effect on fatigue life was discussed using the data on specimens sections, surface relief and fracture surface observations in SEM and TEM observations of thin foils as well as time-dependent degradation processes.

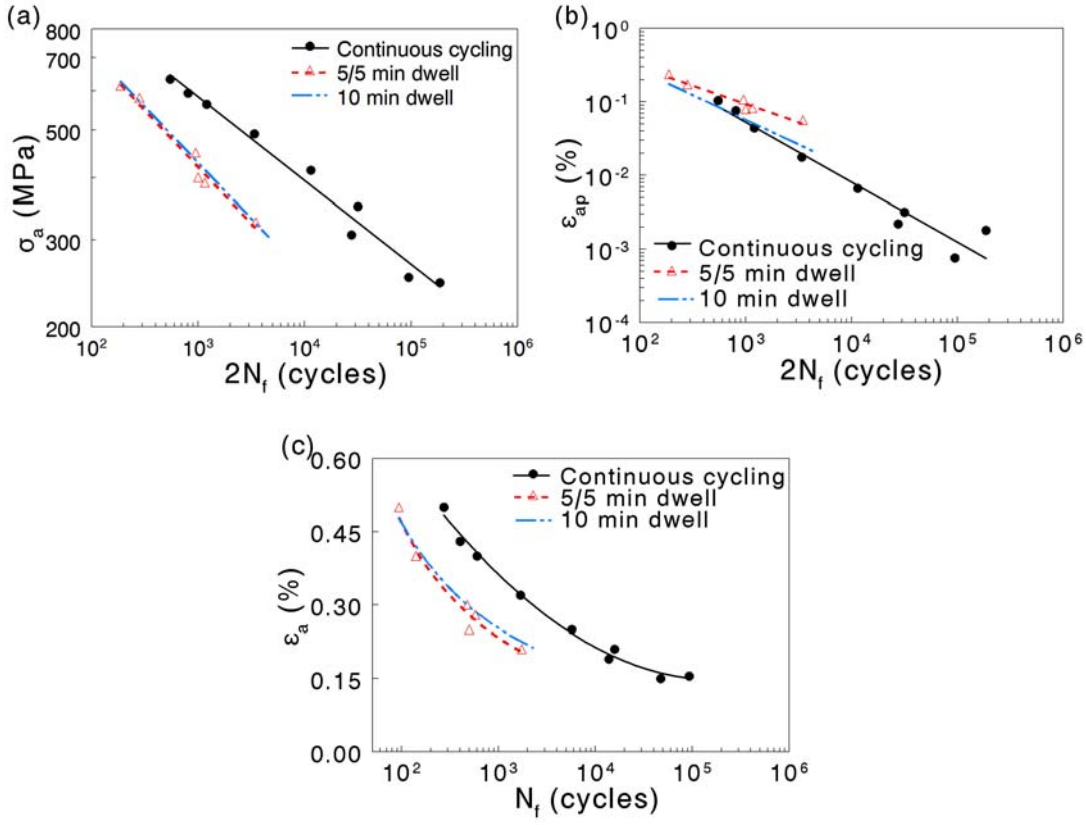

Fig. 1**.** Fatigue life curves (a) Basquin representation, (b) Coffin-Manson representation, (c) total strain representation

Numerical Simulation and Calibration of the Cyclic Behavior of Structural Steel Under Different Loading Protocols

A.I. Mohabeddine[a*], Y.W. Kouidri [a,b], J.M. Castro[a], J.A.F.O. Correia[a]

[a] Civil Engineering, *FEUP, Portugal.*
[b] Civil Engineering, *USTHB , Algeria.*
**Corresponding author: up201610371@fe.up.pt*

Keywords: Cyclic; Chaboche model; Calibration; Multiple curve fitting.

Accurate finite element simulation of the cyclic behavior of structural steel in the commercial software ABAQUS [1] requires the use of advanced material plasticity model. The Chaboche model [2] or the combined nonlinear isotropic/kinematic hardening model is widely used where cyclic plasticity is involved. The isotropic component (Eq. 1) captures the cyclic hardening/and or softening behavior of the material through the enlargement and decrease of the yield surface.

$$\sigma^0 = \sigma|_0 + Q_\infty(1 - e^{-b\varepsilon^{pl}}) \tag{1}$$

Whereas, the kinematic hardening component (Eq. 2) describes the translation of the yield surface in stress space through the backstress α. The backstress evolution law is expressed as:

$$\dot{\alpha_k} = C_k \frac{1}{\sigma^0}(\sigma - \alpha)\dot{\varepsilon}^{pl} - \gamma_k \alpha_k \dot{\varepsilon}^{pl} \tag{2}$$

The calibration of the parameters is a complex task that can be realized using experimental cyclic coupon test data. The model requires different parameters between the transient behavior and the stabilized behavior reached after few cycles [3]. If the interest is only on the stabilized behavior, the remaining issue is the different cyclic behavior observed under different strain amplitudes. Thus, the nonlinear kinematic hardening parameters show a high variability for the same steel subjected to different strain amplitudes. This issue has been observed in several studies as in [4], [5].

In order to tackle this issue and obtain one set of parameters for different strain amplitudes, the calibration of the kinematic hardening parameters has been carried out in this study using multiple curve fitting function [6]. Cyclic coupon experimental test data of different steel grades under different cyclic loading protocols have been provided by [7]. The parameters are summarized in Table 1.

In order to validate the parameters obtained using multiple regression analysis, the experimental coupon tests have been simulated in ABAQUS. Fig.1 illustrates a comparison between the experimental and the numerical simulation results showing a good agreement, where the numerical model captures the experimental behavior under "Ascend cyclic" protocol as described in [8].

Table 1- Nonlinear Isotropic/Kinematic hardening parameters.

Isotropic parameters	$\boldsymbol{\sigma\|0}$ (N/mm^2)	$\mathbf{Q} \infty$ (N/mm^2)	$\mathbf{b_{iso}}$
	269.05	60	4
Kinematic parameters	$\mathbf{C_k}$ (N/mm^2)		$\boldsymbol{\gamma_k}$
	10806		99.35

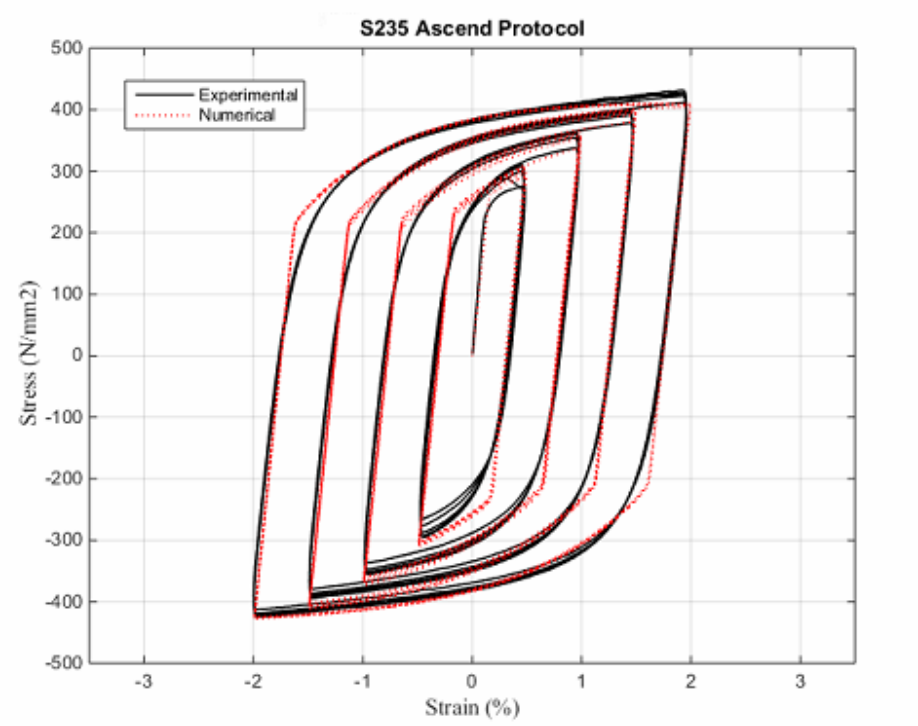

Fig.1. Comparison between experimental and numerical coupon test cyclic behavior.

REFERENCES

[1] Dassault, "ABAQUS User's Manual," ABAQUS/CAE User's Man., pp. 1–847, 2012.

[2] Chaboche, J. -L.: Time-independent constitutive theories for cyclic plasticity. Int. J. Plast. 2(2), 149–188 (1986).

[3] Lemaitre, J., Chaboche, J.-L.: Mechanics of Solid Materials. Cambridge (1990).

[4] Araújo, M., Macedo, L., and Castro, J. M.: Evaluation of the rotation capacity limits of steel members defined in EC8-3. Journal of Constructional Steel Research 135, 11-29 (2017).

[5] Nip, K.H., Gardner, L., Davies, C. M., and Elghazouli, A.Y.: Extremely low cycle fatigue tests on structural carbon steel and stainless steel. J. Constr. Steel Res. 66, 96–110 (2010).

[6] Avinadav, C.: Multiple curve fitting with common parameters using NLINFIT - File Exchange - MATLAB Central," MathWorks, 2016. [Online]. Available: https://www.mathworks.com/matlabcentral/fileexchange/40613-multiple-curve-fitting-with-common-parameters-using-nlinfit. [Accessed: 05-Aug-2018].

[7] Chen, Y., Sun, W., and Chan, T.-M.: Cyclic stress-strain behavior of structural steel with yieldstrength up to 460 N/mm^2. Front. Struct. Civ. Eng. 8 (2), 178–186 (2014).

[8] Chen, Y., Sun, W., Chan, T.-M.: Effect of Loading Protocols on the Hysteresis Behaviour of Hot-Rolled Structural Steel with Yield Strength up to 420 MPa. Advances in Structural Engineering 16(4), 707-719 (2013).

ACKNOWLEDGMENTS

The authors wish to kindly acknowledge Dr. Tak-Ming CHAN for providing experimental data.

A Nonlinear Fatigue Damage Accumulation Model for Fatigue Life Prediction Based on the Isodamage Curves

Ding Liao[a], Qiang Liu[a], Shun-Peng Zhu[a*], José Correia[b], Abílio M.P. de Jesus[b]

[a] *Institute of Reliability Engineering, School of Mechanical and Electrical Engineering, University of Electronic Science and Technology of China, Chengdu 611731, China*
[b] *INEGI, Faculty of Engineering, University of Porto, Porto 4200-465, Portugal*
**Corresponding author: zspeng2007@uestc.edu.cn*

Keywords: Variable amplitude loading; Fatigue; Damage accumulation; Life prediction; Isodamage curve.

ABSTRACT

In practice, engineering components/structures are often subjected to variable amplitude loadings during service time, which usually lead to fatigue failures. In this case, a new nonlinear fatigue damage accumulation model is proposed on the basis of the Subramanyan's model [1], which assumed that the isodamage curves converge at the knee point of the *S-N* curve. The proposed model considers the influence of the current number of loading cycles and load amplitude on the isodamage lines, which also takes into account the mean stress effect on fatigue damage modelling and life prediction [2-3].

The isodamage curves of the proposed model in this paper is given in Eq. (1).

$$D_i = \left(\frac{\lg N_{knee} - \lg N_i}{\lg N_{knee} - \lg n_i}\right)^{(a \lg n_i + b \lg \varepsilon_{a,i})} \tag{1}$$

where D_i is the cumulative damage at the load step i; N_{knee} is the number of cycles at the knee point of the *S-N* curve; N_i is the number of cycles to failure at constant stress amplitude $\varepsilon_{a,i}$, which can be obtained by the *S-N* curves of the material; n_i is the number of loading cycles applied at load step i; a and b are material constants.

In Fig. 1(a), a comparison between tested lives and model predicted lives estimated by the proposed and other four models [1, 4-6] by using experimental data of P355NL1 steel under two-step cyclic loadings [6]. Fig. 1(b) shows the probability density functions of model prediction errors.

In summary, for the steel P355NL1, comparing with the other four models, the proposed model shows better predictions than others under variable amplitude loadings.

REFERENCES

[1] Subramanyan, S.: A cumulative damage rule based on the knee point of the S-N curve. J. Eng. Mater. Technol. 98(4), 316 (1976).
[2] Zhu, S.P., Lei, Q., Wang, Q.Y.: Mean stress and ratcheting corrections in fatigue life prediction of metals. Fatigue & Fracture of Engineering Materials & Structures 40(9), 1343-1354 (2017).
[3] Zhu, S.P., Lei, Q., Huang, H.Z., Yang, Y.J., Peng, W.: Mean stress effect correction in strain energy-based fatigue life prediction of metals. International Journal of Damage Mechanics 26(8), 1219-1241 (2017).
[4] Mesmacque, G., Garcia, S., Amrouche, A., Rubio-Gonzalez, C.: Sequential law in multiaxial fatigue, a new damage indicator. Int. J. Fatigue 27(4), 461–467 (2005).
[5] Manson, S.S., Halford, G.R.: Practical implementation of the double linear damage rule and damage curve approach for treating cumulative fatigue damage. Int. J. Fract. 17(2), 169–192 (1981).

[6] Rege, K., Pavlou, D.G.: A one-parameter nonlinear fatigue damage accumulation model. Int. J. Fatigue 98, 234–246 (2017).
[7] Correia, J.A.F.O. *et al.*: Fatigue life response of P355NL1 steel under uniaxial loading using Kohout-Věchet model. Procedia Eng. 160, 109–116 (2016).

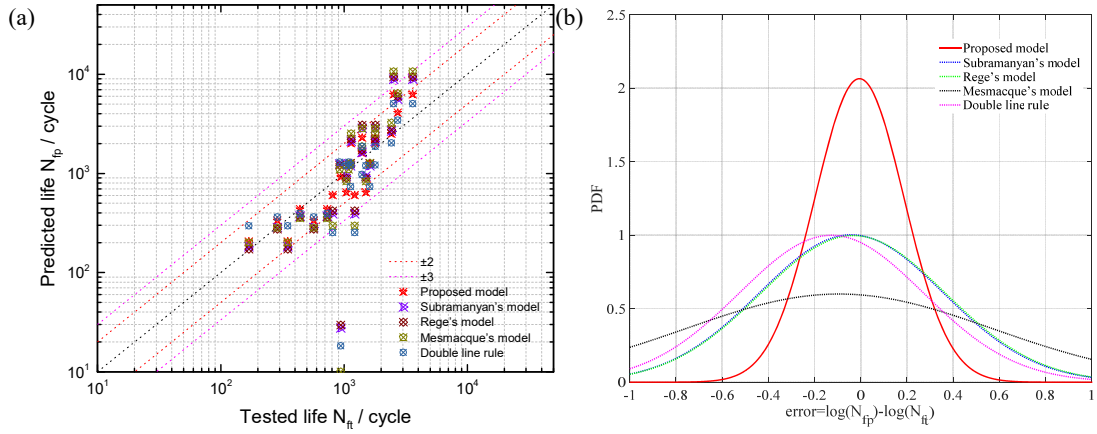

Fig. 1 (a) A comparison between tested lives and predicted lives by the proposed and other four models for the P355NL1 steel under two-step cyclic loadings; (b) Probability density functions of model prediction errors

ACKNOWLEDGMENTS

The authors would like to acknowledge the financial support of the National Natural Science Foundation of China (No. 11672070 and 11302044) and the China Postdoctoral Science Foundation Funded Project (No. 2015M582549) and China Postdoctoral Science Special Foundation (No. 2017T100697) and the Fundamental Research Funds for the Central Universities (No. ZYGX2016J208).

Research on LCF Testing and Lifing Solutions of a Larger Curvic Coupling

FAN Menglong[a,b], XUAN Haijun[a,b*], HUANG Xiannian[a,b], HONG Weirong[a]

[a] *High-speed Rotating Machinery Laboratory, Engineering Faculty, Zhejiang University, Hangzhou 310027, China*
[b] *Collaborative Innovation Center for Advanced Aero-engine, Beijing 100083, China*
**Corresponding author: marine@zju.edu.cn*

Keywords: Large curvic coupling; LCF testing; Finite element analysis; Fatigue life prediction; Crack propagation; Fretting fatigue.

ABSTRACT

Curvic couplings are widely used in turboshaft engine as rotor connecting structures because of its advantages of load bearing capability, accurate positioning and automatic centering. Under working conditions, the curvic coupling is subjected to the joint action of high centrifugal load and high axial compression preload. Therefore, low cycle fatigue (LCF) is a common failure mode of the curvic coupling. The study of low cycle fatigue life is particularly important for the design of large size curvic coupling. For this reason, a pair of large size curvic coupling with the diameter greater than 200 millimetres has been designed to study the LCF life. Then the LCF life test of this specimen was carried out on the high speed spin tester in Zhejiang University. Meanwhile, elastic-plastic finite element analysis was done to get the maximum stress or strain to determine the fatigue risk points, and to calculate the crack expansion path and the growth rate. Finally, the fatigue life of the curvic coupling had been calculated by Masson-Coffin formula and revised by Morrow formula because of the influence of average stress. It is found that the fatigue life Nf of the analysis is much higher than the life obtained by the spin testing. By analysing the displacement, fretting fatigue mode was considered. Then the fretting fatigue life of a large curvic coupling was calculated by a Non-Linear-Continuous-Damage model. The fretting fatigue life fall within the scatter bands of ±2N (±50%). As conclusions, firstly, the predicted crack initiation location correlated well with testing results that the fatigue source was on the tooth root where the stress was max. Secondly, the rate of crack propagation of this curvic coupling is very fast. Finally, the fatigue mode of this large curve coupling was fretting fatigue and its fretting fatigue could be accurately predicted by a Non-Linear-Continuous-Damage model.

Relationship Between Microstructural Features and Fatigue Behaviour of Al-based Alloy in Green Chemical Processing

I. Pettera, R. Sesanab*

[a] *Department of Applied Science and Technology, Politecnico di Torino, Italy*
[b] *Department of Mechanical and Aerospace Engineering, Politecnico di Torino, Italy*
**Corresponding author: raffaella.sesana@polito.it*

Keywords: Al alloy; Green chemical milling; Microstructure; Fatigue resistance; Casting defects.

ABSTRACT

Casting aluminium alloys are already very popular, but they are still finding new applications in a wide range of industrial fields. About 80% of all aluminium casting products derives from aluminium scrap, percentage that is significantly higher than wrought products. In the last years casting technologies have been considerably developed, so now it is possible to achieve higher quality components. In the same time, the continuous industrial development imposes new machining processes after casting, in order to get an appropriate structure or the desired geometry with good surface quality, evidently in an economically convenient way and with no any negative effect on the overall behaviour of the alloy.

In this study, we consider the application of a green chemical milling, Green Etching[1], to B356.2 Aluminum alloy with the aim to remove a controlled thickness layer from the surface with no buckling and maintaining excellent dimensional tolerances. Comparison of the fatigue life of un-treated and chemically treated samples is performed, with the aim to determine how the above mentioned chemical treatment influences the fatigue resistance of the Al alloy to be used in automotive/aircraft industrial application.

The results revealed that the fatigue properties of Al casting alloy are strongly influenced by the presence of casting defects and the fatigue resistance cannot be significantly compromised by the milling treatment despite the surface roughness induced by the treatment (Figure 1 and Figure 2).

(a) (b)

Fig. 1. Base material grinded (a) and Green Etched (b) specimen.

[1] patent pending

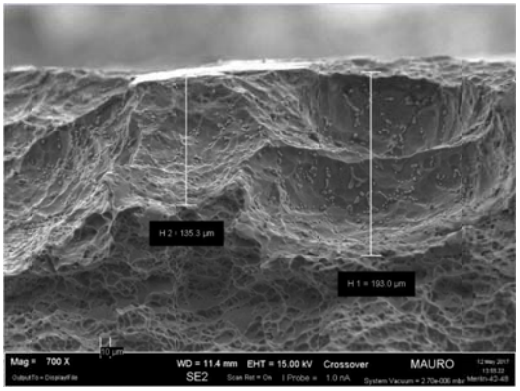

Fig. 2. Surface aspect of Green Etched specimen.

REFERENCES

[1] Ingraffea, Anthony R., Spear, Ashley D.: Effect of chemical milling on low-cycle fatigue behavior of an Al-Mg-S alloy. Corrosion Science Corrosion Science 68, 144–153 (2013).
[2] Rokhlin, S., Kim, J.-Y., Nagy, H., Zoofan, B.: Effect of pitting corrosion on fatigue crack initiation and fatigue life. Engineering Fracture Mechanics 62, 425–444 (1999).
[3] Peter, I., Rosso, M., Bivol, C.: Microstructure and mechanical behaviour of Al-based alloy obtained by liquid forging technique. Metallurgia International XIV (2), 15-19 (2009).
[4] Curà, F., Sesana, R.: Surface factor assessment in HCF for steels by means of empirical and non-destructive techniques. Procedia Structural Integrity 5, 500-507 (2017).
[5] Curà, F., Sesana, R.: Mechanical and thermal parameters for high-cycle fatigue characterization in commercial steels. Fatigue and Fracture of Engineering Materials and Structures 37 (8), 883-896 (2014).
[6] Lichioiu, I., Peter, I., Varga, B., Rosso, M.: Preparation and Structural Characterization of Rapidly Solidified Al-Cu Alloys. J. Mater. Sci. Technol. 30 (4), 394-400 (2014).

ACKNOWLEDGMENTS

The authors wish to thank SIMET srl (TO), RGTECH srl (Bruino, TO) for their collaboration and for the preparation of the samples.

Lattice Distortion and Interlayer Mismatch of Bi4Ti3O12-Based Bismuth Layer-Structured Ferroelectrics

Yu Chen[a,b], Jia-geng Xu[c], Shao-xiong Xie[d], Qing-yuan Wang[a,d*], Jian-guo Zhu[b*]

[a] *School of Mechanical Engineering, Chengdu University, Chengdu 610106, China*
[b] *College of Materials Science and Engineering, Sichuan University, Chengdu 610065, China*
[c] *School of Architecture and Civil Engineering, Chengdu University, Chengdu 610106, China*
[d] *College of Architecture and Environment, Sichuan University, Chengdu 610065, China*
**Corresponding author: wangqy@scu.edu.cn (Qing-yuan Wang); nic0400@scu.edu.cn (Jian-guo Zhu)*

Keywords: Lattice distortion; Interlayer mismatch; Bi4Ti3O12; Oxygen-octahedron; Elastic model.

ABSTRACT

For a sort of W/Cr co-doped Bi4Ti3O12 ceramics (ab. BTWC) as sensitive materials for the high temperature piezoelectric devices, both the lattice distortion and interlayer mismatch of the Bi4Ti3O12 structure were investigated by the lattice stress analysis and elastic mechanics model. In the crystal structure of Bi4Ti3O12, the pseudo-perovskite layers composed of three oxygen-octahedron layers with Bi at the A-site are sandwiched between the bismuth oxide layers, due to a strong combining power between the two layers along the c-axis, the lattice strain have to be constrained in the ab-plane, which causes a structural mismatch between pseudo-perovskite layer and bismuth oxide layer. The interlayer mismatch degree (K) could be determined by the inner stress balance between the two layers and their corresponding bulk modulus, as considering the case of a constant bulk modulus of bismuth oxide layer for BLSF. In addition, both the total strain energy and the lattice parameters in ab-plane vary with the composition of BTWC in a similar trend to the degree of interlayer mismatch, and W-doping has a significant effect on the interlayer mismatch of Bi4Ti3O12. Since the oxygen-octahedron rotates in the ab-plane as well as inclines away from the c-axis, a lattice model to describe the distorted status of oxygen-octahedron was established according to the substituting mechanism of W6+/Cr3+ in Bi4Ti3O12, which is used for investigating the variation of orthorhombic distortion degree (a/b) of BTWC with the content of W6+/Cr3+.

Fig. 1. A conventional solid reaction process for preparing BTWC ceramics (detailed process could be found in [4, 5]).

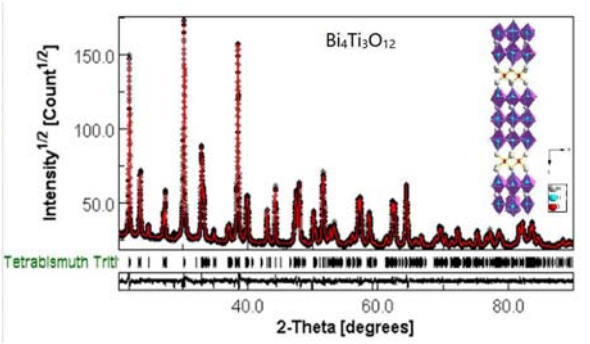

Fig. 2. The observed, calculated , and difference plots for the fit to the XRPD patterns of Bi4Ti3O12 after Rietveld refinement at 295 K.

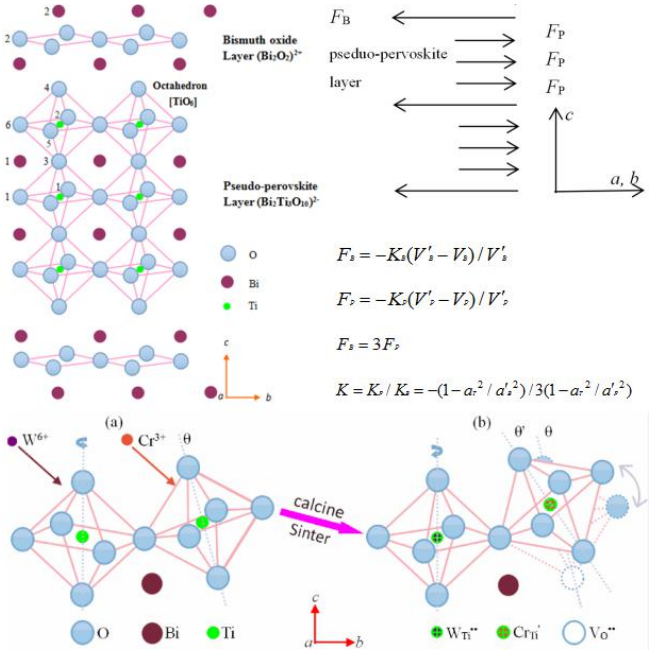

Fig. 3. (a) A perspective drawing of Bi4Ti3O12 along the [110] direction of the undistorted Fmmm parent structure (between 1/4c and 3/4c of an unit cell); (b) Stress analysis for the pseudo-perovskite layer of Bi4Ti3O12; (c) Status change of oxygen-octahedron in Bi4Ti3O12 , (left) before W/Cr codoping; (right) after W/Cr codoping.

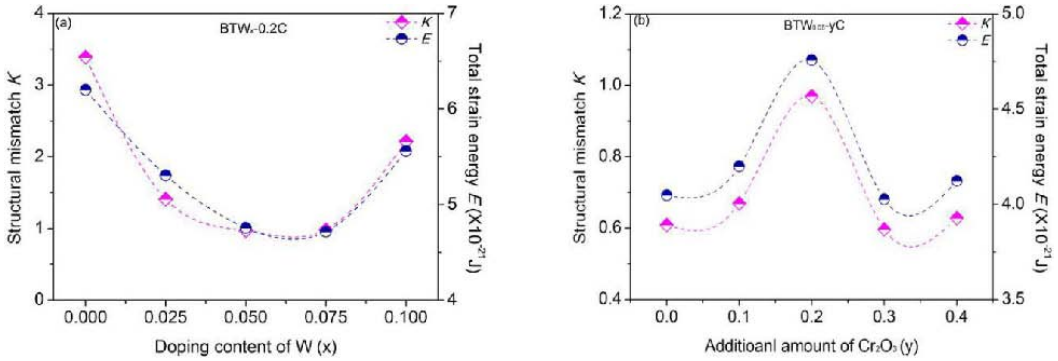

Fig. 4. Variation of the structural mismatch degree and total strain energy with the composition for BTWC ceramics, (a) varying with x, (b) varying with y.

REFERENCES

[1] Aurivillius, B.: Arkiv kemi 1: 499-512 (1949).
[2] Wiegers, G. A.: Progress in Solid State Chemistry 24 (1-2), 1-139 (1996).
[3] Shi, J., Zhu, R., Liu, X. et al.: Materials 10(9), 1093 (2017).
[4] Chen, Y., Pen, Z., Wang, Q. et al.: Journal of Alloys and Compounds 612, 120-125 (2014).
[5] Chen, Y., Miao, C., Xie, S. et al.: Materials & Design 90, 628-634 (2016).

ACKNOWLEDGMENTS

This work was supported by the Applied Basic Research Program from Sichuan Province (2017JY0091), National Natural Science Foundation of China (Grant No. 11702037, 11572057 and 51332003), China Postdoctoral Science Foundation Funded Project (2017M623025), Special Funding for PostDoctoral Research Projects from Sichuan Province (2017, presided over by Yu Chen).

Creep-Fatigue Damage Evaluation in Single-Edge-Notch Specimens of Nickel-based GH4169 Superalloy

R. Wang[a,b], J. Wang[a], S. Guo[a,b], H. Chen[b], X. Zhang[a*], S. Tu[a]

[a] *Key Laboratory of Pressure Systems and Safety, Ministry of Education, School of Mechanical and Power Engineering, East China University of Science and Technology, Shanghai 200237, P.R. China*
[b] *Department of Mechanical & Aerospace Engineering, University of Strathclyde, Glasgow, G1 1XJ, UK*
**Corresponding author: xczhang@ecust.edu.cn*

Keywords: Notch effect; Creep-fatigue; Strain energy density; Crack initiation.

ABSTRACT

Damage evaluation on creep-fatigue interaction is a significant factor in life management of rotating components in aviation, aerospace and nuclear industries. Studies on creep-fatigue life prediction models for smooth specimens have continuously made progress in the last fifty years. Some of them have been coded in the structural design procedures. However, geometric discontinuities, including bolt holes, corners, non-uniform cross sections, etc., are extremely common in practical cases. Then, the effects of mean stress, stress-stain concentration and varying residual stress need to be taken into account [1]. Under this circumstance, traditional damage rules such as stress based time fraction (TF) rule [2] and strain based ductility exhaustion (DE) rule [3] cannot meet the requirement for crack initiation life prediction.

Nickel-based superalloys are often selected for intermediate-temperature applications. The aircraft turbine disks in China, which are made by nickel-based GH4169 superalloy, comprise extremely complex geometries. GH4169 superalloy has been found to exhibit good mechanical properties and corrosion resistance, excellent weld ability and long-term thermal stability. Microstructurally, it usually shows their extremely high strength from the Ni_3Nb type γ" precipitation and partially by Ni_3Al type γ' precipitation, and to even greater extent from precipitates within the solid solution γ matrix. However, an obvious degradation of mechanical properties occurs at temperatures above 650 °C due to the fact that strengthening γ" precipitation heavily transforms to the equilibrium δ phase.

Notch specimens are widely used in investigating geometric discontinuities because notch roots always experience complex multiaxial stress-strain state even under uniaxial loading waveforms. Local stress and strain levels are usually much higher in the vicinities of notch roots than remote positions. The lives of low cycle fatigue without dwell periods are always reduced by notches due to the stress-strain concentration [4], while the notches usually play strengthening roles in pure creep loading conditions in nickel-based superalloys [5]. A general problem under creep-fatigue conditions is that how the presence of notch influences the creep-fatigue performances and endurances.

In order to get a comprehensive understanding of notch effect on creep-fatigue behaviours, two groups of single-edge-notch specimens with different root radius were machined out and creep-fatigue experiments at 650 °C under global strain-controlled loading conditions were carried out. Then an accurate model for creep-fatigue damage evaluation based on linear damage summation (LDS) and energy dissipation criterion (EDS) was developed. Finally, finite element method (FEM) was used to verify the feasibility of the proposed model and further discuss the evolutional processes of stress-strain responses and damage fields in the vicinities of notch roots. The above-mentioned three procedures are listed in detail as follows:

(i) A series of cylindrical bars with the dimensions Φ16 × 200 mm of were extracted from as-received materials through the usage of EDM wire-cut machine. After that, standard heat treatment was applied to all specimens. The heat-treated bar were subsequently fine machined according to specified shapes and dimensions of single-edge-notch specimens. In order to ensure the surface integrity of specimens, the notches were carefully polished down to 1 μm diamond finish. Then the specimens were tested at 650 °C on a MTS servo-hydraulic testing system. To realize a global strain-controlled mode, a high-temperature extensometer crossing 25 mm gauge-length (as well as notch area) was attached to the surface of specimen.

(ii) The damage evaluation model is an extension of our previous modified strain energy density exhaustion (SEDE) method [6]. Fatigue and creep damage per cycle were separately calculated, and the corresponding accumulated ones over cycles were used to determine crack initiation life. The evaluation of fatigue damage combined the equivalent inelastic strain range and Ostergren's energy-based equation [7]. The evaluation of creep damage considered mean stress effect, advanced stress relaxation and a critical creep damage expression. In addition, multiaxial ductility factor (MDF) was incorporated to consider the effect of stress triaxiality on creep damage.

(iii) Two necessary portions were included in simulating various geometric discontinuities and loading waveforms. Firstly, Chaboche's cyclic hardening constitutive model was used to study cyclic stress-strain response, and Norton-Bailey model was used to describe creep and relaxation behaviour during dwell periods. The programs of constitutive equations are embedded in ABAQUS software. Secondly, the objective of UVARM subroutine is to define the output variables of damage fields. All the parameters in constitutive models and the proposed damage evaluation model were obtained from simple uniaxial creep-fatigue tests using uniform specimens, the results of which have been published from one of our previous works [8].

REFERENCES

[1] Berto, F., Vinogradov, A., Filippi, S.: Application of the strain energy density approach in comparing different design solutions for improving the fatigue strength of load carrying shear welded joints. Int J Fatigue 101, 371–384 (2017).

[2] Robinson, EL.: Effect of temperature variation on the long-time rupture strength of steels. Trans ASME 74(5), 777–781 (1952).

[3] Priest, RH., Ellison, EG.: A combined deformation map-ductility exhaustion approach to creep–fatigue analysis. Mater Sci Eng 49(1), 7–17 (1981).

[4] Sakane, M., Zhang, S., Kim, T.: Notch effect on multiaxial low cycle fatigue. Int J Fatigue 33(8), 959–968 (2011).

[5] Yu, QM., Wang, Y., Wen, ZX., Yue ZF.: Notch effect and its mechanism during creep rupture of nickel-base single crystal superalloys. Mater Sci Eng A 520(1), 1–10 (2009).

[6] Wang, RZ., Zhang, XC., Tu, ST., Zhu, SP., Zhang, CC.: A modified strain energy density exhaustion model for creep–fatigue life prediction. Int J Fatigue 90, 12–22 (2016).

[7] Ostergren, WJ.: A damage function and associated failure equations for predicting hold time and frequency effects in elevated temperature, low cycle fatigue. J Test Eval 4(5), 327–339 (1976).

[8] Wang, RZ., Zhang, XC., Gong, JG., Zhu, XM., Tu, ST., Zhang, CC.: Creep-fatigue life prediction and interaction diagram in nickel-based GH4169 superalloy at 650 °C based on cycle-by-cycle concept. Int J Fatigue 97, 114–123 (2017).

ACKNOWLEDGMENTS

The author would like to acknowledge gratefully for the financial support through National Natural Science Foundations of China (51371082, 51322510) and the 111 project. The author Run-Zi Wang is grateful for the support from China Scholarship Council (CSC). The author Xian-Cheng Zhang is also grateful for the support by Shanghai Pujiang Program, Young Scholar of the Yangtze River Scholars Program, and Shanghai Technology Innovation Program of SHEITC (CXY-2015-001).

Fatigue of Additive Manufacturing Metals

Symposium F-AMF-ICMFM

Organized by:

Gianni Nicoletto, Italy

Stefano Beretta, Italy

Abilio de Jesus, Portugal

Philippe Emile, Airbus, Europe

Ludvík Kunz, Czech Republic

Yves Nadot, France

Thomas Niendorf, Germany

Mohsen Seifi, USA

Nima Shamsaei, USA

Sérgio O. Tavares, Portugal

Effects of Porosity and Surface Roughness on High Cycle Fatigue Behavior of Additively-Manufactured 17-4 PH Stainless Steel

S. Romano[a*], B. Torries[c], B. Paudel[c], S. Beretta[a], M. Seifi[b], N. Shamsaei[c]

[a] *Politecnico di Milano, Italy*
[b] *Case Western Reserve University & ASTM International, USA*
[b] *Auburn University, USA*
**Corresponding author: simone.romano@polimi.it*

Keywords: High Cycle Fatigue; Additive Manufacturing; Stainless steel; Surface Roughness; Porosity.

ABSTRACT

The effect of surface roughness and subsurface porosity on fatigue behavior of 17-4 PH stainless steel (SS) fabricated via laser-based powder bed fusion (L-PBF) is investigated and modelled utilizing a crack growth approach. The employed material is the most commonly used precipitation hardened (PH) stainless steel in many fatigue-critical applications. Additive manufactured parts being prone to subsurface porosity and surface roughness, their fatigue behavior should be truly characterized before they can be used under cyclic loading. Round specimens with uniform gage sections were designed and force-controlled fatigue tests were conducted to generate high cycle fatigue data. Some specimens were kept in their as-build condition without any post-manufacture machining to study the effects of surface roughness. The rest of the specimens were machined with different depths; 0.5 mm for half of them and 1.5mm for the other half to investigate the effect of deep versus shallow marching on the fatigue behavior of L-PBF 17-4 PH SS. Computed tomography (CT) scanning was employed to characterize subsurface pores in fatigue specimens to provide a means for establishing porosity-property relationships. Cyclic crack growth data was also generated using three-point bending testing on L-PBF 17-4 PH SS single-edge notch specimens to be used in a predictive fatigue model based on the crack growth concept. This approach assumes the pores and surface roughness can serve as the initial crack in additive-manufactured parts and that fatigue strength can be estimated based on the most detrimental defect present in the relevant material volume. In detail, the comparison of the fatigue properties with measurements of the defects at the fracture origin and defect population measured by CT scan allowed us to investigate the effect of sub-surface defects as well as defects brought up to the surface due to the machining process onto the prospective fatigue behavior of AM 17-4 PH SS parts.

Impact of Various Surface Treatments on the Fatigue Behaviour of Additive Manufactured AlSi12

Dieter Fetzer[b], Steffen Greuling[a*], Klaus Müller-Lohmeier[b], Mattias-Manuel Speckle[b], Wolfgang Weise[a]

a Esslingen University of Applied Sciences, Department of Mechanical Engineering, Strength of Materials Lab (LWF), Kanalstraße 33, 73728 Esslingen, Germany

b Festo AG & Co. KG, 73734 Esslingen, Germany

** Corresponding author: steffen.greuling@hs-esslingen.de*

Keywords: Additive Manufacturing; Selective Laser Melting; Aluminum Silicon; S-N curve; Surface Treatment

ABSTRACT

Additive manufacturing (AM) offers new and unique possibilities to design and produce complex shaped components. Furthermore, Al-alloys fulfil the requirements in lightweight design in many areas of mechanical and automotive applications. Additive manufacturing is already established in prototyping. However, for applications in structural engineering and serial productions many questions still have to be solved. Mechanical and metallurgical properties of AlSi12 cast materials are available [1]. For components made of AlSi12 by additive manufacturing and especially for serial applications and under dynamic loading many further tests are necessary [2,3,4].

Objective of this work will be testing of additive manufactured AlSi12 specimens under static and dynamic loading applying various surface finishing methods. The microstructure and failure mechanisms of crack initiation and propagation will be investigated. The specimens were produced by selective laser melting [5] using a SLM 250 HL machine of SLM Solutions. Specimens tested under static loading build up directions of 0°, 45°, 50° and 90° were applied, see Fig 1. For dynamic loading only a build up direction of 90° was used. Tests were carried out under R-ratio of R=0.1. The following surface treatments were applied:

- additive manufactured (as printed)
- turning
- polishing
- shot peening (MHG SMG 25/1, micro glass balls < 50 µm, approx. 4 min)
- turning and deep rolling
- grinding and deep rolling

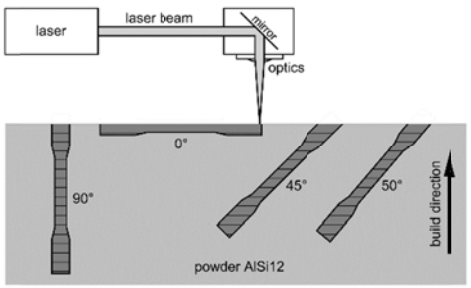

Fig. 1. Sketch of laser scanning and build up direction

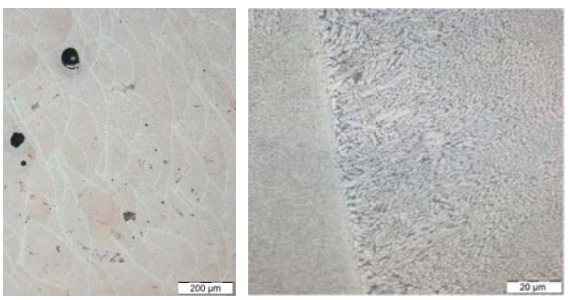

Fig. 2. Polished sections of additive manufactured AlSi12

The microstructure of AlSi12 shows a very fine-grained structure (Fig. 2), which is common for additive manufactured Al-alloys. This microstructure leads to high static strength values, higher values than corresponding cast materials. However, the microstructure shows a certain amount of pores. By using density measurements a porosity of about 3.4% was observed. The surface roughness of various specimens were measured and micrographs of specimen surfaces produced by various finishing methods were documented. Polishing and deep rolling lead to much lower surface roughness compared to turning and grinding. However, for polished surfaces pores at the surface were detected.

Results of dynamic testing are shown in Fig. 3. The diagram shows S-N-curves for a failure probability of P_A=50%. Shot peening and deep rolling lead to an increase in fatigue strength due to compressive residual stresses. As printed and turned surfaces with relatively high surface roughness lead to crack initiation at the surface. Also for polished specimens cracks start at pores at the surface. For shot peened and especially for deep rolled specimens cracks will be initiated at pores below the surface. Hence, further objective will be the reduction of porosity.

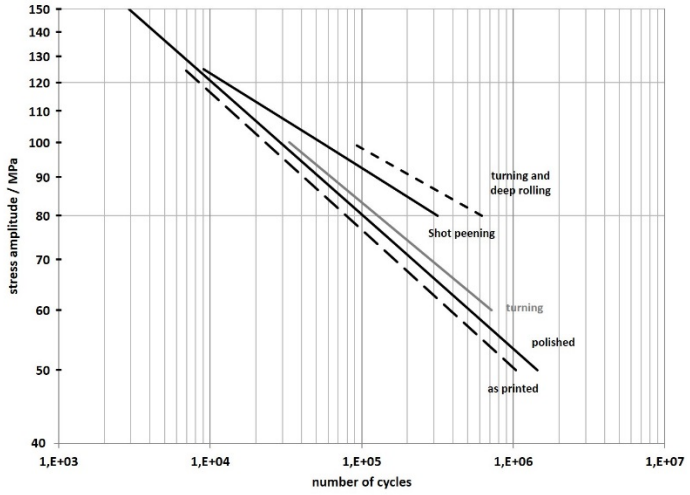

Fig. 3. S-N curves for additive manufactured AlSi12 and applying various surface treatments. Results are valid for a failure probability of P_A=50 %

REFERENCES

[1] Aluminium Taschenbuch: Band 1: *Grundlagen und Werkstoffe*, Verlag Beuth (2011).

[2] Kaufmann, H., Wagener, R., Melz, T.: Anforderung an ein Bemessungskonzept für zyklisch beanspruchte additiv gefertigte Bauteile, DVM-Bericht 401, 1. Tagung des Arbeitskreises Additiv gefertigte Bauteile und Strukturen, Berlin (2016).

[3] Wörner, S., Friederich, H., Jung, U.: Additiv gefertigte Bauteile für den Maschinen- und Automobilbau, DVM-Bericht 401, 1. Tagung des Arbeitskreises Additiv gefertigte Bauteile und Strukturen, Berlin (2016).

[4] Spierings, A.B.: SLM Materialeigenschaften: Aktueller Stand und Trends "erweiterte Designmöglichkeiten mit SLM“, 8. SWISS RaPiD Forum 2012, St. Gallen, Switzerland, August 29, 2012, Verlag: ETH Zürich.

[5] Richard, H.-A. , Schramm, B.: Th. Zipsner (Hrsg.), *Additive Fertigung von Bauteilen und Strukturen*, Springer Fachmedien Wiesbaden (2017).

ACKNOWLEDGMENTS

Parts of this work were carried out during project works of A. Avdyli, F. Lehnert, M. Irion, A.E. Meinel, M. Koch, P. Schwarz and M.E. Giolito at the lab of materials testing at mechanical engineering department of University of Applied Sciences Esslingen. Many thanks also to E. Schuch and U. Merk for supporting evaluation and drawing of diagrams.

Roughness Reduction and Increase of Fatigue Performance of LBM Components by Plasma Electrolytic Polishing

S. Reichelt[a*]

[a] *Airbus, Airbus Central R&T, Taufkirchen, Germany*
**Corresponding author: Sarah.reichelt@airbus.com*

Keywords: Laser Beam Melting; Roughness; Surface Defects; Fatigue.

ABSTRACT

In the course of the industrialization of the Additive Manufacturing (AM) process of metallic components, the surface finish of the final parts is a key milestone. 'As-built' AM surfaces feature a high initial surface roughness (i.e. Ra > 10 µm), which often exceeds the specification for technical applications. In order to apply AM for highly stressed and cyclically loaded components, the as-built surface roughness needs to be reduced. Since conventional surface finishing processes as grinding or blasting often show a limited applicability to complex shaped AM parts, a plasma electrolytic polishing process was developed (3D SurFin®). Within the present study, AM plates and fatigue samples were produced in a powder bed laser beam system (LBM). The roughness reduction by means of the plasma electrolytic polishing process was proven for different treatment times. Also, a notable improvement of the fatigue performance was achieved after a treatment with the plasma electrolyte polishing process. For reference, machined specimens were analysed as well and all results are compared to the performance of as-built samples.

Surface roughness sensitivity of Ti-6Al-4V parts obtained by SLM and EBM: Effect on the HCF

B. Vayssette[a*], N. Saintier[a], C. Brugger[a], M. El May[a]

[a]*Arts et Metiers Paristech, I2M, CNRS, Talence 33400, France*
**Corresponding author: bastien.vayssette@ensam.eu*

Keywords: HCF; SLM; EBM; Surface Roughness; Ti-6Al-4V; FEM.

ABSTRACT

Selective Laser Melting (SLM) and Electron Beam Melting (EBM) are powder bed fusion processes which allow to build parts by successive addition of layers directly from 3D-CAD models. Among the advantages are the high degree of freedom of design and the small loss of material, which explain the increase of Ti-6Al-4V parts obtained by these processes.

However Ti-6Al-4V parts produced by SLM and EBM contain defects (surface roughness, porosity, residual stresses) which decrease significantly the High Cycle Fatigue (HCF) life. In order to minimize the porosity and the residual stresses, post-processing like Hot Isostatic Pressing (HIP) and Stress Relieving are often conducted. The modification of the surface roughness by machining is very costly and not always possible, especially for parts with complex design. The aim of this work is to evaluate the effect of the surface roughness and microstructure of Ti-6Al-4V parts produced by SLM and EBM on the HCF life.

5 sets of specimens were tested in tension-compression and torsion (R=-1): Hot-Rolled (reference); SLM HIP machined ; SLM HIP « As-Built » ; EBM HIP machined ; EBM HIP « As-Built ». For every condition, microstructures characterization, observations of the fracture surface of the specimens and surface analysis were carried out respectively by Optical Microscope (OM), Scanning Electron Microscope (SEM), 3D optical profilometer and X-ray tomography. The results of the fatigue testing show a significant decrease of the HCF life due to the surface roughness.

Along with experimental testing, numerical simulations using FEM were conducted from surface scans obtained by profilometry and volume scans obtained by tomography. Based on extreme values statistics, a methodology is proposed in order to take into account the effect of the surface roughness on the HCF life.

Finally a crystal plasticity model is introduced to give a better understanding of the mechanisms leading to the crack initiation especially the competition of the stress localization between the microstructure orientation and the surface roughness.

Influence of Surface Orientation and Segmentation on the Notch Fatigue Behavior of As-Built DMLS Ti6Al4V

G. Nicoletto[a*], R. Konecna[b]

[a]*Department of Engineering and Architecture, University of Parma, Italy*
[b]*Department of Materials Engineering, University of Žilina, Slovakia*
**Corresponding author: gianni.nicolettol@unipr.it*

Keywords: Direct metal laser sintering; Ti6Al4V; Notch fatigue; Surface quality.

ABSTRACT

The on-going drive for a full exploitation of metal additive manufacturing (AM) technology by industrial sectors such as aerospace, energy, motor racing and medical is pushing for new know-how development supporting the design and qualification of load-bearing metal parts. Among the different metal AM processes, the direct metal laser sintering (DMLS) is considered here. One factor negatively affecting the fatigue performance of a DMLS part is the as-built surface of inferior quality compared to conventionally machined surfaces. A geometrically complex DMLS part may be characterized by the presence of geometrical notches that act as stress concentrators. The interaction of the layer-by-layer geometrical notch generation and its rough as-built surface with respect to the notch fatigue behavior is the topic of this study.

The accuracy and quality of a geometrical notch is influenced by specific DMLS process features. The layer-by-layer generation approximates a semi circular notch geometry by segmentation as shown in the example of Fig. 1. The impact of segmentation depends on the ratio λ/R where λ is the layer thickness and R is the radius and on the local orientation θ with respect to the building direction: when θ approaches 0-deg the local geometry is increasingly stepped, when θ approaches 90-deg the actual geometry merges to the nominal geometry.

Another AM process-dependent factor is introduced in the scheme of Fig. 2: a DMLS surface can be classified as down-skin or up-skin depending on the orientation with respect to the vertical build direction. While the surfaces generated by the layer-by-layer process are nominally the same, different local heat transfer and melt pool support conditions result in practice in down-skin surfaces that are rougher than the up-skin counterparts due to the formation of dross.

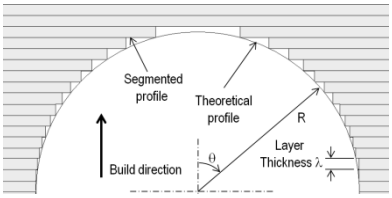

Fig. 1. Segmented geometry resulting from the layer-by-layer fabrication of a semicircular detail.

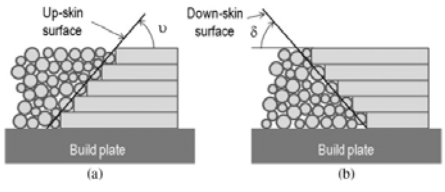

Fig. 2. Definition of DMLS surface orientation.

This contribution is aimed at: i) the investigation of the combined effect of these two factors, (i.e. surface orientation and layer-by-layer construction) on the surface quality of an as-built notch; ii) the quantification of the notch fatigue behavior of the as-built DMLS Ti6Al4V. The study exploits the miniature specimen approach recently proposed to efficiently study the directional smooth fatigue

behavior of DMLS metals, [1]. Fig. 3a shows a mini specimen (22 x 5 x 7 mm^3) oriented orthogonally to the build direction. The mini specimen is cyclic loaded in plane bending with a load ratio R = 0 and it can be used to investigate either the smooth material behavior when the tensile stress is applied to the flat top surface or the notch fatigue behavior when the tensile stress is applied to the notch root, [2]. For this study two batches of mini specimens were produced with an EOS M290 system with notches in the up-skin and in the down-skin orientation. The resulting surface qualities of the 2-mm-radius notches are shown in Figs. 3b and 3c. As expected the down-skin notch is considerably rougher.

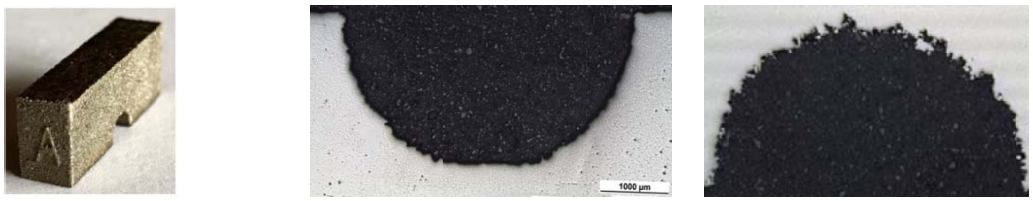

a) b) c)

Fig. 3. a) Notched mini specimen; b) Up-skin round notch; c) Down-skin round notch (R = 2 mm).

The fatigue test results of in terms of max nominal bending stress vs. number of cycles for the un-notched test configuration and for the two sets of notched mini specimens are plotted in Fig. 4. Type A+ refers to an up-skin notch and Type A− to a down-skin notch. The fatigue data appear well-behaved with a reduced scatter. The up-skin fabrication condition is associated to a slightly better fatigue behavior than the down-skin condition. According the empirical notch fatigue factor K_f definition (i.e. smooth fatigue strength/notched fatigue strength), the present geometry with a stress concentration factor K_t = 1.63 is associated to K_f = 2.0 for up-skin notch and K_f = 2.6 for down-skin notch in DMLS Ti6Al4V.

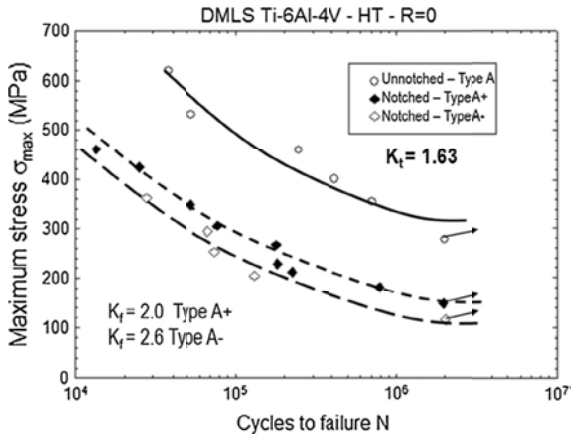

Fig. 4. Fatigue behavior of smooth and up-skin vs. down-skin circular notches in DMLS Ti6Al4V.

REFERENCES

[1] Nicoletto, G.: Anisotropic high-cycle fatigue behavior of Ti-6Al-4V obtained by powder bed laser fusion. International Journal of Fatigue 94, 255-262 (2017).

[2] Nicoletto, G.: Directional and notch effects on the fatigue behavior of as-built DMLS Ti6Al4V. International Journal of Fatigue 106, 124-131 (2018).

ACKNOWLEDGMENTS

The research was supported by the project Slovak VEGA grant No. 1/0685/2015. Specimen production by the company BEAM-IT Fornovo Taro (Italy) (www.beam-it.eu) is gratefully acknowledged.

As-built Sharp Notch Geometry and Fatigue Performance of DMLS Ti6Al4V

M. Frkan[a*], G. Nicoletto[b], R. Konecna[a]

[a] *Department of Materials Engineering, University of Zilina, Slovakia*
[b] *Department of Engineering and Architecture, University of Parma, Italy*
**Corresponding author: martin.frkan@fstroj.uniza.sk*

Keywords: Fatigue; Notch; Selective laser melting; Ti6Al4V.

ABSTRACT

The on-going drive for a full exploitation of metal additive manufacturing (AM) technology by industrial sectors such as aerospace, energy, motor racing and medical is pushing for new know-how development supporting the design and qualification of load-bearing metal parts. Among the different metal AM processes, here the Selective Laser Melting (SLM) is investigated. Specific features characterize metal parts obtained by the SLM processing of a powder bed, namely i) the complex microstructure due to the layer-wise production and ii) the surface finish which is considerably rougher than conventionally machined parts. A third specific feature is related to the adoption of light weight design tools, such as topological optimization, that develop complex part geometries with reentrant corners and notches that are difficult to inspect and whose surface finish may not be post processed and improved.

While static properties are relatively unaffected by the surface characteristics, the response of as-built metal parts of complex geometry is strongly and negatively affected by dynamic service conditions.

Fatigue testing is typically an expensive and time consuming activity. Because of the inherent material data scatter, multiple specimens are required to characterize one material state under a specific test condition. The metal AM technology places an additional burden on fatigue testing as specimens production is costly in terms of material and AM system usage since metal powders are expensive and AM system require large investments.

Recently, an innovative miniature specimen geometry has been proposed to address the negative issues involved in fatigue testing of AM metals, [1]. Fig. 1 shows a miniature specimen (22x5x7 mm^3) compared to a standard 80 mm long rotating bending specimen. As the specimen unit cost depends on i) its volume and ii) the time required for its production, the new specimen geometry allows a remarkable cost saving when compared to a standard specimen geometry. The mini specimen is loaded in cyclic plane bending instead of rotating bending but it shares the same reference section properties and therefore size- and loading-type effects are reasonably similar. The testing method based on mini specimens was validated using DMLS Ti6Al4V specimens. The miniature specimen concept has been also extended to the study of the notch fatigue behavior of DMLS Ti6Al4V, [2]. A mild notch geometry was found to be associated to multiple notch fatigue factors in dependence of its orientation with respect to the build direction.

Fig. 1. Comparison of standard vs. miniature specimens for fatigue testing of AM metals.

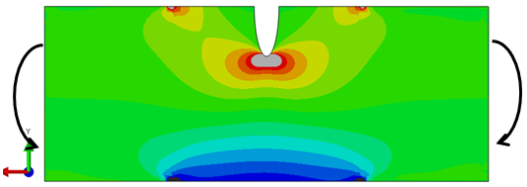

Fig. 2. Stress distribution in mini specimens with a semi-elliptical notch subjected to plane bending.

In this contribution the miniature specimen concept is applied to the investigation of the influence of a sharp notch geometry. To guarantee a correlation with the mild notch fatigue results of [2], the semi-circular notch with to a semi-elliptical notch. Fig. 2 shows the elastic stress distribution due to an applied bending moment obtained by an elastic finite element analysis. The stress concentration factor for this semi-elliptical notch with b/a = 0.25, where a = 2 mm and b = 0.5 mm are the major and minor semi-axes, is given by $K_t = 5$. The mini specimens are subjected to cyclic plane bending with a load ratio R = 0. Batches of these notched specimens made of DMLS Ti6Al4V were produced with an EOS M 290 system operated at a maximum laser power of 400 W and a layer thickness of 60 µm and subsequently stress relieving heat treated in a vacuum furnace.

Specimens were produced with the long axis of the notch parallel to the build direction i.e. Type A+ in Fig. 3a and with long axis perpendicular to build direction, i.e. Type C in Fig. 3b, to investigate the geometrical accuracy and surface roughness of a fine detail, such as the notch, in dependence of the layer-by-layer SLM processing of the powder bed. Fig. 3 shows the different quality of the notches in terms of accuracy and roughness with a well-defined Type A+ notch and an irregular Type C notch.

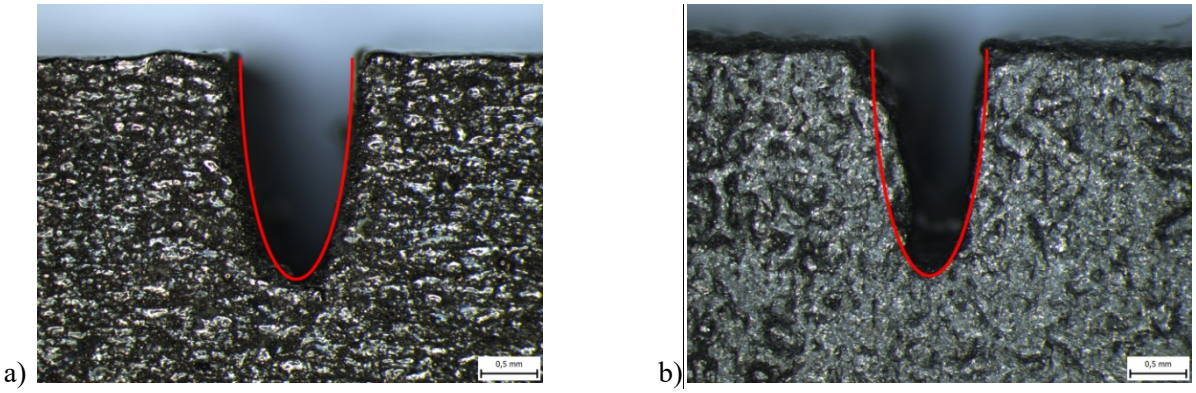

Fig. 3. Magnified view of semielliptical notches a) Type A+, b) Type C.

The fatigue test results of in terms of maximal nominal bending stress vs number of cycles for the unnotched test configuration and for two sets of notched mini specimens of as-built DMLS Ti6Al4V are plotted in Fig. 4. The fatigue data appear well-behaved with a reduced scatter for the Type A+ notch. The Type C is instead characterized by a larger scatter although the average behavior is not too different from the other direction. Compared to the reference smooth fatigue behavior, the notch effect is significant. According an empirical definition of the notch fatigue factor K_f (i.e. ratio between smooth fatigue strength/notched fatigue strength), the present mini specimen geometry with a stress concentration factor $K_t = 5$ is associated to $K_{f,A+} = 3$ and and $K_{f,C} = 2.4$.

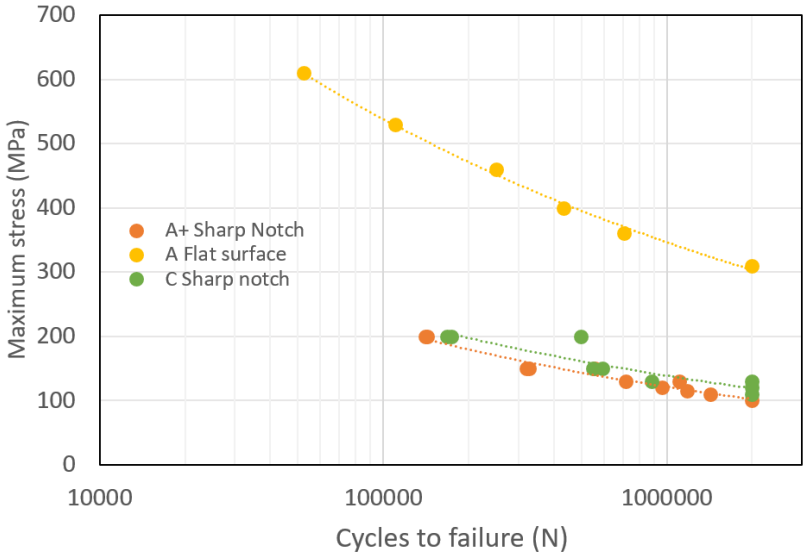

Fig. 4. Directional fatigue behavior of DMLS Ti6Al4V in the presence of sharp notches.

REFERENCES

[1] Nicoletto, G.: Anisotropic high-cycle fatigue behavior of Ti-6Al-4V obtained by powder bed laser fusion. International Journal of Fatigue 94, 255-262 (2017).

[2] Nicoletto, G.: Directional and notch effects on the fatigue behavior of as-built DMLS Ti6Al4V. International Journal of Fatigue 106, 124-131 (2018).

ACKNOWLEDGMENTS

The research was supported by the Slovak VEGA grant No. 1/0685/2015. Specimen production by the company BEAM-IT in Fornovo Taro (Italy) www.beam-it.eu is gratefully acknowledged.

Variable amplitude loading effect of notched additive manufactured Ti6Al4V with as-built surfaces

M. Kahlin[a,b]*, H. Ansell [a,c], J. J. Moverare[b]

[a] *Saab AB, Aeronautics, SE-581 88 Linköping, Sweden*
[b] *Division of Engineering Materials, Linköping University, SE-581 83 Linköping, Sweden*
[c] *Division of Solid Mechanics, Linköping University, SE-581 83 Linköping, Sweden*
**Corresponding author: magnus.kahlin@saabgroup.com*

Keywords: Additive manufacturing; Ti6Al4V; Variable amplitude loading; Stress concentration; Notch.

ABSTRACT

Additive manufacturing (AM) is generally considered to be very attractive for the aerospace industry in which AM could contribute to lightweight designs and thereby extend flight range and reduce fuel consumption. There are however a number of challenges, for example inferior fatigue properties, that need to be solved before AM could be used to its full potential in aerospace applications.

The fatigue behaviour of smooth, un-notched, additive manufactured specimens with rough as-built surface have already been widely studied with constant amplitude fatigue loading. However, these investigations cannot predict the response for most aerospace components since these would have geometries that include notches and radii, that would act as stress concentrations. Moreover, most aerospace components are exposed to variable amplitude loading which does not always give a consistent material behaviour compared to constant amplitude loading due to effects of overloads and load sequence order. In this study, the effect of a geometrical notch which rough as-built surface has been investigated with both constant [1] and variable [2] amplitude loading. The constant amplitude notch effect have been determined for both laser sintered and electron beam melted Ti6Al4V material with rough as-built surface and these results were used to predict fatigue life for variable amplitude loading with the Short-FALSTAFF (Fighter Aircraft Loading STAndard For Fatigue) load sequence [3,4] using a cumulative damage approach. The predicted results were verified by variable amplitude fatigue experiments which showed good consistency with the predictions. In addition to this, hot isostatic pressing (HIP) was found to have no impact on the fatigue properties when applied to parts with rough as-built surfaces.

REFERENCES

[1] Kahlin, M., Ansell, H., Moverare, J.J.: Fatigue behaviour of notched additive manufactured Ti6Al4V with as-built surfaces. Int J Fatigue (2017).
[2] Kahlin, M., Ansell, H., Moverare, J.J.: Fatigue behaviour of additive manufactured Ti6Al4V, with as-built surfaces, exposed to variable amplitude loading. Int J Fatigue (2017).
[3] Joint publication of Flugzeugwerke Emmen, Switzerland; Laboratorium für Betriebsfestigkeit (LBF), Germany; National Aerospace Laboratory (NLR), Netherlands; and Industrie-Anlagen-Betriebsgesellschaft mbH (IABG) G. FALSTAFF: Description of a fighter aircraft loading standard for fatigue evaluation (1976).
[4] CEAT Report M7681900, Centre d'Essais Aeronautique de Toulouse, Toulouse (1980).

ACKNOWLEDGMENTS

This work was financially supported by Saab AB, the Swedish Foundation for Strategic Research and the European Commission, through the Clean Sky 2 programme which all are greatly acknowledged.

An Overview on Fatigue Behavior of Additive Manufactured Parts and Progress Toward Standardization

N. Shamsaei[a*], M. Seifi[b]

[a] *Department of Mechanical Engineering, Auburn University, USA*
[b] *ASTM International and Case Western Reserve University, USA*
**Corresponding author: shamsaei@auburn.edu*

Keywords: Additive manufacturing; Fatigue; Mechanical behavior; Standardization; Qualification.

ABSTRACT

As more industries are adopting metal additive manufacturing (AM) technologies in load-bearing applications, a deep understanding of mechanical behavior, and in particular fatigue behavior, of AM parts becomes a necessity. In addition, while some standards for certification, qualification and documentation of AM processes, materials characterizations and mechanical behavior exist, many of these standards still need to be further modified/developed as we learn more about various aspects of mechanical and fatigue behavior of AM parts. In this presentation, the need for understanding the AM process-structure-property-performance relationships as they pertain to the fatigue behavior is highlighted. Various aspects of fatigue and fracture behavior of AM parts including the effects of build orientation, surface roughness, size, etc. will be discussed utilizing a comprehensive set of experimental data. This will be followed by a discussion on the lack of AM specific standards and limitations associated with using currently available qualification standards. Finally, some of the recent standardization activities with a focus on critical property measurements and relating the specimen property to part performance will be presented.

VHCF response of Gaussian SLM AlSi10Mg specimens: Effect of stress relieve heat treatment

A. Tridello[a*], C.A. Biffi[b], J. Fiocchi[b], P. Bassani[b], G. Chiandussi[a], M. Rossetto[a], A. Tuissi[b] , D.S. Paolino[a]

[a] *Department of Mechanical and Aerospace Engineering, Politecnico di Torino, 10129 Turin, Italy.*
[b] *CNR ICMATE – Institute of Condensed Matter Chemistry and Technologies for Energy, 23900 Lecco, Italy.*
**Corresponding author: andrea.tridello@polito.it*

Keywords: Selective Laser Melting (SLM); Very High Cycle Fatigue (VHCF); AlSi10Mg alloy; Heat treatment: Gaussian specimen.

ABSTRACT

In the last decades, the use of Additive Manufacturing (AM) techniques for the production of metallic components used in structural applications has rapidly increased. Among the AM techniques, Selective Laser Melting (SLM) is one of the most used, especially for Aluminum alloys as the AlSi10Mg alloy. SLM permits to manufacture parts characterized by very good quasi-static mechanical properties [1], that can even outperform those measured on parts manufactured with traditional subtractive technologies. Nonetheless, defects originating during the AM process (e.g., porosities induced by vaporization of light elements, incomplete melting of powder and residual oxide layers) may significantly affect the fatigue response of SLM parts. Therefore, High Cycle Fatigue (HCF) and Very High Cycle Fatigue (VHCF) can be critical and should be properly investigated to guarantee a safe and conservative design of SLM parts subject to fatigue.

According to the literature, the optimization of the process parameters and the proper design of the AM process (e.g., specimen orientation with respect to the building direction, heating of the building platform) can help to reduce the defect population and to enhance the fatigue response [2]. Moreover, the removal of the surface layer in AM parts has proved to improve the fatigue response [2] since superficial defects are generally more critical than internal ones [3]. Heat treatments could also affect the fatigue response, even if they do not permit to reduce the defect population. The effect of traditional heat treatments, which are usually applied to cast components, has been already investigated in the literature (for example the T6 heat treatment for the AlSi10Mg alloy in [2]). However, different heat treatments, specific for SLM parts, are being proposed by producers of SLM equipments and their effect on the HCF and the VHCF response is still under investigation.

The present paper compares the VHCF response of SLM AlSi10Mg specimens in two working conditions: as built and subjected to a standard heat treatment for stress relieve [4,5]. The heat treatment consisted of heating for two hours at 320°C and cooling in air down to room temperature. A significant increment of the material ductility was obtained after heat treatment: the elongation to failure (ε_f) was about four times the ε_f value of the non-treated material. Ultrasonic tests at 10^9 cycles were performed on SLM-built specimens (only a fine polishing is performed, according to [6]) before and after the heat treatment. To properly estimate the defect size distribution and to reliably assess the VHCF response [3], Gaussian specimens with large loaded volumes [7] were used for the ultrasonic tests. Fig. 1 shows the Gaussian specimen geometry used for the experimental tests.

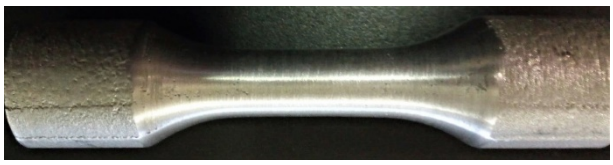

Fig. 1. Gaussian specimen used for the ultrasonic VHCF tests.

Fracture surfaces were investigated with the optical and the Scanning Electron Microscope (SEM) to assess the distribution of defect size. The fatigue strength at different number of cycles was statistically compared to assess the effect of the heat treatment on the VHCF response. The obtained microstructure and microhardness of heat treated and as built specimens were investigated and compared. Finally, a correlation among mechanical properties, microstructure and fatigue behaviour was proposed.

REFERENCES

[1] Kempen, K., Thijs, L., Van Humbeeck, J., Kruth, J.-P.: Processing AlSi10Mg by selective laser melting: parameter optimisation and material characterisation, Mater. Sci. Tech. Ser. 31:8, 917-923 (2015).

[2] Brandl, E., Heckenberger, U., Holzinger, V., Buchbinder, D.: Additive manufactured AlSi10Mg samples using Selective Laser Melting (SLM): Microstructure, high cycle fatigue, and fracture behaviour. Mater. Design 34, 159–169 (2012).

[3] Murakami, Y. Metal Fatigue: Effects Of Small Defects And Nonmetallic Inclusions. 1st ed. Elsevier Ltd, Oxford, UK (2002).

[4] Renishaw plc, Laser Meting: Aluminum AlSi10Mg_25mm_AM250-400W Parameter Validation, 2014.

[5] J. Fiocchi, A. Tuissi, P. Bassani, C.A. Biffi, Low temperature annealing dedicated to AlSi10Mg selective laser melting products, Journal of Alloys and Compounds 695C, 3402-3409 (2017).

[6] Tridello, A.: VHCF response of Gaussian specimens made of high-strength steels: comparison between unrefined and refined AISI H13. Fatigue Fract. Engng. Mater. Struct. 40(10), 1676–1689 (2017).

[7] Paolino, D.S., Tridello, A., Chiandussi, G., Rossetto, M.: On specimen design for size effect evaluation in ultrasonic gigacycle fatigue testing. Fatigue Fract. Engng. Mater. Struct. 37, 570–579 (2014).

ACKNOWLEDGMENTS

The Authors acknowledge the Piedmont Region Industrial Research Project STAMP (Sviluppo Tecnologico dell'Additive Manufacturing in Piemonte, MIUR – POR FESR 2014/2020 – Azione 3 Piattaforma Tecnologica "Fabbrica Intelligente") and Accordo Quadro CNR/Regione Lombardia n. 3866 del 17/07/2015 FHfFC for financial support, BeamIT for technical assistance.

Mechanical behaviour of AM lattice structures under static and cyclic loading

K. Burkamp[a*], L. Heine[a], J. Kunz[b], M. Voshage[c], C. Broeckmann[a], J.H. Schleifenbaum[c,d]

[a]*Institute for Materials Applications in Mechanical Engineering (IWM), RWTH Aachen University, Augustinerbach 4, 52062 Aachen, Germany*
[b]*Institute of Applied Powder Metallurgy and Ceramics at RWTH Aachen e.V. (IAPK), Augustinerbach 4, 52062 Aachen, Germany*
[c]*Digital Additive Production (DAP), RWTH Aachen University, Steinbachstraße 15, 52074 Aachen, Germany Germany*
[d]*Fraunhofer Institute for Laser Technology (ILT), Steinbachstraße 15, 52074 Aachen, Germany*
**Corresponding author: k.burkamp@iwm.rwth-aachen.de*

Keywords: fatigue; laser-powder bed fusion; additive manufacturing; lattice structure; cyclic loading.

ABSTRACT

Additive Manufacturing (AM) gives new freedom of constructive possibilities to design engineers. Many structures with features like cavities or thin beams are impossible to build using conventional methods such as casting or machining. Using AM even finest lattice structures can be produced, and they have high potential to be used as frameworks for transducing loads in structural components. However, until now the study about the failure behaviour of lattice structures under static [1,2] and cyclic loading is insufficient, especially for those lattice structures produced with laser-powder bed fusion (L-PBF) followed by hot isostatic pressing (HIP). In this work both static bending load and cyclic axial loading on X2CrNiMo17-12-2 steel lattice structures produced by L-PBF were investigated. An $f_2$ccz lattice structure, which showed best mechanical properties in preliminary tests, was used in all mechanical tests [1]. This work also investigated the influence of laser power in L-PBF process and the influence of HIP treatment after L-PBF process on mechanical properties of lattice structures. To investigate fracture behaviour of a single lattice cell, static bending tests were performed in-situ in scanning electron microscope (SEM) with slowly and continuously increasing load. Fig. 1 shows detailed damage evolution at the critical node of the lattice structure. Due to the notch effect at the marked node, a crack initiates at the inside of the structure and grows towards the outside.

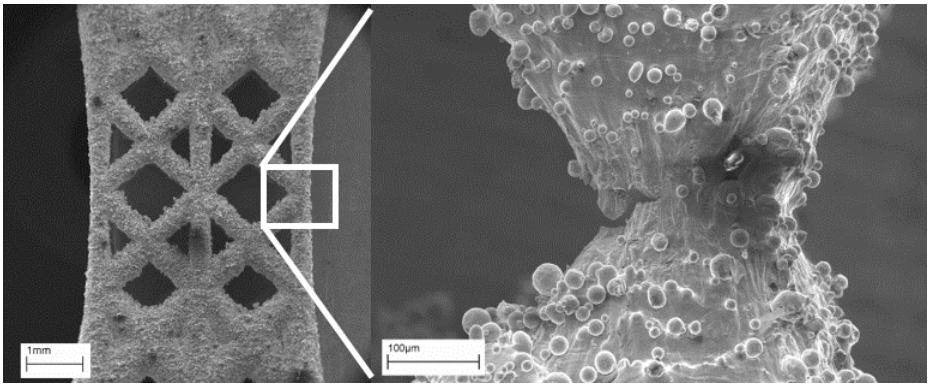

Fig. 1. SEM in-situ crack observation on $f_2$ccz lattice structure during static bending

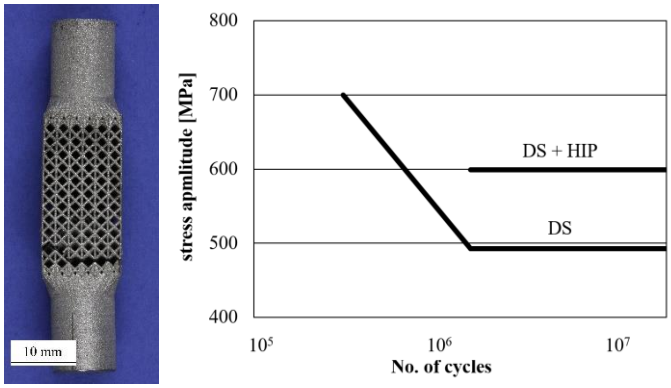

Fig. 2. Geometry of cracked specimen and S-N-curves of as-built (DS) compared to HIP treatment (DS+HIP)

Regarding geometric properties, different Laser parameters mainly influence dimensional accuracy, porosity and surface roughness of the specimen. It was found that, HIP treatment after L-PBF process significantly increases fatigue strength of the structure, whereas a change in process parameters (different laser powers) did not have a large impact on fatigue behaviour. Fig. 2 shows the specimen geometry for cyclic loading with an alternating load amplitude at $R = -1$ and compares S-N-curves of lattice structures in reference state and after HIP treatment. During fatigue testing the lattice structures provide excellent emergency running properties before failure. If one node fails in the first place, the overall stiffness of the structure drops, the entire structure is still able to withstand further load cycles. The SEM graph in Fig. 3 (a) shows that, the crack initiation occurs at an inhomogeneous position, which causes a notch effect at the surface. Striations of crack propagation can be seen in Fig. 3 (b).

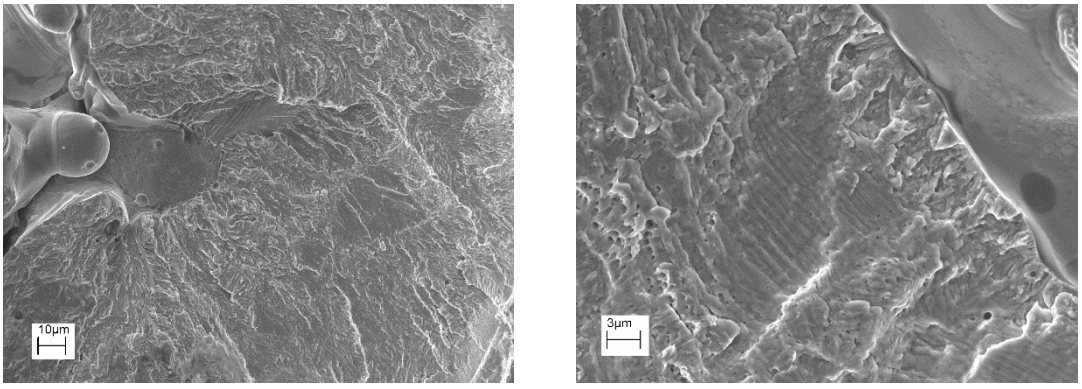

(a) (b)

Fig. 3. Close up of fracture origin (a) and striations on fracture plane (b)

REFERENCES

[1] Merkt, S.: Qualifizierung von generativ gefertigten Gitterstrukturen für maßgeschneiderte Bauteilfunktionen, Dissertation, RWTH Aachen University (2015)

[2] Wauthle, R.: Effects of build orientation and heat treatment on the microstructure and mechanical properties of selective laser melted Ti6Al4V lattice structures. Additive Manufacturing, 77-84 (2015).

Fatigue Crack Growth and Threshold of Materials Prepared by Additive Manufacturing

L. Kunz[a*], G. Nicoletto[b], R. Konečná[c],

[a]*Institute of Physics of Materials, Academy of Sciences of the Czech Republic, Brno, Czech Republic*
[b]*Department of Engineering and Architecture, University of Parma, Italy*
[c]*Department of Materials Engineering, University of Žilina, Slovakia*
**Corresponding author: kunz@ipm.cz*

Keywords: Direct metal laser sintering; Ti6Al4V; IN 718; Growth of long fatigue cracks; Threshold for crack growth

ABSTRACT

Static properties of many metals and alloys produced by additive manufacturing (AM) are well comparable to the static performance of conventionally fabricated materials. Suitably chosen parameters of AM process and application of hot isostatic pressing can reduce the process-driven defects in such a way that the ultimate tensile strength, yield stress and elongation correspond to the materials produced in the traditional way. In contrast to the static performance the fatigue strength and the fatigue limit are strongly susceptible to the details of microstructure, surface quality and small defects, which remain in material even after applying optimally selected process parameters and post-processing treatment.

The damage tolerant design and the prediction of the fatigue life of components with cracks require quantified description of the propagation of long fatigue cracks. Particularly, the knowledge on the behaviour of cracks in the threshold region for propagation is of utmost importance. From the investigation of the conventional materials it is well known that the crack propagation is only weakly influenced by material microstructure in the range of higher crack rates, i.e. the Paris region. On the other hand, the microstructure, loading conditions and environment strongly influence the crack growth near the threshold. Because the microstructure of AM materials often differs substantially from that of conventionally produced ones, it is obvious that the knowledge and data available for conventionally manufactured materials cannot be applied for materials prepared by AM.

The contribution brings results on the experimental determination of the fatigue crack growth and threshold values of the stress intensity factor for two different and often applied engineering materials namely a superalloy IN 718 and titanium alloy Ti6Al4V. Specimens of IN 718 were manufactured on a RENISHAW A250 machine and specimens of Ti6Al4V on an EOSINT M 270 system. The process parameters i.e. the laser power, layer thickness, scanning speed and mode were optimised by the company BEAM-IT Fornovo Taro, Italy.

Experimental determination of the fatigue crack growth rates was performed on CT specimens with characteristic dimension w = 30 mm and thickness 6 mm. The specimens fulfilled the requirements of the ASTM E647 Standard. Tests were conducted at room temperature. The length of the fatigue cracks was optically monitored on polished lateral sides of specimens by means of CCD cameras situated on travelling supports.

Fatigue tests were performed on two different types of fatigue testing machines, namely a resonant Roell/Amsler HFP 5100 machine and an electrodynamic testing system INSTRON E3000 with linear motor technology.

For IN 718 it has been found that the fatigue crack growth resistance in the build direction in the threshold region was substantially lower than that of conventionally manufactured alloy. The threshold value of the stress intensity factor range ΔK_{th} was 3.0 $MPam^{1/2}$, which is only one third of the value for IN 718 manufactured conventionally [1, 2]. The low value can be explained by (1) the specific very fine microstructure of the DMLS material, (2) low boron content and (3) residual stresses. In the region of high crack growth rates the difference between the additive and conventionally manufactured material decreases.

For Ti6Al4V it was found that the crack propagation and threshold values for crack growth are dependent on the heat treatment applied to the as-built material. The influence of three heat treatments on crack growth and material microstructure were investigated. The stress relieving at 380 °C for 8 h results in substantial improvement of the fatigue crack growth resistance when compared to the as-built material, although the microstructure is nearly identical in both cases. The stress relieving at 740 °C for 2 h changed the microstructure only slightly. The average crack growth rate remained unchanged, however the scatter of experimental data decreased. The heat treatment at 900 °C for 2 h resulted in substantial change of the microstructure and small improvement of the threshold value. The fatigue crack growth resistance of material heat treated at 900 °C correlates with the conventionally manufactured alloy [3]. It has been found that under suitably chosen processing parameters the crack propagation characteristics do not depend on the direction of the crack propagation relative to the direction of the specimen building.

In both studied materials the crack growth was transgranular. The crack propagation mechanism in IN 718 consists in planar cyclic slip in the region ahead of the crack tip. The cyclic loading leads to gradual damage of suitably oriented slip bands and development of microcracks. The main crack grows by their linking. This mechanism operates both in the threshold and in the Paris region. Only at very high growth rates exceeding 0.1 μm/cycle formation of striations on the fracture surface was observed, which means that the plastic blunting model can be considered as suitable for the crack growth. In Ti6Al4V alloy the crack propagates through very fine structure consisting of needles of α' martensite (380 °C), fine needles of α phase in β matrix (740 °C) or lamellar α+β structure (900 °C). The original boundaries of columnar β grains do not influence the crack paths.

The discussion is focused on the influence of the specific features of the structure produced by the additive technologies, its directionality due to the layer structure and also to the influence of the residual stresses of all three types.

The main conclusion is that under optimized AM processing parameters the resistance against growth of long cracks may achieve the properties of conventionally produced materials. However, for reliable damage tolerant design it is imperative to have the crack growth data reflecting the applied processing parameters. This is particularly true for the threshold area.

REFERENCES

[1] Mercer, C., Soboyejo, A. B. O., Soboyejo, W. O.: Micromechnisms of fatigue crack growth in a forged Inconel 718 nickel-based superalloy. Mat. Sci. Eng. A270, 308-322 (1999).
[2] Clavel M., Pineau, A.: Frequency and wave-form effects on the fatigue crack growth behavior of alloy 718 at 298 and 823 K. Met. Trans. A 9A, 471–480 (1978).
[3] Konečná, R., Kunz, L., Bača, A., Nicoletto, G.: Resistance of direct metal laser sintered Ti6Al4V alloy against growth of fatigue cracks. Eng. Fract. Mech. 185, 82-91 (2017).

ACKNOWLEDGMENTS

The research was supported by the project Slovak VEGA grant No. 1/0685/2015. Specimen production by the company BEAM-IT Fornovo Taro (Italy) (www.beam-it.eu) is gratefully acknowledged.

Fatigue properties of Ti-6Al-4V thin parts produced by additive manufacturing: Effect of various post-treatments

T. Persenot[a], A. Burr[b], G. Martin[b*], E. Maire[a], J-Y. Buffière[a], R. Dendievel[b]

[a]*INSA Lyon, CNRS, MATEIS, F-69621 Villeurbanne, France*
[b]*Univ. Grenoble Alpes, CNRS, Grenoble INP, SIMAP, F-38000 Grenoble, France*
**Corresponding author: guilhem.martin@simap.grenoble-inp.fr*

Keywords: Electron Beam Melting; Titanium alloys; Fatigue; X-ray microtomography; Post-treatments

ABSTRACT

Designing structural parts including cellular or lattice structures fabricated by additive manufacturing is very promising. However, applications will remain limited as long as the fatigue performances of such structures are not understood and controlled. The objective of this work is to investigate the fatigue properties of Ti-6Al-4V as-built thin parts produced by Electron Beam Melting (EBM). To mimic the behaviour of thin parts or struts, a specific geometry was used to produce tensile specimens with a nominal diameter of 2 mm. Thus, the gauge length of those specimens can be seen as single beams constituting the lattice structures. Fatigue mechanisms have been first identified from cyclic tension-tension tests (constant stress amplitude, R=0.1). Every sample was characterized by laboratory X-ray microtomography before and after failure with a voxel size of 2.5 microns. The extensive use of X-ray microtomography allows to reveal the defects inherited from the EBM process: porosity, plate-pile like defects, roughness. SEM and tomographic observations of the fracture surfaces help to identify the critical defects responsible for the fatigue failure. It was found that crack initiation always occurs at the surface from thin and relatively deep (up to 200 µm) notch-like defects as illustrated in **Fig. 1**. Fatigue performances of as-built samples are therefore rather low in comparison with wrought materials. Various post-treatments: chemical etching, hot isostatic pressing as well as ultrasonic shot peening have been performed to increase the fatigue resistance. Traditional machining was not investigated as it is considered as an inappropriate solution for complex geometries such as lattice structures. The effects of each of those treatments on the fatigue properties are investigated and related to the "healing" of the aforementioned defects. Finally, adequate combinations of these post treatments are shown to significantly improve the fatigue performances.

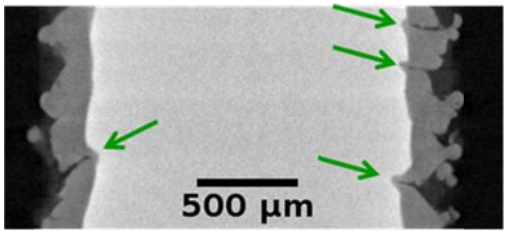

Fig. 1. Notch-like defects observed in the as-built conditions (dark grey) and partially removed by chemical etching (light grey).

ACKNOWLEDGMENTS

The authors would like to thanks the French Agence Nationale de la Recherche (ANR) and the French Fondation de Recherche pour l'Aéronautique et l'Espace (FRAE) for the financial support of the project entitled "Fabrication Additive et FAtigue de Structures Cellulaires Intégrées en AEronautique" (FA2SCINAE-ANR-15-CE08-0038-03). P. Emile and C. Archambeau from AIRBUS are also gratefully acknowledged for fruitful discussions.

Defects and Scale Effect in LCF for AlSi10Mg Obtained by SLM

S. Beretta[a], S. Romano[a*], S. Foletti[a], S.P. Zhu[a,b]

[a] *Department of Mechanical Engineering, Politecnico di Milano, Italy*

[b] *School of Mechatronics Engineering, University of Electronic Science and Technology of China, China*

**Corresponding author: simone.romano@polimi.it*

Keywords: Defects; Additive manufacturing; Scale effect; LCF; HCF.

ABSTRACT

In the recent years, additive manufacturing (AM) has introduced outstanding opportunities for various applications. The fundamentals and working principle of AM offer several advantages, including significant material and mass saving, near-net-shape capabilities, superior design and geometrical flexibility and significant reduction of concept-to-validation time [1]. These reasons have raised the interest of space and aerospace companies, as well as automotive, medical, and energy industries.

One of the main limiting drawbacks is the difficulty to achieve a good and stable material quality. This is mainly referred to the poor surface roughness and compliance to strict tolerances and to the ineluctable presence of manufacturing defects. A literature review of two of the most used lightweight alloys in the space and aerospace sectors (AlSi10Mg and Ti6Al4V) [2] showed the applicability of the defect tolerant design [3] for assessing the fatigue limit of parts containing manufacturing defects. In fact, the defects can be treated as short cracks at stress levels close to the fatigue limit. The scatter is a combination of the inherent variability and dependence on the defect size, which can be simply described by the Murakami's √area parameter [4].

In this presentation we will describe a series of LCF experiments onto cylindrical samples of AlSi10Mg obtained by SLM with a different cross section. The results show that there is, as expected from the 'weakest-link' concepts [5], a difference in the size of the maximum defect at the fracture origin. However, there is not significant difference among the e-N diagram of the three specimen size. The implementation of crack growth model based on ΔJ_{eff} clearly shows that the difference in crack propagation lifetime counteracts the 'weakest-link' effect.

REFERENCES

[1] Zhai, Y., Lados, D.A., LaGoy, J. L.: Additive manufacturing: Making imagination the major limitation, JOM 66 (5), 808-816 (2014).

[2] Beretta, S., Romano, S.: A comparison of fatigue strength sensitivity to defects for materials manufactured by AM or traditional processes, Int. J. Fatigue 94 (2), 178-191 (2017).

[3] Murakami, Y.: Metal Fatigue: Effects of Small Defects and Nonmetallic Inclusions, Elsevier, Oxford, 2002.

[4] Romano, S., Brückner-Foit, A., Brandão, A., Gumpinger, J., Ghidini, T. and Beretta, S.: Fatigue properties of AlSi10Mg obtained by additive manufacturing: Defect-based modelling and prediction of fatigue strength. Engineering Fracture Mechanics 187, 165-189 (2018).

[5] Wormsen, A., Sjödin, B., Härkegård, G. and Fjeldstad, A.: Non-local stress approach for fatigue assessment based on weakest-link theory and statistics of extremes. Fatigue & Fracture of Engineering Materials & Structures 30 (12), 1214-1227 (2007).

Characterisation of the Cyclic Material Behaviour of AlSi10Mg and Inconel 718 produced by SLM

M. Scurria[a*], B. Möller[b], R. Wagener[b], T. Melz[a,b]

[a]*Research Group of System Reliability, Adaptive Structures and Machine Acoustic SAM, Technical University of Darmstadt, Germany*
[b]*Fraunhofer Institute for Structural Durability and System Reliability LBF, Darmstadt, Germany*
**Corresponding author: scurria@sam.tu-darmstadt.de*

Keywords: SLM; AlSi10Mg; Inconel; Cyclic material behaviour.

ABSTRACT

The flexibility in design offered by advanced additive manufacturing technologies makes this process more and more attractive for the automotive as well as aircraft industry, especially for the realisation of metal components. Nevertheless, while on the one hand additive manufacturing paved the way from new design solutions which were not possible before, on the other hand it represents a new process still not being standardised and, therefore, exploitable. In this work, the cyclic material behaviour of two different metals produced by additive manufacturing technologies is evaluated. Small-scale specimens produced by Selective Laser Melting (SLM) of Aluminium AlSi10Mg and Inconel718 powder are first subjected to Incremental Step Tests (IST) [1] in order to evaluate the cyclic stress-strain behaviour of the material. In order to define the initial conditions, specimens oriented along the powder deposition direction in X (0°, lying), XZ (45°) and Z (90°, standing) directions or lying orthogonal to the powder deposition direction with respect to the building platform are produced using standard process parameters (Fig.1, left). Individually adapted support structures, needed for lying (X direction) structures and surfaces with downskin angles up to 45°, are subsequently removed.

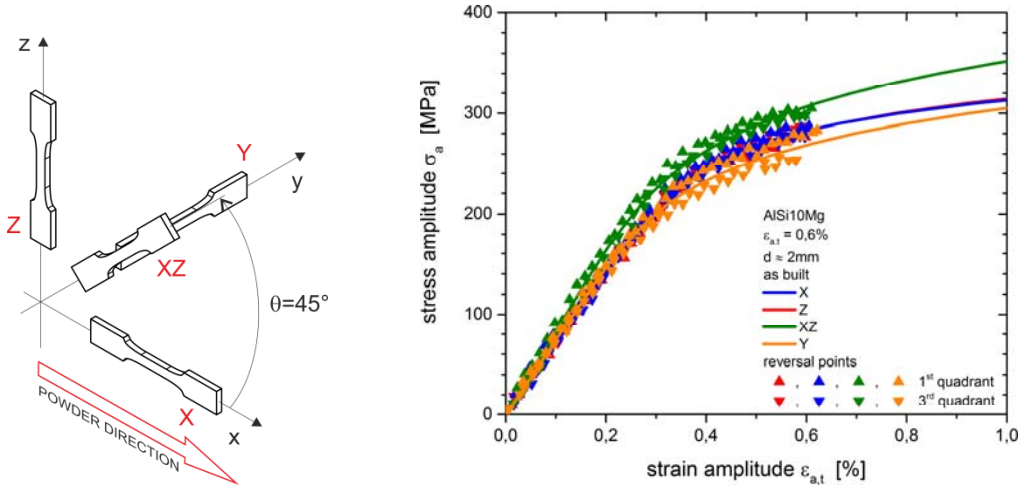

Fig. 1. Results of the Incremental Step Tests performed at a maximum strain amplitude of $\varepsilon_{a,t}$ = 0.6% on specimens of 2 mm thickness (right) produced with four different building orientations (left).

Half of the specimens are left as built, and the other half is polished, so that the influence of the surface condition including removed support structures is investigated The effects of removed support

structures, variation thickness, four building orientations surface conditions and an additional heat treatment on the cyclic stress-strain behaviour of the material is evaluated. In Fig. 1 (right), the cyclic stress-strain curves resulting from ISTs of 2 mm thick AlSi10Mg specimens for the investigated building orientations (X, XZ, Z and Y) show an anisotropic behaviour. Beyond that, based on the knowledge obtained, relevant parameters are identified and characterised through the cyclic stress-strain behaviour. Hereafter, the specimens are subjected to force controlled cyclic loading and the results of the tests are processed to evaluate the fatigue strength of the materials analysing the S-N curves in the range of $10^4 \div 10^7$ cycles to failure.

REFERENCES

[1] Landgraf, R.W., Morrow, J., Endo, T.: Determination of the cyclic stress-strain curve, Journal of Materials, JMLSA 4, 176-188 (1969).

ACKNOWLEDGMENTS

The authors would like to acknowledge the Federal Ministry for Economic Affairs and Energy for its financial support within the project “VariKa” and the Federal Ministry of Education and Research for supporting the project “BadgeB”.

Application of Data Science Approach to Fatigue Property Assessment of Laser Powder Bed Fusion Stainless Steel 316L

M. Zhang[a], C.N. Sun[b], X. Zhang[c], P.C. Goh[d], J. Wei[b], D. Hardacre[d], H. Li[a*]

[a]*Singapore Centre for 3D Printing, Nanyang Technological University, Singapore*
[b]*Singapore Institute of Manufacturing Technology, ASTAR, Singapore*
[c]*Faculty of Engineering, Environment & Computing, Coventry University, United Kingdom*
[d]*Lloyd's Register Global Technology Centre, Singapore*
**Corresponding author: lihua@ntu.edu.sg*

Keywords: Fatigue; Fuzzy rules; Quality assessment; Selective laser melting; Stainless steel 316L.

ABSTRACT

Laser powder bed fusion (L-PBF) is a popular additive manufacturing (AM) technique for fabricating metal parts. Prior work by the authors shows that stainless steel 316L processed by L-PBF exhibits different high cycle fatigue fracture behaviour from the conventionally manufactured forms [1]. For the optimally-processed samples, fatigue fracture is characterised by intergranular crack initiation at dendritic grain boundaries, whereas for samples containing critical pores or lack of fusion defects, crack initiation is driven by such defects. Identifying the critical defect size for the transition between the microstructure- and porosity-driven failure modes is important for controlling the fatigue properties.

Besides the different failure mechanisms, the general empirical relation between static and fatigue properties, where the fatigue endurance limit is approximately half of the tensile strength for conventional ferrous metals [2], is not valid for L-PBF stainless steel 316L [3]. This is because while the ultrafine grains produced by the rapid cooling process gives rise to superior tensile strength, the beneficial effect on fatigue properties is offset by the microstructure defects, which compromise fatigue strength at long life.

Results from the prior works indicate that factors such as porosity and static tensile properties are important and could be used as the input variables for fatigue property assessment of L-PBF stainless steel 316L. However, recognising these variables does not address the uncertainties associated with the process. Specifically, it involves a large number of processing variables, such as laser power, scan speed and hatch pattern, which induce different thermal histories such that various porosity and tensile property conditions are possible in the final part depending on the selection of the build conditions. For instance, with over-melting, the loss of low melting point alloying elements could lead to strength degradation without impacting porosity, whereas with under-melting, the same reduction in material strength could be due to the generation of lack of fusion defects. As these conditions produce different microstructures and defects, they need to be modelled separately. Besides, complete information of the material properties are often not available and crude estimations based on expert knowledge have to be made with regards to the fabrication quality of the parts. The complex interplay between the input variables and fatigue properties, as well as the ambiguity associated with determining the values of the input variables, make modelling the fatigue properties of L-PBF materials a non-trivial task.

Conventional practices to account for such elements of uncertainty involve applying reduction factors on fatigue curves, but this approach will lead to conservative designs. The nonlinear material behaviour could be modelled by computational techniques, among which the artificial neural network (ANN) have been successfully applied in a number of material science fields for process control and property prediction [4, 5]. This system can effectively handle complex empirical data for which analytical solutions cannot be easily obtained; it could potentially be applied for modelling the fatigue problem of L-PBF stainless steel 316L.

However, one of the shortcomings of neural network is that it adopts attributes of the 'black box', which is not desirable considering the uncertainties associated with fatigue modelling. The fuzzy logic, which describes input variables by a set of linguistic terms, could provide the desired physical meaning and transparency to the system, and address the problem of imprecise and insufficient information. For example, key fatigue assessment indicators, including porosity condition and static tensile properties, could be related to fatigue life via the 'if-then' rules:

Rule 1: If porosity fraction is low and tensile strength is high and ductility is high, then fatigue life is long.

Rule 2: If porosity fraction is low and tensile strength is low and ductility is low, then fatigue life is short.

The implementation of such rules allows the states between acceptable and non-acceptable porosity and strength conditions to be defined imprecisely by fuzzy boundaries. Moreover, in view of the difficulty in generating a large amount of fatigue data, the fuzzy system allows easier result verification as it is based on physical understanding of the system [6]. Prior knowledge on the relations between input and output variables could also be used for formulating the fuzzy rules.

Considerable high cycle fatigue data has been generated by the authors to allow an examination of the applicability of data-driven approach to fatigue property assessment of L-PBF stainless steel 316L. Samples with representative porosity and tensile properties were produced by adjusting L-PBF processing parameter and subjected to load-controlled fatigue tests. The adaptive neuro-fuzzy inference system (ANFIS), which incorporates fuzzy logic into the neural network, will be tested for fatigue life prediction by using porosity fraction, tensile strength and ductility as the input variables.

REFERENCES

[1] Zhang, M., Sun, C.-N., Zhang, X., Goh, P. C., Wei, J., Hardacre, D. and Li, H.: Fatigue and fracture behaviour of laser powder bed fusion stainless steel 316L: Influence of processing parameters. Mater. Sci. Eng. A 703, 251-261 (2017).
[2] Tóth, L. and Yarema, S.Y.: Formation of the science of fatigue of metals. Part 1. 1825–1870. Materials Science 42(5), 673-680 (2006).
[3] Zhang, M., Sun, C.-N., Zhang, X., Goh, P. C., Wei, J., Li, H. and Hardacre, D.: Elucidating the Relations Between Monotonic and Fatigue Properties of Laser Powder Bed Fusion Stainless Steel 316L. JOM 70(3), 390–395 (2018).
[4] Ozerdem, M.S. and Kolukisa, S.: Artificial neural network approach to predict the mechanical properties of Cu–Sn–Pb–Zn–Ni cast alloys. Mater. Des. 30(3), 764-769 (2009).
[5] Wang, H., Zhang, W., Sun, F. and Zhang, W.: A Comparison Study of Machine Learning Based Algorithms for Fatigue Crack Growth Calculation. Materials 10(5), 543 (2017).
[6] Schooling, J., Brown, M. and Reed, P.: An example of the use of neural computing techniques in materials science—the modelling of fatigue thresholds in Ni-base superalloys. Mater. Sci. Eng. A 260(1-2), 222-239 (1999).

ACKNOWLEDGMENTS

This work was supported by the Singapore Economic Development Board (EDB) Industrial Postgraduate Programme (IPP).

Tensile and Fatigue Properties Simulation of Additive Manufactured Ti-6Al-4V Alloy with Microstructure Sensitive Model

Dianyin Hu[a,b,c*], Jinchao Pan[a], Jianxing Mao[a], Rongqiao Wang[a,b,c]

[a] *School of Energy and Power Engineering, Beihang University, Beijing 100191, China*
[b] *Collaborative Innovation Center of Advanced Aero-Engine, Beijing 100191, China*
[c] *Beijing Key Laboratory of Aero-Engine Structure and Strength, Beijing 100191, China*
**Corresponding author: hdy@buaa.edu.cn (D.Y. Hu)*

Keywords: Tensile and fatigue; Microstructure sensitive model; Additive manufacturing; Damage.

ABSTRACT

The mechanical properties of titanium alloy is determined by the form, orientation and volume fraction of α and β grains, as well as the defects existing in the grain boundaries. When it comes to additive manufacturing, such as the selective laser melting (SLM), the dependence of mechanical properties on microstructures turns out to be more prominent, due to the separate cooling process of laser-melt material. Thus, inhomogeneity should be effectively captured to represent local stress/strain distribution, involving grain size, orientation and the evolution of defect. Therefore, this paper is motivated to formulate constitutive and damage models combining representative microstructural information.

The grain size and grain orientation provide constraints for material local deformation, generating great influence on local stress/strain state. The defects in titanium alloy manufactured by SLM include pores resulting from entrapped gas, un-melt particles/regions introduced by missing laser scanning, serving as the source of damage. The un-melt particles/regions detached from the matrix result in void nucleation. The voids and pores cause discontinuity in material, leading to the nucleation of crack as well as the final fracture of structures.

To represent the mechanical property under the consideration of above microstructures, we employ internal state variable (ISV) damage model to simulate the tensile process and microstructure sensitive fatigue (MSF) model to describe the fatigue property. Defining the void volume ratio of the original volume as the damage, the ISV damage model describe the process of void nucleation, growth and coalescence and calculate the total volume fraction of defects to get total damage, then the damage is used to reduce the modulus. The MSF model describes the total fatigue life by three parts, including the crack incubation at a micro-notch, the microscale crack growth and the macroscale crack growth until fracture. Model validations are carried out on series of existing data, which exhibit good agreement between prediction and experiments.

Residual Stresses and Distortion Compensation in Additive Manufacturing

A. Yaghi[a*], S. Ayvar-Soberanis[b], S. Moturu[c], R. Bilkhu[b], S. Afazov[a]

[a] *Manufacturing Technology Centre (MTC), United Kingdom*
[b] *Advanced Manufacturing Research Centre (AMRC), United Kingdom*
[c] *Advanced Forming Research Centre (AFRC), United Kingdom*
**Corresponding author: anas.yaghi@the-mtc.org*

Keywords: Additive Manufacturing; Laser Powder Bed Fusion (L-PBF); Finite Element (FE) Modelling; Distortion Compensation and Mitigation; Residual Stress Simulation; Surface Machining; Electronic Speckle Pattern Interferometry (ESPI); Contour Method.

ABSTRACT

This paper presents the methodology and findings of a novel piece of research with the purpose of understanding residual stresses and mitigating distortion caused by the combined processes of additive manufacturing (AM) and post machining to final specifications. The research work started with the AM building of a stainless steel 316L industrial impeller that was then machined by removing around 0.5mm from certain surfaces of the impeller's blades and hub. Distortion and residual stresses were experimentally measured.

The manufacture of the impeller by AM and then post machining was numerically simulated by applying the finite element (FE) method. Distortion and residual stresses were simulated and validated. The quantification of residual stresses can play an important role in the management of fatigue during service. The FE distortion was used in a numerical procedure to reverse distortion directions in order to produce a new impeller with mitigated distortion. The results have shown that distortions in the new impeller, on average, have reduced to less than 50% of the original non-compensated values.

Damage Accumulation in Press-Fit Joints of AM Parts Subjected to Static and Cyclic Loading

A. Brückner-Foit[a*], I. Bacaicoa[a], S. Horn[a], F. Brenne[a], T. Niendorf[a]

[a] *Institute for Materials Engineering, University of Kassel, Kassel, Germany*
**Corresponding author: a.brueckner-foit@uni-kassel.de*

Keywords: Press-fit joint; Damage accumulation; In-situ testing; DIC.

ABSTRACT

Parts manufactured by AM have to be integrated into more complex structures, as additive manufacturing of simple parts is too time consuming and, consequently, too expensive. A typical scenario is that there is a structured part made by AM and conventionally manufactured shaft or hub with a press-fit joint in between. Under operational conditions, the joint is subjected both to static and to vibrational loading. However, it may be unsafe to employ classical design rules even under static loading, as these implicitly assume a limited amount of surface roughness, which may be exceeded in AM parts without additional surface finishing.

Under vibrational loading, the differences are even more pronounced between press-fit joints with conventionally manufactured parts and those including AM parts, as the surface roughness of the AM parts strongly influence the failure mechanisms. First, a high value of the roughness implies that there are significant micro-notches from which cracks may initiate. Second, roughness tips may introduce a certain amount of form fit and additional adhesive forces, especially if the AM part has a higher hardness than the conventionally manufactured part. This implies that a new testing procedure has to be defined for press-fit joints including AM parts subjected to vibrational loading, as the classical fretting test cannot take the benefit of an additional form fit into account.

The basic idea of the AM specific testing procedure presented here is to use a classical flat dog-bone fatigue specimen with a press-fit joint in the centre. This specimen is then subjected to tensile or fatigue loading with the deformation field in the region of the joint monitored by a long-distance optical microscope and digital image correlation. Consequently, the onset of damage can be detected quite early and the role of micronotches and roughness tips can be analysed. First results using an AM steel shaft pressed into a steel specimen will be given. The three-dimensional nature of the damage process in the joint will be further studied using high resolution computer tomography (μ-CT).

Fatigue Behaviour, Modelling and Applications

Symposium G-FBMA-ICMFM

Organized by:

Teresa Morgado, Portugal

Rui Martins, Portugal

Alexandre Velhinho, Portugal

Filipe Silva, Portugal

On the Fatigue Resistance of Rotary Endodontic Instruments Subjected to Electrochemical Polishing and to an Autoclave Sterilization Cycle

Pedro Santos[a], Rui F. Martins[b*], António Ginjeira[c]

[a]*Department of Mechanical and Industrial Engineering, Universidade Nova de Lisboa, Portugal*
[b]*UNIDEMI, Department of Mechanical and Industrial Engineering, Universidade Nova de Lisboa, Portugal*
[c]*Faculty of Dental Medicine, Universidade de Lisboa, Portugal*
**Corresponding author: rfspm@fct.unl.pt*

Keywords: Electrochemical Polishing; Autoclave cycle; Endodontic Instruments; Fatigue Resistance; Ni-Ti Alloys.

ABSTRACT

The research herein presented aimed to determine the influence of surface finishing and of the application of an autoclave sterilization cycle in the fatigue resistance of Hyflex® CM endodontic instruments (ref. 20/.04 and ref. 20/.06).

Several combinations of electrochemical parameters, namely voltage, flow rate and duration, were considered during the experiments, but the best surface finish was obtained after the application of 30 volt, at a flow rate of 1, and for a period of 3 seconds. The endodontic files were weighed before and after the polishing procedure using a microbalance. The weight variation of the polished files was below 1.01mg and the fatigue resistance of all polished endodontic instruments increased between 30% (ref..06/20) and 80% (ref. .04/20) when compared with the fatigue resistance of the endodontic files in the as-fabricated condition.

Concerning the autoclave's sterilization cycle, no definitive conclusions about its influence on the fatigue resistance of endodontic files could be drawn, since the polished instruments ref. .06/20 showed higher fatigue resistance (+52%) after being submitted to an autoclave's cycle, and, inversely, polished instruments ref. .04/20 showed a lower fatigue resistance after the autoclave's cycle had been applied.

ACKNOWLEDGMENTS

The authors would like to thank the Portuguese Foundation for Science and Technology through project ref. UID/EMS/00667/2013.

Determination of the Stress Intensity Factors K_I, K_{II}, K_{III} and K_{eq} Induced at Crack Tip of Compact Tension Specimens Subjected to Torsional Loading

Luís Ferreira[a], Rui F. Martins[b*]

[a]*Department of Mechanical and Industrial Engineering, Universidade Nova de Lisboa, Portugal*
[b]*UNIDEMI, Department of Mechanical and Industrial Engineering, Universidade Nova de Lisboa, Portugal*
**Corresponding author: rfspm@fct.unl.pt*

Keywords: Mode III loading; Torsional loading; CT specimens; Stress intensity factors; Finite Element Analysis.

ABSTRACT

Fatigue crack growth in mechanical components can lead to catastrophic failure. Additionally, crack growth rates and crack growth path will depend on the type and magnitude of the applied loads, as well as on the thickness of the solid bodies, the crack length, and the mechanical properties of the material, just to mention a few.

Moreover, crack growth under mode I loading is very well documented in opposition to what relates to mode III loading, with few studies on the subject.

The paper herein presented shows the Stress Intensity Factors values (SIFs), K_I, K_{II} and K_{III}, obtained for *Compact Tension* (CT) specimens with different thicknesses, namely 2.5 mm; 3 mm; 5 mm; 7.5 mm; 10 mm, that were subjected to some torsional loads (6 $N.m$; 7.5$N.m$; 9 $N.m$). The CT specimens, which were analysed using the Finite Element Method (FEM), were modelled with two cracks that had grown experimentally from a fatigue pre-crack along two directions (+70º and -70º), and for diverse crack lengths (a/L=0.00; a/L=0.25; a/L=0.50; a/L=0.75; a/L=1.00). The equivalent SIFs were calculated from the results of K_I, K_{II} e K_{III}, using the criterion of Richard or Pook. Additionally, a polynomial regression function considering all the obtained results was achieved, allowing to obtain K_I, K_{II}, K_{III} and K_{eq} by specifying the thickness of the specimen, the crack length and the applied torque.

It was observed that, even if a mode III loading was applied, mode I was locally dominant at the crack tip, followed by mode III and mode II, in that order of relevance. It was also observed that the maximum and minimum equivalent SIFs occurred at the lateral surfaces of the CT specimen, resulting in a bigger crack growth rate in those locations.

ACKNOWLEDGMENTS

The authors would like to thank the Portuguese Foundation for Science and Technology through project ref. UID/EMS/00667/2013.

Mean Stress Effect on Fatigue Behavior of Austenitic Stainless Steel in Air and LWR Conditions

W. Chen[a*], P. Spätig[a], H.P. Seifert[a]

[a] *Laboratory for Nuclear Materials, Nuclear Energy and Safety Research Division, Paul Scherrer Institute, 5232 Villigen-PSI, Switzerland*
**Corresponding author: wen.chen@psi.ch*

Keywords: Fatigue; Mean stress; LWR; Austenitic stainless steel.

ABSTRACT

Mean stress is induced from asymmetric cyclic loading. Positive mean stress is generally a beneficial to fatigue life and negative mean stress is detrimental to fatigue life. Goodmann [1], Gerber, Morrow [2], Soderberg methods are commonly applied to correct mean stress effect for fatigue life prediction. Recently findings show that these conventional methods do not apply to austenitic stainless steels that are used in Light Water Reactor (LWR) conditions [3, 4]. Austenitic stainless steels are primarily applied in fabrication of internal components of pressure vessels and reactor coolant piping systems. Temperature transients and fluctuation as well as mechanical loading, such as dead weight and water pressure, can induce mean stress. Although a great deal of fatigue investigations have been carried out on austenitic stainless steels working in air and LWR environment, and the corresponding JSME and ASME codes are documented to guide the fatigue design [5-7], mean stress effect is not fully addressed and understood in the aspect of quantifying mean stress effect and its cooperative effects with LWR environmental factors. This knowledge gaps can bring significant uncertainty in treating the fatigue of austenitic stainless steels in LWR condition correctly.

In this work, the influence of mean stress on fatigue behaviour of 316L austenitic stainless steel in air and LWR environment 288 °C has been studied using load-controlled tests. Hollow specimens were used and tested under simulated LWR water environment with our in-house built water loop system. Both positive mean stress (+50 MPa) and negative mean stress (-20MPa) were observed having beneficial effect on fatigue life. This is tentatively attributed to secondary hardening [8, 9]. The test results are illustrated in the Fig. **1** and Fig. **2** below showing the results obtained in high-purity hydrogen-water chemistry typical of boiling water reactor and in high-temperature air respectively [10]. Tests in air are still under progress. In order to gain insight into the physical micro-mechanism controlling the fatigue behaviour under mean stress and environmental influence, the microstructures evolution was investigated via TEM and ECCI characterization on samples cut from interrupted fatigue tests. The fatigue tests were also supplemented with fractographical SEM striation spacing measurement and EBSD characterization around cracks.

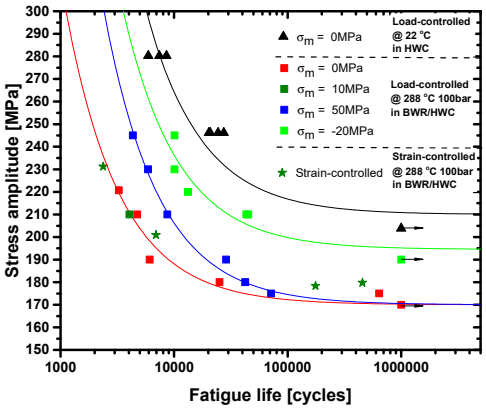

Fig. 1. Stress amplitude vs. fatigue life scatters and fitted curves in LWR environment at 288 °C and 22 °C with and without mean stress under load control; Average stress amplitude vs. fatigue life scatters (green stars) in LWR environment at 288 °C under strain control.

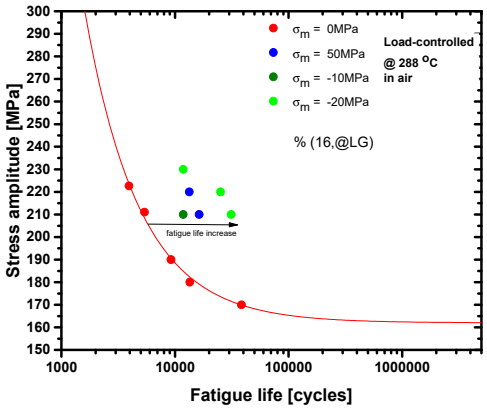

Fig. 2. Stress amplitude vs. fatigue life scatters and fitted curve in air condition at 288 °C with and without mean stress under load control.

REFERENCES

[1] Midmore, L.: Environmentally Assisted Fatigue Gap Analysis and Roadmap for Future Research. 1nd edn. Electric Power Research Institute, California (2011).
[2] Bae, K.H.: A simple life prediction method for 304L stainless steel structures under fatigue-dominated thermo-mechanical fatigue loadings. Materials Science and Engineering a-Structural Materials Properties Microstructure and Processing 529, 370–377 (2011).
[3] Solomon, H.D.: Influence of Mean Stress on the Fatigue Behavior of 304L SS in Air and PWR Water. In: ASME 2005 Pressure Vessels and Piping Conference, ASME, Colorado, 87-97 (2005).
[4] Solomon, H.D.: Fatigue limit and hysteresis behavior of type 304L stainless steel in air and PWR water, at 150 °C and 300 °C. In: 15th International Conference on Environmental Degration, TMS, Colorado, 583–603 (2011).
[5] Miura, N.: High-cycle fatigue behavior of type 316 stainless steel at 288 °C including mean stress effect. International Journal of Fatigue 11(28), 1618-1625 (2006).
[6] Kamaya, M.: Influence of strain range on fatigue life reduction of stainless steel in PWR primary water. Fatigue & Fracture of Engineering Materials & Structures 12(40), 2194-2203 (2017).
[7] Magnus, D., Bremberg, S.: Fatigue margins for austinitic stainless steels in ASME boiler and pressure vessel code- a literature study. 1nd edn. Swedish Radiation Safety Authority, Sweden (2012).
[8] Yuan, X.: Effect of mean stress and ratcheting strain on the low cycle fatigue behavior of a wrought 316LN stainless steel. Materials Science and Engineering: A 677, 193-202 (2016).
[9] Spätig, P.: Mean stress effect on fatigue life of 316L austenitic steel in air and simulated boliing water reactor hydrogen waer chemistry environment. In: 17th Int. Conference on Environmental Degradation of Materials in Nuclear Systems - Water Reactors. TMS, Ottawa (2015).
[10] Leber, H.S.: Thermo-Mechanical and Isothermal Low-Cycle Fatigue Behavior of Type 316L Stainless Steel in High-Temperature Water and Air. Corrosion 10(69), 1012-1023 (2013).

ACKNOWLEDGMENTS

The authors would like to acknowledge the financial support from the Swiss Federal Nuclear Safety Inspectorate (ENSI). Many thanks are addressed to B. Baumgartner, H. Kottmann, and R. Schwenold (all at PSI) for their excellent technical support.

Ultra-Long Life Fatigue Crack Initiation and Growth of TC17 Alloy

Hanqing Liu[a], Zhiyong Huang[a*], Qingyuan Wang[b**]

[a] *School of Aeronautics and Astronautics, Sichuan University, Chengdu 610065, China*
[b] *School of Mechanical Engineering, Chengdu University, Chengdu 610006, China*
**Corresponding author: huangzy@scu.edu.cn*
***Corresponding author: wangqy@scu.edu.cn*

Keywords: TC17 alloy; Very high cycle fatigue; Frequency effect; Crack initiation; Short crack growth.

ABSTRACT

Fatigue behavior of TC17 alloy was investigated at the stress ratio of 0.5 in the lab ambient. Fatigue test was conducted at 20 kHz using ultrasonic fatigue tester up to 109 cycles. Frequency effect was studied using the electromagnetic fatigue tester at the frequency of 110Hz additionally. Fatigue crack initiation and short crack propagation of TC17 alloy were investigated. A transition of fatigue crack initiation site happed to TC17 alloy from specimen surface to the interior site at the present test condition. The interior induced fatigue failure always happened to the TC17 alloy with the fatigue life exceeded 107¬ cycles. Interior short crack activities were influenced by the crystal orientation of the material, which resulted in faceted morphology crack initiation area. The crack initiation depth influenced the initiation area and impacted the fatigue resistance of the material.

Comparison of Optimized Walker and Goodman Methods

I. Vízková[a], J. Papuga[a*], M. Lutovinov[a], M. Nesládek[a]

[a] *Fac. of Mech. Engng., Czech Technical University in Prague, Technická 4, 166 07 Prague 6, Czech Republic*
**Corresponding author: papuga@pragtic.com*

Keywords: Fatigue prediction; Mean stress effect; Goodman; Walker; Cast iron.

ABSTRACT

Goodman formula is commonly used in the industry for the mean stress effect (MSE) evaluation. If conclusions of the relatively recent papers (see e.g. [1]-[6]) are checked, it becomes apparent, that the Goodman method leads to unreliable and in most cases to very conservative results. Often, a new MSE model is suggested and proved to be better than the Goodman method, but the test set used for the validation remains small, limited to less than 10 materials ([2]-[5]). If a sufficient number of experimental validation data is used, the data sets contain various issues as e.g. discussed in [7] or hereafter by the data set in [1].

The recent work by Dowling et al. [1] is very extensive in comparison with other papers. New research papers are based on it (e.g. [8]). The authors of [1] compared results of four methods for the MSE inclusion (Goodman, Morrow, SWT and Walker). For these methods, they compared computed equivalent completely reversed stress amplitudes with the stress amplitudes for a fully reversed cycle at the same number of cycles for all experimental points. Goodman, Morrow and SWT methods are strictly defined using the existing material parameters, but the Walker method contains additional fitting exponent:

$$\sigma_{a,eq} = \sigma_{max}\left(\frac{1-R}{2}\right)^{\gamma}. \tag{1}$$

By using the Basquin formulation of the S-N curve

$$\sigma_{a,eq} = AN^{b} \tag{2}$$

Dowling et al. transform the mix of Eqs. (1) and (2) by logarithms to the multiple linear formulation

$$\log N = \frac{1}{b}\log \sigma_{max} + \frac{\gamma}{b}\log\left(\frac{1-R}{2}\right) - \frac{1}{b}\log A. \tag{3}$$

Use of the linear regression leads to the best fit of the Walker parameter to all data of the given data set. Thanks to it, this method leads to the best results in [1]. Many models (Goodman, Soderberg, Morrow) use a linear formulation of the MSE and differ only by one stress parameter designated as *M* here:

$$\sigma_a = \sigma_{a,eq}\left(1 - \frac{\sigma_m}{M}\right). \tag{4}$$

We decided to check if a similar regression optimization of this generalized Goodman model really leads to results inferior to the Walker model. This formula leads to the non-linear regression study of

$$\log N = \frac{1}{b}\log \sigma_a + \frac{1}{b}\log\frac{M}{A} - \frac{1}{b}\log(M - \sigma_m). \tag{5}$$

The test set used by Dowling suffers from some inconsistencies (it is a mix of data sets with differing stress and strain controls of the amplitude and mean values; some of stress-controlled experiments were

overstrained at the start or during the tests; etc.). We decided to build a new testing dataset while keeping strict rules for accepting new data items. The coefficient of determination R^2 is used as the target value for both regressions of (3) and (5), and also as the parameter comparing both mean stress effect methods.

The summary of the evaluation can be found in Table 1. The results are also provided for various axial load modes and for various material groups. The biggest differences between both models can be found for cast irons (see an example in Fig. 1, referring to tests of Rausch [9] on EN-GJV-450) and then for aluminium alloys in the push-pull case. The difference of regression results is not substantial in other cases. Because the linear Soderberg model, which is usually proposed as the optimum solution for brittle materials is included also in the generalized Goodman method, the poorer performance of the linear MSE model compared with the Walker formula should be of interest to general engineering audience.

Table 1. Results of the R^2 coefficients for various scenarios.

Load mode	Plane bending			Push-pull					All
Material group	Al alloy	Steel	All	Al alloy	Cast iron	Steel	Ti alloy	All	All
Number of sets	3	1	4	4	3	11	1	19	23
Walker	0.824	0.832	0.826	0.876	0.817	0.803	0.918	0.827	0.826
Goodman	0.818	0.831	0.821	0.814	0.688	0.817	0.901	0.800	0.804

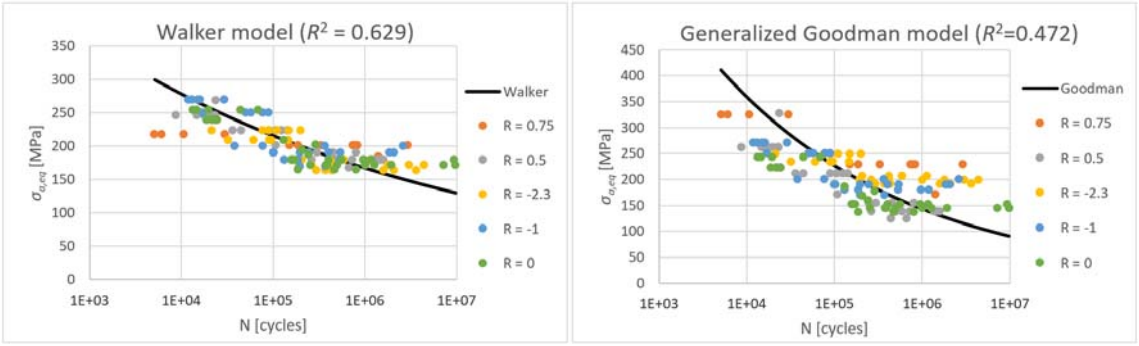

Fig. 1**.** Resulting best fit curves compared with the individual experimental data for the Ra1 test set from Rausch [9].

REFERENCES

[1] Dowling, N. E., Calhoun, C. A., Arcari, A.: Mean stress effects in stress-life fatigue and the Walker equation. Fatigue & Fracture of Engineering Materials & Structures 32(3), 163-179 (2009).

[2] Chu, C.-C.: Comparison of Mean Stress Correction Methods for Fatigue Life Prediction. In: SAE 2000 World Congress. Detroit, pp. 1-7. SAE International, Michigan (2000).

[3] Wang, S.-J., Dixon, M. W., Huey, Jr., Cecil O., Chen, S.-C.: The Clemson Limit Stress Diagram for Ductile Parts Subjected to Positive Mean Fatigue Loading. Journal of Mechanical Design 122(1), 143-146 (2000).

[4] Kwofie, S.: An exponential stress function for predicting fatigue strength and life due to mean stresses. International Journal of Fatigue 23 (9), 829-836 (2001).

[5] Sekercioglu, T.: A new approach to the positive mean stress diagram in mechanical design. Materialwissenschaft und Werkstofftechnik 40(9), 713-717 (2009).

[6] Niesłony, A., Böhm, M.: Mean stress effect correction using constant stress ratio S–N curves. International Journal of Fatigue 52, 49-56 (2013).

[7] Papuga, J.: Quest for Fatigue Limit Prediction Under Multiaxial Loading. Procedia Engng 66, 587-597 (2013).

[8] Burger, R., Yung-Li, L.: Assessment of the Mean-Stress Sensitivity Factor Method in Stress-Life Fatigue Predictions. Journal of Testing and Evaluation 41(2), 200-206 (2013).

[9] Rausch, T.: Zum Schwingfestigkeitsverhalten von Gusseisenwerkstoffen unter einachsiger und mehrachsiger Beanspruchung am Beispiel von EN-GJV-450. [PhD thesis]. Shaker Verlag, Aachen (2011).

ACKNOWLEDGMENTS

Authors acknowledge the support from the ESIF, EU Operational Programme Research, Development and Education, and from the Center of Advanced Aerospace Technology, Fac. of Mech. Eng., Czech Technical University in Prague (CZ.02.1.01/0.0/0.0/16_019/0000826), and from Ministry of Education Youth and Sport and CTU in Prague (the grant No. SGS17/175/OHK2/3T/12).

Evaluation of Stress Intensity factors and J-Integral using a 3 Point Bend Specimen

Ricardo Dias[a], Teresa L. M. Morgado[a,b,c*]

[a] *DEMI – Mechanical and Industrial Engineering Department, FCT NOVA - Faculty of Science and Technology, Universidade Nova de Lisboa, Lisboa, Portugal*
[b] *UNIDEMI – Research and Development Unit for Mechanical and Industrial Engineering, FCT NOVA - Faculty of Science and Technology, Universidade Nova de Lisboa, Lisboa, Portugal*
[c] *IPT – Polytechnic Institute of Tomar, Tomar, Portugal*
**Corresponding author: email: t.morgado@fct.unl.pt;*

Keywords: Crack Propagation; Conventional Finite Element method; XFEM; ABAQUS.

ABSTRACT

This work presents a three dimensional numerical study, using a single edge notched bending (SENB) specimen. The specimen was obtained from a railway component with the specification ASTM A148 90-60 [1]. The principal objective of this work is to conduct a convergence studies with the aim of determine the best methodology to evaluate the stress intensity factors and the J-integral solutions.

This study verifies the validity of the two techniques used to evaluate the stress intensity factors and J-Integral solutions, the conventional finite element method (Contour Integral) and the Extended Finite Element Method (XFEM). The main goal of this study is to show how accurate this concepts are in the fracture mechanical domain. The results were compared to those available on the literature.

The specimen considered in this study was the SENB specimen, an acronym for Single Edge Notch Bending specimen. There are three forces applied on the horizontal specimen: P above the specimen, P/2 on each of the two top corners, B is the thickness and S is equal to 4W where W is the height. The stress intensity factor expression is given by equation (1) [2].

$$K_I = \frac{P.S}{B.W^{\frac{3}{2}}}\left(2{,}9\left(\frac{a}{w}\right)^{1/2} - 4{,}6\left(\frac{a}{w}\right)^{3/2} + 21{,}8\left(\frac{a}{w}\right)^{5/2} - 37{,}6\left(\frac{a}{w}\right)^{7/2} + 38{,}7\left(\frac{a}{w}\right)^{9/2}\right) \quad (1)$$

The mesh used in both methods was made through an optimisation study and can be described for both conventional and XFEM method in Fig. 1 and 2, respectively.

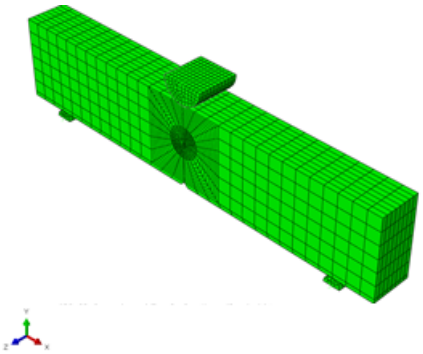

Fig. 1. The mesh used in the conventional method.

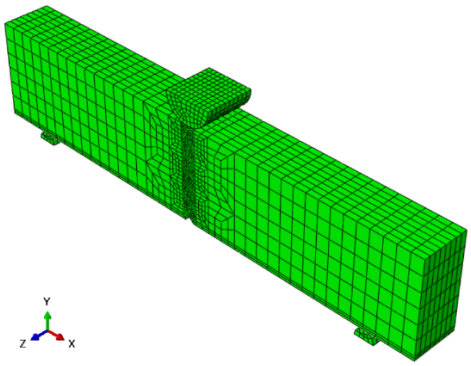

Fig. 3. The mesh used in the XFEM method.

Tables 1 and 2 resume the main results of this work.

Table 1. Numerical Stress Intensity Factor vs Analytical Stress Intensity Factor.

Methods	SIF [MPa $\sqrt{mm}$]	SIF Ref [MPa $\sqrt{mm}$]	Error [%]
Conventional	1839.874	1787.675	2.918
XFEM	1787.897	1787.675	0.011

Table 2. Numerical J Integral vs Analytical J Integral.

Methods	J-Integral [N/mm]	J-Integral Ref [N/mm]	Error [%]
Conventional	14.882	14.049	5.922
XFEM	13.825	14.049	1.601

This results show that both methods proved to be adequate for the evaluation of the stress intensity factor and the J-Integral. Additionally, can also be concluded that XFEM produced better results than the Conventional method and reveal to be capable of represent discontinuities with precision.

REFERENCES

[1] Morgado, T.L.M., Brito, A.S.: Study of casting defects and fatigue limit models of a railway component. Thirteenth International ASTM/ESIS Symposium on Fatigue and Fracture Mechanics. In: 39th National Symposium on Fatigue and Fracture Mechanics (2013).
[2] Morgado, T.L.M.: Fatigue Life Extension Study in Cast Steel Railway Couplings Used in Freight Trains. International Journal of Mechanical Engineering and Applications. Special Issue: Structural Integrity of Mechanical Components 3(2-1), 1-6 (2015).

ACKNOWLEDGMENTS

The authors from FCT NOVA would like to acknowledge Fundação para a Ciência e a Tecnologia (FCT, I.P.) for financial support via PEst-OE/EME/UI0667/2014.

Study of the Fatigue Limit of Cast Aluminium Alloy AlSi7Mg

Beatriz Arraiano[a], Teresa L. Morgado[a,b,c*], Alexandre Velhinho[d,e]

[a] *DEMI – Mechanical and Industrial Engineering Department, FCT NOVA - Faculty of Science and Technology, Universidade Nova de Lisboa, Lisboa, Portugal*
[b] *UNIDEMI – Research and Development Unit for Mechanical and Industrial Engineering, FCT NOVA - Faculty of Science and Technology, Universidade Nova de Lisboa, Lisboa, Portugal*
[c] *IPT – Polytechnic Institute of Tomar, Tomar, Portugal*
[d] *DCM – Department of Materials Science FCT NOVA - Faculty of Science and Technology, Universidade Nova de Lisboa, Lisboa, Portugal*
[e] *CENIMAT – Materials Research Center, FCT NOVA - Faculty of Science and Technology, Universidade Nova de Lisboa, Lisboa, Portugal*
**Corresponding author: t.morgado@fct.unl.pt*

Keywords: AlSi7Mg; Foundry Process; Manufacturing Defects; Fatigue Limit Prediction.

ABSTRACT

An AlSi7Mg alloy was chosen for this study. This alloy presents very good casting characteristics, with excellent properties after heat treatment, high corrosion resistance and a low level of thermal expansion, which is very advantageous for the manufacture of engines or other components subject to heat and/or thermal fatigue during their life cycle. It is thus widely used in both the automotive and aeronautics industries, and its study is therefore of the utmost importance [1, 2].

The main objectives of this study were the analysis of the defects intrinsic to the sand casting process of an AlSi7Mg alloy component, and the estimation of the fatigue limit using empirical equations. This calculation is based on the relationships envolving the maximum area of defects and the Vickers hardness of the material [3].

The component studied has small dimensions (volume, $V = 167.37\ cm^3$, surface area, $S = 433.45\ cm^2$) and exhibits geometric discontinuities which provide a demarcation between several distinct zones. In this study, three components (A, B and C) were produced by sand casting. Slices were retrieved from each component, and those slices were cut in 4 samples each, as represented in Fig. 1.

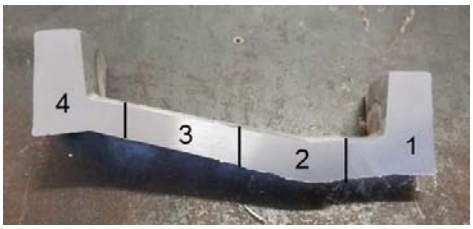

Fig. 1. Samples identification.

Vickers hardness tests were performed on the previously prepared samples. Six indentations were performed per test, using a force of 10Kgf, applied for 10 seconds, following the ASTM E384-2016 standard. To validate these results, a normality test was conducted.

The next step was the inspection of the entire area of each sample using a Leica DMI 500 scanning optical microscope to measure and obtain the distribution of defects and corresponding areas. In this experimental procedure the ImageJ software was used and the images processed, as shown in Fig. 2.

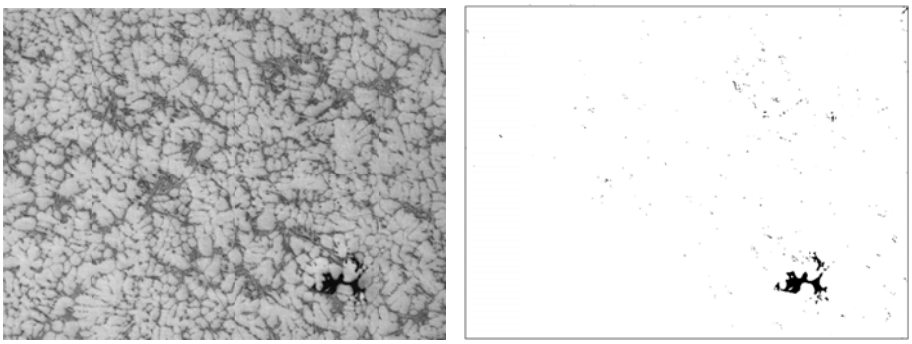

a) b)

Fig. 2. Image processing: a) original microscope image; b) image processed for area counting.

Having the total defect area for each component, the fatigue limit, σ_w, was calculated using the equations deduced by Ueno et al. [4], from the work of Murakami et al. [5], as shown in equations 1 and 2.

$$\sigma_w = \frac{1.43(75 + HV)}{(\sqrt{area})^{\frac{1}{6}}} \quad if \ \sqrt{area} < 1400\mu m \tag{1}$$

$$\sigma_w = \frac{1.43(450 + HV)}{(\sqrt{area})^{\frac{1}{3}}} \quad if \ \sqrt{area} > 1400\mu m \tag{2}$$

A hardness value of 56.09 HV was obtained in this study for the AlSi7Mg alloy, with an average area of defects of 6618149 μm^2. A fatigue limit σ_w = 53 MPa was obtained from the fatigue life prediction study, corresponding to an infinite service life ($N_f > 10^7$).

REFERENCES

[1] Arraiano, B.: Estudo de durabilidade de peças em alumínio vazado AlSi7Mg. Faculdade de Ciências e Tecnologia (2017).

[2] Arraiano, B., Morgado, T.L., Velhinho, A., Machado, C.M., Teixeira, J. P.: Aluminium Alloys Behaviour in the foundry Process, CIBEM2017, Lisbon, Portugal (2017).

[3] Tajiri, A., Nozaki, T., Uematsu, Y., Kakiuchi, T.: Fatigue limit prediction of large scale cast aluminum alloy A356. Procedia Mater. Sci. 3, 924–929 (2014).

[4] Ueno, A., Nishida, M., Miyakawa, S., Yamada, K., Kikuchi, S.: ΔKth estimation of aluminum die-casting alloy by means of √ area method. *Recent Adv. Struct. Integr. Anal. Proc. Int. Congr.* 3, 99–103 (2014).

[5] Murakami, Y., Endo, M.: Effects of defects, inclusions and inhomogeneities on fatigue strength. *Int. J. Fatigue* 16(3), 163–182 (1994).

ACKNOWLEDGMENTS

The authors from FCT NOVA would like to acknowledge Fundação para a Ciência e a Tecnologia (FCT, I.P.) for financial support via PEst-OE/EME/UI0667/2014 and LA25-2013-2014.

A Study of the Shot Peening Effect on the Fatigue Life Improvement of Al 7475-T7351 3PB Specimens

N. Ferreira[a], J.A.M. Ferreira[a], C. Capela[a,b*], J.D.M. Costa[a], J. de Jesus[a]

[a] *CEMMPRE, Department of Mechanical Engineering, University of Coimbra, Portugal*
[b] *ESTG, Department of Mechanical Engineering, Instituto Politécnico de Leiria, Portugal*
**Corresponding author: ccapela@ipleiria.com*

Keywords: Aluminium Alloys; Shot Peening; Fatigue.

ABSTRACT

Shot peening is a widely used mechanical surface treatment in the automotive and aerospace industries to improve the fatigue life of metallic components. The indentation of each impact produces local plastic deformation (increase in hardness) whose expansion is constrained by the adjacent deeper material, resulting in a field of surface compressive stresses, with positive effect on fatigue strength [1].

The main shot peening process parameters are the beads material and diameter, process intensity, exposure time, coverage, air pressure, impact angle and nozzle characteristics [2]. Fatigue life improvement on shot peening aluminium parts can be, mainly attributed to the compressive residual stresses in the sur-face region, which very often overcompensates the worsening of surface morphology [3]. Peening of aluminium alloys, with steel shot can be quite detrimental to fatigue performance. Luo et al. [4], using steel beads, obtained only an increase of 7% in fatigue life for 7075-T6 aluminium specimens, while, on the contrary, Sharp et al. [3], peening with lighter materials, such as glass or ceramic beads, decreased surface roughness and improved the fatigue strength significantly.

The understanding of the improvement in fatigue strength due to surface peening needs still to be better studied in order to enable the development of less conservative designs based on more accurate fatigue life and prediction models. The objective of this paper is to evaluate the shot peening effect, using two different bead diameters and bead materials on the fatigue strength of aluminium 7475-T7351 alloy subjected to pulsating bending. A systematic study was carried out on the roughness, surface hardening, residual stress profiles and fatigue life. Three point bending (3PB) fatigue tests were conducted. Residual stresses were evaluated by X-Ray diffraction, and the fracture surface was observed and analysed with a Scanning Electron Microscope.

Fatigue tests were carried out, using round bone dog specimens 8 mm diameter in centre of the specimens and tested in three points bending (3PB). All tests were performed with the stress ratio R=0.1, using an Instron EletroPuls E10000 machine (shown in Fig. 1).

Five batches of samples were prepared: A reference batch of ground and polished specimens and others four with shot peened surfaces different bead diameters of glass and steel bead.

Fig. 2 summarizes the fatigue test results plotted in terms of the stress amplitude versus the number of cycles to failure. As is usual in this type of test the results show a significant dispersion. Since, for this type of loading the initiation of the fatigue process is much localized, the roughness is as or more important than the residual stresses resulting from the shot peening. It concluded that shot peening does not introduce significant improvement on fatigue life and that the use of glass beads is potentially beneficial.

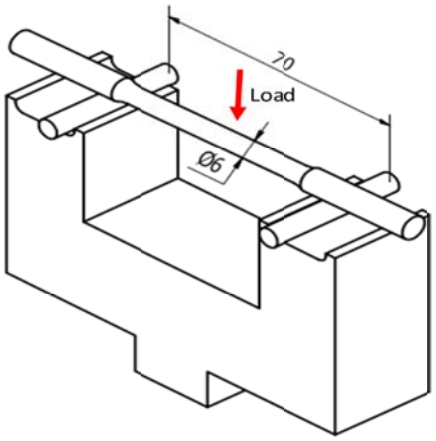

Fig. 1. Fatigue testing apparatus.

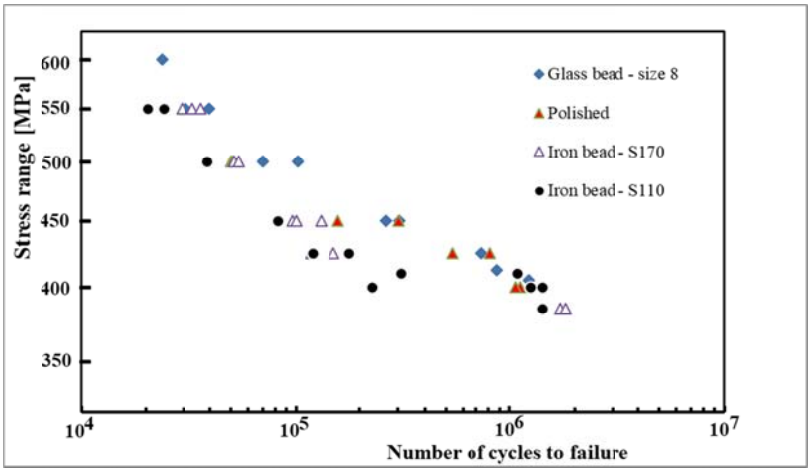

Fig. 2. S-N curves.

REFERENCES

[1] Miková, K., Bagherifard, S., Bokůvka, O., Guagliano, M., Trško, L.: Fatigue behavior of X70 microalloyed steel after severe shot peening. Int. J. Fatigue 55, 33-42 (2013).
[2] Kumar, H., Singh, S., Kumar, P.: Modified Shot Peening Processes - A Review. Int. J. Eng. Sci. Emerg. Technol. 5(1), 12–19 (2013).
[3] Sharp, P.K., Clayton, J.Q., Clark, G.: The fatigue resistance of peened 7050-T7451 aluminium alloy-repair and retreatment of a component surface. Fatigue Fract Eng Mater Struct 17(3), 243–52 (1994).
[4] Luo, W., Noble, B., Waterhouse, R.B.: The effect of shot peening intensity on the fatigue and fretting behaviour of an aluminium alloy. In: Niku-Lari A., Editor. Advances in surface treatments, vol. 2. Oxford: Pregamon Press, 145–153 (1988).

ACKNOWLEDGMENTS

The authors would like to acknowledge OGMA-Indústria Aeronáutica de Portugal, Alverca, Portugal, for the collaboration in the supply of materials and samples used in this project and shot-peening processing. The authors thank also the sponsoring of this research by FEDER funds through the program COMPETE – Programa Operacional Factores de Competitividade – and by national funds through FCT – Fundação para a Ciência e a Tecnologia –, under the project UID/EMS/00285/2013.

Additive Manufactured Components Designed by Topology Optimization: Fatigue Behaviour Considerations

S.M.O. Tavares[a*]

[a] *Faculty of Engineering of University of Porto, Porto Portugal*
**Corresponding author: sergio.tavares@fe.up.pt*

Keywords: Additive manufacturing; Topology optimization; Fatigue behaviour; Soderberg criterion; FKM.

ABSTRACT

Current trend in additive manufacturing (AM) processes has been creating new design methodologies for structural components, allowing new approaches to structural optimization. AM processes unleash freedom for geometrical design, including the adoption of radical geometries achieved by topology optimization, which can result in significant reductions of component weight. However, these new geometries are obtained considering the mass reduction objective for a given static strength value. These typical procedures may have implications in the fatigue strength due to stress concentrations.

This communication analyses data about the material fatigue strength processed by AM, evaluating the differences between the fatigue strength of raw material and additively manufactured material. In addition, will be analysed some common examples of aeronautical parts, topological optimized and manufactured by AM, assessing stress concentration factors and stress gradients, due to notches with low radius of curvature or other geometrical discontinuities.

For comparison purposes, typical fatigue design criteria will be considered, namely Soderberg criterion and FKM criterion, evaluating the stress concentration of some examples presented in the literature, and their effect on the fatigue strength of the part. This initial study aims to raise the debate about topology optimization beyond the static strength objectives, presenting some initial studies about this topic, as Holmberg *et al.* [3] and Jeon *et al.* [4] works.

REFERENCES

[1] ANSI/ASME Standard for Design of Transmission Shafting B106.1M (1985).
[2] VDMA: FKM Guideline: Analytical strength assessment of components: made of steel, cast iron and aluminum materials in mechanical engineering', 6th ed., Frankfurt am Main, VDMA Verlag GmbH (2012).
[3] Holmberg, E., Torstenfelt, B., Klarbring, A.: Fatigue constrained topology optimization. Structural and Multidisciplinary Optimization 50 (2): 207-219 (2014).
[4] Jeong, S.H., et al.: Topology optimization considering the fatigue constraint of variable amplitude load based on the equivalent static load approach. Applied Mathematical Modelling 56: 626-647 (2018).

Full-Field Deformation Measurements and Material Identification

Symposium I-FDMI-ICMFM

José Xavier, Portugal

Paulo Tavares, Portugal

Marco Rossi, Italy

Gil Andrade-Campos, Portugal

On the Finite Element Model Updating and the Virtual Fields Method in the Identification of Elasto-Plastic Models

J.M.P. Martins[a,b], S. Thuillier[a], A. Andrade-Campos[b*]

[a] *Université de Bretagne Sud, FRE CNRS 3744, IRDL, F-56100 Lorient, France*
[b] *Centre for Mechanical Technology and Automation (TEMA), GRIDS Research Unit, Mechanical Engineering Department, University of Aveiro University, Country*
**Corresponding author: gilac@ua.pt*

Keywords: Parameter identification; Full-field methods; Elastoplasticity; VFM; FEMU.

ABSTRACT

The identification of material parameters, for a given constitutive model, can be seen as the first step before any practical application. In the last years, the field of material parameters identification received an important boost with the development of full-field measurement techniques, such as Digital Image Correlation [1-3]. These techniques enable the use of heterogeneous displacement/strain fields, which contain more information than the classical homogeneous tests. Consequently, different techniques have been developed to extract material parameters from full-field measurements [4]. In this study, two of these techniques are addressed, the Finite Element Model Updating (FEMU) and the Virtual Fields Method (VFM) [5-7]. The main idea behind FEMU is to update the parameters of a constitutive model implemented in a finite element model until both numerical and experimental results match. The FEMU process is guided by the following objective function:

$$f(\boldsymbol{\xi}) = \frac{1}{n_s}\sum_{i=1}^{n_s}\left\{\frac{1}{n_p}\sum_{j=1}^{n_p}\left[\left(\frac{\varepsilon_{xx}^{num}-\varepsilon_{xx}^{exp}}{\varepsilon_{xx}^{exp}}\right)^2+\left(\frac{\varepsilon_{yy}^{num}-\varepsilon_{yy}^{exp}}{\varepsilon_{yy}^{exp}}\right)^2+\left(\frac{\varepsilon_{xy}^{num}-\varepsilon_{xy}^{exp}}{\varepsilon_{xy}^{exp}}\right)^2\right]_j+\left(\frac{F^{num}-F^{exp}}{F^{exp}}\right)^2\right\}_i . \quad (1)$$

The VFM makes use of the Principle of Virtual Work and does not require any finite element simulation. In this study, the framework of finite strains theory is adopted, thus the Principle of Virtual Work is written using a Lagrangian (or material) description. Assuming static conditions and neglecting the body forces, the cost function has the following form:

$$\varphi(\boldsymbol{\xi}) = \sum_{i=1}^{n_s}\left(\int_{\Omega_0}\mathbf{P}(\boldsymbol{\xi},\boldsymbol{\varepsilon}^{exp}):\mathrm{Grad}\mathbf{u}^*\,dV-\int_{\partial\Omega_0}\overline{\mathbf{T}}\cdot\mathbf{u}^*\,dS_0\right)_i^2 . \quad (2)$$

Though both techniques proved their feasibility in linear and non-linear constitutive models, it is rather difficult to rank their robustness in plasticity. The purpose of this work is to perform a comparative study in the case of elasto-plastic models. Details concerning the implementation of each strategy are presented. Moreover, a dedicated code for VFM within a large strain framework is developed. The reconstruction of the stress field is performed through a user subroutine. A heterogeneous tensile test (Fig. 1) is considered to compare FEMU and VFM strategies.

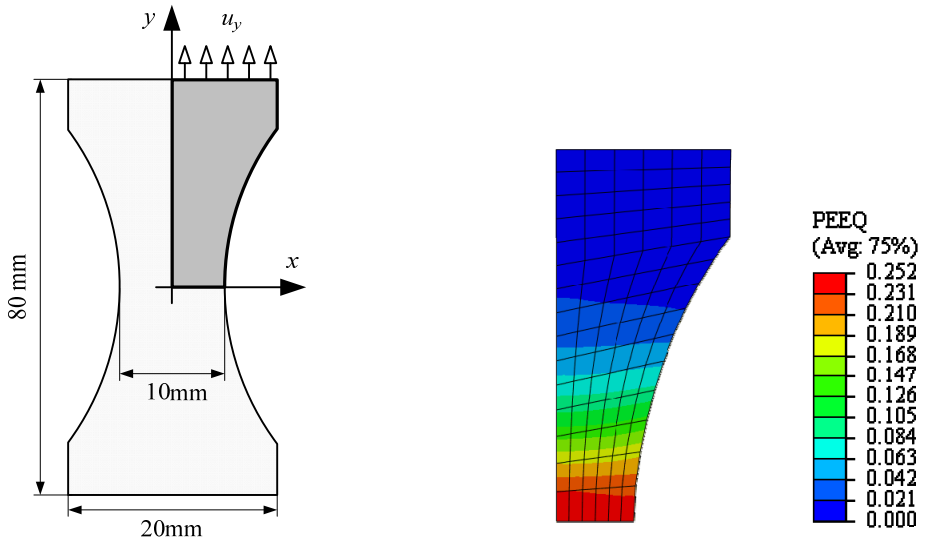

Fig. 1. Specimen geometry and corresponding finite element model. Equivalent Plastic strain distribution after a displacement of 3 mm.

REFERENCES

[1] Avril, S., et al.: Overview of Identification Methods of Mechanical Parameters Based on Full-field Measurements, Exp. Mech. 48, 381–402 (2008).
[2] Kim, J.-H., Serpantié, A., Barlat, F., Pierron, F., Lee, M.-G.: Characterization of the post-necking strain hardening behavior using the virtual fields method, Int. J. Solids Struct. 50(24), 3829–3842 (2013).
[3] Cooreman, S., Lecompte, D., Sol, H., Vantomme, J., Debruyne, D.: Identification of Mechanical Material Behavior Through Inverse Modeling and DIC. Exp. Mech 48, 421-433 (2008).
[4] H. Haddadi and S. Belhabib, Int. J. Mech. Sci., 62, pp.47-62 (2012).
[5] Rossi, M., Pierron, F., Štamborská, M.: Application of the virtual fields method to large strain anisotropic plasticity. Int. J. Solids Struct. 97-98, 322-335 (2016).
[6] Pierron, F., Grédiac, M.: The virtual field method – Extracting constitutive mechanical parameters from full-field deformation measurements. Springer, New York (2012).
[7] Marek, A., Davis, F. M., Pierron, F.: Sensitivity-based virtual fields for the non-linear virtual fields method. Comput. Mech. 60, 409-431 (2017)

ACKNOWLEDGMENTS

The authors gratefully acknowledge the financial support of the Portuguese Foundation for Science and Technology (FCT) under the project P2020-PTDC/EMS-TEC/6400/2014 (POCI-01-0145-FEDER-016876) by UE/FEDER through the program COMPETE 2020. The authors also would like to acknowledge the Région Bretagne (France) for its financial support. J.M.P. Martins is also grateful to the FCT for the PhD grant SFRH/BD/117432/2016.

The Effect of Overloads on Fatigue Crack Propagation Measured by DIC, BEMI and Synchrotron

M. Thielen[a], M. Marx[a*], C. Motz[a]

[a] *Department of Materials Science and Engineering, Saarland University, Germany*
**Corresponding author: m.marx@matsci.uni-sb.de*

Keywords: Fatigue crack growth; Overload; Residual stresses; Plasticity induced crack closure.

ABSTRACT

The key of understanding fatigue crack propagation lies in the knowledge of local stresses, the driving force of cracks. Because local stresses are hardly accessible in experiments, the stress intensity factor is used since Paris and Erdogan [1] to relate crack parameters and external load to fatigue crack growth in a simple way. Nevertheless, in various cases this simple law fails e.g. in the case of an overload (OL) [2,3]. The mechanisms of the OL effect, residual stresses (RS) in front of the crack tip and plasticity induced crack closure (PICC) due to the plastic wake, have been studied. Specifically, a crack in S960Q steel has been followed before OL, after OL, at maximum retardation and recovery. We present the mapping of stress and strain fields induced by OLs on a fatigue crack and their influence on transient crack growth retardation. This investigation was performed by calibrated magnetic Barkhausen noise (MBN) microscope [4] and digital image correlation (DIC) based on in-situ SEM imaging. Both results were compared to synchrotron x-ray diffraction.

We observe a strong correlation of the local fatigue crack growth rate (Fig. 1a) with the micro RS distribution obtained from 2D mappings by MBN with a spatial resolution of 10 µm (Fig. 1b): The RS field after the overload explains in the first instance the successive retardation while the DIC results reveal the influence of these RS on crack tip's opening reactions and strain fields under external loads. While strain fields show a strong decrease due to the OL, differences in crack opening stresses remain rather low at first, but prevail in the further part of the OL region.

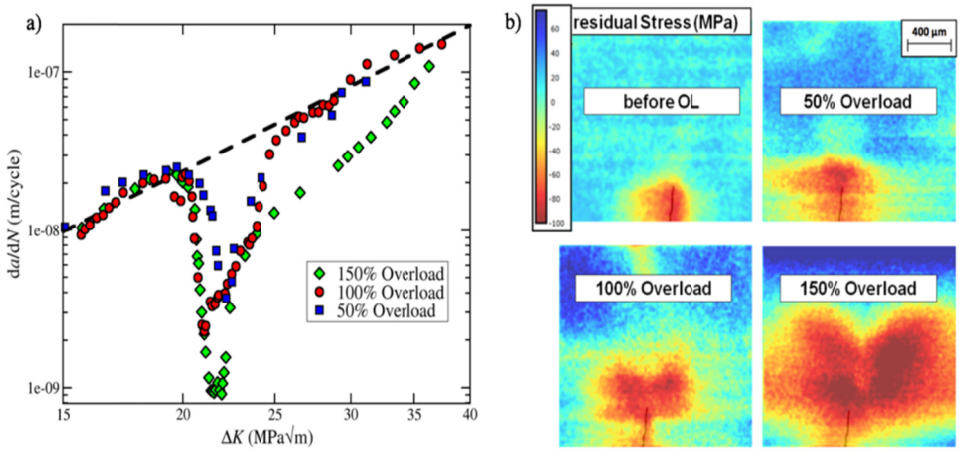

Fig. 1. a) Transient crack growth speed after OL differing from the linear Paris behaviour under constant force amplitude loading. At K = 20 MPa√m different OLs have been applied. Higher OLs lead to stronger deceleration over a longer period. **b)** Influence of the OL level on the RS distribution, measured with MBN. Before OL, the surrounding closure stresses are visible. Applying an OL increases the stress field. Higher OLs lead to higher compressive RS in amplitude as well as in a wider spatial distribution.

We investigated also the PICC at the crack flanks and the superposition of crack tip stresses with RS in front of the crack tip. From the MBN, compressive RS were found near the crack flanks and after the OL inside the entire plastified region in front of the crack tip. From these measurements, changes in crack growth speed could be correlated with the distribution of the RS. Strong changes in the distribution due to the crack growth could not be observed. The influence of PICC and RS could be distinguished by careful examination of crack tip opening displacement (CTOD) and crack tip strain fields measured by DIC. The crack tip opening is delayed because of compressive crack flank contact stresses. The elastic response after opening, the change of CTOD with *K*, can only be explained by RS interaction with crack tip fields that, contrary to PICC, still acts after opening the crack. With increasing growth through the OL region, closure becomes more important since a larger part of the crack is affected by the OL PICC. At the same time, the RS becomes less pronounced as the crack tip strain fields exceed the OL region.

Calculations based on these changes described the observed changes in fatigue crack growth accurately (Fig. 2). These are not claimed to build a properly predictive model, but the combined measurements open the possibility of physical interpreting underlying effects and provide thereby useful information for more sophisticated modelling and simulation approaches. Concluding we interpret the results as follows: The RS effect on the strain fields can be associated to be more significant than PICC at maximum retardation with a change of mechanisms on reacceleration.

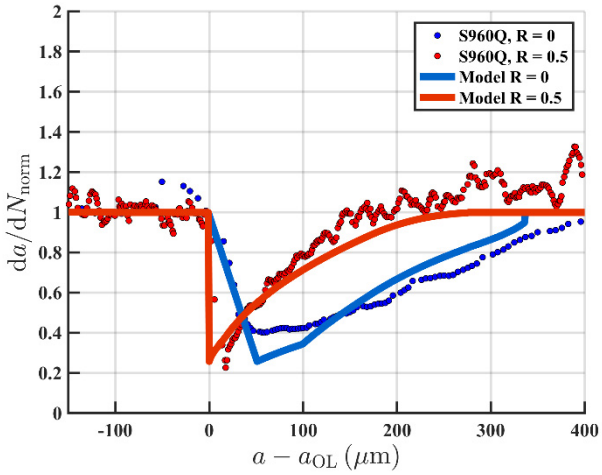

Fig. 2. a) Crack propagation rate of steel S960Q under different load rations (R = 0.5 and R = 0), experimental data are compared with the model which will be presented.

REFERENCES

[1] Paris, P.C., Erdogan, F.: A critical analysis of crack propagation laws. J. Basic Eng. 85(4), 528-533 (1963).
[2] Bichler, C., Pippan, R.: Effect of single overload in ductile metals: A reconsideration, Eng. Fract. Mech. 75(8), 1344-1359 (2007).
[3] Lopez-Crespo, P., Withers, P.J., Yusof, F., Dai, H., Steuwer, A., Kelleher, J.F., Buslaps, T.: Overload effects on fatigue crack-tip fields under plane stress conditions: surface and bulk analysis, Fat. Fract. Eng. Mater. Struct. 36(1), 75-84 (2013).
[4] Boller, C., Altpeter, I., Dobmann, G., Rabung, M., Schreiber, J., Szielasko, K., Tschuncky, R.: Electromagnetism as a means for understanding materials mechanics phenomena in magnetic materials. Materialwissenschaft und Werkstofftechnik 42(4), 269-278 (2011).

ACKNOWLEDGMENTS

We thank the Deutsche Forschungsgemeinschaft DFG for funding this project under grant MA3322/6-1 and we thank the Fraunhofer Institute of Non-Destructive Testing (IzfP) for the permission of using BEMI.

Methodology for ULCF Data Reduction Using Local Boundary Conditions Provided by Digital Image Correlation

J. Xavier[a,b*], J.C.R. Pereira[a,c], A.M.P. de Jesus[a,c], A.A. Fernandes[a,c]

[a]*INEGI, University of Porto, Portugal*
[b]*CITAB, University of Trás-os-Montes e Alto Douro, Portugal*
[c]*Faculty of Engineering, University of Porto, Portugal*
**Corresponding author: jxavier@inegi.up.pt*

Keywords: Finite element method; Digital image correlation; Ultra-low-cycle fatigue.

ABSTRACT

Steel structural components, as it is the case of pipelines, are typically loaded in scenarios of ultra-low-cycle-fatigue (ULCF). These conditions can engender large deformations and fracture which can yield structural instability. Both monotonic ductile and low-cycle fatigue (LCF) damage mechanism can occur on steel components. ULCF damage features can be analysed combining LCF and monotonic ductile fracture. Data reduction carried out by combining both experimental damage data to retrieve material damage behaviour under these extreme loading conditions is required. The use of notched planar specimens on ULCF tests emerged as an effective alternative to the smooth planar ones, since the notch presence contributes to the instability reduction during the cyclic loading. Furthermore, shorter fatigue lives are attained using notched planar specimens in contrast with the results of smooth ones. Moreover, a finite element analysis to derive the stress/strain histories at the critical locations is typically required with the use of notched plane specimens.

The identification of parameters governing the damage models can be analysed by combining numerical and experimental data. The experimental techniques can generate both global and local information to calibrate the numerical models. However, full-field optical techniques (FFOTs) are attractive to this purpose. Moreover, concerning the measurements of large plastic deformations, non-contact optical methods are advantageous over point-wise contact counterpart techniques. FFOTs of displacement and strain measurements have been increasingly used in experimental solid mechanics [1]. These techniques can be generically sorted, according to the physical phenomenon involved in the measurements, as white-light (digital image correlation, geometric moiré, grid method, deflectometry) and interferometric (moiré and speckle interferometry, shearography) methods. The choice of a given technique can be driven by several criteria as the cost, the set-up apparatus (simplicity, flexibility, sensitivity to vibrations), the performances (resolution, spatial resolution...), the measuring quantity (displacement, strain...), and the length scale of observation (from structural down to micro or nano) [2]. In contrast with punctual techniques, these methods provide full-field data and are contact-free. This type of experimental data has allowed new insights into different engineering problems, as, for instance, gradient fields due to material heterogeneities [3], fracture cracking characterisation [4], damage and fracture model evaluation [5], high strain rate characterisation of advanced composite materials [6], validation of phenomenological numerical models [7], and multi-parameter identification from single test configurations [8]. Among FFOTs, non-interferometric methods, based on image and signal processing, have been increasingly used, such as digital image correlation (DIC) [9].

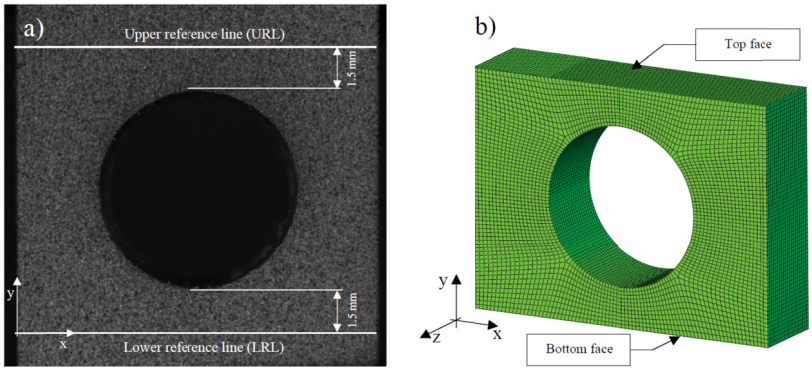

Fig. 1. Definition of local boundary conditions for the numerical simulation of notched specimens: a) region of interest of notched plane specimens; b) submodelling finite element mesh of notched plane specimens.

In this work, fatigue tests in the ULCF regime are analysed by combining finite element simulations of submodeling regions enhanced by experimental data in the form of real boundary conditions provided by DIC. The use of DIC on the ULCF tests of notched plane specimens allows the development of a new numerical approach. This new approach consists on the application of local boundary conditions obtained from the displacement fields at the region of interest of the specimens, as presented in Fig. 1. The analysis is presented on a series of X52, X60, X60TT, X65 and X65TT steel grades.

REFERENCES

[1] Rastogi, P.: Photomechanics. Springer Verlag, Berlin Heidelberg (2000).
[2] Grédiac, M.: The use of full-field measurement methods in composite material characterization: Interest and limitations. Composites Part A: Applied Science and Manufacturing 35, 751–761 (2004).
[3] Pereira, J., Xavier, J., Morais, J., Lousada, J.: Assessing wood quality by spatial variation of elastic properties within the stem: case study of P. pinaster in the transverse plane. Canadian Journal of Forest Research 44(2), 107–117 (2004).
[4] Xavier, J., Oliveira, J., Monteiro, P., Morais, J., de Moura, M.: Direct evaluation of cohesive law in mode I of Pinus pinaster by digital image correlation. Experimental Mechanics 54(5), 829–840 (2014).
[5] Arteiro, A., Catalanotti, G., Xavier, J., Camanho, P.: Direct evaluation of cohesive law in mode I of Pinus pinaster by digital image correlation. Experimental Mechanics 54(5), 829–840 (2014).
[6] Koerber, H., Xavier, J., Camanho, P., Essa, Y., de la Escalera, F.M.: High strain rate behaviour of unidirectional and textile composites under compression and combined compression-shear loading. International Journal of Solids and Structures 54, 172–182 (2015).
[7] Xavier, J., Pereira, J.C.R., de Jesus, A.M.P.: Characterisation of steel components under monotonic loading by means of image-based methods. Optics and Lasers in Engineering 53, 142–151 (2014).
[8] Xavier, J., Avril, S., Pierron, F., Morais, J.: Novel experimental approach for longitudinal-radial stiffness characterisation of clear wood by a single test. Holzforschung 61(5), 573–581 (2007).
[9] Sutton, M., Orteu, J.-J., Schreier, H.: Image correlation for shape, motion and deformation measurements: Basic concepts, theory and applications. Springer US (2009).

ACKNOWLEDGMENTS

The authors acknowledge the Fundação para a Ciência e Tecnologia for their financial support through the SFRH/626 BD/80091/2011 Grant and Ciência 2008 program. The European Commission is also acknowledged through the Research Fund for Coal and Steel that is funding the ULCF project (RFSR-CT-2011-00029). Finally authors gratefully acknowledge the funding of SciTech - Science and Technology for Competitive and Sustainable Industries (NORTE-01-0145-FEDER-000022), R&D project cofinanced by Programa Operacional Regional do Norte ("NORTE2020"), through Fundo Europeu de Desenvolvimento Regional (FEDER).

The Natural Neighbour Radial Point Interpolation Method to Predict the Compression and Traction Behaviour of Thermoplastics

D.E.S. Rodrigues[a*], J.Belinha[a,b], R.M. Natal Jorge[a,c], L.M.J.S. Dinis[a,c]

[a] *Institute of Science and Innovation in Mechanical and Industrial Engineering (INEGI), Portugal.*
[b] *School of Engineering, Polytechnic of Porto (ISEP), Department of Mechanical Engineering, Portugal.*
[c] *Faculty of Engineering of the University of Porto (FEUP), Department of Mechanical Engineering, Portugal.*
**Corresponding author:* drodrigues@inegi.up.pt

Keywords: Natural Neighbour Radial Point Interpolation Method (NNRPIM); Elastoplasticity; Thermoplastics.

ABSTRACT

Nowadays, the Finite Element Method is the most used discretization technique in structural computational mechanics. However, recently, new discretization techniques - such as meshless methods [1] - have been proposed. These numerical techniques are able to handle some of the FEM's drawbacks, such as the re-meshing requirement in crack propagation or large deformations problems. Meshless methods only need an unstructured nodal mesh to discretize the problem domain, and the numerical integration of the discrete system of equations obtained from the Galerkin weak form is performed using a background integration mesh. Additionally, the nodal connectivity is imposed using the influence-domain concept, which allows to construct the interpolation functions. The Natural Neighbour Radial Point Interpolation Method (NNRPIM) is a recently developed truly meshless method, which in this work is used to analyse thermoplastics (used in additive manufacturing processes) assuming an elasto-plastic behaviour. Benchmark numerical examples are solved in both traction and compression, and in the end, the NNRPIM results obtained are compared with FEM solutions.

REFERENCES

[1] Belinha, J.: Meshless Methods in Biomechanics - Bone Tissue Remodelling Analysis. Lecture Notes in Computational Vision and Biomechanics 16, Tavares, João Manuel R.S., Jorge, Renato Natal Eds., Springer Netherlands (2014).

ACKNOWLEDGMENTS

The authors truly acknowledge the funding provided by Ministério da Ciência, Tecnologia e Ensino Superior – Fundação para a Ciência e a Tecnologia (Portugal), under grants: SFRH/BPD/111020/2015 and SFRH/BD/121019/2016, and by project funding MIT-EXPL/ISF/0084/2017 and UID/EMS/50022/2013 (funding provided by the inter-institutional projects from LAETA). Additionally, the authors gratefully acknowledge the funding of Project NORTE-01-0145-FEDER-000022 – SciTech – Science and Technology for Competitive and Sustainable Industries, co-financed by Programa

Operacional Regional do Norte (NORTE2020), through Fundo Europeu de Desenvolvimento Regional (FEDER).

Fracture Analysis of Semi-Circular Bend (SCB) Specimen: A Numerical Study Based on Meshless Methods

Farid Mehri Sofiani[a*], Behzad V. Farahani[a,b], J. Belinha[b,c]

[a] *FEUP, Faculty of Engineering, University of Porto, Dr. Roberto Frias Street, 4200-465, Porto, Portugal.*
[b] *INEGI, Institute of Science and Innovation in Mechanical and Industrial Engineering, Dr. Roberto Frias Street, 400, 4200-465, Porto, Portugal.*
[c] *ISEP, Mechanical Engineering Department, School of Engineering, Polytechnic of Porto, Rua Dr. António Bernardino de Almeida, 431, 4249-015 Porto, Portugal.*
**Corresponding author: up201600432@fe.up.pt*

Keywords: Fracture characterization; RPIM; NNRPIM; FEM; SIF.

ABSTRACT

A variety of numerical analysis has been carried out by Finite Element Method (FEM), and Extended FEM (XFEM) on Semi-circular Bend (SCB) specimens to evaluate its material behaviour, in particular fracture characterization. This work concentrates on calculating stress intensity factor (SIF) and strain energy release rate (G) on this specimen, assuming an elastic brittle behaviour. In order to obtain the required variable fields, two advanced discretization techniques are addressed: The Radial Point Interpolation Method (RPIM) and the RPIM Natural Neighbour version (NNRPIM). In this work, peak load (P_{max}) is assessed with both RPIM and NNRPIM and the corresponding results are compared with those obtained by XFEM. Furthermore, force-displacement curves of the SCB specimen are numerically implemented and the process from initiation to propagation is investigated, leading to produce a high accurate solution in comparison to the literature. Besides, the internal fields are monitored adjacent to the cracked area.

REFERENCES

[1] Belinha, J.: Meshless Methods in Biomechanics - Bone Tissue Remodelling Analysis. Lecture Notes in Computational Vision and Biomechanics 16, Tavares, João Manuel R.S., Jorge, Renato Natal Eds., Springer Netherlands (2014).
[2] Lim, I.L., Johnston, I.W., Choi, S.K.: Stress intensity factors for semi-circular specimens under three-point bending. Eng. Fract. Mech. 44(3), 363–382 (1993).
[3] Xie, Y., Cao, P., Jin, J., Wang, M.: Mixed mode fracture analysis of semi-circular bend (SCB) specimen: A numerical study based on extended finite element method. Comput. Geotech. 82, 157–172 (2017).
[4] Farahani, B.V., Tavares, P.J., Moreira, P.M.G.P., Belinha, J.: Stress intensity factor calculation through thermoelastic stress analysis, finite element and RPIM meshless method. Eng. Fract. Mech. 183, 66–78 (2017).
[5] Farahani, B.V., Tavares, P.J., Belinha, J., Moreira, P.M.G.P.: A Fracture Mechanics Study of a Compact Tension Specimen: Digital Image Correlation, Finite Element and Meshless Methods. Procedia Struct. Integr. 5, 920–927 (2017).

ACKNOWLEDGMENTS

The authors acknowledge the funding by Ministério da Educação e Ciência, Fundação para a Ciência e a Tecnologia (FCT-Portugal), under grants PD/BD/114095/2015 and SFRH/BPD/111020/2015 and by project funding MIT-EXPL/ISF/0084/2017. Additionally, the authors gratefully acknowledge the funding of Project NORTE-01-0145-FEDER-000022 – SciTech – Science and Technology for Competitive and Sustainable Industries, co-financed by Programa Operacional Regional do Norte (NORTE2020), through Fundo Europeu de Desenvolvimento Regional (FEDER).

Fatigue Behaviour of Welded Joints

Investigation of Mechanical Properties and Fatigue of Friction Stir Spot Welded Light Metals

A. Atak[a*], A. Sik[a]

[a] *Industrial Product Design, Gazi University, Turkey*
**Corresponding author: ahmet.atak@gazi.edu.tr*

Keywords: Friction stir spot welding; Joining of Magnesium; Joining of Aluminium; Fatigue of Light Metals; Welding of Light Metals.

ABSTRACT

Light metals such as aluminum and magnesium alloys find extensive use in land and air transport vehicles, electronics, computer and sporting goods industries. In order to reduce weight and thus save fuel, many studies are carried out on the development of new engineering materials, which have lightweight and high fatigue strength, especially for the automotive and aviation industry. One of the first metals remembered in this field is magnesium, which has lower density (35% lighter than aluminum and 65% lighter than titanium). In contrary to these advantages, joining of light metal alloys with fusion based welding methods have some problems. Since the fusion welding of light metal sheets is difficult, friction stir welding (FSW) method frequently used for joining of these. Studies has shown that shoulder profile of welding tool, which apply pressure on material, affects the welding quality in FSW method. In order to understand these effects various shoulder profile has been studied and understood.

FSW method has been investigated and used for joining of materials since 70's. In this paper, the pinless shoulder profile designs of stir tool and the mechanical properties and fatigue strength of magnesium and aluminum alloy sheets, which are joined with these stir tools, are aimed to investigate. In order to realize this, shoulder profiles were designed and manufactured accordingly. Subsequently, magnesium and aluminum alloy sheets for automotive and aviation applications were joined with friction stir spot welding (FSSW). Finally, mechanical properties of joined materials such as tensile, tensile shear, bending and fatigue strength were tested.

As a result, it has been verified that light metal alloys such as magnesium alloy AZ31B and aluminum alloy EN AW 2024-T4 with good ductile and fatigue strength can easily be joined with FSSW. Moreover, joining of light metals with FSSW method has been demonstrated with comparative test and analysis in engineering applications.

Improvement of Fatigue Life of Welded Strenx 700MC Steel by Ultrasonic Impact Treatment

M. Jambor[b], F. Nový[b], O. Bokůvka[b], L. Trško[a*], J. Lago[c]

[a] *Research Center of the University of Žilina, University of Žilina, Slovakia*
[b] *Department of Materials Engineering, University of Žilina, Slovakia*
[c] *Lago Nástrojáreň s. r. o., Veľké Rovné, Slovakia*
**Corresponding author: libor.trsko@rc.uniza.sk*

Keywords: Ultrasonic impact treatment; Strenx 700MC steel; Weld; Fatigue life.

ABSTRACT

Advanced high strength low alloy (HSLA) steels are now applied into production of welded structures to reduce their weight while maintaining the loading capacity. These steels are usually thermo-mechanically processed to obtain various special types of microstructures, which results in superior mechanical properties, when compared to their commonly processed equivalents, without necessity of increasing the amount of alloying elements to maintain simple weldability. The main issue of application of HSLA steel is the partial recrystallization of the microstructure during the welding process what causes that the weld often does not exhibit the superior mechanical properties as the HSLA base material [1].

Ultrasonic Impact Treatment (UIT) [2] is a one of surface strengthening methods which promises a possibility to improve fatigue properties of welded joints from HSLA steels. Fatigue test specimens were machined from a welded sheet metal of Strenx 700MC with 10 mm thickness according to Figure 1a. Three parameters of UIT treatment (Figure 1b) were carried out to analyse, which will provide the best performance. First treatment was carried out with contact force of 85 N, second treatment was again with 85 N contact force, but the surface of the specimen was passed two times. Third treatment was carried out with contact force of 135 N. The UIT treatment created a deep layer with compressive residual stresses in whole welded joints: weld metal (Figure 2a), heat affected zone (Figure 2b) and base material (Figure 2c).

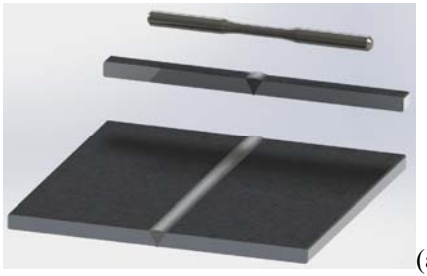
(a)


(b)

Fig. 1. Manufacturing of specimens from Strenx welded sheet metal (a) and UIT surface treatment (b).

Fatigue tests were carried out in rotating bending loading mode with cycle asymmetry ratio R = -1 at loading frequency of f = 35 Hz, with a run-out number of cycles at $N = 1 \times 10^8$. Results of the fatigue test have showed that all three types of UIT treatment have increased the fatigue life of welded Strenx steel (Figure 3). Best performance was obtain after two passes with contact force of 85 N, mainly at number of cycles lower than $N = 1 \times 10^7$, where fatigue strength is slightly higher than of specimens treated with one pass at 85 N contact force. It is interesting to note that the treatment with 135 N contact force had only a small positive influence on the fatigue life, however the scatter of the results increased significantly.

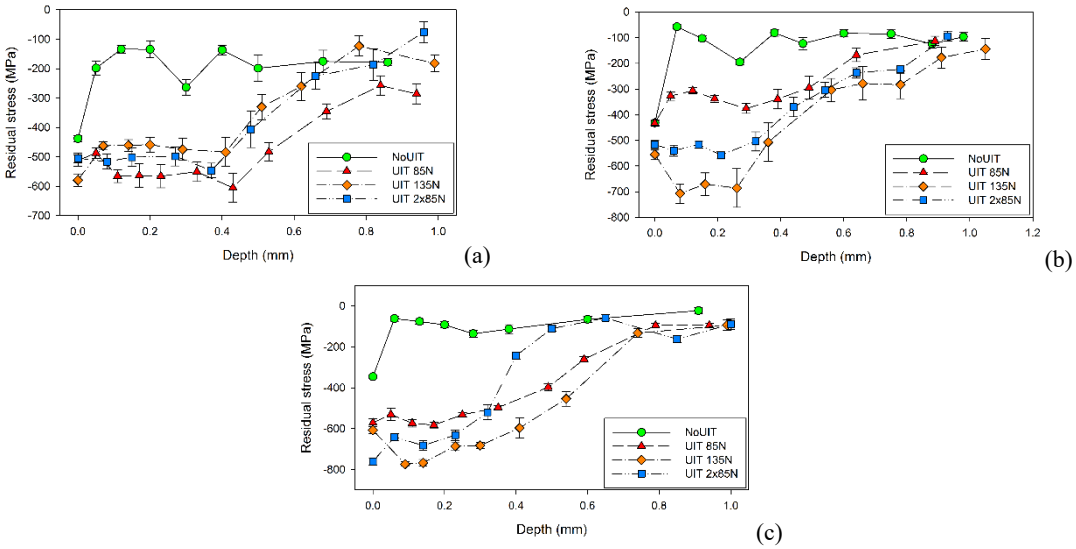

Fig. 2. Residual stress before and after UIT treatment with different parameters: (a) weld metal, (b) heat affected zone and (c) base metal.

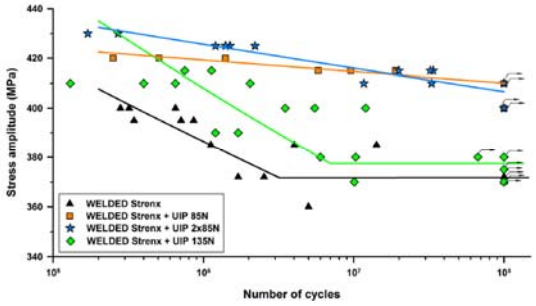

Fig. 3. Results of rotating bending fatigue tests of welded Strenx steel and after treatment with UIT.

Similar behaviour of the fatigue life with increasing intensity of the surface treatment was observed in [3] where too extensive treatment parameters created deeper layer of compressive residual stresses, however the influence on fatigue life was not so positive as using of treatments with lower intensity. This is usually related to surface damage after extensive treatment e. g. creation of micro-cracks. In case of weld fatigue also significant role play the weld defects present in the volume of material because they often serve as fatigue crack initiation points, thus they overcome the effect of the surface treatment.

REFERENCES

[1] Lago, J., et. al.: Improvement of fatigue endurance of welded S355 J2 structural steel by severe shot peening. Surface Engineering 9(33), 715-720 (2017).
[2] Zhang, H., et. al.: Effects of ultrasonic impact treatment on pre-fatigue loaded high-strength steel welded joints. International Journal of Fatigue (80), 278-287 (2015).
[3] Trško, L., et. al.: Influence of Severe Shot Peening on the Surface State and Ultra-High-Cycle Fatigue Behavior of an AW 7075 Aluminum Alloy. Journal of Materials Engineering and Performance 6(26), 2784–2797 (2017).

ACKNOWLEDGMENTS

The research was supported by project APVV-16-0276, APVV-16-0300, APVV-14-0096 and VEGA 1/0951/17.

Influence of Tool Geometry on Fatigue Behavior of Friction Stir Welded T-Joints

N. Manuel[a, b], P. Martins[b], J.D.M. Costa[b], A. Loureiro[b*]

[a] *Escola Superior Politecnica do Namibe, Rua Amilcar Cabral, Namibe, Angola*
[b] CEMMPRE, Mechanical Engineering Department, University of Coimbra, Rua Luís Reis Santos, 3030-788 Coimbra, Portugal
**Corresponding author: altino.loureiro@dem.uc.pt*

Keywords: Tool geometry; Friction stir weld; T-joints; Aluminium alloys; Fatigue behaviour.

ABSTRACT

T-joints in aluminium alloys are widely used in many industrial applications, such as hull and boat decks, railroad roof panels or the Space Shuttle external tanks. The fusion welding processes present limitations in the realization of these joints, as they cause defects and distortion in the welds. Friction stir welding does not have these drawbacks, but is little studied for this type of joints. Hou et al [1] and Cui et al [2] studied the influence of the radius of the fillet between the skin and stringer on the mechanical strength of the T-joints. Krasnowski [3] states that, from the technological point of view, chamfer arrangements are preferable because they ease the execution of the job. The study of fatigue behaviour of these joints is still limited [3, 4], and neither deals with the influence of technological parameters.

The aim of this study was to analyse the influence of tool geometry and FSW welding parameters on the morphology, mechanical strength and fatigue resistance of T-welds in dissimilar aluminium alloys.

The welds were made by friction stir welding in 3 mm thick sheets of AA 6082-T6, as skin, and AA 5083-H111, as stringer, in the configuration indicated in Fig. 1a). The designation of this joint preparation is T-butt. For this purpose, two tools with different pin geometry were used, as shown in Fig. 1b) and c). Two series of welds were produced, one with the CRP tool, with the designation 65BRP-3, and another with the PP tool, with the designation 65BPP-2, both with the same welding parameters: tool rotational speed - 660 rpm; traverse speed - 30 mm / min; tool plunge depth - 5.7 mm. The specimens were drawn transversely to the weld direction, and subjected to metallographic tests, hardness tests, skin tensile tests and fatigue. The tensile fatigue tests were performed on the skin with a stress ratio R = 0.02, a stress range of 100-200 MPa and a frequency between 15 and 25 Hz.

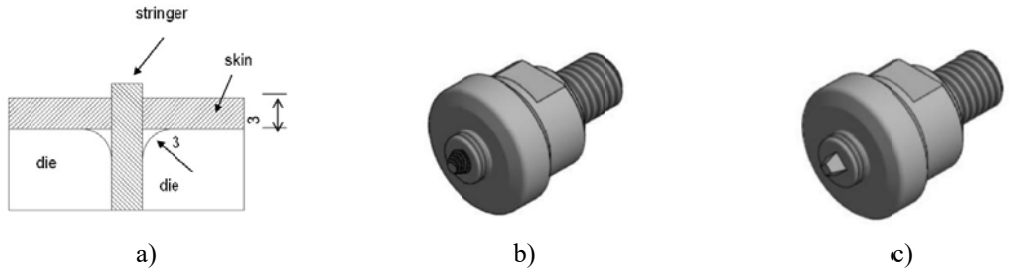

a) b) c)

Fig. 1. a) T-butt joint preparation; b) tool with conical threaded pin (CRP); c) tool with pyramidal progressive pin (PP).

The welds did not show any defects in their cross-section, but a significant loss of skin hardness was obtained, as shown in Fig. 2. This loss of hardness is due to the dissolution of the hardening precipitates

in the weld because the skin is a thermally treatable alloy. This loss of hardness was similar for the two sets of welds and corresponded to a loss of mechanical strength of the skin about of 41%.

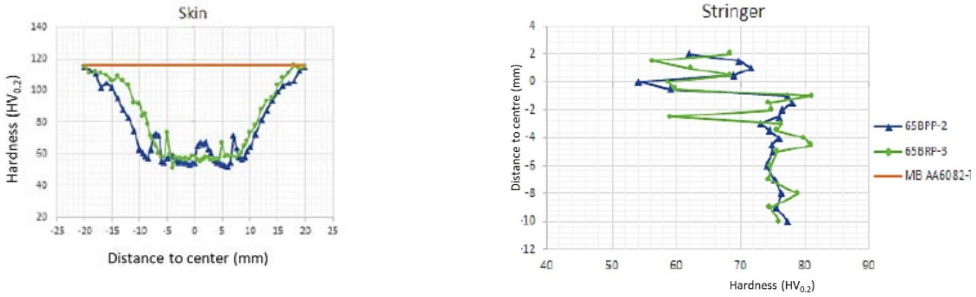

a) b)

Fig. 2. Hardness profiles for: a) the skin; b) the stringer.

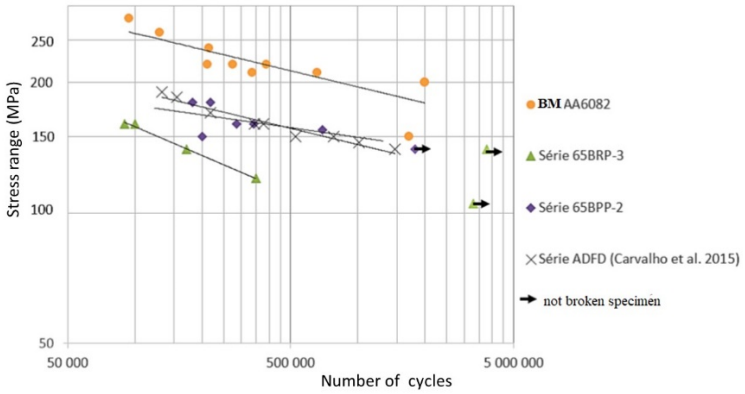

Fig. 3. S-N curves for the welding series 65.

Fig. 3 shows the S-N curves for the base material, for the two series studied and for a third series previously performed with the same PP tool. It is found that any of the series has lower fatigue strength than the base material. However, the series made with the conical threaded pin tool (CRP) has lower resistance than the one with the pyramid pin tool (PP). This behaviour results from the presence of a line of oxides in the welds of the 65BRP-3 series. All specimens failed in the heat-affected zone.

REFERENCES

[1] Hou, X., Yang, X., Cui, L., Zhou, G.: Influences of joint geometry on defects and mechanical properties of friction stir welded AA6061-T4 T-joints. Materials and Design 53, 106–117 (2014).
[2] Cui, L., Yang, X., Xie, Y., Hou, X., Song, Y.: Process parameter influence on defects and tensile properties of friction stir welded T-joints on AA6061-T4 sheets. Materials and Design 51, 161–174 (2023).
[3] Krasnowski, K.: Technology of friction stir welding of aluminium alloy 6082 T-joints and their behaviour under static and dynamic loads. Materialwissenschaft und Werkstofftechnik 46(3), 256–268 (2015).
[4] Tavares, S.M.O., Castro, R.A.S., Richter-Trummer, V., Vilaça, P., Moreira, P.M.G.P., de Castro, P.M.S.T.: Friction stir welding of T-joints with dissimilar aluminium alloys: mechanical joint characterisation. Science and Technology of Welding & Joining 15(4), 312–318 (2010).

ACKNOWLEDGMENTS

This research is sponsored by FEDER funds through the program COMPETE – Programa Operacional Factores de Competitividade – and by national funds through FCT – Fundação para a Ciência e a Tecnologia, under the project UID/EMS/00285/2013.

Increase in Fatigue Strength of Friction Stir Welded Joints of an Aluminium Alloy by Laser Peening

Y. Sano[a*], K. Masaki[b], T. Sano[c]

[a] *ImPACT Program, Japan Science and Technology Agency, Japan*
[b] *National Institute of Technology, Okinawa College, Japan*
[c] *Division of Materials and Manufacturing Science, Graduate School of Engineering, Osaka University, Japan*
**Corresponding author: yuji.sano@jst.go.jp*

Keywords: A6061-T6; FSW; Laser peening; Residual stress; Fatigue.

ABSTRACT

Laser peening (LP) is an emerging surface technology which can introduce compressive residual stress by simply irradiating laser pulses to metallic materials covered with transparent plasma-confining medium (liquid or solid) [1-3]. Most recently, the authors have invented a novel process of laser peening without using any confining medium. This technology was named “dry-LP” and would largely expand the application of laser peening [4].

In this study, laser peening was applied to friction stir welded (FSW) joints to enhance the fatigue properties through the introduction of compressive residual stress on the surface [5]. As shown in Fig. 1, fatigue specimens were cut out from FSW A6061-T6 aluminum alloy plates with a thickness of 3 mm by wire electric discharge machining (EDM). Both crown and root sides of the specimens were treated by laser peening with a frequency-doubled Nd:YAG laser (λ = 532 nm). Laser pulses with an energy of 60 mJ and a duration of 8 ns were focused down to 0.7 mm onto the specimens.

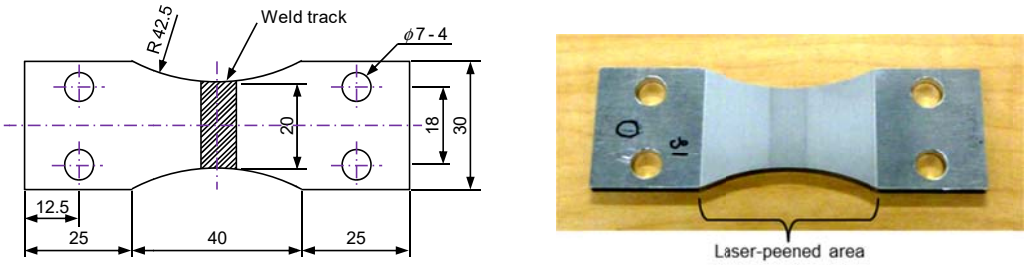

Fig. 1. Shape and dimensions of specimen (light) and external view after laser peening (right).

The effects of laser peening on the fatigue properties were studied through plane bending fatigue testing with a stress ratio of R = -1 and frequency of 22 Hz in ambient conditions. The results are summarized in Fig. 2, showing that the fatigue strength of unwelded base material (BM) specimens was 110 MPa at 10^7 cycles and laser peening (LP) enhanced the strength by 60 MPa to 170 MPa, in spite of increase in surface roughness due to the direct irradiation of the laser pulses to the bare surface of the specimens. On the other hand, the fatigue strength of FSW specimens was 90 MPa and laser peening enhanced it by 30 MPa to 120 MPa. This increment is a half compared to that in the unwelded BM specimens; however the fatigue strength of the FSW specimens after laser peening was higher than that of the unwelded specimens.

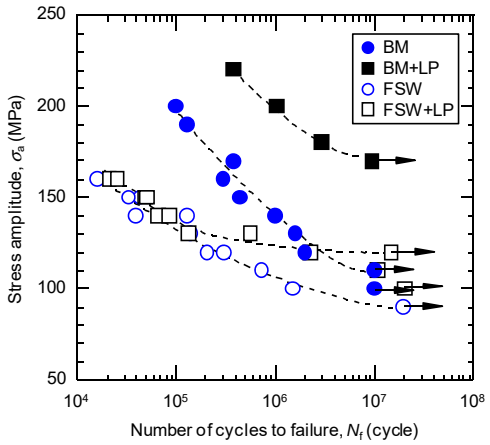

Fig. 2. S-N diagram of A6061-T6 base material (BM) and friction stir welded (FSW) joints.

The outline of the laser peening technology and the effects on the fatigue properties of friction stir welded A6061-T6 joints will be presented together with the results on the surface roughness, hardness, residual stress and fracture surface of the specimens.

REFERENCES

[1] Sano, Y., Mukai, N., Okazaki, K., Obata, M.: Residual stress improvement in metal surface by underwater laser irradiation. Nucl. Instrum. Methods Phys. Res. B 121, 432-436 (1997).

[2] Sano, Y., Yoda, M., Mukai, N., Obata, M., Kanno, M., Shima, S.: Residual stress improvement mechanism on metal material by underwater laser irradiation. J. Atomic Energy Soc. Japan. 42, 567-573 (2000).

[3] Sano, Y., Obata, M., Kubo, T., Mukai, N., Yoda, M., Masaki, K., Ochi, Y.: Retardation of crack initiation and growth in austenitic stainless steels by laser peening without protective coating. Mater. Sci. Eng. A 417, 334-340 (2006).

[4] Sano, T., Eimura, T., Kashiwabara, R., Matsuda, T., Isshiki, Y., Hirose, A., Tsutsumi, S., Arakawa, K., Hashimoto, T., Masaki, K., Sano, Y.: Femtosecond laser peening of 2024 aluminum alloy without a sacrificial overlay under atmospheric conditions. J Laser Appl. 29, 012005-1-7 (2017).

[5] Sano, Y., Masaki, K., Gushi, T., Sano, T.: Improvement in fatigue performance of friction stir welded A6061-T6 aluminum alloy by laser peening without coating. Mater. Des. 36, 809-814 (2012).

Mechanical Characterization of Successive Double-Sided LBW of Dissimilar AA2024-T3/AA7075-T6 T-Joints

P.I.P. Oliveira[a], J.C.S. Melo[a], J.D.M. Costa[a*], A.J.R. Loureiro[a], J.A.M. Ferreira[a]

[a] CEMMPRE, Mechanical Engineering Department, University of Coimbra, Rua Luís Reis Santos, 3030-788 Coimbra, Portugal
**Corresponding author: jose.domingos@dem.uc.pt*

Keywords: Laser beam welding; Double sided T-joint; Dissimilar aluminium alloys; AA2024-T3; AA7075-T6; AA4047; Fatigue behaviour.

ABSTRACT

The interest of aviation industry in reducing the weight of airplane structures and in decreasing both cost and time of aircraft manufacturing are the main reasons to investigate the laser beam welding (LBW) as a joining technology to replace the riveted joints in stiffened panels [1]. The main drawbacks for this replacement are the welding defects such and the reduction in mechanical properties due to the welding process. Beyond the porosity caused by hydrogen rejection during the weld pool solidification, the porosity formed by keyhole instability plays an important role in LBW difficulties [2]. The porosity can be affected by welding parameters such as the wire feeding angle [3] and incident beam angle [4]. The solidification cracking can be avoided by using filler wire with high silicon content [5] and with feed rate high enough to compensate the crack formation during the solidification [6]. Moreover, welding parameters like welding speed and feed rate of filler wire have influence on weld strength [7]. Aluminum alloys of 2xxx and 7xxx series have been widely used in manufacturing of riveted aeronautic structures due to their high strength to weight ratio, but both are considered not easily weldable by fusion welding [1], due to defect formation during welding. Therefore, few works have studied dissimilar laser welded T-joints of 2xxx and 7xxx series.

Thus, this research evaluated the effect of laser beam welding parameters on morphology and mechanical properties of successive double-sided laser beam welded T-joints that were performed with 2 mm thickness sheets of AA2024-T3 as skin and AA7075-T6 as stringer, and with a 1 mm wire of AA4047 as filler metal. Different weld series were carried out by the variation of welding parameters such as laser beam power, laser beam diameter, incident beam angle, incident beam position and welding speed, presented in the Fig. 1. The effect of welding parameters on weld bead dimensions and microstructure were analysed by optical and scanning electron microscopies. The influence of these parameters on macroporosity was measured by mean of radiographies. Moreover, pull-out, hoop and fatigue tests were carried out and the microhardness were measured. The results pointed out that the welding parameters affect the weld bead dimensions and porosity, but they did not indicate relevant effect of the parameters on microstructure and microhardness profiles. Furthermore, it was verified that some weld bead dimensions have influence on pull-out and hoop test results. The fatigue tests showed that the S-N curves obtained for the several weld series are different when plotted in terms of nominal stress, as shown in Fig. 2. The Fig. 3 shows the comparison between the S-N curves of the same weld series for nominal stress and local stress indicating that there were no significant changes in slope of the curves neither in coefficient of determination (R^2) pointing out that geometric factors were not the cause for the fatigue data scatter.

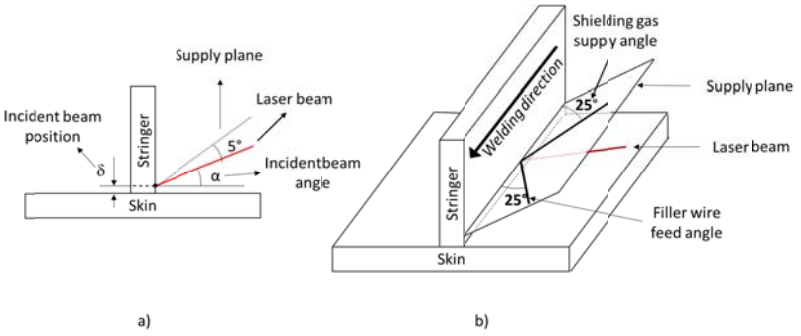

Fig. 1. Schematic diagram of T-joint welding.

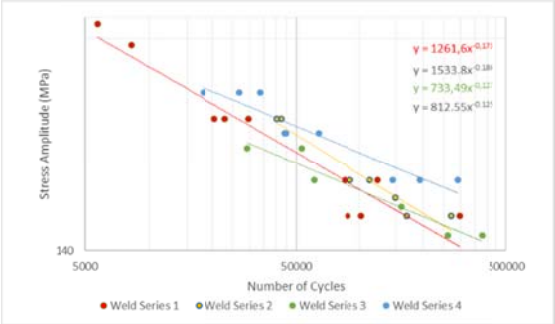

Fig. 2. Comparison among S-N curves for nominal stress

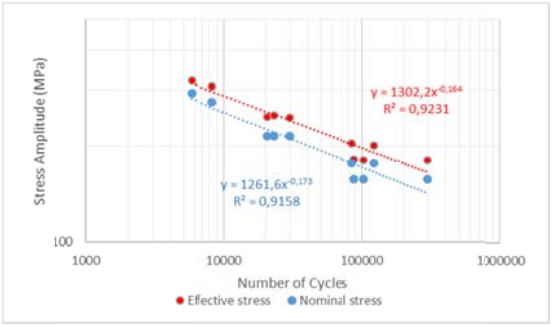

Fig. 3. Comparison between SN curves for effective and nominal stress of weld series 1

REFERENCES

[1] Dittrich, D., Standfuss, J., Liebscher, J., Brenner, B., Beyer, E.: Laser beam welding of hard to weld Al alloys for regional aircraft fuselage design – First results. Physics Procedia 12, 113-122 (2011).

[2] Pastor, M., Zhao, H., Martukanitz, R.P., Debroy, T.: Porosity, underfill and magnesium loss during continuous wave Nd:YAG laser welding of thin plates of aluminum alloys 5182 and 5754. Welding Research Supplement, 207-216 (1999).

[3] Tao, W., Yang, Z., Chen, Y., Li, L., Jiang, Z., Zhang, Y.: Double-sided fiber laser beam welding process of T-joints for aluminum aircraft fuselage panels: Filler wire melting behavior, process stability, and their effects on porosity defects. Optics and Laser Technology 52, 1-9 (2013).

[4] Ventzke, V., Riekehr, S., Horstmann, M., Haack, P., Kashaev, N.: One-side Nd:YAGlaser beam welding for manufacture of T-joints made of aluminium alloys for aircraft construction. Welding and Cutting 13(4), 245-249 (2014).

[5] Enz, J., Riekehr, S., Ventzke, V., Kashaev, N.: Influence of the Local Chemical Composition on the Mechanical Properties of Laser Beam Welded Al-Li Alloys. Physics Procedia 39, 51-58 (2012).

[6] Cicalã, E., Duffet, G., Andrzejewski, H., Grevey, D.: Continuous Welding of Al-Mg-Si Alloys with Nd:YAG Laser Irradiation: Tensile Properties Optimization of T-joint Seams. Lasers in Engineering 20, 195-211 (2010).

[7] Prico, A., Acerra, F., Squillace, A., Giorleo, G., Pirozzi, C., Prico, U., Bellucci, F.: LBW of similar and dissimilar skin-stringer joints. Part I: process optimization and mechanical characterization. Advanced Materials Research 38, 306-319 (2008).

ACKNOWLEDGMENTS

This research is sponsored by FEDER funds through the program COMPETE – Programa Operacional Factores de Competitividade – and by national funds through FCT – Fundação para a Ciência e a Tecnologia, under the project UID/EMS/00285/2013. The authors thanks to Fundiven by support to carry out radiographies.

Low-Cycle Fatigue

Low Cycle Fatigue Life Estimation of P91 Steel by Strain Energy Based Approach

B. Das[a], A. Singh[a*]

[a] *Department of Mechanical Engineering, Indian Institute of Technology Patna, India*
**Corresponding author: akhil@iitp.ac.in, akhilendra.singh@gmail.com*

Keywords: Low cycle fatigue; Masing; Bauschinger strain; Fatigue toughness.

ABSTRACT

1. Introduction

In the present study strain energy based analytical models are used to predict the fatigue life of P91 steel subjected to strain controlled loading. P91 steel being used in pressure vessel and many other components for ultra-supercritical fossil fired and nuclear power plants are subjected to repeated thermal stresses. Cyclic loadings arising due to thermal stresses produces severe strain in the material thereby causing low cycle fatigue (LCF) failure of the engineering components. Since the low cycle fatigue failure is mainly caused by the cyclic plastic strain ($\Delta\varepsilon_p$), thus plastic strain energy can be considered as a crucial parameter to describe the damage mechanism [1, 2]. Golos et al. [1] proposed a single damage criterion based on strain energy density to characterize both low and high cycle fatigue regimes of pressure vessel steel. Callaghan et al. [3] analysed low cycle fatigue behaviour of 2.25Cr–1Mo steel using energy based approach and predicted fatigue toughness to crack propagation. Thus models based on energy dissipation during first cycle and averages of cycles are developed to assess the fatigue life.

2. Experimental Procedures

The P91 material used in this study were austenized at 1050^0C for 90 min, air-cooled followed by tempering at 760^0C for 60 min. Uniaxial strain controlled low cycle fatigue tests at ambient temperature are conducted on P91 steel in the normalized and tempered condition. All fatigue tests were carried at constant strain rate of 0.001 s^{-1} until complete separation of the specimens or when the peak stresses got reduced by 30 %.

3. Results and Discussions

The stress-strain response of P91 steel subjected to strain controlled loading at strain amplitudes of 0.3-0.5 % are summarised in Table 1. It can be observed from Table 1 that plastic strain amplitude increases with increase in imposed strain amplitudes. It can be concluded that at higher amplitudes material had undergone severe plastic deformation, thus resulting in reduction in fatigue lives. P91 material showed small deviation from ideal masing type behaviour and can be referred as near masing behaviour. The masing behaviour can be further examined by the variation in bauschinger strain with plastic strain range. The progressive increase in basuchinger strain infers that the P91 steel follows near masing behaviour. The analytical energy models based on energy dissipated in first cycle(W_1^p) and average of the energy dissipated from first to fifth cycle (W_{avg}^p). The relationship between energy and number of cycles to failure can be expressed as:

$$W_1^p = A_1(2N_f)^{b_1} \quad (1)$$

$$W_{avg}^p = A_2(2N_f)^{b_2} \quad (2)$$

Table 1. Cyclic stress-strain response and fatigue life data of P91 steel

Values at $0.5N_f$				
Total strain amplitude (%) $(\Delta\varepsilon_t/2)$	Elastic strain amplitude (%) $(\Delta\varepsilon_e/2)$	Plastic strain amplitude (%) $\Delta\varepsilon_p/2$	Stress amplitude (MPa) $\Delta\sigma/2$	Number of cycles to failure (N_f)
0.3	0.23	0.07	512.54	4965
0.4	0.275	0.125	587.90	1644
0.5	0.29	0.21	587.20	945

Fig. 1 (a) and (b) shows the accuracy of the predicted number of reversals to failure based on energy dissipated in first cycle and average of cycles. The figure depicts that the above models successfully correlates experimental and predicted fatigue lives within small deviation. The prediction of fatigue life based on the average of cycles is more accurate than energy dissipated in first cycle. The cumulative plastic strain energy or fatigue toughness was found to increase with increasing number of cycles to failure [4].

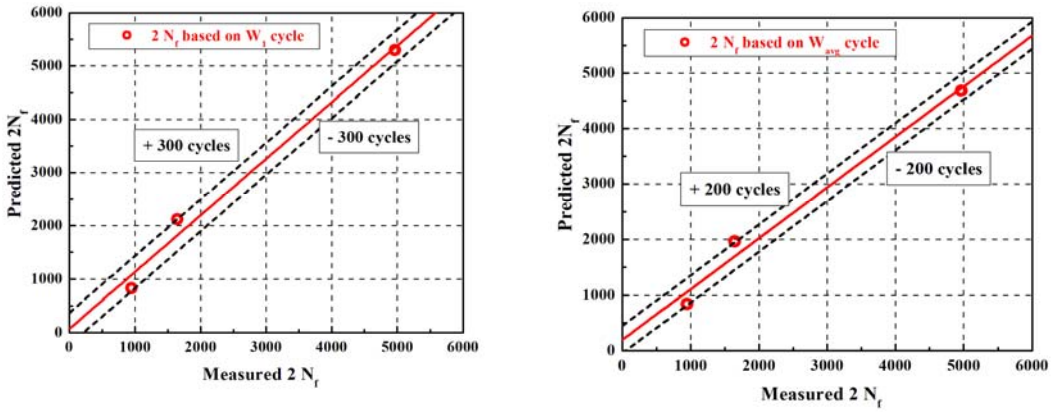

(a) (b)

Fig. 1. Predicted number of reversals to failure based on (a) first cycle and (b) average of first to fifth cycles.

REFERENCES

[1] Golos, K., Ellyin, F.: A Total Strain Energy Density Theory for Cumulative Fatigue Damage. Journal of Pressure Vessel and Technology 110, 36-41 (1988).

[2] Ellyin, F., Kujawski D.: Plastic Strain Energy in Fatigue. Journal of Pressure Vessel and Technology 106, 342-347 (1984).

[3] Callaghan, MD., Humphries, SR., Law, M., Ho, M., Bendeich, P., Li, H.: Energy-based approach for the evaluation of low cycle fatigue behaviour of 2.25Cr–1Mo steel at elevated temperature 527, 5619–5623 (2010).

[4] Sarkar, P.P., De, P.S., Dhua, S.K., Chakraborti, P.C.: Strain energy based low cycle fatigue damage analysis in a plain C-Mn rail steel. Materials Science & Engineering A 707(7),125–135 (2017).

Evaluation of Strain Controlled Fatigue and Crack Growth Behaviour of Al-3.4Mg Alloy

P. Kumar[a], A. Singh[a*]

[a] *Department of Mechanical Engineering, Indian Institute of Technology Patna, India*
**Corresponding author: akhil@iitp.ac.in; akhilendra.singh@gmail.com*

Keywords: Fatigue crack growth; Low cycle fatigue; Chaboche kinematic hardening model; XFEM.

ABSTRACT

Present study focuses on fatigue performance of Al-3.4Mg (AA5754) alloy having 3.4 weight % of Magnesium (Mg). Chemical composition of alloy is confirmed by Inductive coupled plasma-Optical Emission spectroscopy (ICP-OES) test. Fatigue crack growth (FCG) and low cycle fatigue (LCF) tests are performed for as received and precipitation strengthened AA5754 alloy. The presence of magnesium (Mg) makes this alloy highly resistive towards corrosion therefore it can be a good choice for marines and cryogenics applications. In these applications the components are subjected to varied dynamic loadings. Therefore, their fatigue performance investigation under cyclic loads is important for safe design. The alloy has been heat treated for improved mechanical strength and further tested for fatigue life. Precipitation strengthening heat treatment (PSHT) process significantly alters the strength of Al-Mg alloys [1–3]. PSHT comprises of heating the alloy at *530*°C (above Mg-solvus temperature) for 2 *hours* followed by quenching at room temperature water thereafter reheating (annealing) at *250*°C for 6 *hours* and cooling in furnace itself. Micro-structural images of as received and PSHT alloy are shown in Fig. 1(a) and Fig 1(b).

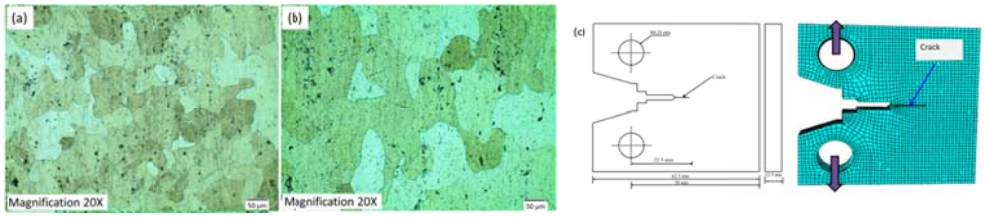

Fig. 1. Microstructure of (a) as received and (b) PSHT Al-3.4Mg alloy (c) Compact tension specimen with meshed model.

Table 1. Mechanical properties and Fatigue crack growth test results

Alloy condition	Tensile strength (MPa)	Hardness (VHN)	ΔK_{th} (MPa-m$^{1/2}$)		Fatigue life (Cycle)	
			R=0.1	R=0.5	R=0.1	R=0.5
As received alloy	257	81	2.66	2.64	109294	53414
PSHT alloy	320	68	3.86	3.23	212998	67033

Fatigue crack growth test is performed at load ratio (R=P_{max}/P_{min}) of 0.1 and 0.5 on compact tension (CT) specimen. Mechanical properties and FCG test results are presented in Table 1. Experimental results depict that heat treated alloys offer higher resistance against crack growth during fatigue loading. Higher fatigue life for PSHT alloy is attributed due to the less crack path deflection or crack tortuosity, smoother fracture surface and redistribution of grain structure [4, 5]. The crack growth behaviour of the material is

numerically modelled by eXtended Finite Element Method (XFEM). Fig.1(c) represents discretised model of the CT specimen. The enriched displacement approximation at any point can be written as [6]:

$$\boldsymbol{u}^h(\mathbf{x}) = \sum_{j=1}^{N} \phi_j(\mathbf{x}) \left[\boldsymbol{u}_j + H(\mathbf{x})\boldsymbol{a}_j + \sum_{\alpha=1}^{4} F_\alpha(\mathbf{x})\boldsymbol{b}_j^\alpha \right] \tag{1}$$

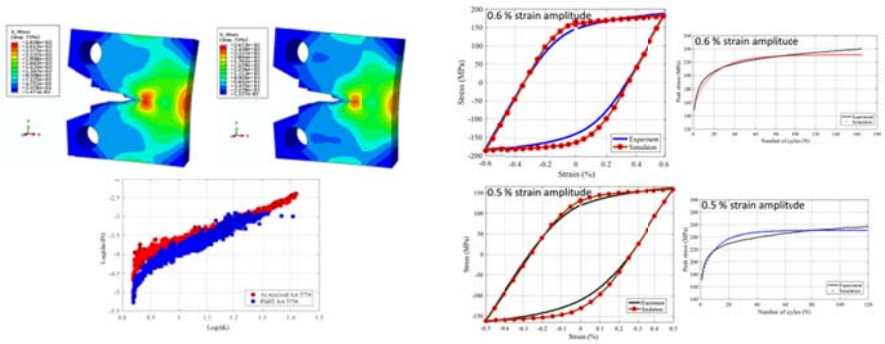

(a) (b)

Fig. 2. (a) Deformed model of crack growth by XFEM and experimental Paris curve for as received and PSHT Al-3.4Mg alloys (b) Experimental and simulated hysteresis loops and fatigue life for as received AA5754.

The stress distribution shown in Fig. 2(a) illustrate higher stresses at crack vicinity and lower crack growth for PSHT AA5754 alloy which signifies that it offers higher resistance towards crack growth. Strain controlled LCF test is performed for two strain ranges of 1.0 % and 1.2 % on flat specimen prepared according to ASTM E606 standard. Improvement in tensile strength and refined grain structure results in enhancement of fatigue life which is shown in S-N curve presented in Fig. 2(b). Cyclic hardening behaviour is observed for both as receive and PSHT alloys. Kinematic hardening model postulated by Chaboche [7] is used to simulate the hysteresis loops using finite element method (FEM). Chaboche kinematic hardening model combined with isotropic hardening model is used to simulate the experimental hysteresis loops and fatigue life as shown in Fig. 2(b). The present study concludes that higher fatigue strength during LCF test and lower crack growth rate by FCG test is obtained for precipitation strengthened AA5754 alloy as compared with as received alloy.

REFERENCES

[1] Seong-Jong, K.I.M., Seok-Ki, J.A.N.G., Min-Su, H.A.N., Seong-Kwon, K.I.M., Jong-Sin, K.I.M.: Effects of precipitation strengthening heat treatment for Al-Mg alloy. Transactions of Nonferrous Metals Society of China 21(6), 1218–1224 (2011).

[2] Starink, M.J., Zahra, A.M.: Low-temperature decomposition of Al-Mg alloys: Guinier-Preston zones and L12 ordered precipitates. Philosophical Magazine A 76(3), 701-714 (1997).

[3] Hales, S.J., McNelley, T.R.: Microstructural evolution by continuous recrystallization in a superplastic Al-Mg alloy. Acta Metallurgica 36(5), 1229–1239 (1988).

[4] Pao, P.S., Jones, H.N., Cheng, S.F., Feng, C.R.: Fatigue crack propagation in ultrafine grained Al–Mg alloy. International Journal of Fatigue 27, 1164–1169 (2005).

[5] Shou, W.B., Yi, D.Q., Liu, H.Q., Tang, C., Shen, F.H., Wang, B.: Effect of grain size on the fatigue crack growth behavior of 2524-T3 aluminum alloy. Archives of Civil and Mechanical Engineering 16(3), 304–312 (2016).

[6] Pathak, H., Singh, A., Singh, I.V.: Fatigue crack growth simulations of 3-D problems using XFEM. International Journal of Mechanical Sciences 76, 112-131 (2013).

[7] Chaboche, J.L.: On some modifications of kinematic hardening to improve the description of ratchetting effects. International Journal of Plasticity 7(7), 661–678 (1991).

Description of Steel S355J2 and S355J0 Fatigue Behaviour by Canteli et al. Model in Low and High Cycles Regime

S. Seitl[a*], P. Miarka[a], S. Blasón[b], A. Canteli[b]

[a] *High Cycle Fatigue Group, Institute of Physics of Materials, Academy of Sciences of The Czech Republic, Czech Republic*
[b] *Department of Department of Construction and Manufacturing Engineering, Universidad de Oviedo, 33203 Gijon, Spain*
**Corresponding author: seitl@ipm.cz*

Keywords: S355; Steel; Fatigue; ProFatigue; Canteli et al. model; S-N curve.

ABSTRACT

The use of S355 high strength steel in civil engineering to design structures of bridges, cranes or simple engineering parts allows material and economical savings meeting the strict construction requirements. The knowledge of the fatigue resistance of material plays the key role during design and maintenance of the bridge structures. In the paper the fatigue behaviours of S355J2 and S355J0 are analysed using statistical models. The data consist of results from low cycle and high cycle fatigue and different number of various investigated specimens. In particular, the software ProFatigue is used for derivation of the probabilistic S–N field from experimental fatigue data. The program, based on a former regression Weibull model, allows the estimation of the parameters involved in the S–N field model, providing an advantageous application of the stress based approaches in the fatigue design of mechanical components. The results obtained are compared with the customary Wöhler-curve, represented as a straight line in a double-logarithmic scale.

Table 1. Chemical composition in percentage by weight (wt. %) of the S355 J2 and S355J0 steel grades according to EN 10025-2:2004 standard.

	Steel grade	C (max.%)	Mn (max.%)	Si (max.%)	P (max.%)	S (max.%)	N (max.%)	Cu (max.%)	CEV (max.%)
EN 10025-2:2004	S355J0	0.2	1.6	0.55	0.035	0.035	0.012	0.55	0.47
	S355J2	0.2	1.6	0.55	0.03	0.03	-	0.55	0.47

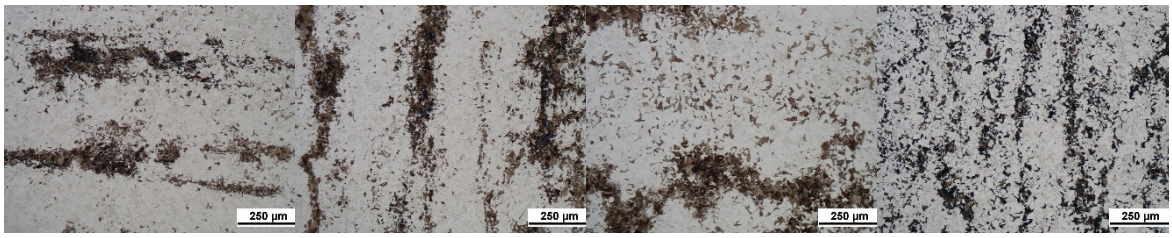

a) S355 J0A b) S355 J0B c) S355 J2A d) S355 J2B

Fig. 1. Structure of the HS S355 J0 and S355 J2 steel grades: the crack was propagating in the horizontal direction (etched with 2% Nital, light optical microscope).

Weibull model for minima:

$$F(N;\Delta\sigma) = 1 - exp\left[-exp\left(\frac{(\log N - B)(log\Delta\sigma - C) - \lambda}{\delta}\right)\right];\ (logN - B)(log\Delta\sigma - C) \geq \lambda\,, \qquad (1)$$

where B is a threshold value of the lifetime, C is the endurance or fatigue limit for $NN \longrightarrow \infty$, and λ, δ, β are the location, scale and shape Weibull parameters, respectively. The percentiles curves are hyperbolas sharing the asymptotes log $N = B$ and log $\Delta\sigma = C$, whereas the zero percentile curve represents the minimum possible number of cycles required to achieve failure for different values of log $\Delta\sigma$.

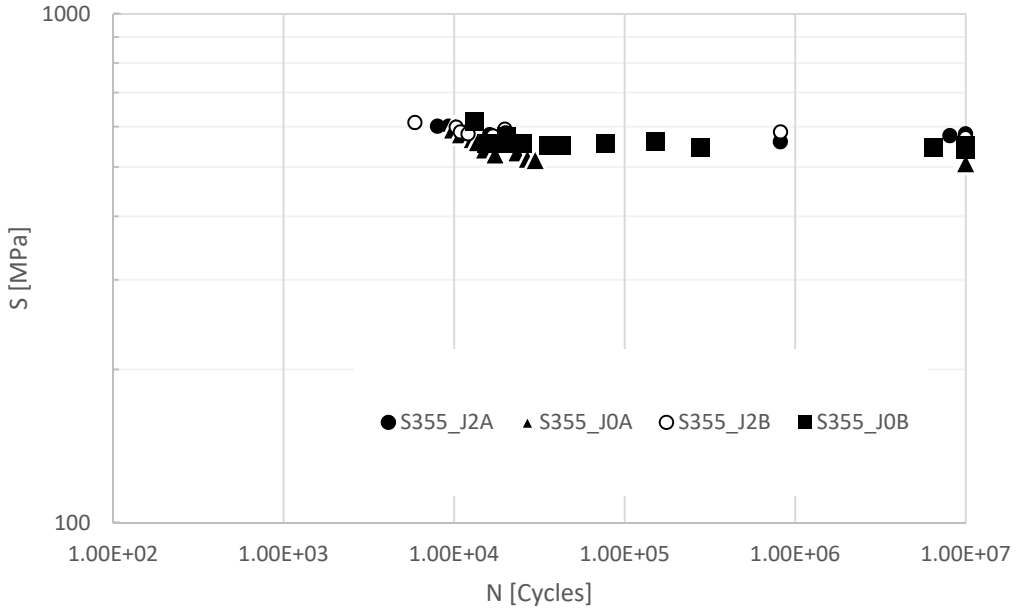

Fig. 3. Different S–N curves resulting from analysis of experimental results performed on S355 J2 and S355 J0.

REFERENCES

[1] de Jesus, M.P., Matos, R., Fontoura, B.F.C., Rebelo, C., Simoes da Silva, L., Veljkovic, M.: A comparison of the fatigue behavior between S355 and S690 steel grades. Journal of Construction Steel Research 79, 140–150 (2012).
[2] Lewandowski, J., Rozumek, D.: Cracks growth in S355 steel under cyclic bending with fillet welded joint. Theoretical and Applied Fracture Mechanics 86, 342–350 (2016).
[3] Gao, W., Wang, D., Cheng, F., Di, X., Deng, C., Xu, W.: Microstructural and mechanical performance of underwater wet welded S355 steel. Journal of Materials Processing Technology 238, 330–340 (2016).
[4] Pawliczek, R., Prazmowski, M.: Study on material property changes of mild steel S355 caused by block loads with varying mean stress. International Journal of Fatigue 80, 171–177 (2015).
[5] Rozumek, D., Marciniak, Z., Lesiuk, G., Correia, J.A.F.O.: Mixed mode I/II/III fatigue crack growth in S355 steel. Procedia Structural Integrity 5, 896–903 (2017).

ACKNOWLEDGMENTS

The Czech Science Foundation under the contract No. 17-01589S supported this research. The research was conducted in the frame of IPMinfra supported through project No. LM2015069 of MEYS.

Applicability of Critical Distances Theory to Extreme-Low-Cycle Fatigue

J.C.R. Pereira[a,b*], J. Xavier[b,c], J.A.F. Correia[a,b], A.M.P. de Jesus[a,b],

L. Susmel[d], A.A. Fernandes[a,b]

[a] *Faculty of Engineering, University of Porto, Portugal*
[b] *INEGI, University of Porto, Portugal*
[c] *CITAB, University of Trás-os-Montes e Alto Douro, Portugal*
[d] *Department of Civil and Structural Engineering, The University of Sheffield, United Kingdom.*
**Corresponding author: jxavier@inegi.up.pt*

Keywords: Theory of critical distances; Ultra-low-cycle fatigue; Finite element method; Pipeline materials.

ABSTRACT

Pipelines can be submitted to extreme loading scenarios, which can engender structural instability in the form of large deformations and fracture by both monotonic plastic deformations of cyclic loads. Both monotonic ductile and low-cycle fatigue (LCF) damage mechanisms can occur for X52, X60 and X65 piping steel grades. The evaluation and prediction of this type of failure, characterized by large-scale plastic yielding associated to high levels of stress triaxiality, are still not completely understood, deserving significant research effort in recent times [1-6]. ULCF using smooth testing is very challenging since the imposed strain levels lead generally to specimen's instabilities. The use of notched specimens is frequently an alternative option since strain localization helps to overcome the specimens buckling. Nevertheless the non-uniform stress/strain fields raised other challenges concerning the data reduction. In this respect, the Theory of Critical Distances (TCD) that has been proposed to allow fatigue life predictions for notched components under high-cycle and low-cycle fatigue regimes [7-10], is proposed in this paper to address the data reduction of ULCF data carried out using smooth and notched specimens. The extension of the TCD to monotonic failure prediction [11] is a good indication of its possibilities for the ULCF that is considered a transient process between the LCF and monotonic failure.

This paper originally addresses the applicability of the Theory of Critical Distances in the framework of LCF and ULCF fatigue regimes. Moreover, the proposed approach includes the application and comparison of the point, line and area methods associated to the TCD. An experimental program is carried out on several specimen geometries manufactured from X52 piping steel. Smooth and notched planar specimens are submitted by cyclic loading under tension/compression in order to obtain the fatigue lives within the range of 10^1-10^4 cycles. In addition, cyclic bending tests on notched planar specimens are also included. Finite element analyses are performed on the whole set of small-scale tests allowing deriving elastoplastic stress/strain fields along the potential crack paths. The numerical data is subjected to a post processing in order to find characteristic lengths that can be treated as a fatigue property in accordance to TCD strategy.

REFERENCES

[1] Pereira, J.C.R., de Jesus, A.M.P., Xavier, J., Fernandes, A.A.: Ultra low-cycle fatigue behaviour of a structural steel. Engineering Structures 60, 214–222 (2014).

[2] Xavier, J., Pereira, J.C.R., de Jesus, A.M.P.: Characterisation of steel components under monotonic loading by means of image-based methods. Optics and Lasers in Engineering 53, 142–151 (2014).
[3] Pereira, J., De Jesus, A.M.P., Xavier, J., Fernandes, A.A.: ULCF assessment of X52 piping steel by means of cyclic bending tests. Journal of Constructional Steel Research 138, 663-674 (2017).
[4] Pereira, J., Van Wittenberghe, Jeroen, De Jesus, A., Thibaux, P., Correia, J.A.F.O., Fernandes, A.A.: Damage Behaviour of Full-Scale Straight Pipes under Extreme Cyclic Bending Conditions. Journal of Constructional Steel Research 143, 97-109 (2018).
[5] Pereira, J.C.R., De Jesus, A.M.P., Fernandes, A.A., Varelis, G.: Monotonic, low-cycle fatigue and ultra-low cycle fatigue behaviors of the X52, X60 and X65 piping steel grades. Journal of Pressure Vessels Technology 138 (3), Paper No. 031403 (9 pages) (2016).
[6] Pereira, J.C.R., de Jesus, A.M.P., Fernandes, A.A.: A new ultra-low cycle fatigue model applied to the X60 piping steel. International Journal of Fatigue 93 (1), 201-213 (2016).
[7] Susmel, L., Taylor, D.: Fatigue Design in the Presence of Stress Concentrations. The Journal of Strain Analysis for Engineering Design 38(5), 443-452 (2003).
[8] Taylor, D.: The Theory of Critical Distances: A New Perspective in Fracture Mechanics. Oxford: Elsevier (2007).
[9] Susmel, L., Taylor, D.: An elasto-plastic reformulation of the theory of critical distances to estimate lifetime of notched components failing in the low/medium-cycle fatigue regime. Journal of Engineering Materials and Technology 132(2), 0210021–0210028 (2010).
[10] Susmel, L., Taylor, D.: Estimating lifetime of notched components subjected to variable amplitude fatigue loading according to the elasto-plastic Theory of Critical Distances. Journal of Engineering Materials and Technology 137(1), 011008-011023 (2015).
[11] Susmel, L., Taylor, D.: On the use of the Theory of Critical Distances to predict static failures in ductile metallic materials containing different geometrical features. Engineering Fracture Mechanics 75, 4410–4421 (2008).

ACKNOWLEDGMENTS

The authors acknowledge the Fundação para a Ciência e Tecnologia for their financial support through the SFRH/626 BD/80091/2011 Grant and Ciência 2008 program. The European Commission is also acknowledged through the Research Fund for Coal and Steel that is funding the ULCF project (RFSR-CT-2011-00029). Finally authors gratefully acknowledge the funding of SciTech - Science and Technology for Competitive and Sustainable Industries (NORTE-01-0145-FEDER-000022), R&D project cofinanced by Programa Operacional Regional do Norte (“NORTE2020”), through Fundo Europeu de Desenvolvimento Regional (FEDER).

Applications/Case Studies

Microinclusion and Fatigue Performance of Bearing Rolling Elements

E. Ossola[a], S. Pagliassotto[b], S. Rizzo[b], R. Sesana[a*]

[a]*DIMEAS, Politecnico di Torino, Italy*
[b]*Central Lab - Product Development, Tsubaki Nakashima, Italy*
**Corresponding author: raffaella.sesana@polito.it*

Keywords: Fatigue; Bearing; Microinclusion, Structural damage.

ABSTRACT

Many phenomena are involved in damage of rolling elements of bearings. Rolling contact fatigue is the main cause of failure, along with contact pressure related fatigue and dimensional instabilities effect. Most of those are well known, and are described by wide experimental, analytical and numerical literature. Damage phenomena are related to material properties and manufacturing processes, respectively. Particularly, the damage evolution might be affected by some microinclusions present in the material. This influence is related to mechanical properties, dimension, composition, shape and location of inclusions.
This research activity is focused on the C70, 100Cr6 and 100CrSiMn6-4 steel alloys. Relation between microinclusions and fatigue life is here investigated. These alloys exhibit a different behaviour with respect to fatigue damage and failure mechanism.

Results of experimental testing run on some test bench are compared to some analytical models (as those proposed by Eshelby and Murakami), for given set of operation conditions. Failures are then analysed to relate life of rolling elements to the microinclusion parameters. The research activity is aimed to investigate whether a microinclusion threshold parameter could be defined, to be related to the life bearing requirements. This analysis is performed by comparing analytical and experimental results of several models and different alloys.

REFERENCES

[1] Mura, T.: Micromechanics of defects in solids, Ch 4. 2nd ed. Dordrecht: Martinus Nijhoff (1987).
[2] Fajdiga, G., Ren, Z. and Kramar, J.: Comparison of virtual crack extension and strain energy density methods applied to contact surface crack growth. Eng. Fract. Mech. 74, 2721–2734 (2007).
[3] Tasgetiren, S., Aslantas, K.: A numerical study of the behavior of surface cracks under dry-sliding conditions. Mater. Des. 24, 273–279 (2003).
[4] Murakami, Y., Yokohama, N.N.: Influence of hydrogen trapped by inclusions on fatigue strength of bearing steel. In: Beswick JM, editor. Proc of ASTM Symposium Bearing Steel Technology. ASTM STP1419; 113–124 (2002).
[5] Fujimatsu, T., Nagao, M., Nakasaki, M., Hiraoka, K.: Analysis of stress around nonmetallic inclusions under rolling contact surface 13(1), Sanyo Tech Rep, 62–65 (2006).
[6] Yamakawa, K., Kizawa, K., Oguma, N., Kida, K.: The influence of subsurface defect on stress distributions under rolling contact fatigue conditions. Koyo Eng J., 24–28 (2004).
[7] Frith, P.H.: Fatigue tests on rolled alloy steels made in electric and open-hearth furnaces. J. Iron Steel Inst.180, 26–33 (1955).
[8] Unigame, Y., Hiraoka, K., Takasu, I., Kato, Y.: Evaluation procedures of nonmetallic inclusions in steel for highly reliable bearings. In: Beswick JM, editor. Bearing Steel Technology-Advances and State of the Art in Bearing Steel Quality Assurance, ASTM STP 1465. American Society for Testing and Materials; 34–41 (2007).

[9] Ioannides, E, Harris, T.A.: A new fatigue life model for rolling bearings. ASME J Tribology 107, 367–378 (1985).
[10] Harris, T.A.: Fatigue limit stress: a new and superior criterion for life rating of rolling bearing materials. In: Beswick JM, editor. Proc of ASTM Symposium Bearing Steel Technology. ASTM publication STP1419, 474–492 (2002).

Dimensional Stability on Fatigue Performance of Wheel Bearing Rolling Elements: Case Studies

E. Brusa[a], C. Sammarco[b], S. Rizzo[b], R. Sesana[a*]

[a]*DIMEAS, Politecnico di Torino, Italy*
[b]*Central Lab - Product Development, Tsubaki Nakashima, Italy*
**Corresponding author: raffaella.sesana@polito.it*

Keywords: Fatigue; Bearing; Dimensional stability.

ABSTRACT

Rolling bearings are critical automotive and mechanical components. For high loaded bearings, the steel rolling elements are subjected to failure having a direct impact on overall bearing fatigue life performance. Fatigue phenomena involve both rolling contact fatigue and material fatigue damage processes.

Metallurgical, mechanical, geometrical, physical properties affect fatigue behaviour and they can be controlled also by precise manufacturing process parameters. Despite accurate manufacturing, during the working condition, dimensional stability of some rolling elements within the bearing can be affected and distribution of stresses can strongly change with respect to design thus affecting fatigue performance. Failure can then occur for load values different and lower from design indications.

In the present research 100Cr6 and 100CrMnSi6-4 alloys, undergoing different thermal treatments, involving hardening, undercooling and tempering are analysed. Rolling elements in the selected alloys are subjected to fatigue tests and, while testing and after failure, metallurgical and dimensional parameters are measured.

The present paper reports about failure cases in rolling elements and investigates on the relation between dimensional stability and fatigue performance involving metallurgical, processing and dimensional analysis.

REFERENCES

[1] Rizzo, S., Pagliassotto, S.: Fatigue Performance Improvements of Wheel Bearing Rolling Elements, SAE Int. J. Passeng. Cars - Mech. Syst. 10(3), 797-804 (2017).
[2] Sadeghi, F., Jalalahmadi, B., Slack, T.S., Raje, N., Arakere, N.K.: A Review of Rolling Contact Fatigue, J. Tribol 131(4), 041403 (2009).
[3] Sri Siva, R., Arockia Jaswin, M., Mohan Lal, D.: Enhancing the wear resistance of 100Cr6 bearing steel using cryogenic treatment, Tribology transactions 55(3), 387-393 (2012).
[4] Efremenko, V.G., Shimizu, K., Noguchi, T., Efremenko, A.V., et al.: Impact-abrasive-corrosion-wear of Fe-based alloys: Influence of microstructure and chemical composition upon wear resistance, Wear 305(1–2), 155-165 (2013).
[5] Baldissera, P., Delprete, C.: Fatigue focused optimization of treatment parameters - A case study about Deep Cryogenic Treatment. In: Advances in Fracture and Damage Mechanics X, Tonković, Z., Aliabadi, M.H. Trans Tech Publications, Uetikon, 498-501 (2012).

A Novel Hot-Spot Stress Calculation for Tubular Welding Joints Used in Agricultural Sprayers

G. Fortese[a*], A. Carpinteri[a], I. Iturrioz[b], C. Ronchei[a]
D. Scorza[a], S. Vantadori[a], A. Zanichelli[a]

[a] *Department of Engineering & Architecture, University of Parma, Parco Area delle Scienze 181/A, 43124 Parma, Italy*
[b] *Mechanical Post- Graduate Program, Federal University of Rio Grande do Sul, Sarmento Leite 425, CEP 90050-170, Porto Alegre, Brazil*
**Corresponding author: giovanni.fortese@studenti.unipr.it*

Keywords: Critical plane-based criteria; Hot-spot approach; Initial crack growth direction; Random loadings; Welded joints.

ABSTRACT

The H-shaped structural components used in agricultural sprayers consist of tubular elements fillet-welded as T-joints. Such components are particularly prone to fatigue failures being subjected, under service condition, to forces that are random in nature. In such a context, the localisation of hot-spots represents an important step in multiaxial fatigue assessment of H-structural components. In the present paper, a novel approach aimed both to localise hot-spots in tubular welded joints and to estimate initial crack growth direction is employed. In particular, such an approach is based on the joint application of the hot-spot stress approach [1] and the time-domain multiaxial critical plane-based criterion by Carpinteri et. al for random loadings [2-4]. Experimental and numerical results are compared in terms of both hot-spots location and crack growth direction.

REFERENCES

[1] Hobbacher, A.: Recommendations for fatigue design of welded joints and components. International Institute of Welding IIW-1823-07 (ex XIII- 2151-07/XV-1254-07) (2008).
[2] Carpinteri, A., Spagnoli, A., Vantadori, S.: A multiaxial fatigue criterion for random loading. Fatigue and Fracture of Engineering Materials and Structures 26, 515-522 (2003).
[3] Carpinteri, A., Spagnoli, A., Vantadori, S., Bagni, C.: Structural integrity assessment of metallic components under multiaxial fatigue: the C–S criterion and its evolution. Fatigue and Fracture of Engineering Materials and Structures 36, 870-883 (2013).
[4] Carpinteri, A., Spagnoli, A., Vantadori, S.: A review of multiaxial fatigue criteria for random variable amplitude loads. Fatigue and Fracture of Engineering Materials and Structures 40, 1007-1036 (2017).

ACKNOWLEDGMENTS

The authors gratefully acknowledge the financial support of the Italian Ministry of Education, University and Research (MIUR) the National Council for Scientific and Technological Development (CNPq - Brazil) and the Coordination for the Improvement of Higher Education Personnel (CAPES – Brazil).

Voids as Fatigue Palliative in a Shrink-Fitted Shaft

D. Erena[a], C. Navarro[a*], J. Vázquez[a], J. Domínguez[a]

[a]*Departamento de Ingeniería Mecánica y Fabricación, Universidad de Sevilla, Spain*
**Corresponding author: cnp@us.es*

Keywords: Fretting; Voids; Palliative; Numerical model; Fitted shaft.

ABSTRACT

High stress concentrations and wear appear in a shrink-fitted shaft near the edge of the contact. Due to these stresses cracks rapidly initiate. This combination of events is known as fretting fatigue. Several solutions to increase fatigue life are usually found in practice, they include the introduction of compressive residual stresses (with shot peening for example), a slot in the shaft outside of the contact, an increase of the shaft´s diameter in the contact zone, etc. This paper makes a new suggestion based on an increasingly popular technique that allows the manufacturing of pieces of difficult shapes, and nearly impossible to make with other techniques: additive manufacturing. It has already been studied for another geometry showing that it is possible [1,2]. The idea is to introduce an internal void with a toroidal shape beneath the contact making it more flexible, thus, reducing the stresses near the stress concentration. Fig. 1 shows a cross section of this geometry.

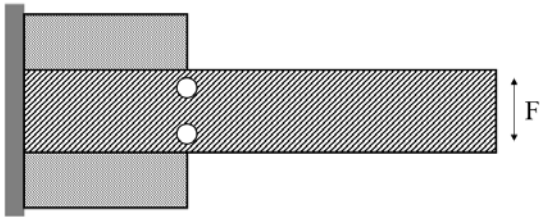

Fig. 1**.** Pressed fitted shaft with an internal void as a stress reliever.

The shrink-fitted shaft has been numerically simulated with FEM. This work analyses and compares the stress and strain fields and Smith-Watson-Topper multiaxial fatigue parameter in the areas sensitive to fretting with respect to a case with homogeneous material (no internal voids). Various configurations changing different parameters like size and position of the void, radial interference and friction coefficient have been considered.

REFERENCES

[1] Miller, G.R., Keer, L.M.: Interaction between a rigid indenter and a near-surface void or inclusion. J. Appl. Mech. 50, 615-620 (1983).
[2] Erena, D., Vázquez, J., Navarro, C., Domínguez, J.: Internal voids as a stress reliever and palliative in fretting fatigue. In: 7th International Conference on Fatigue Design, Fatigue Design 2017, 29-30 November 2017, Senlis, France (2017).

ACKNOWLEDGMENTS

This research was supported by the Ministerio de Economía y Competitividad through the project DPI2014-59160-P.

Fretting Fatigue and Crack Initiation Analysis of GH80A at High Temperature

Yu Zhai[a], Zhiyong Huang[a*], Qingyuan Wang[a]

[a] *School of Aeronautics and Astronautics, Sichuan University, Chengdu 610064, China*
**Corresponding author: huangzy@scu.edu.cn*

Keywords: Crystal plasticity; Nickel-based superalloy; Crack propagation; Fretting fatigue; High temperature.

ABSTRACT

Nickel-based superalloy has been widely used in aero-engines and gas turbines due to its superior mechanical properties. In order to investigate the high temperature fretting fatigue behaviour of GH80A in very high cycle fatigue and observe the crack path propagation clearly, the rectangular cross-section specimen are designed. The S-N curves of GH80A were obtained at 400ºC and 800ºC. By observing the fretting wear morphology of the specimen and the fracture surface, it was found that the crack always initiated at the border of the wear zone. It can be clearly observed from the side face of the specimen that the direction of the crack path always shows a certain initiation angle and points to the inside of the wear zone. Finally, for the sake of analysing the local stress distribution with fatigue and fretting load which affect the crack initiation, the pad-specimen contact model was established by FEM software ABAQUS combined with crystal plasticity. The contact stress/strain fields calculated by this approach, combined with either the Fatemi-Socie (FS) or Smith-Watson-Topper (SWT) multiaxial fatigue parameters, allow us to analysis the crack initiation process. The crack propagation simulation results are in good agreement with the experimental results.

Fatigue Crack Propagation

An Improved Prediction of the Effective Range of Stress Intensity Factor in the Presence of Plasticity-Induced Shielding in Fatigue Crack Growth

Bing Yang[a], M.N. James[b,c*], J.M. Vasco-Olmo[d], F.A. Díaz[d]

[a] *State Key Laboratory of Traction Power, Southwest Jiaotong University, Chengdu, China*
[b] *School of Engineering, University of Plymouth, Plymouth, England*
[c] *Department of Mechanical Engineering, Nelson Mandela Metropolitan University, Port Elizabeth, South Africa*
[d] *Departamento de Ingeniería Mecánica y Minera, University of Jaén, Jaén, Spain*
**Corresponding author:* mjames@plymouth.ac.uk

Keywords: CJP model; Plastic enclave; Plasticity-induced crack closure; Crack tip shielding; Fatigue crack growth rate prediction.

ABSTRACT

The CJP model is a meso-scale model of crack tip displacement and stress that was proposed a few years ago as an attempt to better capture the elastic forces induced by the plastic enclave that surrounds a growing fatigue crack and hence enable direct prediction of the effective range of crack driving force. The model was a development of earlier work that had achieved some success in measuring the wake contact pressure arising from the plastic enclave that surrounds a growing fatigue crack [1]. The theoretical model in Mode I loading was extended from a stress-based version that could be fitted to full-field photoelastic images of the crack tip region [2, 3], to one that utilised digital image correlation and could be applied directly to displacement fields on metallic specimens [4]. The next step in the development of the model involved extending it to deal with combined Mode I and Mode II loading which, in principle, would open up its use to include characterising surface roughness-induced shielding as well as plasticity-induced shielding [5].

Experimental verification of the concepts in the CJP model followed a little more slowly than the theoretical developments, reflecting factors such the complexity of phase-stepping photoelastic fatigue experiments, the development of software necessary to automate the CJP model solution from photoelastic and DIC images, and the training of new PhD students. Over the last several years, however, researchers from the University of Jaen in Spain, Gifu University in Japan and Southwest Jiaotong University in China have been making considerable progress in experimental verification of the model.

The objective of the work described in reference [2] was to identify the real influence or effect on the applied elastic field, of stresses arising from plastic deformation associated with crack growth. Reference [4] notes that the CJP model essentially treats the crack as a plastic inclusion in an elastic body. This approach leads to the definition of a stress intensity factor perpendicular to the crack plane, called K_F, which drives crack growth in an analogous fashion to K_I and is modified by the incorporation of shielding force components acting perpendicular to the crack. The shielding effect of the plastic enclave is also accounted for via a new retarding stress intensity factor K_R that accounts for shielding forces acting in the plane of the crack, and the model also defines an interfacial shear stress intensity factor, K_S, which is included to capture compatibility-induced shear components of shielding that would perhaps be more applicable to Mode II or III loading.

It is possible to explore the influence of these various stress intensity parameters on crack tip fields through a comparison between experimental crack tip field fringe patterns and those provided by the

model using a range of values for K_F, K_R, and K_S. As an example of this, reference [2] indicates that the introduction of interfacial shear stresses causes migration along the crack path of the join between the fringe loops on either side of the crack path. This is perhaps more pronounced in the crack wake, but both ahead and behind the crack, the shape of the join between the loops of common fringe order changes from a sharp 'V' to more of a 'U' shape. This phenomenon has been observed before in photoelastic images in the presence of crack closure but the discussion in reference [2] is probably the first time that it could be assigned, most probably, to the effect of interfacial shear stresses.

Sufficient experimental work has now been performed by various researchers across a range of stress ratio values, specimen geometries and materials to conclude that the original hypothesis by the proposers of the model, that the model could be used to evaluate the effective stress intensity factor in the presence of plasticity-induced shielding, is correct [e.g. 6, 7]. Nowell *et al.* [7] have recently published a paper in which he discusses the CJP model and presents a slightly simplified version of the force diagram given in reference 2. He goes on to show that his own experimentally-based analysis of DIC data provided by Vasco-Olmo [8] and demonstrates that the combined $K_F + K_R$ parameter is very similar to the measured effective value of ΔK found using their own experimental technique. Nowell *et al.* [7] express reservations regarding the split of ΔK into the K_F and K_R terms although they go on in their paper to show that the split into what they call "applied and residual terms" may be helpful, even for measurements taken very close to the crack tip. However, a major driver behind the development of the CJP model was to obtain a better physical understanding of the role of various possible forces in plasticity-induced shielding. The multi-parameter approach of the model is proving useful in such investigations and is shedding light on, for example, overloads and plasticity-induced shielding.

This paper will present work done at Plymouth and Jaen over the last two years that shown an improved rationalisation of fatigue crack growth date data across a range of stress ratio values and specimen geometries and also summarise current work aimed at directly predicting the effective range of stress intensity factor and fatigue crack growth rates using the CJP model and a calibration curve approach.

REFERENCES

[1] Pacey, M.N., Patterson, E.A., James, M.N.: A new photoelastic model for studying fatigue crack closure, Experimental Mechanics 45(1), 42-52 (2005).

[2] Christopher, C.J., James, M.N., Patterson, E.A., Tee, K.F.: Towards a new model of crack tip stress fields, International Journal of Fracture 148, 361-371 (2007).

[3] Christopher, C.J., James, M.N., Patterson, E.A., Tee, K.F.: A quantitative evaluation of fatigue crack shielding forces using photoelasticity, Engineering Fracture Mechanics 75, 4190-4199 (2008).

[4] James, M.N., Christopher, C.J., Yanwei Lu and Patterson, E.A.: Local Crack Plasticity and its Influences on the Global Elastic Stress Field, International Journal of Fatigue 46, 4-15 (2013).

[5] Christopher, C.J., Laboviciute, G., James, M.N., Patterson, E.A.: Extension of the CJP model to mixed Mode I and Mode II, Frattura ed Integrità Strutturale 7 25, 161-166 (2013).

[6] James, M.N., Christopher, C.J., Díaz Garrido, F.A., Vasco-Olmo, J.M., Toshifumi Kakiuchi, Patterson, E.A.: Interpretation of plasticity effects using the CJP crack tip field model, Solid State Phenomena 258, 117-124 (2017).

[7] Nowell1, D., Dragnevski, K.I., O'Connor, S.J.: Investigation of Fatigue Crack Models by Micro-scale Measurement of Crack Tip Deformation. International Journal of Fatigue, doi.org/10.1016/j.ijfatigue.2018.01.015 (2018).

[8] Vasco Olmo, J.M.: Experimental evaluation of plasticity induced crack shielding effect using full field optical techniques for stress and strain measurement. PhD thesis, University of Jaén (2014).

Crack Closure Behaviour in Notched Ductile Cast Iron Specimens

M. Cova[a*], S. Beretta[b], A. Pourheidar[b]

[a]*SACMI Imola S.C.,Italy*
[b]*Department of Mechanical Engineering, Politecnico di Milano, Italy*
**Corresponding author: matteo.cova@sacmi.it*

Keywords: R-curve; Ductile Cast Iron; Kitagawa; Crack closure.

ABSTRACT

This paper deals with a crack closure approach to explain an unexpected crack propagation behaviour of Ductile Cast Iron (DCI). Four series of notched specimens (Fig. 1) were tested under axial fatigue with the aim of deriving the material's Kitagawa-Takahashi diagram [1]. The notches had a half-penny shape and were machined by EDM. Non-propagating cracks longer than 1 mm were observed in run-out specimens (Fig. 2). The standard El-Haddad formulation [2] couldn't fit the experimental data. Consequently, crack-closure behaviour of the material was investigated. The concept of the R-curve [3] and the use of a modified Kitagawa-Takahashi diagram as proposed by Maierhofer *et al.* [4] were used in order to reproduce the experimental behaviour.

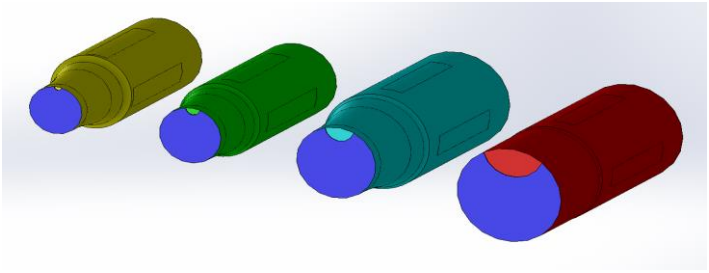

Fig. 1. Section view of the notched specimens.

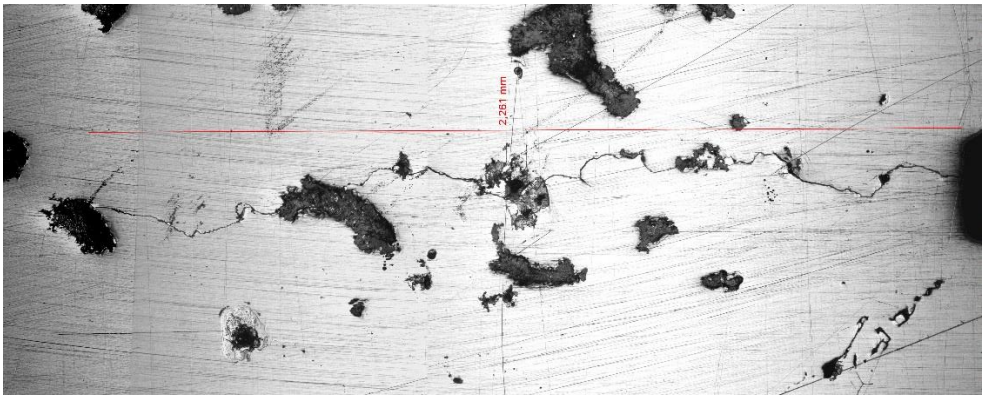

Fig. 2. Non propagating crack after 108 cycles, emanating from the border of the EDM notch (bottom).

REFERENCES

[1] Kitagawa, H., Takahashi, S.: Applicability of fracture mechanics to very small cracks or the cracks in the early stages. In: Proceedings of the Second International Conference on Mechanical Behavior of Materials. Metals Park, OH: American Society for Metals, 627–631 (1976).
[2] El Haddad, M.H., Topper, T.H., Smith, K.N: Prediction of non propagating cracks. Eng Fract Mech 11, 573–584 (1979).
[3] Maierhofer, J., Kolitsch, S., Pippan, R., Gänser, H.-P., Madia, M., Zerbst, U.: The cyclic R-curve – Determination, problems, limitations and application. Engineering Fracture Mechanics 198, 45-64 (2018).
[4] Maierhofer, J., Gänser, H.-P., Pippan, R.: Modified Kitagawa–Takahashi diagram accounting for finite notch depths. International Journal of Fatigue 70, 503-509 (2015).

ACKNOWLEDGMENTS

M. Nanni and M. Villa of SACMI are gratefully acknowledged for performing the fatigue tests and metallographic analysis. L. Patriarca of Politecnico di Milano is gratefully acknowledged for support in FCG testing.

Numerical Analysis of the Influence of Crack Growth Scheme on Plasticity Induced Crack Closure Results

D. Camas[a*], J. Garcia-Manrique[a], F.V. Antunes[b], A. Gonzalez-Herrera[a]

[a] *Department of Civil and Materials Engineering, University of Malaga, Spain*
[b] *Department of Mechanical Engineering, University of Coimbra, Portugal*
**Corresponding author: dcp@uma.es*

Keywords: Finite element analysis; Crack growth scheme; Fatigue crack closure; Node release.

ABSTRACT

Fatigue crack closure has been studied by means of finite element method for a long time. Most work has been performed considering bi-dimensional models. Lately, as in fracture analysis [1,2], the use of three-dimensional models has been extended [3–5]. Nevertheless, the methodology employed has been taken from that developed for bi-dimensional cases.

There is a great number of previous bi-dimensional studies which analyse different numerical parameters and optimise them [6–8]. The current computational capabilities allow a comprehensive study of the influence of the different modelling parameters in a similar way to those studies carried out with bi-dimensional models, with the advantage, that the evolution along the thickness of the analysed parameters can be taken into consideration.

In particular, one of the key issues is related to the crack growth scheme. A fatigue analysis implies a crack growth. Each change in loading conditions implies to solve a nonlinear problem. When running a finite element analysis, it is impossible to consider all the cycles involved in a real fatigue problem. The computational cost would be unacceptable.

Experimentally, an aluminium alloy 2024-T3, when loading conditions are K_{max}=25MPa·m$^{1/2}$ and R=0.1, the crack growth rate is in the order of 1μm/cycle [9]. Numerically, the usually accepted element size recommendation by McClung implies an element size in the order of 60μm. Even employing more restrictive models the element sizes are in the order of 16 or 8μm. Thus, numerical rates are in the order of this size per cycle, which are unrealistic when comparing with experimental ones.

Usually, the crack growth is carried out changing the boundary conditions. A node ahead of the crack is released at each loading cycle in order to obtain a strain fields as continuous as possible. In the literature, one or two load cycles between node releases are usually performed. However, in three-dimensional analyses usually only one load cycle is applied because of the numerical cost. Instead of applying one or two cycles it might seem more appropriate to apply more cycles between node releases. So, the scope of this work is to analyse the influence of the number of load cycles between node releases in the opening and closure results.

For this purpose, a CT aluminium specimen has been modelled three-dimensionally and several calculations have been made in order to evaluate the influence of the number of load cycles between node releases. The results are analysed in terms of crack closure and opening values. Eight different cases have been analysed for a 3mm specimen thickness. The load applied is which corresponds to a stress intensity factor K=25MPa·m$^{1/2}$, the plastic wake length previously developed is 0.4 times de Dugdale's plastic

zone size (r_{pD}), the allowed penetration is 5e-8m and the minimum element size is 90 times smaller than r_{pD} . Two different stress ratios are considered R=0.1 and 0.3. For each one four different number of load cycles between node releases are considered ranging from 1 to 8 cycles. The material behaviour shows a weak hardening and the stress-strain curve employed is the one which represent the cyclic behaviour of the material.

The study shows that the number of load cycles after releasing the last nodes has more influence on the results than the previous load cycles between node releases. The main conclusion is that it seems more appropriate to analyse the crack opening and closure in terms of stresses than in terms of displacements, because these results are more stable against the number of load cycles.

REFERENCES

[1] Camas, D., Garcia-Manrique, J., Gonzalez-Herrera, A.: Numerical study of the thickness transition in bi-dimensional specimen cracks. International Journal of Fatigue 33, 921–928 (2011).

[2] Camas, D., Lopez-Crespo, P., Gonzalez-Herrera, A., Moreno, B.: Numerical and experimental study of the plastic zone in cracked specimens. Engineering Fracture Mechanics 185, 20-32 (2017).

[3] Chermahini, R.G., Shivakumar, K.N., Newman Jr, J.C., Blom, A.F.: Three-Dimensional aspects of plasticity-induced fatigue crack closure. Engineering Fracture Mechanics 34, 393–401 (1989).

[4] Roychowdhury, S., Dodds Jr., R.H.: A numerical investigation of 3-D small-scale yielding fatigue crack growth. Engineering Fracture Mechanics 70, 2363–2383 (2003).

[5] Gonzalez-Herrera, A., Zapatero, J.: Tri-dimensional numerical modelling of plasticity induced fatigue crack closure. Engineering Fracture Mechanics 75, 4513–4528 (2008).

[6] McClung, R.C., Sehitoglu, H.: On the finite element analysis of fatigue crack closure-1. Basic modeling issues. Engineering Fracture Mechanics 33, 237–252 (1989).

[7] González-Herrera, A., Zapatero, J.: Influence of minimum element size to determine crack closure stress by the finite element method. Engineering Fracture Mechanics 72, 337–355 (2005).

[8] Antunes, F.V., Camas, D., Correia, L., Branco, R.: Finite element meshes for optimal modelling of plasticity induced crack closure. Engineering Fracture Mechanics 142, 184–200 (2015).

[9] McEvily, A.J., Matsunaga, H.: On fatigue striations. Tansaction B: Mechanical Engineering 17(1), 75-82 (2010).

ACKNOWLEDGMENTS

This work has been supported by the “Plan Propio de Investigación y Transferencia” from Universidad de Málaga and Ministerio de Economía y Competitividad of the Spanish Government through grant reference MAT2016-76951-C2-2-P.

Fatigue Crack Propagation Behaviour of Inconel 625 Manufactured by Laser Powder-Bed Fusion

JR. Poulin[a], V. Brailovski[a*], P. Terriault[a]

[a] *Department of Mechanical Engineering, Ecole de Technologie Superieure, Canada*
**Corresponding author: vladimir.brailovski@etsmtl.ca*

Keywords: Fatigue crack propagation; Laser powder bed fusion; Additive manufacturing; Superalloy.

ABSTRACT

Additive manufacturing (AM) technologies, such as the laser powder bed fusion (LPBF), have gained a significant attention due to their capacity for near net shape manufacture of complex components from various metals and alloys. The aerospace industry is showing a lot of interest in this technology, but given the necessity for flight certification, commissioning new components requires a thorough understanding of the LPBF processing-structure-properties relationship. While the static mechanical properties of LPBF components are found to be generally comparable to those of their wrought counterparts, fatigue resistance of LPBF components continues to raise questions [1]. The latter is of a special concern, since fatigue is responsible for 60% of the total failures of aerospace components [2].

Processing-induced defects, such as pores and inclusions [3], are regularly observed in LPBF-processed material, and since fatigue is governed by changes occurring on the micro and mesoscale levels, such defects have been proven to negatively affect the fatigue life of LPBF components [4]. Moreover, a strong material anisotropy, which is a particular feature of powder bed fusion process, can impact the crack propagation behavior [5]. It must be mentioned however that the literature on this topic mainly focuses on lightweight alloys and no information is available for Inconel 625 (IN625) which is commonly employed in the aerospace industry.

In order to support a damage tolerant approach in the design of fatigue-resistant IN625 LPBF components, compact crack growth specimens (ASTM E647) were manufactured with three build orientations (0, 45 and 90^{o}), subjected to stress relieve annealing (SR, 870^{o}C, 1h), and machined and polished prior to testing. Selected specimens were also subjected to hot isostatic pressing (HIP, 100 MPa and 1120^{o}C for 4h). The absence of pores and inclusions larger than 25 µm in size was confirmed by X-Ray computed tomography of selected machined specimens. The fatigue crack growth behavior was tested according to the ASTM E647 standard using the compliance method and validated with direct optical measurements. The crack-propagation behavior of a wrought Inconel 625 was also studied for comparison.

As compared to the wrought alloy, the LPBF-built IN625 specimens demonstrated an equivalent or higher resistance to crack propagation in the near threshold region (Figure 1a). The threshold stress intensity factor (SIF) for the wrought IN625 alloy was 7.2 MPa*m$^{1/2}$, while SR LPBF specimens showed anisotropic crack growth behavior, with threshold SIF ranging from 7.1 to 11.2 MPa*m$^{1/2}$ (Figure 1b). This difference is attributed to the strongly anisotropic material microstructure resulting from the powder bed processing [6]. In the higher Paris regime, the SR LPBF specimens also performed better than the wrought alloy, the Paris law exponent being 3.2 as compared to 3.5. After HIP, an identical for all the build orientations threshold value of ~11 MPa*m$^{1/2}$ was obtained, this value being close to the highest value obtained for the SR LPBF specimens (0^{o} orientation) (Figure 1c). This outcome is explained by the coarser grained isotropic microstructure resulting from the HIP treatment [3], which promotes the roughness-induced crack closure. After HIP, the crack growth rate in the Paris regime was independent of the build orientation and close to that of the wrought alloy, with the Paris law exponent m ranging from 3.6 to 3.7.

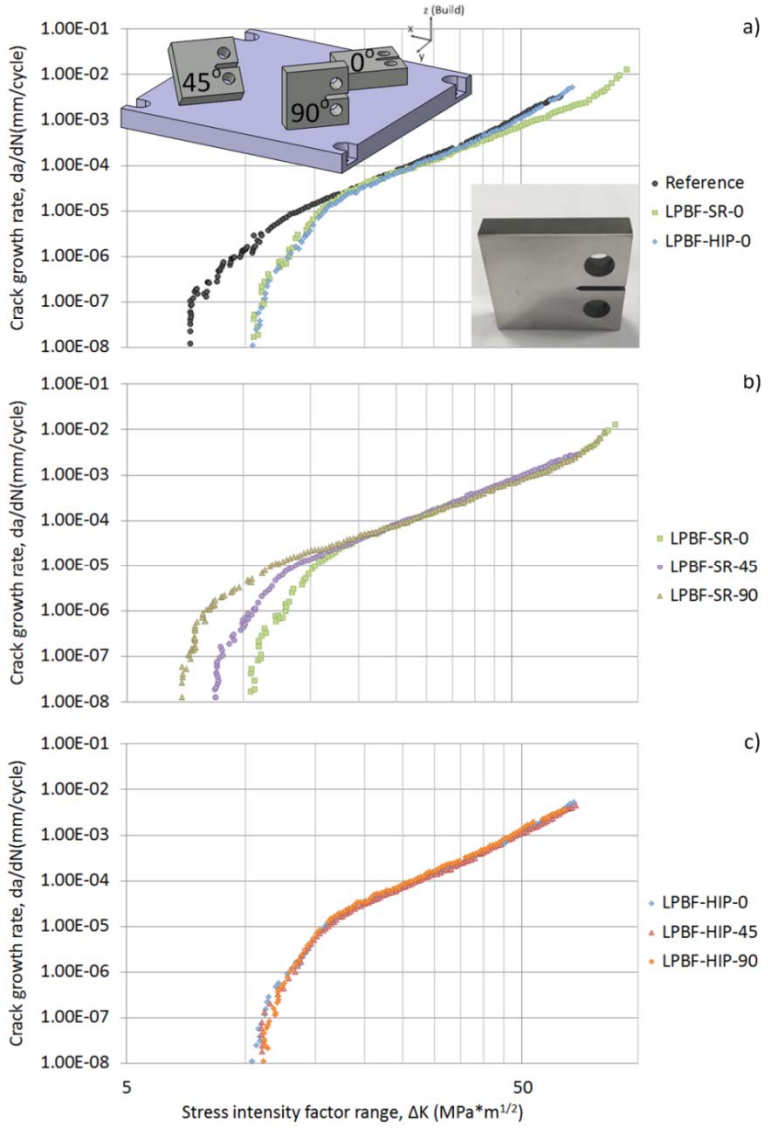

Fig. 1. Paris diagrams for IN625 alloy. Influence of the post-processing conditions: a) LPBF (SR and SR+HIP specimens) versus wrought alloy; Influence of the build orientation: b) SR and c) CR+HIP specimens.

REFERENCES

[1] Yadollahi, A., Shamsaei, N.: Additive manufacturing of fatigue resistant materials: Challenges and opportunities. International Journal of Fatigue 98, 14-31 (2017).
[2] Bhaumik, S.K., Sujata, M., Venkataswamy, M.A.: Fatigue failure of aircraft components. Engineering Failure Analysis 15(6), 675-694 (2008).
[3] Seifi, M., et al.: Defect distribution and microstructure heterogeneity effects on fracture resistance and fatigue behavior of EBM Ti–6Al–4V. International Journal of Fatigue 94, 263-287 (2017).
[4] Akita, M., et al.: Defect-dominated fatigue behavior in type 630 stainless steel fabricated by selective laser melting. Materials Science and Engineering A 666, 19-26 (2016).
[5] Reschetnik, W., et al.: Fatigue crack growth behavior and mechanical properties of additively processed EN AW-7075 aluminium alloy. Procedia Structural Integrity 2, 3040-3048 (2016).
[6] Kreitcberg, A., Brailovski, V., Turenne, S.: Effect of heat treatment and hot isostatic pressing on the microstructure and mechanical properties of Inconel 625 alloy processed by laser powder bed fusion. Materials Science and Engineering A 689, 1-10 (2017).

Analysis of Fatigue Crack Growth Based on Plastic CTOD

F.V. Antunes[a*], R. Branco[a], P. Prates[a]

[a] *CEEMPRE, Depart. of Mechanical Engineering, University of Coimbra, 3030-788, Portugal*
**Corresponding author: fernando.ventura@dem.uc.pt*

Keywords: Fatigue crack growth; Crack tip opening displacement (CTOD); Plastic CTOD.

ABSTRACT

The analysis of fatigue crack propagation is usually conducted by relating the crack advance per unit cycle, da/dN, to the stress intensity factor range, ΔK. Nevertheless, da/dN-ΔK relations have several limitations, namely: (i) such curves are completely phenomenological, not derived from physics, and the fitting parameters have units with no physical justification; (ii) such curves are only valid in the small-scale yielding range; (iii) and da/dN depends on other parameters, including the stress ratio and the load history. In order to overcome the difficulties related to the application of K to the analysis of fatigue crack growth, several concepts have been proposed, namely crack closure, partial crack closure, T-stress or the CJP model. However, these complementary concepts only mitigate the problem, without attacking its real source.

In authors' opinion, the linear elastic ΔK parameter must be replaced by non-linear crack tip parameters, because fatigue crack growth is effectively linked to non-linear processes happening at the crack tip. The parameter proposed to quantify crack tip deformation is the plastic CTOD. Fig. 1 shows typical results of CTOD versus load, measured at a short distance behind crack tip. The plastic CTOD is obtained extracting the elastic deformation. The finite element method was used to obtain these predictions. The modelling of the elastic-plastic behaviour of the material is of major importance. Stress-strain results obtained in smooth specimens cyclically loaded are used to fit the hardening models. da/dN is obtained experimentally using standard specimens. Consequently, fatigue crack growth is studied using da/dN versus $\Delta CTOD_p$ relations. Fig. 2 shows da/dN-$\Delta CTOD_p$ models for different materials. The relation between the numerical ΔCTODp and the experimental da/dN can be used to predict fatigue crack growth rates in other conditions, namely for other loading parameters and for other geometries. Fig. 3 shows predictions of the effect of stress ratio for the 304L stainless steel under plane strain conditions. Note that the plastic CTOD range includes, in a natural way, crack closure and fatigue threshold.

ACKNOWLEDGMENTS

This research was sponsored by FEDER funds through the program COMPETE (under project T449508144-00019113) and by national funds through FCT – Fundação para a Ciência e a Tecnologia, under the project PTDC/EMS-PRO/1356/2014. One of the authors, P.A. Prates, was supported by a grant for scientific research from the Portuguese Foundation for Science and Technology (SFRH/BPD/101465/2014). All supports are gratefully acknowledged. The authors would also like to thank the DD3IMP in-house code developer team for providing the code and all the support services.

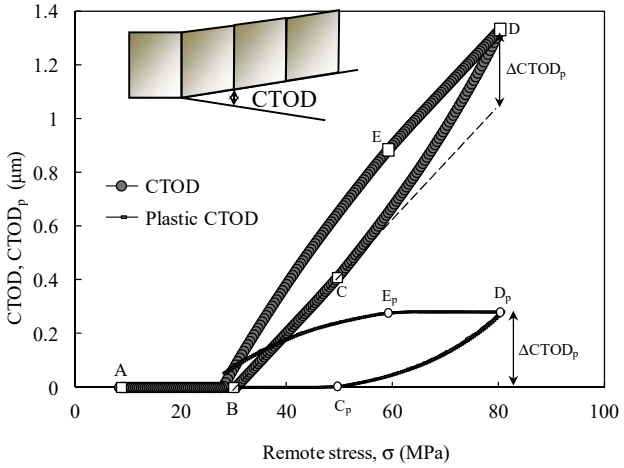

Fig. 1. Effect of load on CTOD (2050-T8 aluminum alloy).

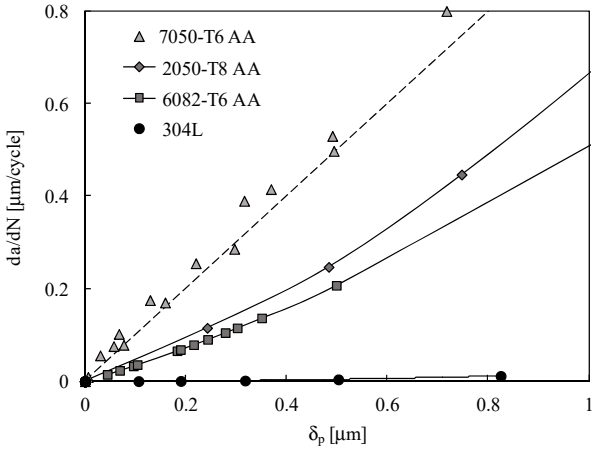

Fig. 2. da/dN versus plastic CTOD range (δ_p) for different alloys.

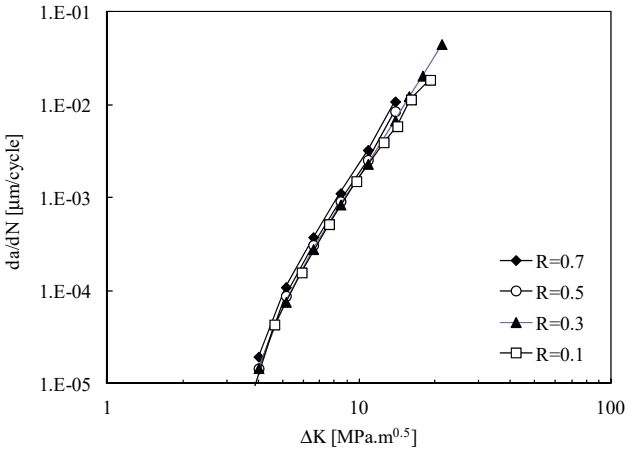

Fig. 3. Prediction of the effect of stress ratio for the 304L stainless steel using the da/dN-δ_p model.

Review of Current Progress in 3D Linear Elastic Fracture Mechanics

A. Kotousov[a*], A. Khanna[a], R. Branco[b], A. De Jesus[c], J. A. Correia[c]

[a]School of Mechanical Engineering, *The University of Adelaide, Australia*
[b]*CEMMPRE, Department of Mechanical Engineering, University of Coimbra, Portugal*
[c]*INEGI, Faculty of Engineering, University of Porto, Portugal*
**Corresponding author: Andrei.kotousov@adelaide.edu.au*

Keywords: LEFM; FE; 3D stress singularities; plates.

ABSTRACT

The aim of this contribution is to provide a brief review of the latest developments in the area of 3D Linear-Elastic Fracture Mechanics. The primary focus of this contribution is on the situations where the classical results, which are normally obtained within the framework of plane theory of elasticity, lead to peculiar results. These situations include analysis of stress and displacement fields near vertex points, generation of the coupled fracture mode under shear loading, application of Williams series expansion to 3D problems as well as fracture scaling.

REFERENCES

[1] Kotousov, A.: Effect of plate thickness on stress state at sharp notches and the strength paradox of thick plates. Int. J. Solids and Structures 47(14–15), 1916–1923 (2010).
[2] He, Z., Kotousov, A., Berto, F.: Effect of vertex singularities on stress intensities near plate free surfaces. Fatigue and Fracture of Eng. Materials and Structures, 38(7), 860–869 (2015).
[3] He, Z., Kotousov, A: On evaluation of stress intensity factor from in-plane and transverse surface displacements. Experimental Mechanics, 56(8), 1385–1393 (2016).
[4] Pook, L.P.: A 50-year retrospective review of three-dimensional effects at cracks and sharp notches, Fatigue and Fracture of Eng. Materials and Structures 36(8), 699–723 (2013).
[5] Kotousov, A., Lazzarin, P., Berto, F., Pook, L.P.: Three-dimensional stress states at crack tip induced by shear and anti-plane loading. Eng. Fracture Mech.108, 65–74 (2013).
[6] He, Z., Kotousov, A., Berto, F., Branco, R.: A brief review of three-dimensional effects near crack front. Physical Mesomechanics 19, 6–20 (2016).
[7] Kotousov, A., Bun, S., Khanna, A.: A new analytical method for the evaluation of transverse displacements and stresses in plane problems of elasticity. Int. J Solids Struct. 118, 89–96 (2017).

Very High Cycle Fatigue

Fatigue Testing at 1000Hz Testing Frequency

M. Berchtold[a]*, I. Klopfer[a]

[a]*RUMUL Russenberger Prüfmaschinen AG Switzerland*
**Corresponding author: mberchtold@rumul.ch*

Keywords: New Resonant Fatigue Testing Machine; Giga cycle fatigue (VHCF); Frequency effects.

ABSTRACT

In 2014 RUMUL could present a new resonant fatigue testing machine, with a testing frequency of 1000Hz. The dynamic load of maximum 50kN peak-peak is produced with an electromagnetic system. Similar to established resonant systems which run on testing frequencies from about 40 up to 250Hz. The static portion of the load is provided by a mechanical spindle, the maximum load of the system is +/- 50kN. Any load ratio can be selected. Flat and round specimen types that are normally used in fatigue testing can be used. The new testing machine offers new possibilities for investigations of material properties in the very high cycle fatigue (VHCF) regime. Compared to other systems used in the field of VHCF testing the RUMUL GIGAFORTE provides several advantages. The size of the machine is smaller and energy consumption less compared to a servo hydraulic system. The actually tested material volume is larger than the material volume that is tested on ultrasonic systems. The testing frequency of 1000Hz allows normally continuous testing, without stopping for cooling down the specimen.

In the past three years the new testing machine was intensively used for example at the laboratory of the Fraunhofer institute IWD Dresden in Germany. Effects of the 1000Hz testing frequency on the fatigue behaviour of the material were observed. This talk shows some example of heating up of the specimen related to the 1000Hz testing frequency and highlights some of the found frequency related effects on fatigue strength.

Fig. 1. 1000Hz Fatigue Testing Machine RUMUL GIGAFORTE with sound enclosure.

A Statistical Definition of Risk-Volume in Components Subject to VHCF

D.S. Paolino[a*], A. Tridello[a], G. Chiandussi[a], M. Rossetto[a]

[a] *Department of Mechanical and Aerospace Engineering, Politecnico di Torino, 10129 Turin, Italy.*
**Corresponding author: davide.paolino@polito.it*

Keywords: Very High Cycle Fatigue (VHCF); Stress Intensity Factor (SIF); Largest defect size.

ABSTRACT

The Very-High-Cycle Fatigue (VHCF) of metallic materials is a quite recent and attractive research field investigating the unexpected fatigue failure of structural metallic parts at number of cycles larger than 10^8 cycles and for stress amplitudes below the conventional fatigue limit.

Experimental results [1] show that the VHCF failure generally originates from internal defects, whose size plays a major role in the VHCF response of metallic materials: the larger the defect size in the stressed volume, the smaller the VHCF life and strength. The size of the stressed volume plays a key role, too: as stated by the statistics of extremes [2,3], the average defect size increases with the size of the stressed volume and, consequently, the VHCF response is significantly affected by the amount of stressed volume. This is generally known as size-effect in VHCF.

In the VHCF literature [2, 4-5], the assessment of size-effect is commonly based on the size of the so-called risk-volume, i.e. the volume of material subject to a stress amplitude larger than the 90% of maximum stress amplitude. The risk-volume is the volume of stressed material in which VHCF failures occur. The assumed 90% threshold is based on the experimental evidence that VHCF failures in material volumes subject to stress amplitudes below this threshold are very rare, even not possible. However, this assumption does not permit to account for the effect of the stress gradient within the risk-volume and may finally lead to large approximations in the evaluation of size-effects.

The present paper proposes an innovative statistical definition of the risk-volume in parts subject to VHCF. The definition is based on the statistical distribution of the critical Stress Intensity Factor (SIF), which is defined as the largest SIF in the entire material volume. The proposed definition can take into account the stress gradient within the entire material volume and its generalness permits to consider the effect of volume size as well as the effect of loading type (bending or tension-compression with different stress ratios).

In order to show the applicability and the effectiveness of the proposed approach, the statistical definition of the risk-volume is applied to two different experimental datasets. The two datasets are obtained by VHCF testing of high-strength steel specimens with two different shapes (details are given in [6]): Gaussian and hourglass specimens with conventional risk-volume (90% definition) of 2330 mm^3 and 194 mm^3, respectively.

Fig. 1 depicts results obtained on the two investigated specimen shapes. Fig. 1a plots the cumulative distribution functions of the risk-volumes computed according to the proposed statistical definition. Fig. 1b shows a good agreement between the experimental and the predicted cumulative distribution functions

of the ratio between σ_{crit}, the local stress at failure location, and σ_{max}, the maximum applied stress in the specimen.

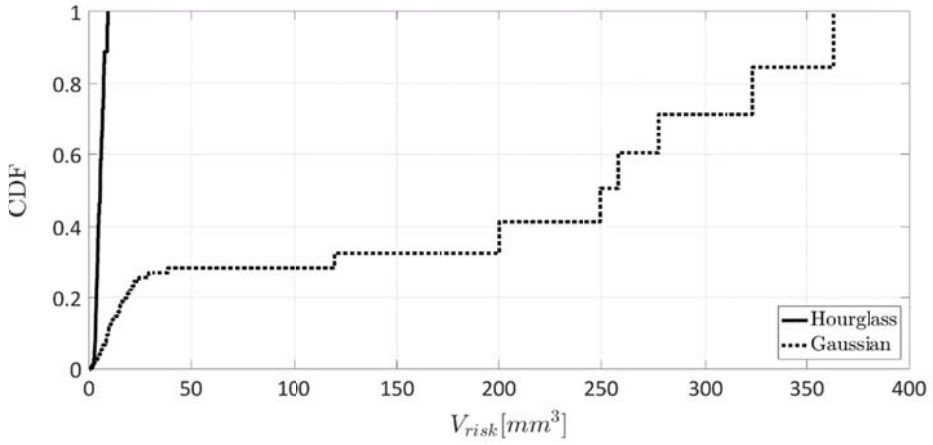

(a)

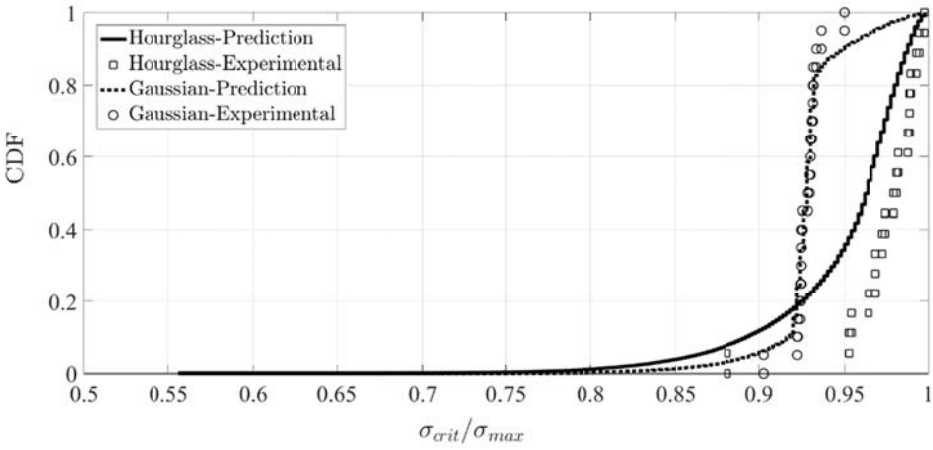

(b)

Fig. 1. Cumulative distribution functions of relevant quantities in Gaussian and hourglass specimens: a) risk-volume; b) ratio between local stress at failure location and maximum stress.

REFERENCES

[1] Bathias, C., Paris, P.C.: Gigacycle Fatigue in Mechanical Practice. 1st ed. CRC Dekker, New York, USA (2004).

[2] Murakami, Y.: Metal Fatigue: Effects Of Small Defects And Nonmetallic Inclusions. 1st ed. Elsevier Ltd, Oxford, UK (2002).

[3] Beretta, S., Anderson, C., Murakami, Y.: Extreme value models for the assessment of steels containing multiple types of inclusion. Acta Mater. 54, 2277-2289 (2006).

[4] Furuya, Y.: Notable size effects on very high cycle fatigue properties of high strength steel. Mater Sci Eng A 528, 5234-5240 (2011).

[5] Paolino, D.S., Tridello, A., Chiandussi, G., Rossetto, M.: On specimen design for size effect evaluation in ultrasonic gigacycle fatigue testing. Fatigue Fract. Engng. Mater. Struct. 37, 570–579 (2014).

[6] Tridello, A., Paolino, D.S., Chiandussi, G., Rossetto, M.: VHCF Response of AISI H13 Steel: assessment of Size Effects through Gaussian Specimens. Procedia Eng. 109, 121-127 (2015).

The Effect of Different Microstructures by Heat Treatment on the VHCF Properties of Low Carbon Steels

A. Giertler[a*], K. Koschella[a], U. Krupp[a]

[a] *Institute of Materials Design and Structural Integrity, University of Applied Sciences Osnabrück, 49009 Osnabrück, Germany*
**Corresponding author: a.giertler@hs-osnabrueck.de*

Keywords: VHCF; Internal crack initiation; Low carbon steel; thermography.

1. Introduction

For mechanically stressed components in mechanical engineering, preferably low-alloyed carbon steels are used. In order to ensure the reliability of the components, the knowledge of the fatigue mechanisms occurring during cyclic loading is of great importance to maintain structural integrity. In this present work, the fatigue properties of a low-alloyed carbon steel 50CrMo4 (Fe-0.5wt%C-1wt%Cr) are examined in the HCF and VHCF regime taking into account different tempering temperatures. For this purpose, two sets of samples were hardened under the same conditions, but annealed at different tempering temperatures, so that one set of samples exhibits a hardness of 37HRC and the other set of 57HRC. The chemical composition of the material, the heat treatment parameters and the mechanical properties are given in Table 1.

Table 1. Chemical composition (wt. %), heat treatment parameters and mechanical properties for the steel 50CrMo4.

Material	C	Cr	Mo	Mn	P	S	Fe	σ_{YS}	σ_{UTS}	HRC
50CrMo4	0.48	1.00	0.18	0.71	0.013	0.010	bal.	MPa	MPa	
37HRC	austenitizing: 850°C (0.5h) oil quench; temper heat treatment: 550°C (1.5h) air-cool							992	1095	37
57HRC	austenitizing: 850°C (0.5h) oil quench; temper heat treatment: 200°C (1.5h) air-cool							1561	2128	57

The martensitic microstructure of the material has been investigated metallographically with respect to microstructural parameters such as martensitic block size, packet size and of the prior austenite grain size. Subsequently, specimens for fatigue tests at laboratory air atmosphere under fully reversed loading (R=-1) in an ultrasonic testing machine (f=20,000Hz) and a resonance testing machine (f=95Hz) were machined from the heat-treated bars. The implementation of a high-resolution digital microscope in the testing machines allows the detection of microstructurally short fatigue cracks and the tracking of their propagation. The use of high resolution thermography during the fatigue tests allows the early detection of local plastic deformation within the martensitic microstructure on the surface of the specimens.

2. Results

Fig. 1 shows the fatigue life S-N diagrams for the two strength levels of 37HRC and 57HRC, respectively. Figure 1a shows the results from the fatigue tests for the hardness of 37HRC. Here only fatigue failures from the surface for all fractured specimens were observed. Since, no fractures above 10^7 cycles were occurring, the assumption of a fatigue limit at 10^6 cycles yields to a respecting fatigue strength of σ_{FL}=490MPa for the test frequency of 95Hz and a fatigue strength of σ_{FL}=680MPa for the test frequency of 20,000Hz. The fatigue strength of σ_{FL}=490MPa has also been confirmed by thermographic measurements using a high-resolution thermos camera in load increase tests at a test frequency of 95Hz. In contrast to the classical fatigue tests, the observation of the specimen surface with the aid of high-resolution thermography showed a yield limit at a stress amplitude of σ_a=396MPa, which is far below the

technical fatigue strength of σ_a=396MPa. This means that even far below the fatigue strength some fatigue damage has to be taken into account, but is obviously blocked by local microstructural features.

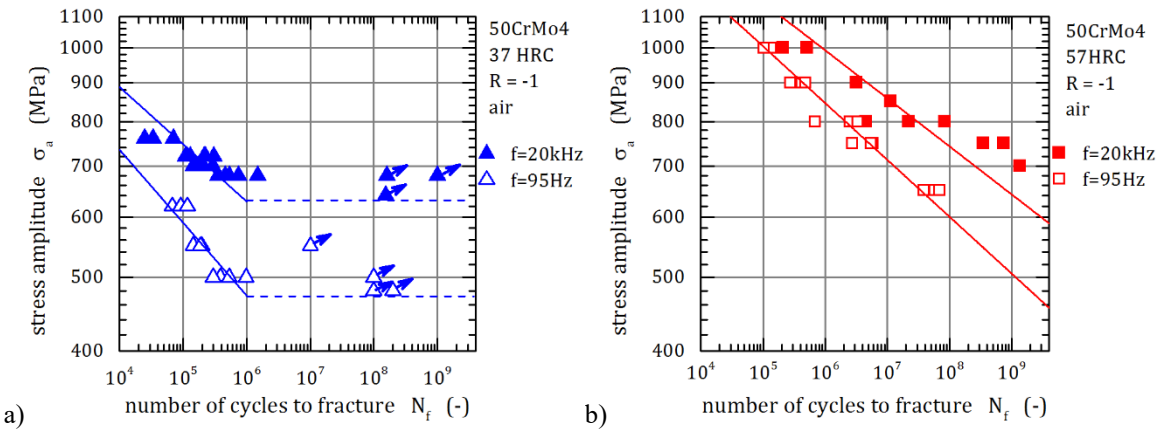

Fig. 1. Wöhler S-N Diagram showing the fatigue life for the steel 50CrMo4 at two testing frequencies of *f*=95Hz and *f*= 20kHz for a) the 37HRC hardness condition and b) for the 57HRC hardness condition.

The pronounced difference in the fatigue strength of Δσ=200MPa for the two test frequencies of 95Hz and 20,000Hz is due to the influence of the strain rate under cyclic loading on the flow stress. According to an analysis by Seeger [1], the supplement thermal stress component σ* (thermally activated Peierls stress) of the flow stress must be applied purely mechanically below a transition temperature T_0 or above a transition rate $\dot{\varepsilon}_T$. Fig. 1b) shows the S-N data for the 57HRC hardness condition. Due to the lower tempering temperature and the resulting higher hardness as well as higher strength of the material, the fatigue life shifts as expected to higher values of the stress amplitude σ_a. The increase in hardness has led to a change in the failure mechanism from pure surface failure to internal crack initiation at nonmetallic inclusions, cf. [2]. The data points shown in Fig. 1b correspond only to internal crack initiation on non-metallic inclusions of the type Al_2O_3. The results for the test frequency of *f*=20,000Hz show a shift to higher values for the fatigue life, which can be attributed to a size effect by changing the specimen geometry.

3. Conclusions

The results from fatigue experiments on the low-alloyed steel 50CrMo4 with respect to the comparison between two hardness conditions, 37HRC and 57HRC, are in agreement with the general relationship where an increasing static strength/hardness correlates with an increase in fatigue strength. In addition, a change in the fracture behavior was determined depending on the material strength. While for the hardness of 37HRC, only surface crack initiation was observed, the crack initiation for the higher hardness of 57HRC took place exclusively in the interior of the specimens at nonmetallic inclusions. A pronounced influence of the testing frequency was found for the test series with 37HRC specimens only. Moreover, it was shown with the aid of high-resolution thermography, which even below the fatigue strength local plastic deformation occurs.

REFERENCES

[1] Seeger, A.: The temperature dependence of the critical shear stress and of work-hardening of metal crystals. The London, Edinburgh, and Dublin Philosophical Magazine and Journal of Science: Series 7, 45:366, 771-773 (1954).

[2] Krupp, U., Giertler, A., Koschella, K.: Microscopic damage evolution during very-high-cycle fatigue (VHCF) of tempered martensitic steel. Fatigue Fract. Eng. Mater. Struct. 40, 1731–1740 (2017).

ACKNOWLEDGMENTS

The German Ministry of Education and Research (BMBF) and the Robert BOSCH GmbH is gratefully acknowledged for financial support of this work.

Effect of Ultrasonic Deep Rolling on High-Frequency and Ultrasonic Fatigue Behavior of TC4

Yi-Xin Liu[a], Yun-Fei Jia[a], Xian-Cheng Zhang[a]*, H. Li[a], Run-Zi Wang[a], Shan-Tung Tu[a]

[a] *Key Laboratory of Pressure Systems and Safety, Ministry of Education, School of Mechanical and Power Engineering, East China University of Science and Technology, Shanghai 200237, P.R. China*
**Corresponding author: xczhang@ecust.edu.cn*

Keywords: Ultrasonic deep rolling; Surface enhancement; High-frequency fatigue; Ultrasonic fatigue.

ABSTRACT

Ultrasonic deep rolling (UDR) is a surface modification method for improving fatigue life by introducing residual compressive stress and refining surface grains. The process controllability of the surface strengthening layer can be achieved by adjusting the frequency, amplitude and applied static pressure of the ultrasonic vibration that is, controlling the magnitude of the residual stress, the degree of work hardening and the depth of the strengthening layer[1]. Compared with traditional deep rolling process, ultrasonic deep rolling could induce deeper residual compressive stress layer and refine the surface grain to nano-scale. For this treatment, grain sizes on the surface layer could be refined to nano-scale and gradually increase with the depth to micro-scale. The surface nano-grains inhibit cracks initiation and interior coarse grains prevent cracks propagation, thus improving fatigue properties.

As well known, the fatigue properties of metallic material with gradient nanostructure have been extensively researched such as fatigue strength in both high cycle fatigue and low cycle fatigue were improved in gradient nanostructured 316L samples compared with coarse-grained samples[2]. The fatigue properties of gradient nanostructured Cu samples was almost 40% higher than that of the CG sample in high cycle fatigue[3].Surface nanocrystallization hardening (SNH) technology was used to treat nickel-based C-2000 superalloys with different process parameters, and the fatigue properties of the C-2000 superalloys were improved in high cycle fatigue[4]. The fatigue properties of surface gradient nanostructured carbon steel S45C, obtained by ultrasonic nano-surface modification (similar to ultrasonic rolling), were greatly improved by optimizing the surface treatment time. [5]

However, previous works mostly concentrated on the fatigue properties of gradient nanostructured samples in low cycle fatigue or high cycle fatigue, only a few studies investigated the properties under the condition of high-frequency or ultrasonic fatigue. Detailed investigations on fatigue behaviours and mechanical properties during high-frequency and ultrasonic cyclic loading are expected for the gradient nanostructured materials. In this work, the surface of TC4 was strengthened by ultrasonic rolling technology and its surface microstructure and high frequency-ultrasonic fatigue properties were systematically tested and analysed. The conclusions of this study are as follows:

1、Fig.1 summarizes the S-N curves of the TC4 original specimen and the ultrasonic-rolled specimen through the high-frequency fatigue test (100 Hz) and the ultrasonic fatigue test (20 kHz). One can note that under the same loading stress amplitude, the fatigue life of TC4 sample after ultrasonic fatigue test is higher than that of high-frequency fatigue test, which indicates the fatigue performance of TC4 titanium alloy is "frequency effect". Throughout the high-frequency and ultra-high frequency fatigue

tests, TC4 original samples unexpectedly have higher fatigue life than ultrasonic rolled samples. Generally speaking, the grain refinement of metallic materials has been proven to be a viable method to increase the fatigue strength, but most of the fatigue tests of the gradient nanostructured materials have been carried out using low frequency cyclic loading. However, in our study, this phenomenon of increasing fatigue life disappeared, which implies the effect of some harmful damages exceeds that of the grain refinement.

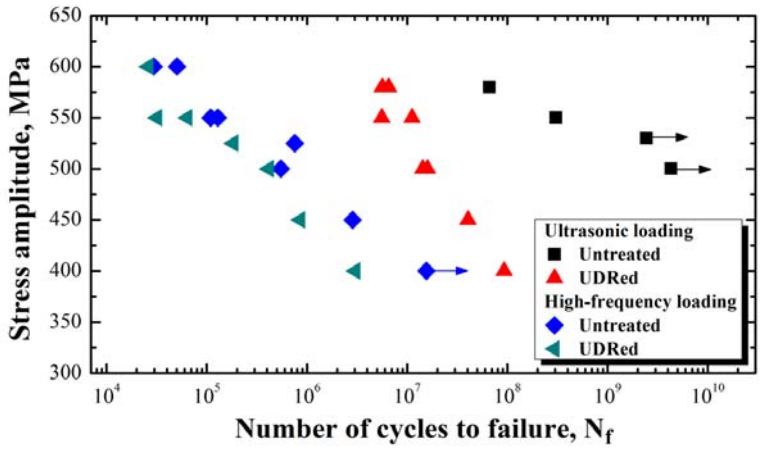

Fig. 1. S-N curves of UDRed and untreated TC4.

2、After vacuum heat treatment, the surface layer TC4 ultrasonic-rolled sample formed a more uniform gradient structure. The fatigue life of the sample after 200℃ and 300℃ treatment slightly increased compared with that of without heat treatment, but when the temperature increased to 400℃ and above, the fatigue life of the sample was greatly reduced.

3、Under the same stress amplitude, compared with ultrasonic fatigue loading, the residual compressive stress on the specimen surface is released faster in the high-frequency fatigue loading process, and the residual compressive stress is lower.

REFERENCES

[1] Ting, W., Dongpo, W., Gang, L., Baoming, G., Ningxia, S.: Investigations on the nanocrystallization of 40Cr using ultrasonic surface rolling processing. Applied Surface Science 255(5), 1824-1829 (2008).
[2] Roland, T., Retraint, D., Lu, K., Lu, J.: Fatigue life improvement through surface nanostructuring of stainless steel by means of surface mechanical attrition treatment. Scripta Mater. 54, 1949-1954 (2006).
[3] Yang, L., Tao, N.R., Lu, K., Lu, L.: Enhanced fatigue resistance of Cu with a gradient nanograined surface layer. Scripta Material 68, 801-804 (2013).
[4] Tian, J.W., Villegas, J.C., Yuan, W., Fielden, D., Shaw, L., Liaw, P.K., Klarstrom, D.L.: A study of the effect of nanostructured surface layers on the fatigue behaviors of a C-2000 superalloy. Materials Science and Engineering: A 468, 164-170 (2007).
[5] Cao, X. J., Pyoun, Y.S., Murakami, R.: Fatigue properties of a S45C steel subjected to ultrasonic nanocrystal surface modification. Applied Surface Science 256(21), 6297-6303 (2010).

ACKNOWLEDGMENTS

The authors would like to acknowledge gratefully for the financial support through National Natural Science Foundations of China (51371082, 51322510) and 111 project. The author X.C. Zhang is also grateful for the support by Shanghai Pujiang Program, Young Scholar of the Yangtze River Scholars Program, and Shanghai Technology Innovation Program of SHEITC (CXY-2015-001).

High Cycle Fatigue of Superelastic NiTi Wires

E. Alarcon[a*], L. Heller[a], P. Sittner[a], S. Arbab Shirani[b], L. Saint-Sulpice[b]

[a] *Department of Functional Materials, Institute of Physics of the Czech Academy of Sciences, Czech Republic*
[b] *Ecole Nationale d'Ingénieurs de Brest, France*
**Corresponding author: alarcon@fzu.cz*

Keywords: NiTi; High Cycle Fatigue; R-phase; Martensitic transformations; Self-heating.

ABSTRACT

In this research work, we address the high cycle fatigue (HCF) behaviour of superelastic NiTi wires. NiTi is an intermetallic alloy capable of reversing deformations up to 10%, thus, outperforming the elastic strain range of metals, which is far below 1%. This particular behaviour results from reversible solid-sate crystallographic phase transformations, which can be activated via stress changes –giving rise to the superelastic property, or by temperature changes –allowing the so-called shape memory effect (see [1] for a detailed description of NiTi thermomechanical behaviour). NiTi is particularly used in biomedical applications. The superelastic property of NiTi-based biomedical devices, such as stents and endodontic files, allows for better functional performances than their stainless-steel counterparts (NiTi devices provide better vessel expansion in the case of stents and more flexibility for teeth root canalisation in the case of endodontic files). However, further development of this technology is hindered by difficulties in the characterization of the cyclic response and lifetimes of NiTi. We consider that one of the main difficulties during NiTi fatigue testing is related to the heterogeneous strain distribution that occurs when the stress-induced phase transformation is activated [2]. As a result, the strain values plotted in Strain-N diagrams reported in the literature might be up to ten times lower than the actual strain leading to crack initiation! To face up this difficulty, we propose in this study to use NiTi hourglass-shaped cylindrical samples for tensile fatigue testing (see Fig.1a). This sample's geometry, although standardized for tensile fatigue testing of metals, has been omitted in NiTi fatigue studies due to difficulties related to samples' size and machining. The cross-section reduction of our samples allows for a more accurate identification of the stress threshold needed for phase transformations, homogenizes the fatigue and deformation mechanisms in the middle of the sample and, helps to prevent the localization of the fatigue failure within the testing machine clamps. We tested NiTi hourglass-shaped samples under to pull-pull fatigue loading ($R = \sigma_{min}/\sigma_{max} = 0.1$) at three different temperatures (40°C, 60°C, and 80°C). As observed in the tensile responses illustrated in Fig.1b, the effect of the temperature on the tensile behaviour of NiTi is twofold. First, by increasing the temperature, the stress threshold for the phase transformation moves up (see the shift of the stress local maximum in Fig.1b). Secondly, at stresses below the martensitic transformation threshold, the tensile response of the sample results more compliant at lower temperatures (see the segments of the tensile curves plotted in continuous lines in Fig.1b). Through x-ray diffraction experiments, we recognized that the continuous drop of stiffness upon increasing the stress is related to an intermediate phase transformation, which is referred in the literature as R-phase transformation. Note that the R-phase transformation is well-pronounced at 32.5°C and 40°C, and almost suppressed at 60°C and 80°C, cases in which the material shows an almost linear response. By evaluating the fatigue behaviour of NiTi samples at different temperatures, we determined the effects of the R-phase transformation in the lifetime of NiTi wires in a tensile stress range bellow the martensitic transformation threshold (High Cycle Fatigue regime). We present the results of the fatigue tests in the form of S-N curves in Fig.2a and in the form of Strain-N curves in Fig.2b. From these curves, we concluded that R-phase transformation plays a detrimental role in the high cycle fatigue behaviour of NiTi. We found that not only the endurance

limit (σ_e) of NiTi exhibiting R-phase transformation is lower than NiTi without R-phase transformation, but also that the stress relief allowed by the R-phase transformation mechanism does not engender any improvement of the lifetime of NiTi in terms of applied strain.

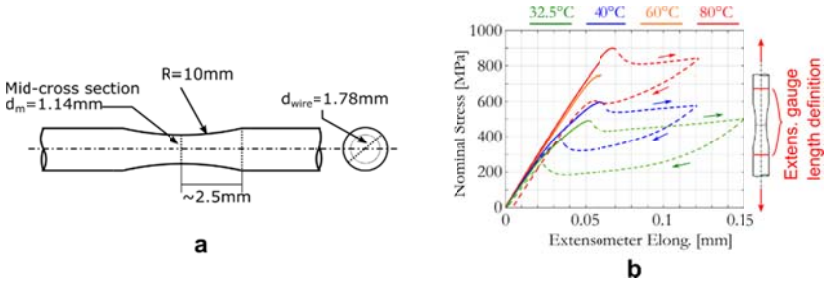

Fig. 1. NiTi Hourglass-shaped samples: a) geometry of the samples; b) loading-unloading tensile response of NiTi hourglass-shaped samples at different temperatures. These tensile responses are plotted in terms of the elongation of a 10mm gauge-length clip-on extensometer attached as shown in the scheme in (b).

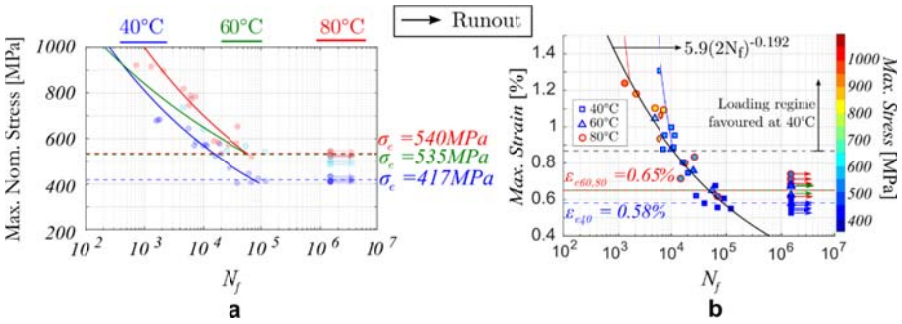

Fig. 2. Fatigue curves of NiTi hourglass-shaped samples at different temperatures: a) stress-N representation; b) Strain-N representation. In (b) the maximum applied stress is represented by marker colors. The maximum applied strain values were calculated using finite element analysis.

As in other structural alloys, we believe that the activation of dissipative mechanisms is the prelude to fatigue crack initiation in NiTi. To prove this hypothesis, we calculated the energy dissipated per cycles in the form of heat by computing infrared temperature field measurements of samples subjected to fatigue testing at different stress levels and temperatures. We post-processed the recorded thermographs using spectral analysis tools, which together with thermomechanical simulations allowed us to quantify the energy loses per cycle in terms of the applied stress. Following the same ideas that founded the Self-Heating technique for fast characterization of the High Cycle Fatigue behaviour of metals [3], we are currently working on the development of an energy-based fatigue model that will allow us to reproduce the high cycle fatigue behaviour of NiTi. With this approach, we also justify the detrimental role of R-phase in the fatigue performance of NiTi.

REFERENCES

[1] Yoneyama, T., Miyazaki, S.: Shape memory alloys for biomedical applications. 1st ed. Woodhead Publishing, Boca Raton, FL 33487, USA (2009).

[2] Sittner, P., Liu, Y., Novak, V.: On the origin of Lüders-like deformation of NiTi shape memory alloys. J Mech Phys Solids 53, 1719–46 (2005).

[3] Munier, R., Doudard, C., Calloch, S., Weber, B.: Determination of high cycle fatigue properties of a wide range of steel sheet grades from self-heating measurements. Int J Fatigue 63, 46-61 (2014).

ACKNOWLEDGMENTS

We kindly acknowledge the financial support of this work provided by the Czech Science Foundation by projects No. 18-03834S and 16-20264S. We further acknowledge city of Brest, France, for partly financing the PhD scholarship of Eduardo Alarcon.

Fatigue Modelling

Application of the Nonlinear Fatigue Damage Cumulative on the Prediction for Rail Head Checks Initiation and Wear Growth

Y. Zhou[a*], D.S. Mu[a], Y.B. Han[a], X.W. Huang[a], C.C. Zhang[a]

[a] *Key Laboratory of Road and Traffic Engineering of the Ministry of Education, Tongji University, China*

**Corresponding author: yzhou2785@tongji.edu.cn; wqhuo2785@163.com*

Keywords: Rail; Nonlinear fatigue damage cumulative; Head check initiation; Wear; Critical plane.

ABSTRACT

Rolling contact fatigue (RCF) crack, such as head checks (HCs) and squats, and wear are the main defects in rails of the railway and metro systems. The coexistence of the RCF crack initiation and wear growth were observed by twin-disc test[1,2] or field tests[3]. For the prediction of the rail head checks initiation, which often occurred at the gauge corner of curve rails, together with the wear growth, existing researches [4] applied Critical Plane and Archard model, in which the cumulative fatigue damage during wear growth and profile evolution was calculated according to the Miner linear fatigue rule[5]. Therefore, the fatigue damage influenced by the sequence and interaction between adjacent wheel-rail loads was considered little which would affect the accuracy of the prediction result [6].

In this paper, the nonlinear fatigue damage cumulative model was modified by combining the damage curve method considering the wheel-rail loading sequence and the fatigue damage method considering the interaction of the loads [7-8]. Based on above modified nonlinear fatigue damage cumulative model, a prediction method for coexistence of HC initiation and wear growth was presented and compared with that by the linear fatigue cumulative model.

Modified nonlinear fatigue damage cumulative model for multi-level loading:

$$\sum D=\left\{\left(\left(\frac{n_1}{N_{f1}}\right)^{\left(\frac{N_{f1}}{N_{f2}}\right)^{\alpha\left(\frac{\sigma_{max1}}{\sigma_{-1}}\right)}}+\frac{n_2}{N_{f2}}\right)^{\left(\frac{N_{f2}}{N_{f3}}\right)^{\alpha\left(\frac{\sigma_{max2}}{\sigma_{-1}}\right)}}+\ldots+\frac{n_{i-1}}{N_{f(i-1)}}\right\}^{\left(\frac{N_{f(i-1)}}{N_{fi}}\right)^{\alpha\left(\frac{\sigma_{max\,i-1}}{\sigma_{-1}}\right)}}+\frac{n_i}{N_{fi}} \quad (1)$$

It was found that the cumulative fatigue damage at the rail material point by the modified nonlinear fatigue damage cumulative model was higher than that of the linear one (See Figure 1). Therefore, the corresponding HC initiation life was the short.

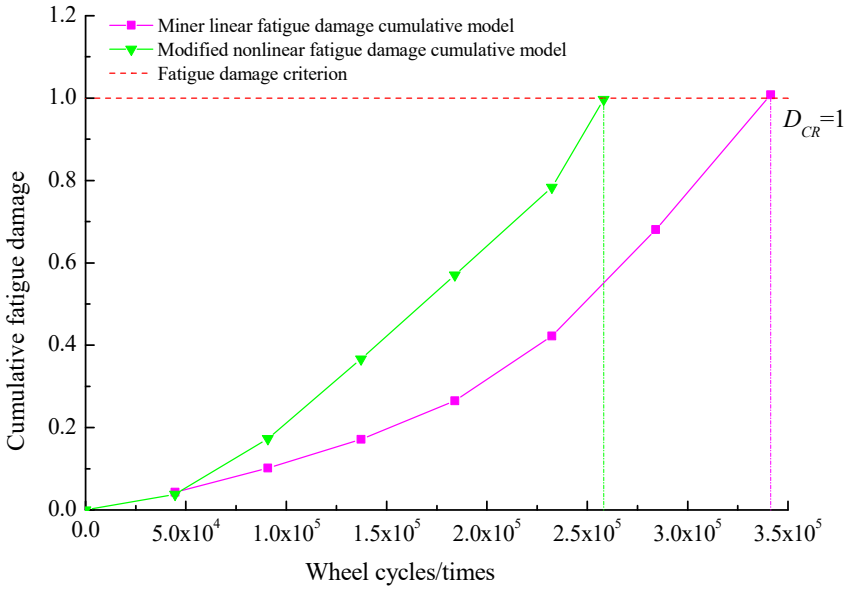

Fig. 1. The cumulative fatigue damage of the rail with the accumulation of wheel cycles. D_{CR} is the fatigue damage cumulative criterion which equals 1.

Taking the U75V heat-treated rail in the high rail of a sharp curve of the China heavy-haul railway as an example, prediction with the modified nonlinear fatigue damage cumulative model showed that head check initiation life was 2.58×10^5 wheel cycles. Comparing with the field sampled and laboratory microscopic observation, the prediction by Miner linear fatigue cumulative model was close to the upper range value by the field observation and that with the modified nonlinear fatigue damage cumulative model were close to the median by the field observation.

REFERENCES

[1] Donzella, G., Mazzù, A., Petrogalli, C.: Competition between wear and rolling contact fatigue at the wheel–rail interface: Some experimental evidence on rail steel. Proceedings of the Institution of Mechanical Engineers, Part F: Journal of Rail and Rapid Transit, 31-44 (2009).
[2] Fletcher, D.I., Beynon, J.H.: Equilibrium of crack growth and wear rates during unlubricated rolling-sliding contact of pearlitic rail steel. Proceedings of the Institution of Mechanical Engineers, Part F: 214, 93-105 (2000).
[3] Zhou, Y., Wang, S.F., Wang, T., et al: Field and laboratory investigation of the relationship between rail head check and wear in a heavy-haul railway. Wear 315(1), 68-77 (2014).
[4] Zhou, Y., Yu, M., Jiang, J.: Effects of rail hardness on rail wear and head check initiation. Journal of the Transportation Research Board 2545(1), 55-65 (2016).
[5] Miner, M.A.: Cumulative damage in fatigue. Journal of Applied Mechanics 12(3), 159-164 (1945).
[6] Zhu, S.P., Huang, H.Z., Xie, L.Y.: Nonlinear fatigue damage cumulative model and the analysis of strength degradation based on the double parameter fatigue criterion. China Mechanical Engineering 19(22), 2753-2761 (2008) (in Chinese).
[7] Fan, Z. C., Chen, X.D., Chen, L., et al.: Fatigue-creep behavior of 1.25Cr0.5Mo steel at high temperature and its life prediction. International Journal of Fatigue 29(6), 1174-1183 (2007).
[8] Manson, S.S., Halford, G.R.: Practical implementation of the double linear damage rule and damage curve approach for treating cumulative fatigue damage. International Journal of Fracture 17(2), 169-192 (1981).

ACKNOWLEDGMENTS

We would like to acknowledge the support of the National Natural Science Foundation of China (51378395, 51678445).

Micromagnetic Based Fatigue Life Prediction of Single-Lip Deep Drilled 42CrMo4+QT

N. Baak[a*], J. Nickel[b], D. Biermann[b], F. Walther[a]

[a] *Department of Materials Test Engineering (WPT), TU Dortmund University, D-44227 Dortmund, Germany*
[b] *Institute of Machining Technology (ISF), TU Dortmund University, D-44227 Dortmund, Germany*
**Corresponding author: nikolas.baak@tu-dortmund.de*

Keywords: Micromagnetic technique; Barkhausen noise; Fatigue performance; Surface condition; Single-lip deep drilling.

ABSTRACT

Non-destructive testing based on micromagnetic techniques, for example magnetic Barkhausen noise (MBN) analysis, are quick and reliable possibilities to detect and classify material parameters like hardness and residual stresses. High-strength steels, like 42CrMo4+QT (1.7225, AISI 4140), are commonly used for highly dynamically loaded parts. Increasing requirements on weight, performance and efficiency of automotive industry claim increasing demands on material properties. The aim of this study is to evaluate the surface conditions of deep drilled round specimens due to drilling parameters and to predict the resulting fatigue strength by micromagnetic measurements. Furthermore, modified process parameters should enhance fatigue life without the need of expensive processing steps, e.g. autofrettage.

MBN is based on unsteady changes in areal expansion of magnetic domains in ferromagnetic materials. The domains are divided by Bloch walls, which move when an external magnetisation occurs. The movement is affected by lattice defects and the magnetostriction. In a constantly changing magnetic field, a characteristic in Bloch wall movement can be observed and traced back to microstructure and residual stresses. The maximum penetration depth of approximately 100 µm is caused by the skin effect, thus it is important to detect the MBN on the crucially surface. [1]

In this study, round specimens with a diameter of 7.5 mm at the measuring length and a single-lip deep drilled hole with a diameter of 5 mm were investigated. The feed f was varied between 0.05 and 0.15 mm by otherwise constant parameters. This dimensions lead to the need of an optimized MBN sensor (Fig. 1 a). The sensor magnetises the specimen from the outer surface. The MBN can be detected by a hall sensor conventionally positioned between the pole shoes or by a customised hall sensor, which fits inside the bore hole in order to detect the MBN information from the influenced inner surface.

a)

b)

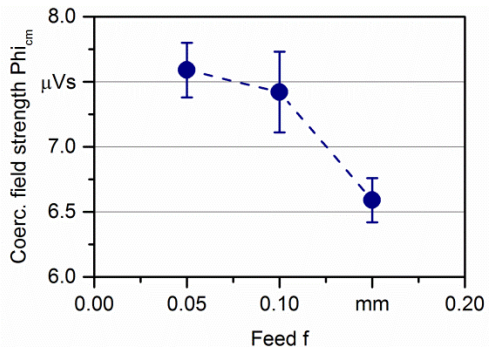

Fig. 1. a) Custom-built MBN sensor for inner surface measurement; b) change of coercive field strength based on MBN (Phi_{cm}) caused by varying feed f.

The MBN measurement was performed using a low magnetisation frequency of 30 Hz and a bandpass filter between 20 and 200 kHz to assure an uniform magnetic field at the inner surface. Fig. 1 b shows the coercive field strength based on MBN (Phi_{cm}) as function of the feed. While Phi_{cm} for f = 0.05 and 0.10 mm does not differ significantly, a profound drop of approx. 1.5 µVs can be detected for f = 0.15 mm. Microstructural investigations on transverse microsections reveal a typical drill microstructure in feed direction. In case of the highest feed f = 0.15 mm, a thin white etching layer was found. Therefore it can be assumed, that MBN correlates with the microstructure of the bore hole surface and the formation of white etching layers.

After the characterisation of the initial surface condition, specimens for all feeds were tested under fully-reversed fatigue loading in so-called load increase tests (LIT). The fatigue tests were instrumented with an extensometer, thermocouples and an alternating current potential drop (ACPD) test setup to evaluate the fatigue deformation and damage behaviour. The material response in form of the plastic strain amplitude $\varepsilon_{a,p}$, change in temperature ΔT, and alternating current potential U_{AC} as function of the number of cycles N can be used to determine the proceeding fatigue damage precisely [2].

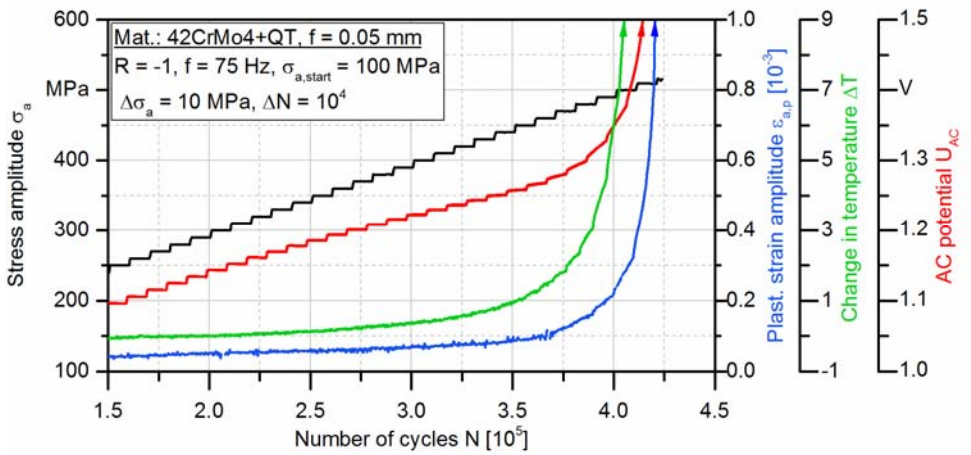

Fig. 2. Instrumented load increase test on 42CrMo4+QT, feed f = 0.05 mm.

Fig. 2 shows exemplary the result of a LIT performed on a specimen drilled with a feed of 0.05 mm. First material response can be detected in an early state of 65% fatigue life, where the change in temperature shifts from a linear to an exponential trend. The stepwise load increase can be observed in AC potential till 85% fatigue life, when U_{AC} increases progressively. Within the same load level, the increase in plastic strain amplitude shows a correlating progressive behaviour. The material reactions were used for the characterisation of the fatigue performance, with the aim to allow an efficient optimisation of drilling parameters. The fatigue strength, predicted based on LIT, was validated in following constant amplitude tests (CAT), which were additionally interrupted for intermittent Barkhausen (MBN) measurements.

REFERENCES

[1] Cullity, B. D., Graham, C. D.: Introduction to magnetic materials. Wiley, Hoboken (2009).
[2] Walther, F.: Microstructure-oriented fatigue assessment of construction materials and joints using short-time load increase procedure. Materials Testing 56, 7-8, 519-527 (2014).

ACKNOWLEDGMENTS

The authors would like to thank the German Research Foundation for financial support within the research project “Investigations on the influence of machining and sulphur content on the fatigue strength of the quenched and tempered steel 42CrMo4+QT” (WA 1672/22, BI 493/83).

Fatigue Life Prediction for Component With Local Structural Discontinuity Based on Stress Field Intensity

Lu Tianyang[a], Zhao Peng[a*], Xuan Fu-zhen[a]

[a] *School of Mechanical And Power Engineering, East China University of Science and Technology, China*
**Corresponding author: pengzhao@ecust.edu.cn*

Keywords: Notch; Fatigue life; Stress field intensity.

ABSTRACT

The impact of notch is one of the major problems that remain to be solved when predicting fatigue life. Because of various shape in notch, the material bears high stress concentration and complex stress gradient in notch root. Traditional methods of fatigue life prediction such as Neuber's rule [1] often overestimate the cycles to crack initiation in tension condition [2]. However, thanks to the increases in computing power, more methods which meet the fatigue mechanism can be applied by using Finite Element Method (FEM).

The fatigue life is determined by the area around notch root. The method of stress field intensity (SFI) was first put forward by Zhen [3] and developed by Yao [4]. This theory assumes that if the stress field intensity at the notch root is the same as that of the smooth one, they have the same fatigue life (Fig. 1).

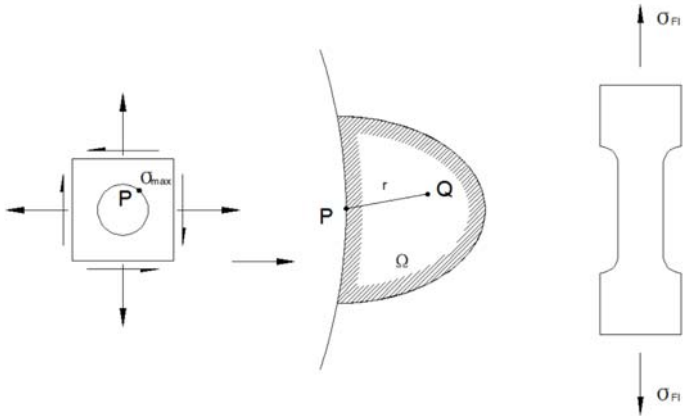

Fig. 1**.** Stress field intensity model.

The notch field intensity is σ_{FI}, given by Eq. (1).

$$\sigma_{FI}=\frac{1}{V}\int_{\Omega} f(\sigma_{ij})\varphi(r)dv \tag{1}$$

Here Ω is fatigue zone, V is the volume of Ω, $f(\sigma_{ij})$ is failure stress function, and $\varphi(r)$ is weight function.

According to the basic idea and realization form of SFI, it conforms to the mechanism of fatigue failure. Compared with other theories, SFI has good fatigue life prediction [5]. Here use a detail engineering notched specimen (Fig. 2) to test this theory. The material under investigation is Q345. The experiment uses a 34kN axial load with load ratio, R=0.1. The section of stress concentration is located on both sides of the middle hole.

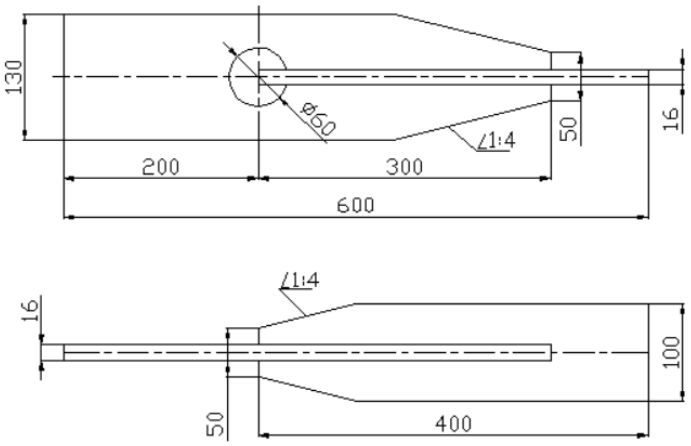

Fig. 2. Schematic of the model component with local structural discontinuities.

After data analysis with the help of FEA, the results are compared with experimental values and other traditional methods of predicting notched fatigue life in Table 1. It shows good prediction effect when SFI is used for specific problems.

Table 1. Fatigue life comparison between estimation and experiment (unit: cycles)

Methods	Local stress-strain approach	Nominal stress approach	Stress field intensity approach	Experimental value
Fatigue life	38741	205213	92534	82043
Deviation	-52.8%	150.1%	12.8%	/

However, the determination of the fatigue zone and weight function of this model depends on experiments when it comes to complex shape. This theory is valuable for further study.

REFERENCES

[1] Neuber, H.: Theory of stress concentration for shear-strained prismatical bodies with arbitrary non-linear stress–strain law. J Appl Mech Trans ASME 28, 544–550 (1961).
[2] Gladskyi, M., Fatemi, A.: Notched fatigue behaviour including load sequence effects under axial and torsional loadings. International Journal of Fatigue 55, 43-53 (2013).
[3] Zheng, C.H.: HCF design method-Stress Field Intensity. Beijing: Tsinghua University (1984) (in Chinese).
[4] Yao, W.X.: Fatigue Life Prediction of Structures. National Defend Industry Press, Beijing (2003) (in Chinese).
[5] Zhang, C.-C., Yao, W.-X.: Typical fatigue life analysis approaches for notched components. Journal of Aerospace Power 28(6), 1223-1230 (2013) (in Chinese).

ACKNOWLEDGMENTS

The authors are grateful for the supports provided by National Natural Science Foundation of China (51475168).

Finite Life and Propagating Crack Considerations for an Extended Interpretation of the Kitagawa-Takahashi Diagram

S. Blasón[a*], M. Muniz-Calvente[a], R. Brighenti[b], J.A.F.O. Correia[c], A.M.P. de Jesus[c], A. Fernández-Canteli[a]

[a] *Dept. of Construction and Manufacturing Engineering, University of Oviedo. C\ Pedro Puig Adam, s/n, 33204 Gijón, Spain*
[b] *Dept. of Engineering and Architecture, University of Parma, Viale delle Scienze 181/A, 43124 Parma, Italy*
[c] *University of Porto, INEGI, Engineering Faculty, Rua Dr. Roberto Frias, 4200-465 Porto, Portugal*
**Corresponding author: blasonsergio@uniovi.es*

Keywords: Fatigue limit; Kitagawa-Takahashi diagram; El-Haddad equation; Probabilistic S-N curve.

ABSTRACT

Considerations resulting from S-N field analyses on the existence or non-existence of fatigue limit [1,2], besides being an everlasting topic of discussion in the fracture mechanics community, give rise to promote a more profound comprehension of some issues related to the Kitagawa-Takahashi (K-T) diagram, thus continuing former works of the authors [3,4]. To do this, arguments are provided to illustrate the necessity of revising some of the influencing concepts in the current conventional interpretation of the K-T diagram, such as the transcendence of considering probabilistic S-N field approaches avoiding arbitrary, deterministic bi- and trilinear S-N models (Fig. 1), which necessarily imply the K-T diagram to be referred to a defined finite lifetime, see [5], the contradictory definition of non-propagating cracks [6] and the necessary identification of the K-T with a particular fatigue mechanism. In this way, a probabilistic extension of the K-T diagram for finite life predictions is ensured even in the VHCF region with multiplicity of mechanisms (Fig. 2). It is hoped that this approach will enhance understanding, effectiveness and reliability of the K-T applications in practical component design.

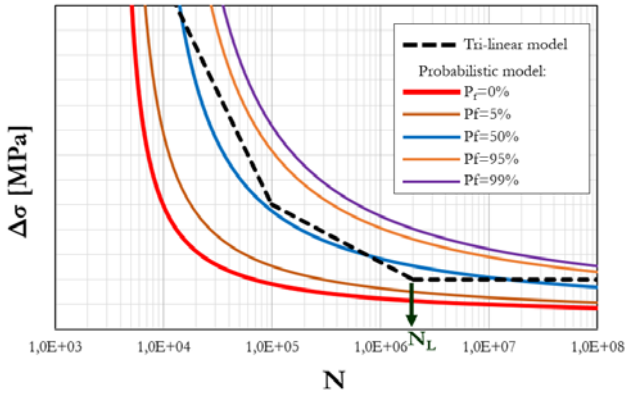

Fig. 1. Schematic representation of probabilistic S-N field, according to [2], and simplistic trilinear S-N field with definition of the kink point, N_L, as lifetime limit to which the K-T diagram is referred.

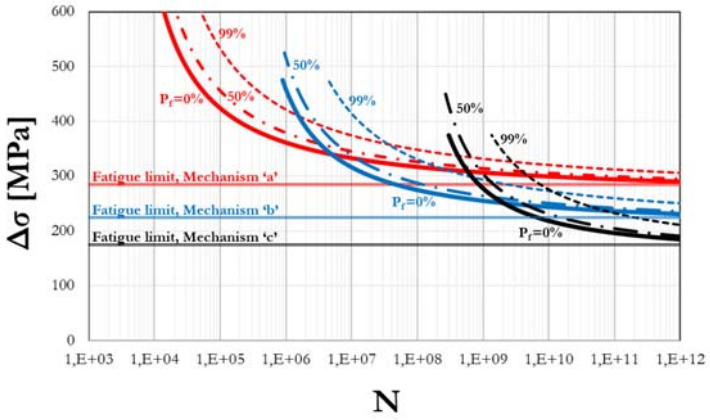

Fig. 2. Schematic probabilistic modelling of the S-N field, including hypothetical successive S-N fields as resulting from different failure mechanisms [1].

REFERENCES

[1] Blasón, S., Muñiz-Calvente, M., Pyttel, B., Fernández-Canteli, A., Castillo, E.: Considerations about the existence or inexistence of a fatigue limit and its implications on current practical design. Fatigue 2018: The 12th Int. Fatigue Congress, Poitiers (2018).

[2] Castillo, E., Fernández-Canteli, A.: A unified statistical methodology for modeling fatigue damage. Springer (2009).

[3] Fernández-Canteli, A., Brighenti, R., Castillo, E.: Towards a probabilistic concept of the Kitagawa-Takahashi diagram. The 4th Conference on Crack Paths, 19-21 September, Gaeta (2012).

[4] Correia, J.A.F.O., De Jesus, A.M.P., Fernández-Canteli, A., Brighenti R., Moreira, P.M.G.P., Calçada, R.A.B.: A procedure to obtain the probabilistic Kitagawa-Takahashi diagram. UPB Scientific Bulletin, Series D: Mechanical Engineering 78(1), 3-12 (2016).

[5] Ciavarella, M., Monno, F.: On the possible generalizations of the Kitagawa-Takahashi diagram and of the el Haddad equation to finite life. The 4th Conference on Crack Paths, 19-21 September, Gaeta (2012).

[6] El Haddad, M., Topper, T., Smith, K.: Prediction of non-propagating cracks. Eng. Fract. Mech. 11, 573–584, (1979).

Evaluation of Regression Tree-Based Durability Models for Spring Fatigue Life Assessment

Y.S. Kong[a,b], S. Abdullah[a*], D. Schramm[b], M.Z. Omar[a], S.M. Haris[a]

[a] *Department of Mechanical and Materials Engineering, Universiti Kebangsaan Malaysia, Malaysia*
[b] *Departmental Chair of Mechatronics, University of Duisburg-Essen, Germany*
**Corresponding author: shahrum@ukm.edu.my*

Keywords: Automobile spring; Fatigue life; Durability models; Regression tree; Scatter band.

ABSTRACT

This paper presents evaluation of pruned regression decision tree for automobile spring fatigue life predictions. Inputs for this regression decision tree models are vehicle ISO 2631 vertical vibrations and suspension frequencies. Design process of a coil spring involved many steps which consumes many time and efforts. Hence, there is a need to generate a prediction model for spring design assistances. Loading time histories were obtained from a quarter car model simulation for spring fatigue life assessment and ISO 2631 vertical vibrations calculations. Obtained force time histories were used to predict fatigue life of spring using strain-life approaches while acceleration time histories were used to obtain ISO 2631 vertical vibration. Together with spring stiffness sensitivities, the spring fatigue life was modelled using regression decision tree. Mean squared error of the generated regression decision tree residuals were analysed. Five sets of independent experimental measurement strain time histories were used to validate the predictions using a conservative approach. Most of the validation data points were lied beyond the acceptable region. Therefore, this proposed regression tree models are providing a good prediction on spring fatigue life to shorten required the design process.

INTRODUCTION

Suspension system of an automobile is subjected to dynamic loading during operating conditions. Coil spring is a part of the suspension system which serves to absorb the dynamic impacts. After accumulated loading cycles reached material's limit, fatigue failure of the coil spring occurred. The critical source that affected fatigue life of the coil spring is the corresponding road profile [1]. Since the coil spring serves to filter the dynamic responses, it contributes to certain degree of vehicle ride quality. Spring stiffness is one of the main parameters which determines the natural frequency of the suspension system. When the road excitation frequencies superimpose with the suspension natural frequency, resonance of the suspension systems happened and caused extra deformation of coil springs [2]. The capability of suspension in filtering responses is reduced and subsequently leads to poor ride quality. Vehicle ride quality is usually quantified using ISO 2631 standard. As proposed in [3], the fatigue life of a vehicle suspension components could be assessed using some nominal point acceleration measurements from suspension systems. Hence, the relationship between vehicle ride quality, spring fatigue life and suspension natural frequency are based on the road excitation sources. This study aims to establish regression tree-based durability models for spring fatigue life predictions. The generated regression-tree based durability models aim to shorten automotive coil spring design process through reducing number of prototypes.

RESULTS AND DISCUSSION

The main results of this work are regression-tree based strain-life durability models. The developed regression tree-based Smith-Watson-Topper (SWT) durability model is shown in Fig. 1. The number of splits is seven and the number of nodes is 15. The fitted regression tree consisted of three levels. With the ISO 2631 vertical vibration and suspension frequency as input, prediction of spring fatigue life was performed. Correlation between regression tree-based model and experimental predicted fatigue lives were analysed using scatter band approach as shown in Fig 2. Three out of five points were fitted nicely into 1:2 or 2:1 correlation curve. It suggested that the regression tree-based durability models could be used for spring fatigue life predictions with acceptable accuracy.

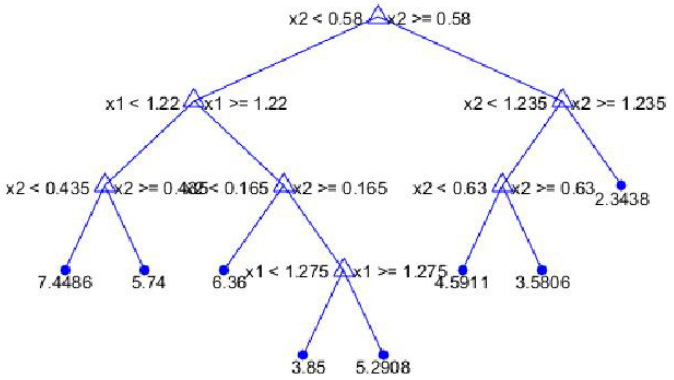

Fig. 1. Regression-based durability models for SWT approach.

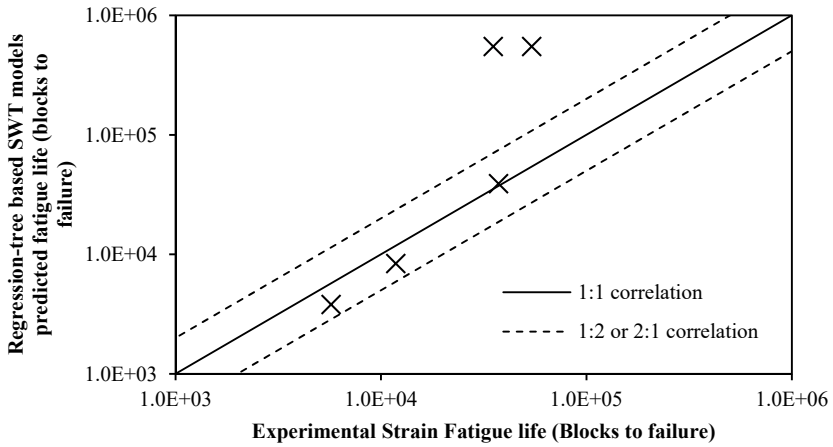

Fig. 2. Correlation between regression-tree based durability models and experimental strain predicted fatigue lives.

REFERENCES

[1] Prasad, S., Prakaash, J., Dayalan, P.: Study and comparison of road profile for representative patch extraction and duty cycle generation in durability analysis. SAE International 2017-060309 (2017).

[2] Wei, C., Taghavifar, H.: A novel approach to energy harvesting from suspension system: half vehicle model. Energy 134, 279–288 (2017).

[3] Halfpenny, A., Hussain, S., McDougall, S., Pompetzki, M.: Investigation of the durability transfer concept for vehicle prognostic applications. 2010 NDIA Ground Vehicle Systems Engineering and Technology Symposium, U.S.A. (2010).

Multiaxial Fatigue

Computational Framework for Multiaxial Fatigue Life Prediction Considering Notch Effect

Ding Liao[a], Shun-Peng Zhu[a*], Yong-Zhen Hao[a], Shen Xu[a]

[a] *Institute of Reliability Engineering, School of Mechanical and Electrical Engineering, University of Electronic Science and Technology of China, Chengdu 611731, China*
**Corresponding author: zspeng2007@uestc.edu.cn*

Keywords: Turbine blade; Critical plane; Multiaxial fatigue; Stress gradient; Life prediction.

ABSTRACT

With the development of aircraft engines, hot section components are often subjected to complex multiaxial loadings, which gives rise to higher-level requirements on its structural integrity and service life. During the design of hot section components like turbine discs and blades, for the sake of meeting requirements including cooling, assembly, driving motion and weight reduction, design scheme with complex cross sections are expected, which contributes to stress concentration in some locations under external loadings. High stress gradient usually triggers crack initiation, which then causes fatigue damage and crack propagation of these components [1]. Complex shape of turbine blades contributes to multiaxial stress/strain states under cyclic loadings, accordingly, modelling concepts that addressing only uniaxial loading condition are not sufficiently for the design requirements. The ever-growing demand on methods for accurate life prediction to ensure the mechanical integrity of these components drives the development of multiaxial fatigue lifing solutions as well as methods considering both size and notch support effects.

Until now, various researches focus on multiaxial fatigue analysis over the past several decades, most of them attempt to propose a sound methodology for assessing fatigue lives of engineering components/materials [2]. Comparing with the uniaxial fatigue models, multiaxial fatigue models are more suitable for real loading conditions [3]. However, it should be pointed out that few of multiaxial fatigue models have been commonly applied in practice [4-5], due to many additional complexities such as varied properties of different materials, manufacturing and testing of specimen, data extraction and analysis, and so on.

Under the effect of stress concentration, fatigue cracks usually initiate at the discontinuities such as holes and notches, in which the structural geometry changes suddenly. Since high stress gradient exists in these components, fatigue crack initiation is conducive to structural failure through crack propagation. Therefore, fatigue life of a component usually relates with fatigue strength of the material at its stress concentration location. In this paper, by adopting the elasto-plasticity FE analysis, a new critical plane damage parameter combining with stress gradient in the border element is proposed, which accounts for the notch effect by introducing a notch support function. Moreover, by coupling with Fatemi-Socie (FS) and Smith-Watson-Topper (SWT) damage criteria, a computational framework for multiaxial fatigue life prediction is established for notched components. By calibration and validation with experimental data of TC4 and GH4169 alloys [6-7], the proposed damage parameter provide more accurate predictions than other three models. In addition, experimental data of turbine blade alloy TC4 and field load spectra of a high-pressure turbine blade are introduced for model validation and comparison. Finally, based on this framework, testing effect can be significant reduced according to the model predictions of engineering components with notch effect.

REFERENCES

[1] Wang, Y.R., Li, H.X., Yuan, S.H., Wei, D.S., Shi, L.: Method for notched fatigue life prediction with stress gradient. J. Aerosp. Power 28(6), 1208–1214 (2013).
[2] Socie, D.F., Marquis, G.B.: Multiaxial fatigue. Warrendale, PA: Society of Automotive Engineers (2000).
[3] Zhu, S.P., Foletti, S., Beretta, S.: Probabilistic framework for multiaxial LCF assessment under material variability. Int. J. Fatigue 103, 371-385 (2017).
[4] Fatemi, A., Shamsaei, N.: Multiaxial fatigue: An overview and some approximation models for life estimation. Int. J. Fatigue 33(8), 948–958 (2011).
[5] Papuga, J.: A survey on evaluating the fatigue limit under multiaxial loading. Int. J. Fatigue 33(2), 153–165 (2011).
[6] China Aeronautical Materials Handbook Editorial Committee, China Aeronautical Materials Handbook vol. 2 Deformation Superalloy & Casting Superalloy, Second ed. Beijing: China Standards Press (2002).
[7] China Aeronautical Materials Handbook Editorial Committee, China Aeronautical Materials Handbook vol. 4 Titanium Alloy, Second ed. Beijing: China Standards Press (2002).

ACKNOWLEDGMENTS

The authors would like to acknowledge the financial support of the National Natural Science Foundation of China (No. 11672070 and 11302044) and the China Postdoctoral Science Foundation Funded Project (No. 2015M582549) and China Postdoctoral Science Special Foundation (No. 2017T100697) and the Fundamental Research Funds for the Central Universities (No. ZYGX2016J208).

Prediction of Fatigue Crack Initiation Life in Notched Cylindrical Bars Under Multiaxial Cycling Loading

R. Branco[a*], J.D. Costa[a], F. Berto[b], A. Kotousov[c], F.V. Antunes[a]

[a]*Department of Mechanical Engineering, University of Coimbra, Portugal*
[b]*Department Mechanical and Industrial Engineering, Norwegian University of Science and Technology, Norway*
[c]*Department Mechanical Engineering, University of Adelaide, Australia*
**Corresponding author: ricardo.branco@dem.uc.pt*

Keywords: Crack initiation; Multiaxial fatigue; Equivalent strain energy density; Life prediction.

ABSTRACT

Most mechanical components with circular cross-sections contain notches because of design requirements. When subjected to multiaxial loading histories, the stress-strain responses at the geometric discontinuities may result in complex fatigue problems, even in cases of low plastic deformation. In this context, the full understanding of the notch effect is pivotal to develop safe and durable products. Moreover, due to the increasingly short product life cycles, lower batch sizes, and the growing need to reduce overall costs, products are developed in smaller time frames. Thus, the rapid assessment of fatigue life in notched members subjected to non-trivial loading scenarios is indispensable to increase efficiency.

This paper proposes a simplified approach to estimate the fatigue crack initiation lifetime in notched round bars subjected to proportional multiaxial loading using the total strain energy density concept. The *modus operandi* consists of developing a fatigue master curve relating the total strain energy density and the number of cycles to failure from only two strain-controlled tests and an adequate elastic-plastic finite-element model. In a second stage, the total strain energy density of the notched samples is computed from representative hysteresis loops obtained via linear-elastic finite-element models. The proposed methodology is tested in cylindrical bars with lateral U-shaped notches and cylindrical bars with transverse holes subjected to different proportional bending-torsion loading histories. Tests are conducted under constant-amplitude loading and the crack detection is performed *in situ* using a high-resolution digital camera. The most likely initiation sites, surface crack paths and surface crack angles in the early stage of crack growth are predict based on principal stress field criteria. After fatigue testing, specimen surfaces are examined by scanning electron microscopy to identify the main failure micro-mechanisms.

Comparison Among Different Multiaxial Fatigue Models for Damage Prediction Under Random Loading

I. Portugal[a,b*], M. Olave[a], A. Zurutuza[c], A. López[c], M. Muñiz-Calvente[b], A. Fernández-Canteli[b]

[a] *Mechanics, IK4-Ikerlan, Spain*
[b] *Construction and Manufacturing Engineering, University of Oviedo, Spain*
[c] *Laulagun Bearings, Spain*
**Corresponding author: iportugal@ikerlan.es*

Keywords: Fatigue models; Multiaxial; Random loading; Stresses; Strains.

ABSTRACT

It is well known that a number of industrial components are exposed to Rolling Contact Fatigue (RCF) during their service life (rail wheels, bearings, cams, gears, etc. [1]). Despite the diversity of shape and operation function of the components implied under which the RCF phenomenon may arise, it affects their performance and lifetime in a characteristic and similar way [2]. The phenomenon of RCF induces crack initiation in the subsurface after having a tug-of-war of stresses and strains what, depending on the particular application culminates in failure. However, finding out the magnitude of those stresses and strains at an a priori unknown location under the surface when the component is subjected to a varying load is a complex task due to the lack of linearity [3]. Furthermore, those components are often exposed to alternated random load conditions during their service life. For this reason, failure prediction models are indispensable to fulfil the requirements of structural integrity of the component as well as to ensure correct operation during its service life.

In this work, a comparison among different multiaxial fatigue models is presented, including orthogonal shear stress and critical plane models based on stresses (such as McDiarmid and Findley) or strains (such as Fatemi-Socie, Smith-Watson-Topper and Brown Miller) [4-9] (See Fig.1). With this aim, the action of randomly distributed load histories is taken into account using a novel methodology based on the calculation of the stress tensor as a function of time, derived by the interpolation of loads with those obtained from response surfaces using FEM models. Following this proposal, the selected parameters related to the failure criterion are estimated, from which the critical values are considered as the reference to determine fatigue damage from the Wöhler curve. Finally, the results obtained from the different multiaxial fatigue models applied to RCF problems under random loading are compared, and their relative discrepancy analysed.

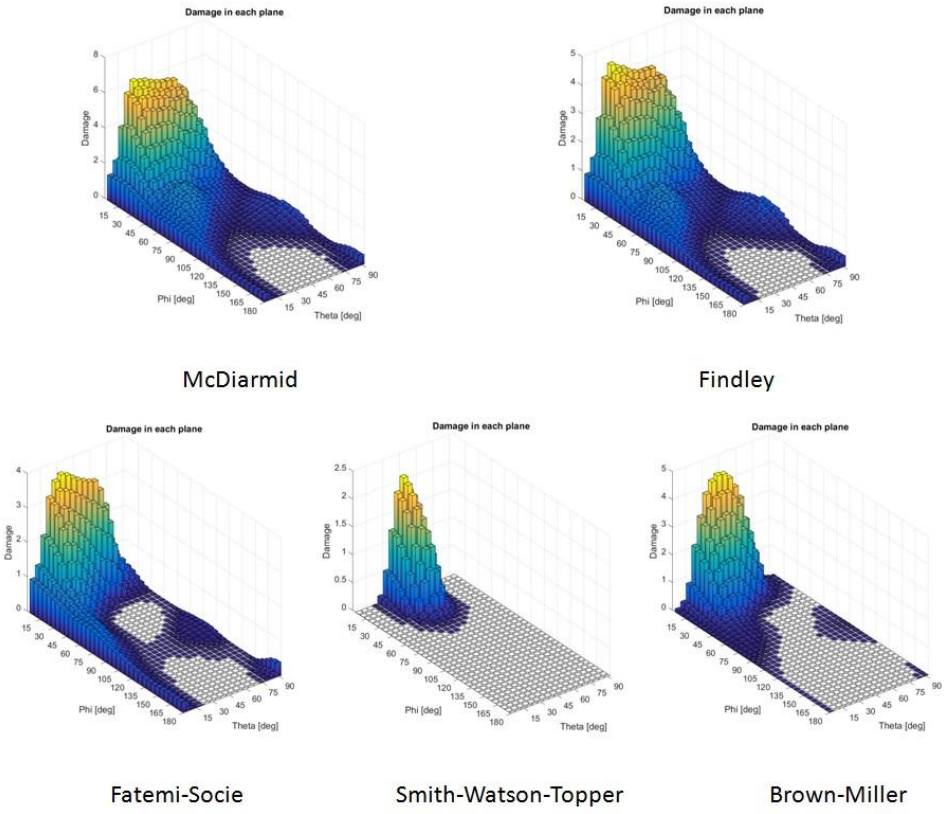

Fig. 1. Damage obtained at each plane from different multiaxial criteria applied to a random loading case.

The methodology proposed allows us to make a comparison among the results from the different fatigue models referred to their degree of safety reserve, as well as their subsequent contrast to the experimental lab results. Thus, the fundamental bases to explore new multiaxial fatigue models in order to obtain a perfect correlation between damage prediction and experimental results are established.

REFERENCES

[1] Donzella, G., Mazzù, A., Petrogalli, C.: Failure assessment of subsurface rolling contact fatigue in surface hardened components. Eng. Fract. Mech. 103, 26–38 (2013).
[2] Ciavarella, M., Monno, F.: A comparison of multiaxial fatigue criteria as applied to rolling contact fatigue. Tribol. Int. 43 (11), 2139–2144 (2010).
[3] Harris, T.A., Kotzalas, M.N.: Essential Concepts of Bearing Technology. 5th edn. CRC (2006).
[4] Papuga, J.: Mapping of fatigue damages, program shell of FE-calculation, Ph.D. thesis (2005).
[5] Carpinteri, A., Ronchei, C., Scorza, D., Vantadori, S.: Critical plane orientation influence on multiaxial high-cycle fatigue assessment. Physical Mesomechanics Journal 18 (4), 348–354 (2015).
[6] Carpinteri, A., Berto, F., Campagnolo, A., Fortese, G., Ronchei, C., Scorza, D., Vantadori, S.: Fatigue assessment of notched specimens by means of a critical plane-based criterion and energy concepts. Theor. Appl. Fract. Mech. 84, 57–63 (2016).
[7] Socie, D.: Advances in multiaxial fatigue. ASTM Edition (1993).
[8] Papadopoulos, I.: Critical Plane Approaches in High-Cycle Fatigue: on the Definition of the Amplitude and Mean Value of the Shear Stress Acting on the Critical Plane. Fatigue Fract. Eng. Mater. Struct. 21 (3), 269–285 (1998).
[9] Anes, V., Reis, L., Freitas, M.D.: Random accumulated damage evaluation under multiaxial fatigue loading conditions. Frat. ed Integrità Strutt. 33, 309–318 (2015).

Fatigue Life Prediction in Multiaxial Fatigue on Low Carbon Steel with a New Critical Plane Model

A.S. Cruces[a*], P. Lopez-Crespo[a], S. Suman[b], B. Moreno[a]

[a] *Department of Civil and Material Engineering, University of Malaga, Spain*
[b] *UTC Aerospace Systems, USA*
**Corresponding author: ascruces@uma.com*

Keywords: Critical plane model; Multiaxial fatigue; Non-proportional; St52-3N.

ABSTRACT

Accurate fatigue designs are crucial to differentiate between efficient use of a material with reliable safety factor and catastrophic failures. Since most of mechanical systems are subjected to complex multiaxial loadings [1], general design codes should be based on multiaxial models. Incorporating multiple loads into design models requires not only the state of stress to be accounted for, but also the material response, the interaction between these loads and their effects over the nucleation and growth of fatigue cracks. Some multiaxial fatigue theories try to condense such information in a damage parameter, while other are based on experimental characterisation of some property measured at the crack tip [2]. The damage parameter approach is used to estimate the damage caused by the load cycles. Critical plane methods present the damage in each cycle with a parameter, normally as combination of several stress-strain values, in a plane where is estimated the crack nucleate and growth. In this work, critical plane models developed by Suman & Kallmeyer [3], Fatemi-Socie [4], Wang-Brown [5], and Liu 1 and Liu 2 [6], are presented and applied to different loading cases. Furthermore the five different models are compared in terms of accuracy of life prediction and discussed.

Fatigue tests were conducted under different multiaxial loading conditions on dog bone shaped tubular hollow specimens [7]. All tests were performed under strain mode with the help of a biaxial extensometer. The material studied was a low carbon steel type St52-3N. Twenty one multiaxial tests were conducted with sinusoidal normal-shear strain with total inversion in-phase and with 90º out-of-phase.

Suman & Kallmeyer developed a new critical plane criterion [3] (see Eq. 1). It is based on the damage parameter where the shear strain range is multiplied by maximum shear stress value at critical plane φ* in their model. The third term in this model is the maximum value of the product of normal stress and shear stress on φ*.

$$(G\Delta\gamma)^{w}\tau_{max}^{(1-w)}\left(1+k\frac{(\sigma\cdot\tau)_{max}}{\sigma_0^2}\right)=AN^{b}+CN^{d} \quad (1)$$

Fig. 1 shows life estimation for each model in-phase and Fig. 3 for out-of-phase. SK estimation are represented with red diamonds, FS with blue squares, WB with green triangles, Liu 1 with black circles and Liu 2 with purple crosses.

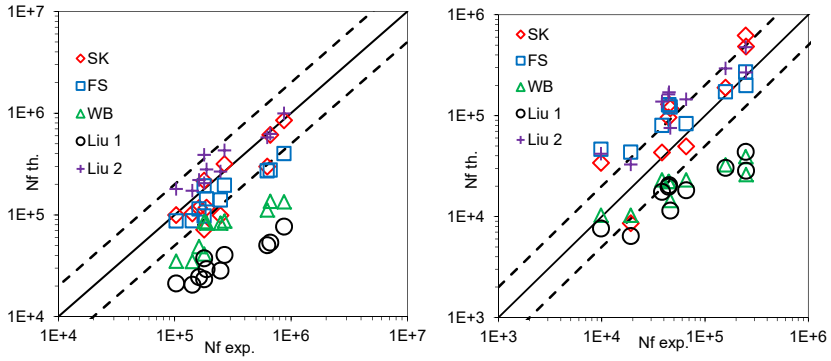

Fig. 1. St52-3N fatigue life predicted for in-phase (left) and out-of-phase (right) loading.

For in-phase loading, SK gives good estimation, with values near the conservative side, as it can be seen for almost all models with the exception of Liu 2. At low cycle fatigue the response is not as good as for high cycle fatigue, as consequence of a low weight of the shear strains in the DP for the fit obtained. FS returns better predictions at low cycle fatigue than SK, with a conservative tendency as it moves to high cycle fatigue. As we can see, between Liu 1 and Liu 2, the second one gives a better result, showing this way the ductile character of the material. WB based on the same model as FS, shows similar results but more conservative maybe considering the normal stress on φ* instead of the normal strain reflect better the hardening effect. For out-of-phase, models predictions move up to the non-conservative side respect to the values returns in-phase. Although SK model estimations are not bad, it presents a considerable dispersion, consequence of the sensitive response of the DP with τ_{max} instead of the low weight of $\Delta\gamma$ at low cycles. WB and Liu 1 results are very close and more conservative for larger experimental life estimations. Among all the damage parameters considered, SK model appeared to give the most effective predictions for fatigue life for wide variety of in-phase and out-of-phase loadings.

REFERENCES

[1] Lopez-Crespo, P., Pommier, S.: Numerical analysis of crack tip plasticity and history effects under mixed mode conditions. Journal of Solid Mechanics and Materials Engineering 2(12), 1567–1576 (2008).

[2] Lopez-Crespo, P., Garcia-Gonzalez, A., Moreno, B., Lopez-Moreno, A., Zapatero, J.: Some observations on short fatigue cracks under biaxial fatigue. Theoretical and Applied Fracture Mechanics 80, 96–103 (2015).

[3] Suman, S., Kallmeyer, A., Smith, J.: Development of a multiaxial fatigue damage parameter and life prediction methodology for non-proportional loading. Frattura ed Integrita Strutturale 10(38), 224–230 (2016).

[4] Fatemi, A., Socie, D.F.: A Critical Plane approach to multiaxial fatigue damage including out-of-phase loading. Fatigue and Fracture of Engineering Materials and Structures 11(3), 149–165 (1988).

[5] Wang, C.H., Brown, M.W.: A path-independent parameter for fatigue under proportional and non-proportional loading. Fatigue Fract Engng Mater Struct 16, 1285–1298 (1993).

[6] Liu, K.C.: A method based on virtual strain energy parameters for multiaxial fatigue life prediction. In: McDowell, D.L., Ellis, R. editors, Advances in Multiaxial Fatigue, ASTM STP 1191, 67–84 (1993).

[7] Mokhtarishirazabad, M., Lopez-Crespo, P., Moreno, B., Lopez-Moreno, A., Zanganeh, M.: Optical and analytical investigation of overloads in biaxial fatigue cracks. International Journal of Fatigue 100(2), 583–590 (2017).

ACKNOWLEDGMENTS

Financial support from Ministerio de Economia y Competitividad through grant reference MAT2016-76951-C2-2-P is greatly acknowledged.

On the Application of Critical Plane Models for Multiaxial Fatigue Prediction of Stainless Steel

A.S. Cruces[a*], P. Lopez-Crespo[a], B. Moreno[a], S. Bressan[b], T. Itoh[c]

[a] *Department of Civil and Material Engineering, University of Malaga, Spain*
[b] *Graduate School of Science & Engineering, Ritsumeikan University, Japan*
[c] *Department of Mechanical Engineering, College of Science & Engineering, Japan*
**Corresponding author: ascruces@uma.es*

Keywords: Multiaxial fatigue; Proportional loading; Non-proportional loading; Critical plane approach.

ABSTRACT

The vast majority of fatigue data available in the literature is based on uniaxial cyclic loading. Nevertheless, the real loading of mechanical components is often quite complex and involves loads in different directions instead of uniaxial loading. In order to have a better understanding of the multiaxial fatigue behaviour, it is desirable to design experiments where loads resemble more accurately the real conditions that appear during service. This involves experiments where both proportional [1] and non-proportional loads are applied to the cracked component. Such loading scenarios often produce interaction effects that are difficult to account for by classic methodology [2]. A very clever way to incorporate the stress state and other interaction effects that appear during the loading cycle is using critical plane methods. Unlike damage tolerance approach [3], critical plane methods are based on global data and not locally measured variables [4].

This paper presents a study of the biaxial fatigue behaviour of 316 stainless steel with several well-known critical plane models; Fatemi-Socie (FS) [5], Wang-Brown (WB) [6] and Liu 1 and 2 [7]. By applying different load paths on the specimens, the capabilities of the different models are assessed, in particular how to take into account hardening and mean stress effects. All the experiments were performed on 316 stainless steel. The specimens were hollow cylindrical geometry. The longitudinal gauge zone was polished by 1 μm alumina particles. The inner surface of the specimen was polished by emery papers up to #2000. The experimental tests were performed with a three actuator fatigue loading rig. Such rig allows (i) the introduction of a fluid inside a hollow specimen, (ii) traction and compression forces to be applied and (iii) torsional force to be applied. Further details about the experimental have been described previously [8]. Fig. 1 shows the six different load paths applied. These have a combination of axial longitudinal loads and inner pressure. Fig. 2 shows life estimation for each model for different load paths. FS results are represented with blue squares, WB with green triangles, Liu I with black circles and Liu II with purple crosses. Conservative predictions are returned at low fatigue life, this is for #6 push-pull path tests. Similar predictions were found previously on structural low carbon steel [6-7]. As the test strain value is reduced a better correlation between prediction and experimental life is obtained. In general, FS presents the best results among the models with the exception of the non-proportional load path #3. There is not a sensitive difference between Liu I and Liu II estimations, although as it was describe previously, they are oriented to different failures modes. It was shown that the different models tend to yield conservative predictions for low cycle fatigue. Energetic based methods show better results than strain based methods for non-proportional. In addition, FS model appears to produce the best estimations for all cases but one non-proportional loading scenario.

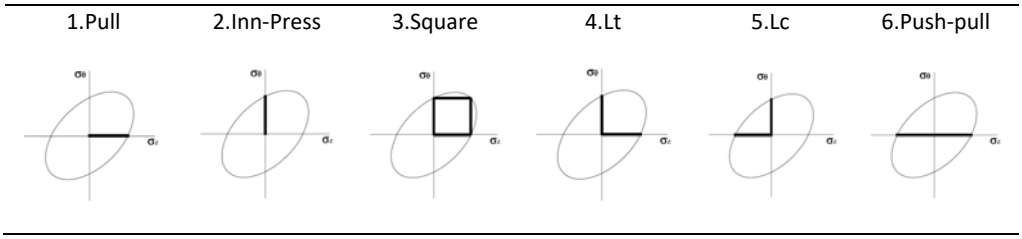

Fig. 1. Schematic of the six different loading paths studied.

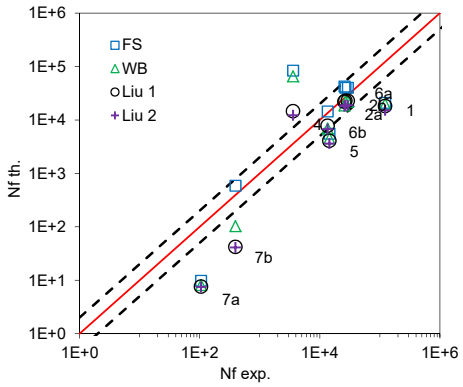

Fig. 2. Critical plane model 316 stainless steel fatigue life predictions for different load paths.

REFERENCES

[1] Lopez-Crespo, P., Pommier, S.: Numerical analysis of crack tip plasticity and history effects under mixed mode conditions. Journal of Solid Mechanics and Materials Engineering 2, 1567–1576 (2008).

[2] Moreno, B., Martin, A., Lopez-Crespo, P., Zapatero, J., Dominguez, J.: Estimations of fatigue life and variability under random loading in aluminum Al-2024T351 using strip yield models from NASGRO. Int. J. Fatigue 91, 414–422 (2016).

[3] Withers, P.J., Lopez-Crespo, P., Kyrieleis, A., Hung, Y.-C.: Evolution of crack-bridging and crack-tip driving force during the growth of a fatigue crack in a Ti/SiC composite. Proceedings of the Royal Society A 468, 2722–2743 (2012).

[4] Mokhtarishirazabad, M., Lopez-Crespo, P., Moreno, B., Lopez-Moreno, A., Zanganeh, M.: Evaluation of crack-tip fields from DIC data: a parametric study. International Journal of Fatigue 89, 11–19 (2016).

[5] Fatemi, A., Socie, D.F.: A critical plane approach to multiaxial fatigue damage including out-phase loading. Fatigue Fract. Engng. Mater. Struct. 11, 149-165 (1988).

[6] Wang H, Brown MW. A Path-Independent Parameter for Fatigue Under Proportional and Non-Proportional Loading. Fatigue Fract. Engng. Mater. Struct. 16(12), 1285–1297 (1993).

[7] Liu K. A method based on virtual strain energy parameters for multiaxial fatigue life prediction. Advances in Multiaxial Fatigue, ASTM STP1191, 67–84 (1993).

[8] Yakada, Y., Morishita, T., Itoh, T.: Effect of interchange in principal stress and strain directions on multiaxial fatigue strength of type 316 stainless steel. Proceedings of Fatigue 2017 Conference, Cambridge, UK (2017).

[9] Lopez-Crespo, P., Moreno, B., Lopez-Moreno, A., Zapatero, J.: Study of crack orientation and fatigue life prediction in biaxial fatigue with critical plane models. Engineering Fracture Mechanics 136, 115–130 (2015).

[10] Mokhtarishirazabad, M., Lopez-Crespo, P., Moreno, B., Lopez-Moreno, A., Zanganeh, M.: Optical and analytical investigation of overloads in biaxial fatigue cracks. Int. J. Fatigue 100(2), 583–590 (2017).

ACKNOWLEDGMENTS

Financial support from Ministerio de Economía y Competitividad through grant reference MAT2016-76951-C2-2-P is greatly acknowledged.

Microstructural Aspects of Fatigue

&

Thermal and Environmental Fatigue

Observation of Dislocation Walls During Cyclic Deformation in an Fe-Si Alloy

H. Shuto[a,b*], A. Onodera[b], S. Arai[c], T. Miyazawa[b], T. Fujii[b]

[a] *R&D Laboratories., Nippon Steel & Smitomo Metal Corporation, Japan*
[b] *School of Materials and Chemical Technology, Tokyo Institute of Technology, Japan*
[c] *Institute of Materials and Systems for Sustainability, Nagoya University, Japan*
**Corresponding author: shuto.87e.hiroshi@jp.nssmc.com*

Keywords: Dislocation structure; Wall structure; Labyrinth structure; High voltage electron microscopy; Iron.

ABSTRACT

It is well known that dislocation structures are formed during fatigue tests in metals. Authors have showed that dislocation structures affect fatigue limit of steels [1]. It implies that fatigue property can be improved if we can control the development of the dislocation structures during cyclic deformation. Although formation mechanisms of the dislocation structures in fcc metals have been discussed in detail, those in bcc metals have not been elucidated yet. For instance, in the case of dislocation walls in the labyrinth structures developed by simultaneous activation of two slip systems, there are disagreements in wall orientations reported in previous studies [2-4]. In this study, therefore, the dislocation structures in a bcc Fe-Si alloy are investigated using high voltage electron microscopy (HVEM), and the formation mechanisms of the dislocation walls in bcc metals are discussed.

Push-pull fatigue tests of Fe-1mass%Si polycrystalline specimens were conducted with constant total strain amplitude of 5×10^{-3} at a strain rate of 4×10^{-3}/s. Plastic strain amplitude during the fatigue test changed from 3.8×10^{-3} to 3.3×10^{-3} as shown in Fig.1. These values are comparable to that reported in previous studies in which the labyrinth structures were observed [2-4]. The tests were stopped after 1000 cycles, and the dislocation structures were observed using the HVEM equipped scanning transmission electron microscopy (STEM) detector (JEM-1000K RS) in Nagoya University.

Vein, wall, and cell structures were found in a fatigued specimen as shown in Fig. 2. The detailed orientation and structure of the walls in a (001) foil were observed in various diffraction conditions as shown in Fig. 3(a)-(c). In the case of $\mathbf{g} = -200$, $\mathbf{g}\cdot\mathbf{b} \neq 0$ because the Burger's vector of bcc metals is parallel to <111>. It means that all of the dislocations existing in the specimen are visible in Fig. 3(a). In Fig. 3(b), all dislocations were visible again. On the other hands, contrast of dislocations in Fig. 3(c) was weaker than those in Fig. 3(a) and Fig. 3(b). Therefore, the wall structures contain the dislocations with $\mathbf{b} = a/2[111]$ and/or $\mathbf{b} = a/2[-1-11]$ because $\mathbf{g}\cdot\mathbf{b}$ becomes zero in Fig. 3(c).

Assuming that the wall structures are consisting of unique dislocations of single slip, the wall structures are arranged parallel to the (111) or (-1-11) plane perpendicular to the Burger's vector of the single slip dislocations [5]. As the (111) and (-1-11) walls are not observed edge-on condition in the (001) foil, the width of the (111) and (-1-11) walls should be larger than that actually observed in Fig. 3. Thus, the walls in Fig. 3 consist of more than two types of dislocations with $\mathbf{b} = a/2[111]$ or $\mathbf{b} = \mathbf{a}/2[-1-11]$. In fcc metals, a set of walls in labyrinth structures is known to be parallel to the planes which bisect the two Burger's vector direction [5]. Adopting this model to the present case, the planes which bisects $\mathbf{b} = a/2[111]$ and $\mathbf{b} = a/2[-1-11]$ are (110) and (001). The (110) walls are observed at edge-on condition in the (001) foil, and the orientation of the walls is consistent with that of walls observed in Fig. 3. The

(001) walls are invisible if the (001) foil was taken from a part of a channel between (001) walls. Therefore, the wall structures observed in this study can be explained self-consistently by considering the labyrinth structures consisting of the (110) and (001) walls.

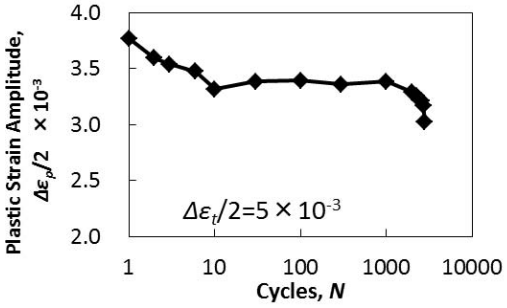

Fig. 1**.** Plastic strain amplitude during fatigue test.

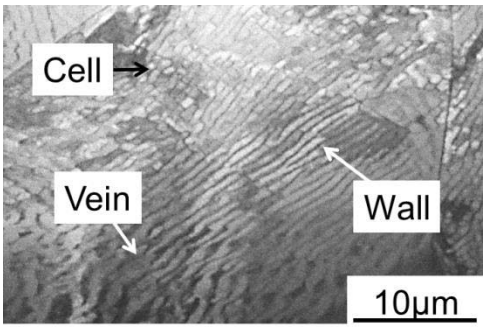

Fig. 2**.** Dislocation structures after 1000 cycles.

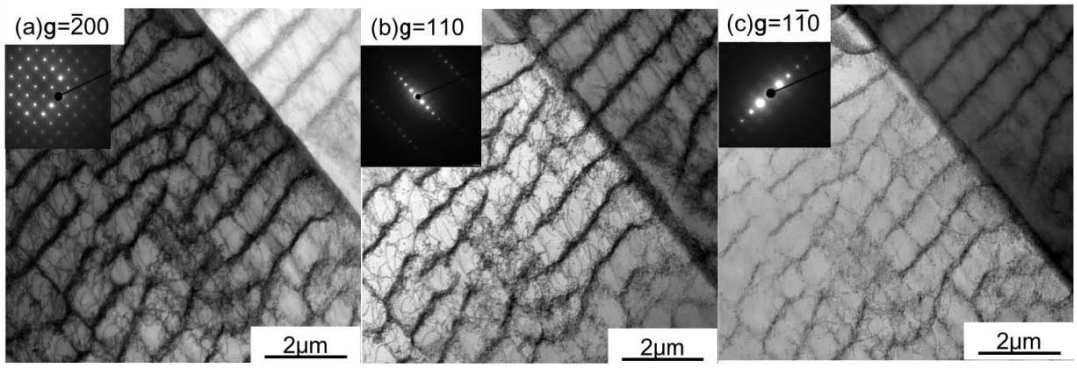

Fig. 3**.** STEM images of wall structures in a grain oriented to [001] observed with various g conditions. (a) **g** = -200, (b) **g** = 110, and (c) **g** = 1-10.

REFERENCES

[1] Shuto, H., Yokoi, T.: CAMP-ISIJ 28, 261 (2015).

[2] Fielding, S., Stobbs, W.: Dislocation structures in fatigued polycrystalline stainless steel. J. Microscopy 130, 279-288 (1983).

[3] Turenne, S., L'espérance, G., Dickson, J.: The orientations of dipolar dislocation structures produced by the cyclic deformation of B.C.C. metals. Acta Metall. 36, 459-468 (1988).

[4] Petrenec, M., Polák, J., Obrtlík, K., Man, J.: Dislocation structures in cyclically strained X10CrAl24 ferritic steel. Acta Mater. 54, 3429-3443 (2006).

[5] Li, P., Li, S., Wang, Z., Zhang, Z.: Fundamental factors on formation mechanism of dislocation arrangements in cyclically deformed fcc single crystals. Progress in Mater. Sci., 56, 328-377 (2011).

ACKNOWLEDGMENTS

Supported by "Nanotechnology Platform Japan" program by the Ministry of Education, Culture, Sports, Science and Technology.

Characterization of the Fatigue Behavior of Mechanical and Thermal Aged Austenitic Power Plant Steel AISI 347

F. Maci[a*], M. Jamrozy[a], R. de Acosta[b], P. Starke[b], C. Boller[b], K. Heckmann[c], J. Sievers[c], T. Schopf[d], F. Walther[a]

[a] *Department of Materials Test Engineering (WPT), TU Dortmund University, 44227 Dortmund, Germany*
[b] *Chair of Non-Destructive Testing and Quality Assurance (LZfPQ), Saarland University, 66125 Saarbrücken, Germany*
[c] *Gesellschaft für Anlagen- und Reaktorsicherheit (GRS) gGmbH, 50667 Köln, Germany*
[d] *Materials Testing Institute (MPA), University of Stuttgart, 70569 Stuttgart, Germany*
**Corresponding author: frankel.maci@tu-dortmund.de*

Keywords: AISI 347; Aging; Multiple amplitude test; Fatigue, Non-destructive testing.

ABSTRACT

For the characterization of the mechanical and thermal aging of materials used in nuclear power plant reactors, an innovative lifetime calculation method is developed based on cyclical investigations and microstructure analysis. The deformation behavior in multiple amplitude and constant amplitude tests is evaluated by non-destructive testing methods based on magnetic, resistometric and electrochemical measurement techniques in order to determine the fatigue properties of AISI 347. To generate a realistic basis of data, cyclic investigations are carried out in air as well as under distilled water conditions. For both environmental conditions, specimens in the initial state and after a mechanical and thermal aging are tested. The validation of both material states shows a significant influence of the aging on the fatigue properties by a lower stress amplitude at failure for the aged specimen, which is about 70% of the stress amplitude at failure of the initial state.

INTRODUCTION

Materials of components in boiling water reactors in nuclear power plants are exposed to aging mechanisms that take influence on the fatigue properties. The hot water and the high pressure environment as well as thermal expansions and compressions through startup and shutdown processes of the reactor lead to mechanical and thermal fatigue, with simultaneous environmental influences. This causes a limit in service time due to crack formation, initiation and growth. To provide a safe and optimized application of the material, an innovative, resource- and time-optimized test method is developed with the aim to estimate the fatigue life. Therefore, total strain-controlled multiple amplitude tests (MAT) are carried out on austenitic stainless steel AISI 347 (X6CrNiNb18-10, 1.4550) instrumented with magnetic, resistometric and electrochemical testing methods to identify critical strain levels. These tests also support the development and improvement of analysis models for crack formation, crack growth and rupture under fatigue loading relevant for lifetime and safety assessments. Validation of the testing results is realized by total strain-controlled constant amplitude tests (CAT) on the previously in MAT identified strain levels. Within this paper, investigations in air and in distilled water conditions are carried out for initial state and after mechanical and thermal aging. The aging process is realized by cyclic investigations in air with a total strain amplitude of 0.3%, a constant strain rate of $0.4 \cdot 10^{-3}$ s^{-1} and a superimposed operational temperature of 240°C. The cyclic investigations are stopped after 50% of the number of cycles to failure (15,725 cycles), which results in a test time of approx. 12.5 hours. The number of cycles to failure was estimated statistically in preliminary tests.

RESULTS AND CONCLUSIONS

In good agreement to preliminary tests [1], no significant influence of the distilled water on the fatigue properties was obtained, so it can be used to extend the field of non-destructive testing and evaluation by electrochemical methods. The correlation between MAT in distilled water for initial state and aged samples (Fig. 1) shows a significant influence of the aging process. The correlated total strain amplitude $\varepsilon_{a,t,cor}$ is the strain value that results in the gauge length, defined by previously carried out calibration tests. The investigations start at a cor. total strain amplitude $\varepsilon_{a,t,start} = 0.05\%$, and the cor. total strain amplitude is increased each 1,800 s for $\Delta\varepsilon_{a,t} = 0.05\%$. Due to the aging process the max. reached cor. total strain level of 0.90% at stress amplitude at failure $\sigma_{a,f} = 750$ MPa for the initial state is reduced down to 0.65% at $\sigma_{a,f} = 535$ MPa. The comparison of the stress amplitude for both material states shows a qualitatively similar curve. At strain levels greater $\varepsilon_{a,t,cor} = 0.30\%$, aged sample reaches lower stress values.

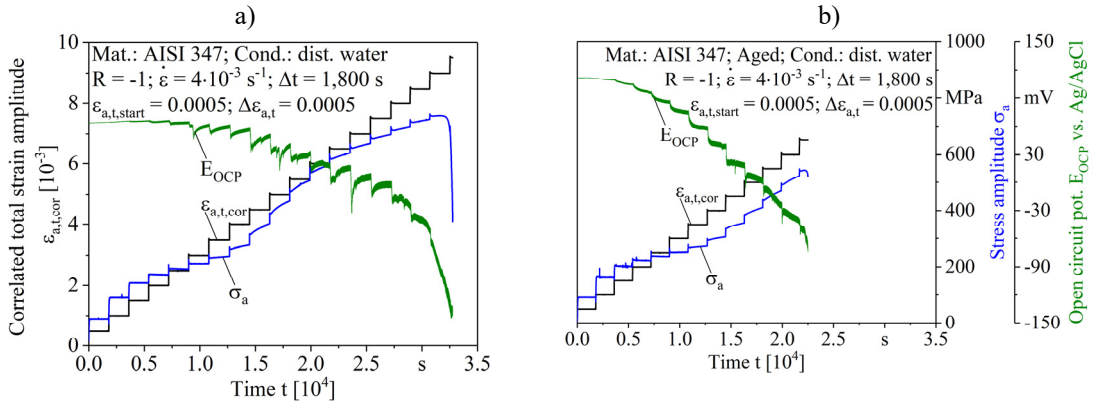

Fig. 1. Total strain-controlled multiple amplitude tests for AISI 347 in distilled water conditions for a) initial state and b) after aging.

The open circuit potential E_{OCP} has been measured and compared for both material states as a further material response. E_{OCP} for the initial state is approximately constant until $\varepsilon_{a,t,cor} = 0.25\%$. For higher strain levels, E_{OCP} drops at the beginning of every step to a local minimum. This drop is due to a steady rupture of the passive film caused by the mechanical loading, which exposes consequently a fresh and active material surface. Up to $\varepsilon_{a,t,cor} = 0.80\%$, E_{OCP} increases during the constant cyclic loading within the strain levels. A reason for this is assumed to be the passivation on the new surface [2]. From $\varepsilon_{a,t,cor} = 0.80\%$ onwards, which is the penultimate strain level, E_{OCP} decreases until failure. E_{OCP} of the aged specimen decreases from the beginning and a passivation effect cannot be observed. The results show, that aging influences the effect of passivation. At $\varepsilon_{a,t,cor} = 0.55\%$ the trend of E_{OCP} decreases again, when compared to the previous strain level. This trend could be shown in the penultimate step for the initial state and for the aged samples. Therefore, the failure of the specimens can be estimated two steps before fracture by measuring E_{OCP}.

REFERENCES

[1] Klein, M., Starke, P., Nowak, D., Boller, C., Walther, F.: Separation of surface, subsurface and volume fatigue damage effects in AISI 348 steel for power plant applications. Materials Testing 58(7-8), 601-607 (2016).

[2] Sun, Y., Rana, V.: Tribocorrosion behaviour of AISI 304 stainless steel in 0.5 M NaCl solution. Materials Chemistry and Physics 129.1, 138-147 (2011).

ACKNOWLEDGMENTS

The authors thank the German Federal Ministry for Economic Affairs and Energy (BMWi) for the financial support within the joint research project “Microstructure-based determination of maximum operation time for corrosion fatigue-loaded materials and components of nuclear technology“ (funding numbers 1501528A, 1501528B, 1501528C, and RS1545).

Micromechanical Simulation of Fatigue in Nodular Cast Iron

M. Lukhi[a*], M. Kuna[a], G. Hütter[a]

[a] *Technische Universität Bergakademie Freiberg, Germany*
**Corresponding author: mehul.lukhi@imfd.tu-freiberg.de*

Keywords: Nodular cast iron; Void ratchetting; Low cycle fatigue; Unit cell model.

ABSTRACT

Nodular cast iron (NCI) is an iron-carbon alloy which exhibits comparable mechanical properties like engineering steels. These favourable properties are due to the shape of the graphite particle present in the matrix. The form of graphite particles is nodular in comparison to other cast iron having graphite particles in flake or vermicular form. The nodularity of the graphite particles can be promoted by the addition of magnesium, cerium etc. The manufacturing cost of NCI is less than of engineering steels. Due to cost-effectiveness and similar mechanical properties, nodular cast iron is widely used in automobile, energy and transportation industries in different applications [1].

The strength and ductility of NCI depend on the shape, size, and distribution of graphite particle along with microstructure of the matrix. There exist also some casting defects in the material which affect the properties of NCI. Most of the structural components in the different industries are subjected to cyclic loading. That is why it is important to understand fatigue mechanisms in the material.

The low cycle fatigue is dominated by high plastic strain accumulation. When elastic – plastic porous materials are subjected to cyclic deformations, they experience an increase in void volume fraction called void ratchetting. This observation is confirmed by experiments and simulations as well [2]–[6]. However, only a few cycles have been simulated until now. We propose that the void ratchetting is a potential mechanism of low cycle fatigue (LCF) in NCI. To confirm this hypothesis, we have created a micromechanics-based axisymmetric Finite-Element unit cell. This cell is subjected to uni-axial cyclic deformations and simulations are carried out till final failure of the model. The unit cell model is described in Fig. The matrix material is defined as an elastic – plastic one with hardening exponent N.

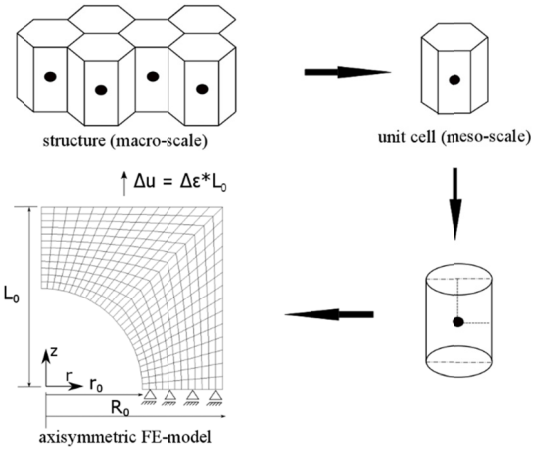

Fig. 1**.** The unit cell model for the nodular cast iron.

When the unit cell is subjected to cyclic deformations, void ratchetting is observed. The macroscopic stress response of model is a cyclic hardening followed by softening. When geometrical softening begins, a sudden drop in macroscopic stress is defined as a failure point in this study. Further internal necking occurs which is associated with coalescence of voids and finally leads to the formation of a macroscopic crack. Komotori *et. al* [6] have indeed observed void growth and coalescence in the ferritic ductile cast iron material under cyclic loading. This is shown in Fig. 2.

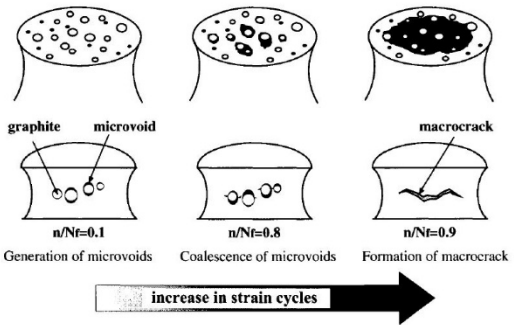

Fig. 2. Void coalescence under cyclic loading [6].

Different strain amplitudes ($\Delta\varepsilon$) are applied and the number of cycles to failure (N_f) is extracted from the simulations. The simulation results are compared with the experimental results collected from the literature [5,6] among others. The effects of hardening models, graphite particle inclusion, the shape of graphite particle, load sequencing and material strength on strain vs life have been studied. From the comparison, it is confirmed that void ratchetting is the relevant low cycle fatigue mechanism in NCI. The simulations results are in qualitative agreement with experimental results but there is a quantitative mismatch. The simulation results better agree quantitatively with experimental results when the non-spherical shape of graphite particles is considered. The first results of studying high cycle fatigue are reported as well. The aim of this research is to gather complete information about fatigue in NCI and optimize the design of NCI microstructure.

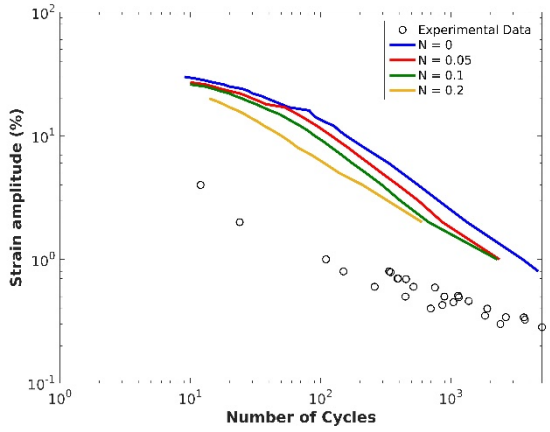

Fig. 3**.** The strain vs life curves extracted from the simulations and experimental data from literature.

REFERENCES

[1] Hütter, G., Zybell, L., Kuna, M.: Micromechanisms of fracture in nodular cast iron: From experimental findings towards modeling strategies - A review. Eng. Fract. Mech. 144, 118-141 (2015).
[2] Gilles, G., Jullien, B.: Analysis of cyclic effects on ductile tearing strength by a local approach of fracture. Adv. Fract. Model. Anal. Eng. Probl. 137, 269–283 (1992).
[3] Rabold, F., Kuna, M.: Cell model simulation of void growth in nodular cast iron under cyclic loading. Comp. Materials Sci. 32(3), 489-497 (2005).
[4] Mbiakop, A., Constantinescu, A., Danas, K.: On void shape effects of periodic elasto-plastic materials subjected to cyclic loading. Eur. J. Mech. A/Solids 49, 481-499 (2015).
[5] Petrenec, M., Tesařová, H., Beran, P., Šmíd, M., Roupcová, P.: Comparison of low cycle fatigue of ductile cast irons with different matrix alloyed with nickel. Proc. Engi. 2(1), 2307–2316 (2010).
[6] Komotori, J., Shimizu, M.: Fracture mechanism of ferritic ductile cast iron in extremely low cycle fatigue. K-T. Rie and P.D. Portella (eds), Low Cycle Fatigue Elasto-Plastic Behav. Mater. 2, 39–44 (1998).

ACKNOWLEDGMENTS

This work is funded by ESF (European social fund) scholarship for Mehul Lukhi under country innovation project (SAB application number: 100284311) in Saxony, Germany. The authors would also like to thank Prof. Peter Hübner for valuable discussions.

On the Sources of Cyclic Slip Irreversibility Leading to Fatigue Crack Initiation

J. Polák[a,b*], V. Mazánová[a], M. Heczko[a]

[a]*Institute of Physics of Materials, Academy of Sciences of the Czech Republic, Czech Republic*
[a]*CEITEC IPM, Institute of Physics of Materials, Academy of Sciences of the Czech Republic, Czech Republic*
**Corresponding author: polak@ipm.cz*

Keywords: Fatigue; Cyclic slip; Irreversibility; Initiation; Persistent slip marking.

ABSTRACT

Experimental studies of the surface relief of the metal single and polycrystals revealed the formation of the pronounced surface relief, which precedes the formation of fatigue cracks [1]. Characteristic feature of the surface relief is the alternation of the areas having original flat surface and the areas in the form of strips with very pronounced profile. These strips, called persistent slip markings (PSMs) result from the localization of the cyclic plastic strain into persistent slip bands (PSBs) and are located where PSBs emerge on the surface. PSMs in individual grains of a polycrystal consist of an extrusion or an intrusion and most often pronounced extrusion is accompanied by parallel intrusion. In single crystal macrobands consisting of numerous alternating extrusions and intrusions are most typical.

Since cyclic plastic strain is localized in PSBs the original explanation of the PSB formation was the random slip within the PSBs [2]. Later physically based models based on the production of point defects [3] and production and migration of point defects [4,5] were proposed.

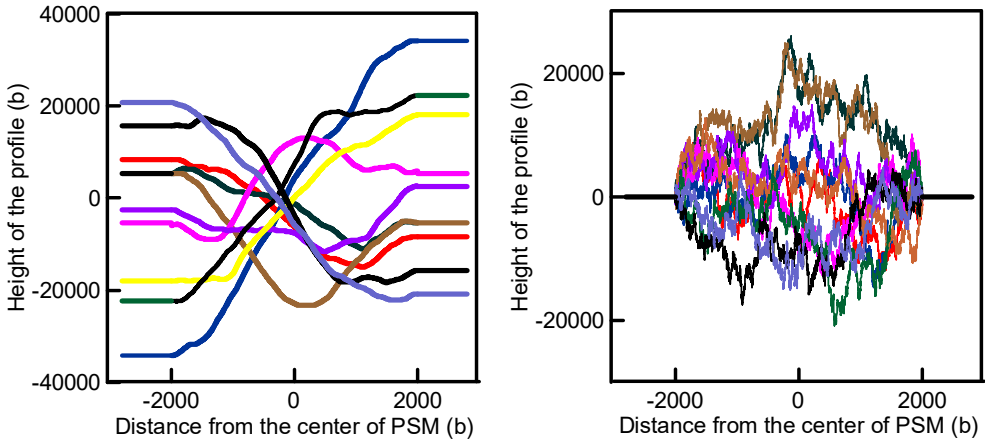

Fig. 1. Profiles of the PSMs generated using two distributions of slip intervals and slip step heights; (a) slip intervals from experiment, random straining; (b) unit slip intervals, symmetrical straining.(b is the modulus of Burgers vector)

Present paper presents simulations of the intensive slip within PSB which leads to the formation of the surface relief. Fig. 1 shows the profiles of PSM produced by random slip using two distributions of slip intervals and slip step heights. Fig. 1a corresponds to the distribution of slip intervals of slip heights found by Weidner et al. [6]. The slips in tensile and compression directions are not correlated and both extrusion and intrusion type profile as well as unidirectional slip steps result. Fig. 1b corresponds to slip interval of unit length (b) and to symmetric straining of PSB with constant plastic strain amplitude 1%.

The predictions of the simulations are compared with several recent experimental findings of the shapes of the PSBs in metal single and polycrystals. Fig. 2 shows typical profiles of PSMs in polycrystalline copper and in stainless steel. In both case PSM consists of a large extrusion accompanied on one or on both sides by a thin intrusion.

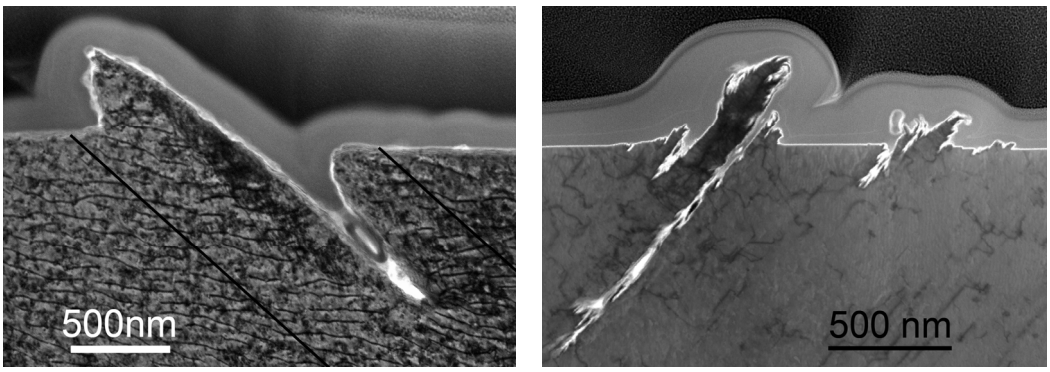

(a) (b)

Fig. 2. Surface profiles of PSMs imaged using STEM, (a) PSM in surface grain of polycrystrystalline copper; (b) PSM in surface grain of austenitic steel

The comparison of random slip simulations with experiments shows that even in the case the simulations are based on experimental assessment of the slip steps during cyclic loading [6] the simulated profiles differ substantially from those recorded experimentally. Contrary to simulations experiments show PSMs consisting of large extrusion and parallel thin intrusions. Also the predicted heights of the PSBs are smaller than observed in experiments for equal number of loading cycles.

In order to arrive at satisfactory agreement with experiment the models based on the dislocation movement and their interactions in the bands of intensive cyclic slip - PSBs - are considered [3-5]. The principal source of the cyclic slip irreversibility is not a random irreversible slip of dislocations but the internal compressive and tensile stresses due production of point defects in PSBs and their systematic migration to the neighbor matrix. The predictions of these models leading to irreversible cyclic clip producing extrusions and intrusions are compared with former and recent experimental documentations of the profiles of PSBs. The advantages and deficiencies of individual models are discussed.

REFERENCES

[1] Man, J., Obrtlík, K., Polák, J.: Extrusions and intrusions in fatigued metals. Part 1. State of the art and history, Philos. Mag. 89(16) 1295-1336 (2009).
[2] May, A.N.: Random Slip Model of Fatigue and Coffins Law, Nature 188(4750) 573-574 (1960).
[3] Essmann, U., Gosele, U., Mughrabi, H.: A Model of Extrusions and Intrusions in Fatigued Metals .1. Point-Defect Production and the Growth of Extrusions, Philos. Mag. A 44(2), 405-426 (1981).
[4] Polák, J.: On the role of point defects in fatigue crack initiation, Mater. Sci. Eng. 92, 71-80 (1987).
[5] Polák, J., Man, J.: Mechanisms of extrusion and intrusion formation in fatigued crystalline materials, Mater. Sci. Eng. A 596, 15-24 (2014).
[6] Weidner, A., Man, J., Tirschler, W. et al.: Half-cycle slip activity of persistent slip bands at different stages of fatigue life of polycrystalline nickel, Mater. Sci. Eng. 492 (1-2), 118-127 (2008).

ACKNOWLEDGMENTS

The present work was conducted in the frame of IPMinfra supported through project no. LM2015069 and the project CEITEC 2020 no. LQ1601 of MEYS. The support by the project RVO: 68081723 is also gratefully acknowledged.

Influence of Heat Treatment Process to the Fatigue Properties of High Strength Steel

V. Chmelko[a*], I. Berta[b], M. Margetin[a]

[a] *Department of Applied Mechanics and Mechatronics, Slovak University of Technology in Bratislava, Slovakia*
[b] *Department of Materials and Technologies, Slovak University of Technology in Bratislava, Slovakia*
**Corresponding author: vladimir.chmelko@stuba.sk*

Keywords: fatigue properties; high strength steel; heat treatment

ABSTRACT

High strength of the steels and their good mechanical properties are achieved by the heat treatment. It is very difficult to choose such procedure and the type of the heat treatment which leads to the balanced mechanical properties in area of the strength, tensibility and fatigue strength. As example can be two practically identical steels with the chemical composition listed in the Tab.1.

Table 1. Comparison of chemical composition of two material

Chemical elements	C	Mn	Ni	Cr	Al	Si	Mo	Cu	Co	V
Material A	0.4	0.65	1.7	0.78	0.028	0.24	0.25	0.11	0.01	0.01
Material B	0.42	0.7	1.85	0.82	0.024	0.25	0.28	0.12	0.02	0.01

Both materials have been heat treated according the prescribed procedure given in Tab.2.

Table 2. Comparison of the heat treatment procedure for two materials

Heat treatment	Forging	Normalization annealing	Annealing to the soft	Oil hardening	Hardening by air	Tempering
Temperature [°C]	1100-850	850-880	680-720	850-880	810-850	560-680

Due to the alleged difference in the severity of these two steels, an experimental program was proposed. The aim was to assess the impact of allegedly different ductility values in terms of the use of steels in cyclic loading. Simple tensile tests as well as cyclical tests in both controlled and controlled mode were performed. A comparison of the tensile curves of the steel is shown in Fig. 1a and shows the difference in strength properties of these two steels. The differences of tensibility were not observed by measurement. Surprising were the differences in cyclic properties of the compared steels which document the comparison of Basquin curves in Fig. 2b.

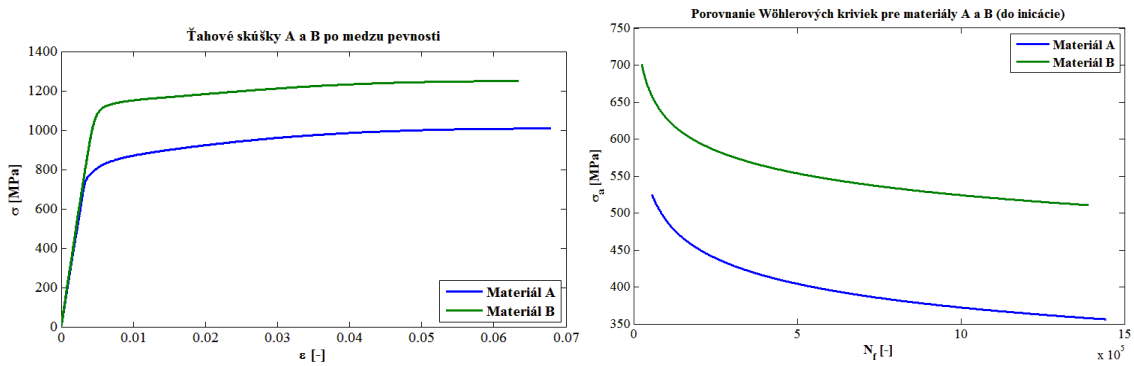

Fig. 1. a/ Comparison of the tensile curves of steels; b/ Comparison of the Basquin curves of the steels.

The tensibilities of those compared steels were practically identical as well as notch toughness. The explanation of those high differences in cyclic properties for comparing steels is necessary to seek in microstructure of the steels (Fig.2)

.

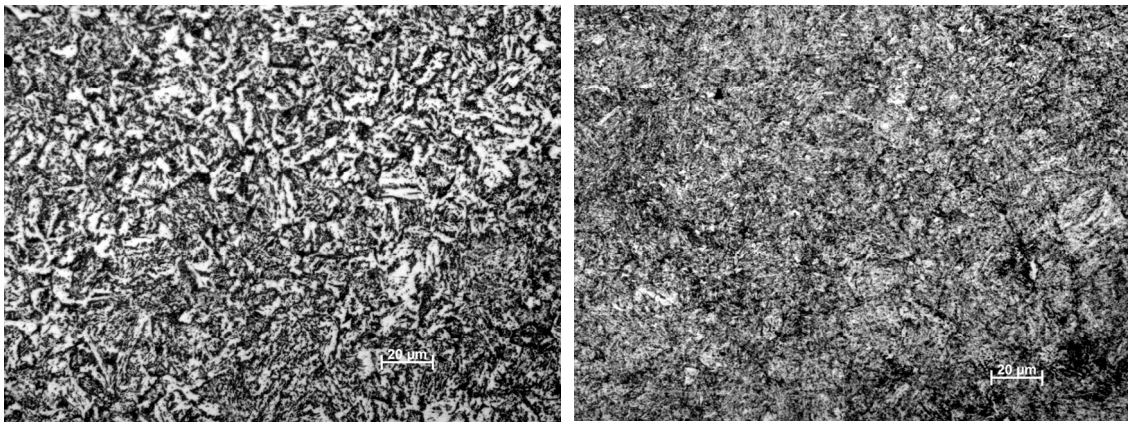

Fig. 2. Comparison of microstructure: on the left – the material A: on the right - material B.

The difference of microstructure is possible to see also from simple optical metallography of both steels. The presence of thickened carbides and the boundaries of the original austenitic grains is the result of different temperatures i.e. longer tempering time in the heat treatment process, which can be proved directly by repeating the heat treatment process of both steels.

ACKNOWLEDGMENTS

This work was supported by the Research & Development Operational Programme funded by the ERDF ITMS: 26240220084 Science city Bratislava.

Microscopic Strain Localization of Ti-6Al-4V Alloy Under Uniaxial Tensile Loading

Guang-Jian Yuan[a], Xian-Cheng Zhang[a*], Shan-Tung Tu[a]

[a] *School of Mechanical and Power Engineering, East China University of Science and Technology, Shanghai 200237*
**Corresponding author: xczhang@ecust.edu.cn*

Keywords: Ti-6Al-4V alloy; Micromechanical modelling; Inhomogeneity.

ABSTRACT

In this paper, Plate specimens (Fig. 1) for tensile tests with two different microstructures (as-received and heat treated) were studied. Micromechanical modelling of Ti-6Al-4V (TC4) alloy by using a representative volume element (RVE) [1] is used to investigate the tensile flow behavior. Voronoi tessellation (VT) model and actual microstructure model were developed to predict the macro macroscopic stress versus strain behaviour, as shown in Fig. 2. Kinematic hardening rule was used to simulate the nonlinear hardening. Results showed that Both VT model and actual microstructure model has good ability to predict the stress-strain response (Fig. 3). The stress and strain distribution (Fig. 4) showed that VT model agreed with the microstructure-based model well. In addition, the microstructure-level inhomogeneity and incompatible deformation between the hard and soft phases are the main reason for damage.

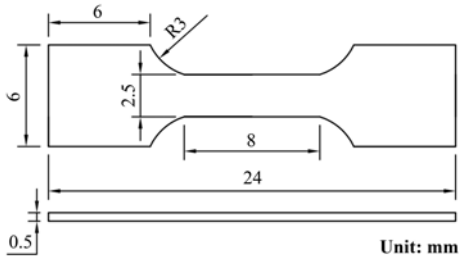

Fig. 1**.** A schematic of the specimen used in the experiment, with gauge length of 8mm, width of 2.5mm and thickness of 0.5mm.

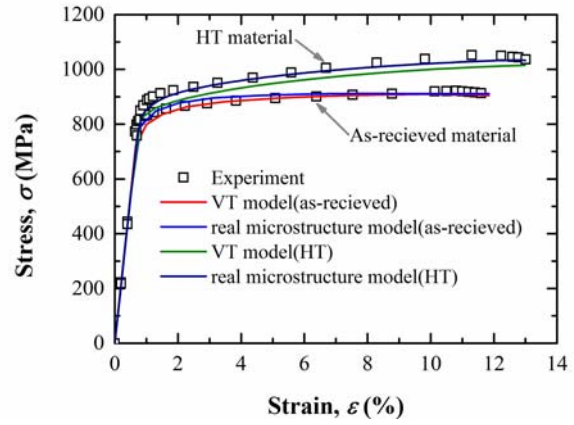

Fig. 2**.** Comparison of stress-strain curve between experiment and simulation results.

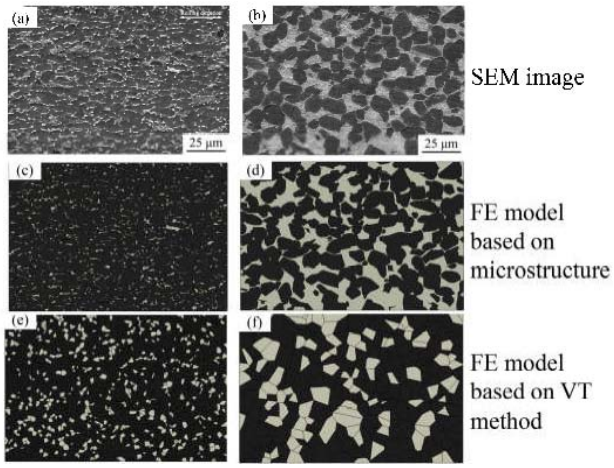

Fig. 3. (a) as-received TC4 SEM image, (b) heat treated TC4 SEM image, (c) as-received TC4 FE model based on microstructure, (d) heat treat TC4 FE model based on microstructure, (e) as-received TC4 FE model based on VT method, (f) heat treat TC4 FE model based on VT method.

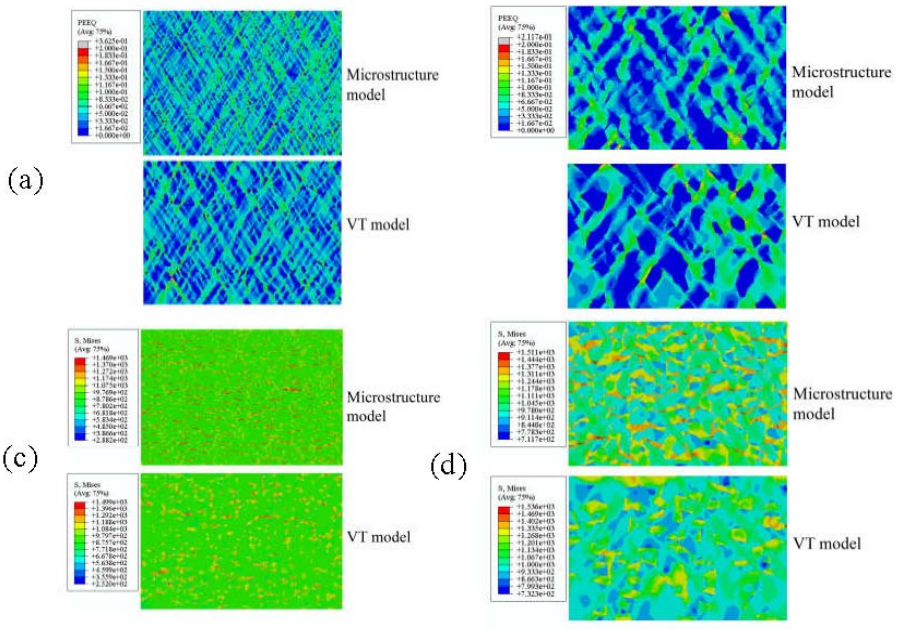

Fig. 4. (a) strain distribution of as-received TC4, (b) strain distribution of heat treated TC4, (c) stress distribution of as-received TC4, (b) stress distribution of heat treated TC4.

REFERENCES

[1] Moeini, G., Ramazani, A., Sundararaghavan, V., Könke, C.: Micromechanical modeling of fatigue behavior of DP steels. Materials Science & Engineering A 689, 89-95 (2017).

ACKNOWLEDGMENTS

The authors would like to acknowledge gratefully for the financial support through NSFC of China (51371082, 51575183) and 111 Project. XZ is also grateful for the support by Shanghai Pujiang Program, Young Scholar of the Yangtze River Scholars Program, and Shanghai Technology Innovation Program of SHEITC (CXY-2015-001).

Thermal Fatigue of H11 Steel in High Pressure Die Casting Conditions

Z. Dadić[a*], D. Živković[a], N. Čatipović[a], I. Marinić-Kragić[a]

[a] *Department of Mechanical Engineering Technology, Faculty of Electrical Engineering, Mechanical Engineering and Naval Architecture, University of Split, Croatia*
**Corresponding author: zdadic@fesb.hr*

Keywords: Tribology; Thermal fatigue; High pressure die casting; Preheating temperature.

ABSTRACT

Results shown in this paper were acquired on prototype wear testing equipment. This paper is a part of experimental research in area of high pressure die casting mould wear (H11). Those equipment was designed to achieve and analyze tribological wear mechanisms of a casting mould such as: thermal fatigue, erosion and adhesion wear. The equipment simulates industry conditions to help predict wear intensity. Testing parameters were set to simulate conditions in high pressure die casting of aluminium. Results for thermal fatigue wear of the mould material are presented for two samples. Samples were tested under same parameters for 10000 testing cycles, except with significantly different preheating temperature. Results are shown graphically by 3D scan before and after the experiment. The wear was also confirmed by mass loss of the tested samples.

Analysis of Complex Waveshape Signals on Environmentally-Assisted Cracking During Low-Cycle in PWR Environment of a 304L Stainless Steel

Thibault Poulain[a], José Mendez[a], Laurent de Baglion[b], Gilbert Hénaff[a*]

[a] *Pprime Institute, UPR 3346 CNRS ENSMA Université de Poitiers, Department of Mechanics and Physics of Materials, Futuroscope Chasseneuil, France*
[b] *Framatome, 1 place Jean Millier, 92 084 La Défense Cedex, France*
**Corresponding author: gilbert.henaff@isae-ensma.fr*

Keywords: Strain rate; Crack growth rate; Striation; Austenitic stainless steel.

ABSTRACT

It is well established that the low-cycle fatigue resistance of austenitic stainless steels used in nuclear power plants is altered by the action of the Primary Water Reactor (PWR) medium circulating in pipes [1]. However, while this degradation is taken into account in design codes, the controlling parameters still need clarification. This is mainly due to the complex interplay taking place between different factors such as strain amplitude, strain rate [2,3]. This is even more complicated when considering complex wave shapes, representative of actual loading conditions, characterised by a strain rate varying during a given fatigue cycle. The present study is precisely tackling this issue in the case of a 304L stainless steel. With this aim, low-cycle tests have been performed on cylindrical polished samples in PWR simulated environment, at a strain amplitude of 0.6% and under push-pull conditions, using triangular waveshapes with fixed strain rates, but also two complex waveshapes characterised by a varying strain rate and noted SIS A and SIS B signals (Fig. 1). The fatigue lives are analysed on the basis of the influence of strain rate and waveshape on crack growth rates, derived from post-mortem striation measurements on fracture surfaces and expressed as a function of the strain intensity factor [4-6]. It is shown that the fatigue lives as the crack growth rates in PWR are controlled by a characteristic time noted T*, corresponding with exposure duration under a positive strain rate with a fully opened crack, and which is significantly different according to the complex signal considered as shown in Fig. 1. Moreover, while the crack growth rate enhancement is time dependent for T*<50s, a saturation in environmental effect is noticed for T*>50s, consistently with the fatigue life data.

REFERENCES

[1] Atkinson, J.D., Forrest, J.E.: Factors influencing the rate of growth of fatigue cracks in RPV steels exposed to a simulated PWR primary water environment. Corrosion Science 25(8-9), 607-631 (1985).
[2] Tsutsumi, K., Dodo, T., Kanasaki, H., Nomoto, S., Minami, Y., Nakamura, T.: Fatigue behavior of stainless steel under conditions of changing strain rate in PWR primary water. Pressure Vessel and Piping Codes and Standards, ASME: New York, 135–141 (2001).
[3] Higuchi, M., Sakaguchi, K., Nomura, Y.: Proceedings of the ASME Pressure Vessels and Piping Conference, Vol 1: Codes and Standards, ed. K. Hasegawa and D.A. Scarth; Vol. 1: 123-131 (2007).
[4] Boettner, R.C., Laird, C., McEvily, A.J.: Crack nucleation and growth in high strain-low cycle fatigue. Transactions of the Metallurgical Society of AIME 233 (2), 379-387 (1965).
[5] Kamaya, M.: Low-cycle fatigue crack growth prediction by strain intensity factor. International Journal of Fatigue 72, 80-89 (2015).

[6] Poulain, T., Mendez, J., Henaff, G., de Baglion, L.: Analysis of the ground surface finish effect on the LCF life of a 304L austenitic stainless steel in air and in PWR environment. Engineering Fracture Mechanics 185, 258-270 (2017).

ACKNOWLEDGMENTS

The authors thank Areva for the financial support and the technical centre of Areva in Le Creusot for the completion of tests in PWR water environment.

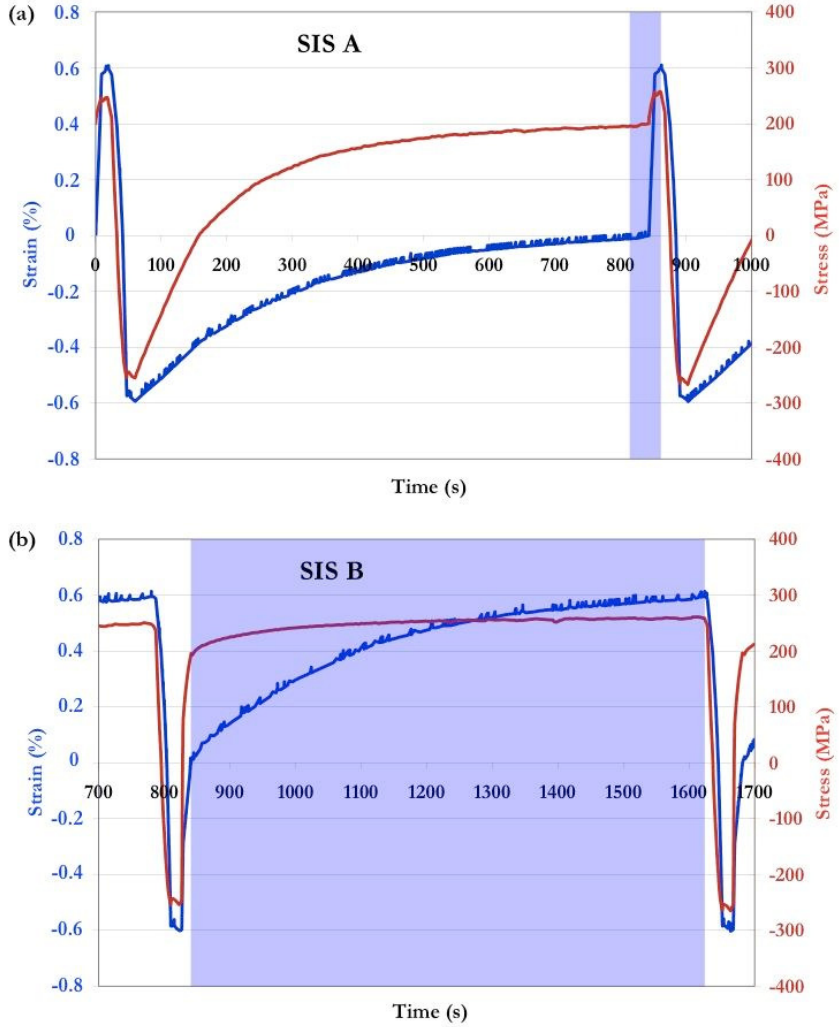

Fig. 1**.** Variation of strain and stress in SIS A and in SIS B signals; Representation of the characteristic time T* by the blue area.

Effect of Heat Treatment on High-Temperature Low-Cycle Fatigue Behavior of Nickel-Based GH4169 Alloy

Xu-Min Zhu[a], Xian-Cheng Zhang[a*], Run-Zi Wang[a], Xu Zeng[a]

[a] *Key Laboratory of Pressure Systems and Safety, MOE, East China University of Science and Technology Shanghai, 200237, P.R. China*

**Corresponding author: xczhang@ecust.edu.cn*

Keywords: High-temperature; Low cycle fatigue; δ phase; Nickel-based alloy.

ABSTRACT

The effect of heat treatment on the strain-controlled fatigue behavior of Nickel-based GH4169 alloy at 650℃ was investigated. The volume fraction of δ phase increases as the longer solution annealing time. At the same time the yield strength and the tensile strength of GH4169 alloy decrease gradually. The heat treatment had almost no effect on fatigue life at strain amplitude higher than 0.6%. However, the fatigue life slight increased with increasing the solution annealing time at strain amplitude lower than 0.5%. The alloy does not exhibited dual-slope Coffin-Manson relationships at 650℃. This makes the alloy exhibited the high-temperature fatigue life higher than the room-temperature fatigue life at low strain amplitude.

In this work, Each HT contained two different steps, the solution annealing and the subsequent ageing [1]. The main difference among different HTs was the processing parameter used in the solution annealing, as listed in Table 1.

Table 1. The processing parameters used for solution annealing in different HTs.

HT1	960 °C for 1 h, AC to 720 °C
HT2	960 °C for 1 h, AC to 900 °C, 900 °C for 4 h, 960 °C for 1 h, AC to 720 °C
HT3	960 °C for 1 h, AC to 900 °C, 900 °C for 20 h, 960 °C for 1 h, AC to 720 °C

The microstructures of as-received and heat-treated GH4169 alloys are shown in Fig. 1.The volume fractions of δ phase in GH4169 alloys after HT1, HT2 and HT3 are respectively 2.71%, 9.13% and 13.79%.

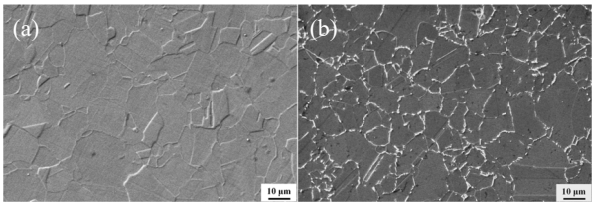

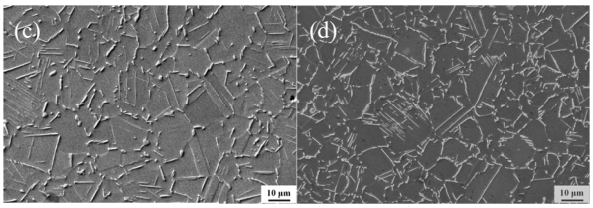

Fig. 1. Microstructures of (a) as-received alloy, and alloys after (b) HT1, (c) HT2, and (d) HT3.

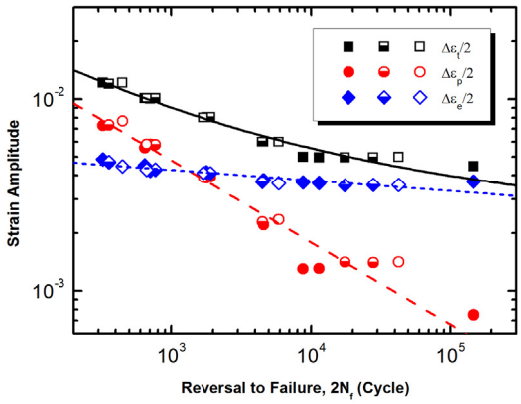

Fig.2. Low cycle fatigue life of GH4169 alloy under 650℃

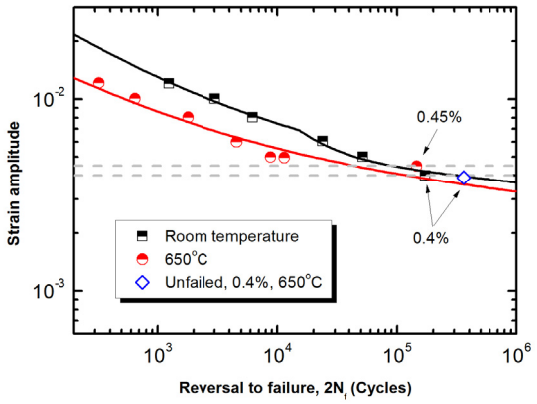

Fig. 3. Comparison of low cycle fatigue life of GH4169 alloy between 650℃ and room temperature

REFERENCES

[1] Donachie, M.J., Donachie, S.J.: Superalloys: A Technical Guide, 2nd edition, ASM International, The Materials Society, Materials Park, Ohio (2002).

ACKNOWLEDGMENTS

The authors would like to acknowledge gratefully for the financial support through National Natural Science Foundations of China (51371082, 51322510) and 111 project. The author X.C. Zhang is also grateful for the support by Shanghai Pujiang Program, Young Scholar of the Yangtze River Scholars Program, and Shanghai Technology Innovation Program of SHEITC (CXY-2015-001).

Evaluation of the Relaxation of Residual Stresses and Their Effects on the Fatigue Strength of Nitrided 42CrMo4 steel: Experimental and Numerical Approaches

R. Bechouel[a,b*], M. Ali Terres[b]

[a] *National Engineering School of Sousse ENISO, University of Sousse, Sousse, Tunisia*
[b] *LMMP, Mechanical Laboratory of Material and Methods, Higher National Engineering School of Tunis, ENSIT, Tunis, Tunisia*
**Corresponding author: bechouel.rafik@gmail.com*

Keywords: Multiaxial fatigue criteria; Numerical Approach; Nitrided steel; Residual Stress relaxation.

ABSTRACT

A numerical approach using FEM for prediction and calculating residual stress and work hardening redistribution during bending fatigue at low cycle fatigue (LCF) has been studied and implemented in the finite element software ABAQUS [4].An experimental evaluation was performed using 3 points bending fatigue test for nitrided steel. The validation of this procedure was carried out by comparing the experimental results taken from XRD measurement to those calculated residual stress profiles. The aptitude prediction for the 42CrMo4 nitrided steel fatigue life was assessed using the multiaxial Crossland criterion with considering the effect of hardening and the stabilized residual stresses.

1. Introduction

Using multiaxial fatigue criterion, such as Crossland's criterion Engineering can predict the fatigue behaviour of nitrided layer [1,3].For this reason, it's necessary to predict the relaxed state of residual stresses after cyclic loading [1,2 et 3]. This work proposes to use a numerical approach based on FE method.

2. Numerical procedure and multi-axial fatigue criterion

2.1 Crossland criterion

To take into account of experimental results [1,3] for calculation HCF strength of nitrided steel Crossland criterion was used. This criterion is expressed by the limitation of equivalent stress Eq (1).

$$\sigma_{eq} = \Delta_{Coct,\,a} + \alpha_c P_{max} \leq \beta_c \quad (1)$$

2.2 Numerical procedure

A 2D finite element model was developed for simulating the 3 points bending loading test using ABAQUS standard software. The finite element model integrates meshing, loading conditions, cyclic material behavior and calculation steps. A nonlinear isotropic-kinematic hardening model was employed in the FE model.The base material constants k, C, c, Q and b of this model for the 42CrMo4 steel were identified from experimental stress-strain hysteresis loops.The obtained values are summarized in Table 1. The results show that the shape of the hysteresis loop (0.85% strain amplitude) is successfully described by the model as shown in Fig 1. The experimental residual stresses and micro-hardness profile of each layer induced by nitrided treatment were introduced under the code ABAQUS as an initial condition using a subroutine written in FORTRAN language.

Table 1. Cyclic behavior law coefficients of 42CrMo4 steel

E(GPa)	ν	K (MPa)	C (MPa)	δ	Q (MPa)	b
201	0.3	980	669420	1064	-636	1046

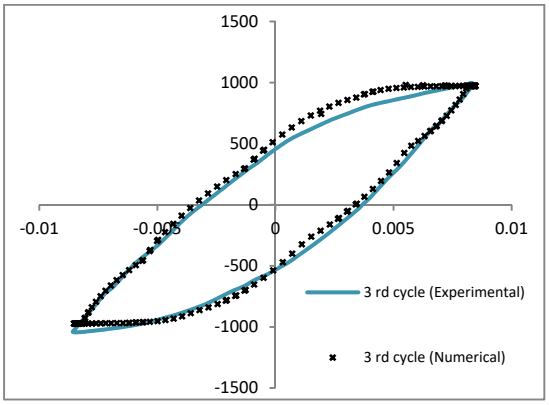

Fig. 1. Comparison between numerical profile and predicted hysteresis loop after 3 cycles.

3. Results and Discussion

The aptitude prediction for the nitrided steel fatigue life was assessed using the multiaxial Crossland criteria with considering the effect of hardening and the stabilized residual stresses. The parameters of Crossland criteria are (α_C=0.3 and β_{0C}=370MPa).The computation results of the new values of (β_{0C} =411 MPa) and their effects on the lines threshold are illustrated in the endurance diagram Fig 2.The Multi-axial criteria is in agreement with experimental results. Experimental and numerical results indicated that the cyclic loading modifies the initial residual stress magnitude of nitrided steel. These modifications are the consequence of plastic strain creation and redistribution during cyclic loading.

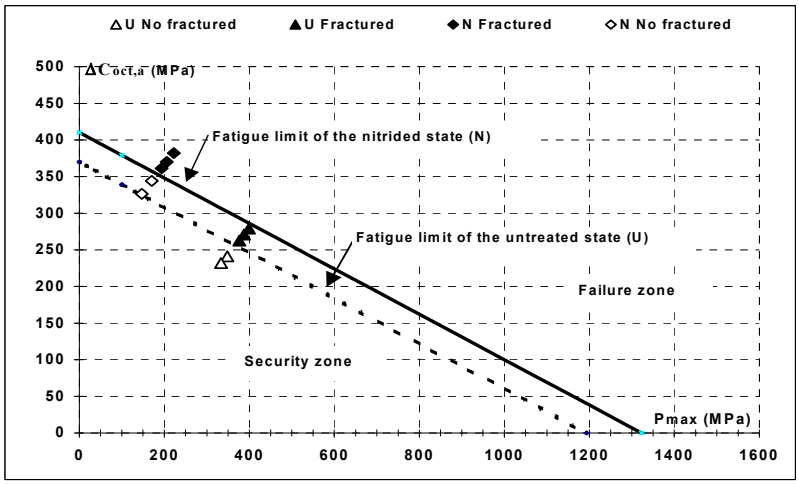

Fig. **2**. Effect of residual stress and hardening on the fatigue strength improvement of nitrided steel.

4. Conclusion

The Numerical approach proposed in this work allows predicting the relaxation of residual stresses induced by ionic nitriding after cyclic loading. Accounting for these surface characteristics by multiaxial fatigue criteria, the fatigue life of nitrided parts has been satisfactory predicted and the beneficial effect of compressive residual stress and hardness are assessed.

REFERENCES

[1] Xie, X.-F., Jiang, W., Luo, Y., Xu, S., Gong, J.-M., Tu, S.-T.: A model to predict the relaxation of weld residual stress by cyclic load: Experimental and finite element modeling. International Journal of Fatigue 95, 293–301 (2017).
[2] Terres, M.A., Bechouel, R., Mohamed, S.B.: Low Cycle Fatigue Behaviour of Nitrided Layer of 42CrMo4 Steel. International Journal of Materials Science and Applications 6(1), 18-27 (2017).
[3] Laamouri, A., Sidhom, H., Braham, C.: Evaluation of residual stress relaxation and its effect on fatigue strength of AISI, 316L stainless steel ground surfaces: Experimental and numerical approaches. International Journal of Fatigue 48, 109–121 (2013).

Fatigue and Fracture of Various Materials

and

Numerical Methods

Advanced Development of Characteristics of the Hysteresis Measurement for Early Detection of Fatigue Damages on Fastening Systems in Concrete

M. Hoepfner[a*]

[a]*Juniorprofessur Befestigungstechnik, Technische Universität Dortmund, Germany*
**Corresponding author: marvin.hoepfner@tu-dortmund.de*

Keywords: Fatigue damage; Hysteresis measurement; Fastening systems; Centroid; Hysteresis loop.

ABSTRACT

To characterize the process of fatigue damages to final failures on fastening systems in concrete, a method for the approximation of hysteresis loops with performance of conformity to measured values and flexibility of different hysteresis forms has been developed. Therefore, an analytical-physical approach, on the basis of viscoelastic material properties and elliptical hysteresis loops according to Lazan [1] in combination to the analytical approximation of hysteresis loops using secondary additive function components [2], was found and applied to experimental fatigue test of fastener systems in concrete. With the resulting hysteresis vector, see Eq. (1), conventional characteristic values of the hysteresis measurement procedure, displacements, stiffness and energies, could also be determined for hysteresis loops with local measurement errors, respectively local limited faulty courses.

$$\vec{H} = \begin{bmatrix} s(t) \\ F(t) \end{bmatrix} = \begin{bmatrix} s_m + s_0 \cdot [\sin(\Omega t + \delta) + a \cdot (\cos(\Omega t + \delta))^m + b \cdot (-\cos(\Omega t + \delta))^m] \\ \frac{C_{zyk}}{b_m} \cdot s_m + C_{zyk} \cdot s_0 \cdot [\sin(\Omega t + \delta_1) + (a-d) \cdot (\cos(\Omega t + \delta_1))^m + (b-e) \cdot (-\cos(\Omega t + \delta_1))^m] \end{bmatrix} \quad (1)$$

$$m = {}^{n}/_{2} \qquad \forall n \in \mathbb{Z} \quad (2)$$

This approximation function allows the mathematical determination of the storage and loss energy, as well as the specific damping, which is used as a character for energy dissipation in the mechanical oscillation process [3], of fastening systems and is used in further correlations with fatigue mechanisms. The parameters *a*, *b*, *d* and *e* in Eq. (1) are calculated by regression analysis, respectively the least squares method [4], and modify the additional adjustment functions in the sinusoidal oscillation of displacement and force. Due to the property of periodic positive and negative values of the adjustment function and the exponent *m*, which is determined according to Eq. (2), a separate effect on loading and unloading phase results. Further investigations of the four variable parameters led to the successful characterisation of an indicator for experimental predictions at an early stage during the test. This property is based on certain geometric changes and curvature of the extreme values in the displacement oscillation and forms of hysteresis areas. The subsequent determination of the hysteresis centroid, as a sensitive characteristic value of the hysteresis measurement, is carried out using the numerical method of individual elements and total centroid of area. Using finite trapezoidal elements, formed by the hysteresis vector described above, the total centroid of the loop can be determined, see Fig.1a. For the comparisons of hysteresis loops depending on the number of cycles, relative values are determined using an imaginary reference system, see Fig. 1b.

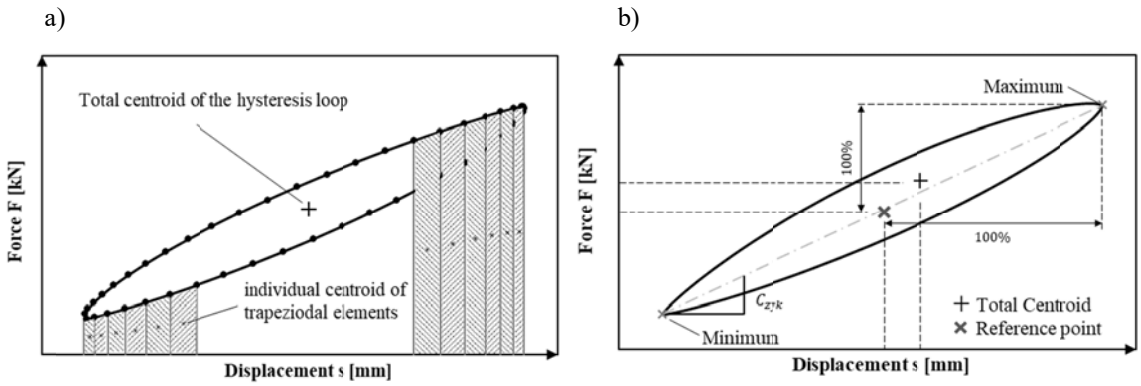

Fig. 1. a) individual centroids of the trapezoidal elements b) imaginary reference point and hysteresis centroid.

The evaluation of the horizontal and vertical positions indicates a permanent asymmetric shape and an inequality between loading and unloading of the displacement in the process. The properties and changes were compared and analysed with the characteristics of the hysteresis measurement method and the approximation.

REFERENCES

[1] Lazan, B. J.: Damping of materials and members in structural mechanics, Pergamon Press, New York (1968).
[2] Lapshin, R.V.: Analytical model for the approximation of hysteresis loop and its application to the scanning tunnelling microscope. Review of Scientific Instruments 66 (9), 4718 (1995).
[3] Dratschmidt, F., Ehrenstein, G.W.: Threaded Joints in Glass Fiber Reinforced Polyamide. Polymer Engineering and Science 37(4), 744-755 (1997).
[4] Grossmann, W.: Grundzüge der Ausgleichsrechnung nach der Methode der kleinsten Quadrate nebst Anwendung in der Geodäsie. Springer Verlag, Berlin/Heidelberg (1969).

Constitutive Modelling of Reinforced Concrete Structures Under Monotonic and Cyclic Loading

L.G. Barbu[a*], X. Martinez[a], S. Oller[a], A.H. Barbat[a]

[a] *Centre Internacional de Mètodes Numèrics en Enginyeria (CIMNE), Universidad Politècnica de Catalunya (UPC), Campus Norte UPC, 08034 Barcelona, Spain*
**Corresponding author: lgratiela@cimne.upc.edu*

Keywords: Reinforced concrete; Serial/parallel rule of mixtures; Damage; Plasticity; Fatigue.

ABSTRACT

This work is centred on the behaviour of a reinforced concrete column-beam union subjected both to monotonic loading and cyclic loading. Reinforced concrete is modelled as a composite material whose properties are dependent on the material properties and constitutive model of its two components: steel and concrete. The behaviour of the composite material will be obtained by means of the serial/parallel rules of mixtures (SP ROM) theory [1].

This method is able to account for the transmission of structural effects from one material to the other implicitly and allows the monitoring of the internal stress-strain state on each component material of the volume afferent to each integration point. Furthermore, its generic integration and equilibrium scheme allows different type of constitutive behaviour for each material that is present in the structure. The methodology thus is highly versatile in this respect.

At the same time, its computational simplicity deems it adequate for performing large-scale numerical analysis while still counting with a significant level of information for each material at each integration point of the structure.

The serial/parallel mixing theory (SP RoM) is based thus on the definition of two different compatibility equations between the strain and stress states of the composite constituent materials: it defines an iso-strain condition on the parallel direction, usually the fiber direction, and it defines an iso-stress condition on the serial direction, usually the remaining directions. Using these compatibility equations in a composite made of matrix and fiber, if the matrix structural capacity is lost due to excessive shear stresses, the iso-stress condition also reduces the shear capacity of fiber, and consequently the composite serial strength is also reduced.

The known variable that enters the algorithm (input) is the strain state ε of the composite material at time $t+\Delta t$. From this input, the S-P RoM has to find a pair of strain/stress tensors for each component that fulfils the equilibrium, compatibility and the constitutive equations in each integration point.

The behaviour of the steel material is modelled by means of the Ultra-Low Cycle Fatigue (ULCF) model presented by Martinez et al. [2], [3]. The model is able to account ULCF effects by incorporating a new law, especially developed for steel materials, that has been designed to reproduce their hardening and softening performance under monotonic and cyclic loading conditions. This law depends on the fracture energy of the material and has been validated on large scale steel models as shown by Barbu et al. [4]. The energy dissipated in each hysteresis loop is monitored and failure under cyclical loads is reached when the total available fracture energy of the material is spent.

A damage model with tension-compression internal variables – Paredes et al. [5] - based on continuum damage mechanics for simulating the opening, closing and reopening of cracks in concrete using only one surface of discontinuity, is used in this work in order to model the constitutive behaviour

of concrete. The model complies with the thermodynamics principles of non-reversible, isothermal and adiabatic processes. Two scalar internal variables have been defined: a tensile damage variable and a compressive damage variable; the threshold of damage is controlled by only one surface of discontinuity and a new parameter that controls the damage variable that should be activated. This parameter is the ratio of tensile stress to compressive stress in the damaged material.

The finite element model that is used in this numerical analysis has been generated with an extremely reduced pre-process time as the generation of the finite elements that contain both a volumetric participation of steel and of concrete has been done automatically, using the same procedure as in [6].

REFERENCES

[1] Rastellini, F., Oller, S., Salomon, O., Oñate, E.: Composite materials non-linear modelling for long fibre reinforced laminates: continuum basis, computational aspects and validations. Computers and Structures 86(9), 879–896 (2008).

[2] Martinez, X., Oller, S., Barbu, L.G. Barbat, A.H., de Jesus, A.M.P.: Analysis of Ultra Low Cycle Fatigue problems with the Barcelona plastic damage model and a new isotropic hardening law. International Journal of Fatigue **73**, 132-142 (2015).

[3] Martinez, X., Oller, S., Barbu, L., Barbat, A.: Analysis of ultra-low cycle fatigue problems with the Barcelona plastic damage model, Computational Plasticity XII. Fundamentals and Applications 352 – 363, ISBN 978-84-941531-5-0 (2013).

[4] Barbu, L.G., Martinez, X., Oller, S., Barbat, A.H.: Validation on large scale tests of a new hardening-softening law for the Barcelona plastic damage model. International Journal of Fatigue 81, 213-226 (2015).

[5] Paredes, J.A., Barbat, A.H., Oller, S.: A compression–tension concrete damage model, applied to a wind turbine reinforced concrete tower. Engineering Structures **33**(12), 3559-3569 (2011).

[6] Barbu, L.G., Escudero, C., Cornejo, A., Martinez, X., Oller, S., Barbat A.: Analysis of pre-tensioned structures by means of a constitutive Serial-Parallel rule of mixtures, Computational Plasticity XIV: Fundamentals and Applications, 471-482. Proceedings of the XIV International Conference on Computational Plasticity, Barcelona, Spain, 5-7 September 2017.

ACKNOWLEDGMENTS

This work has been partially supported by the Spanish “Ministerio de Economía y Competividad” through the projects BIA2015-67807-R - RESCICLO and EUIN2015-62818 - RESSAFE.

Effect of Heat-Treatment on Fatigue Behavior and Microdamage of Trabecular Bone

D. Yang[a*], Y. Wang[a], Y. Chen[b], W. Feng[b], Q.Q. Kong[a], Q.Y. Wang[b,c]

[a] *Institute of Advanced Research, Chengdu University, Chengdu 610106, China*
[b] *School of Mechanical Engineering, Chengdu University, Chengdu 610106, China*
[c] *School of Architecture and Environment, Sichuan University, Chengdu 610065, China*
**Corresponding author: yangdan1234-2004@163.com (D. Yang)*

Keywords: Trabecular bone; Microdamage; Bone fatigue; Organics; Micro-computed tomography.

ABSTRACT

Heat-treatment of xenograft bone is recognized as one of the simple and practical methods to fill the bone voids and overcome the risks of disease transfer during bone transplantation [1]. Investigating the mechanisms of crack initiation, propagation and tissue damage in bone after heat treatment has become a significant topic. While the porous heat-treated trabecular bone may serve as a candidate for xenograft, most of our understanding of microdamage is derived from studies of cortical bone [2]. Different analysis approach is needed to identify the damage in the porous microstructure of trabecular bone.

Microdamage (linear cracks and diffuse damage) accumulates in normal bone during high-intensity training or normal daily activity, which may cause stress fracture or fragility injury but also serve as a toughening mechanism [3]. The heat-treatment leads to the loss of water, organics or even the changes in microstructure. The current study evaluates the fatigue behavior and fatigue-induced damages of the heat-treated bones, in order to gain an insight into the effect of water and organics under fatigue loading and how microdamage accumulates in trabecular bone.

Trabecular bone used was from bovine proximal and distal femur obtained from a local slaughterhouse. The bovine bone has higher strain resistance compared to human one, the fatigue strength was found to be almost identical to that of human [4]. Samples (n=15) were divided into three groups (Control group, G1 and G2) and cut into final cubes of 5*5*6 mm. The marrow existing between trabecular was completely removed. They were immersed in PBS and the temperature was kept under 40°C during preparation process. According to previous literature [5], the dehydration occurs from 40 to 120°C and the loss of organics is finalized at 460°C. The dehydrated group (G1) and organic-removed group (G2) were obtained by placing samples into 60°C or 500°C vacuum oven for 24h.

A compressive cyclic loading is applied at 2Hz between 0.5 N to a normalized stress value σ/E_0 of 0.002 with σ, the load divided by the cross section area and E_0, the initial elastic modulus. The loading is ceased when the reduction of Young's modulus is significant representing the final stage of fatigue life and failure of bone. Before and after fatigue loading, three groups were stained by radio-opaque contrast agents to identify microdamage. Three-dimensional images of cubic trabecular bone were captured by micro-CT to show the microstructure of tissue and distribution of damages. The volume of stained microdamage in the entire specimen was characterized as the damage bone volume fraction [2].

The porous structure of trabecular bone prevents direct observation of microdamage during mechanical testing. The distribution and geometry of microdamage in three dimensions can be observed and assessed by staining approach combined with micro-computed tomography. The dehydration or remove of organics leads to a significant decrease of fatigue life and crack resistance of bone. The main

reasons are attributed to a few large microdamage sites caused by heat-treatment. It is thus suggested that the heated trabecular bone cannot be applied to load-bearing regions of bone.

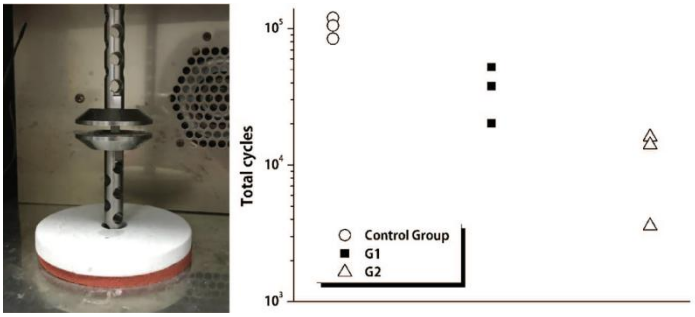

Fig. 1**.** The compression apparatus for fatigue testing (left) and fatigue life of three groups of trabecular bone (right).

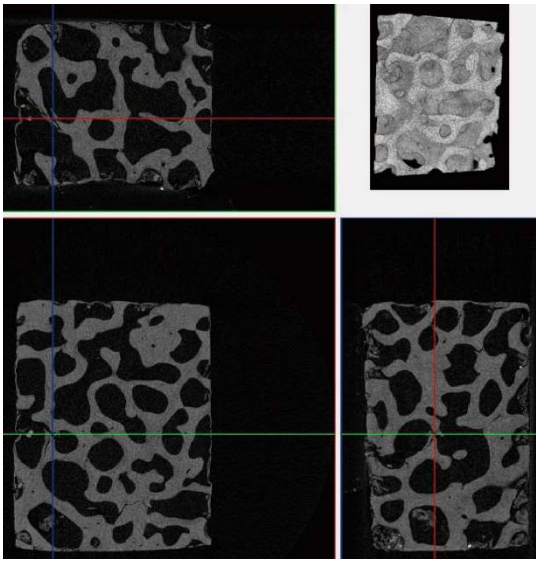

Fig. 2. Typical micro-CT images showing the microstructure and damage of trabecular bone.

REFERENCES

[1] Lau, M., Lau, K., Ku, H., Cardona, F., Lee, J.: Analysis of heat-treated bovine cortical bone by thermal gravimetric and nanoindentation. Composites Part B: Engineering 55, 447–452 (2013).
[2] Goff, M., Lambers, F., Nguyen, T., Sung, J., Rimnac, C., Hernandez, C.: Fatigue-induced microdamage in cancellous bone occurs distant from resorption cavities and trabecular surfaces. Bone 79, 8-14 (2015).
[3] Luo, Q., Leng, H., Wang, X., Zhou, Y., Rong, Q.: The role of water and mineral-collagen interfacial bonding on microdamage progression in bone. Journal of Orthopaedic Research 32, 217-223 (2014).
[4] Fatihhi, S., Rabiatul, A., Harun, M., Kadir, M., Kamarul, T., Syahrom, A.: Effect of torsional loading on compressive fatigue behavior of trabecular bone. Journal of the Mechanical Behavior of Biomedical Materials 54, 21-32 (2016).
[5] Yan, J., Daga, A., Kumar, R., Mecholsky, J.: Fracture toughness and work of fracture of hydrated, dehydrated and ashed bovine bone. Journal of Biomechanics 41, 1929-1936 (2008).

ACKNOWLEDGMENTS

The work was supported by the National Natural Science Foundation of China No. 11572057.

The Elasto-Plastic Analysis of Polymers Subject to Traction and Compression Using Advanced Discretization Techniques

D.E.S. Rodrigues[a*], J.Belinha[a,b], R.M. Natal Jorge[a,c], L.M.J.S. Dinis[a,c]

[a] *Institute of Science and Innovation in Mechanical and Industrial Engineering (INEGI), Portugal.*
[b] *School of Engineering, Polytechnic of Porto (ISEP), Department of Mechanical Engineering, Portugal.*
[c] *Faculty of Engineering of the University of Porto (FEUP), Department of Mechanical Engineering, Portugal.*
**Corresponding author: drodrigues@inegi.up.pt*

Keywords: Polymers; Elasto-plasticity; Meshless methods.

ABSTRACT

Materials such as thermoplastics often have different behaviours when subjected to traction and compression. In those cases, yield criterions need to be appropriately chosen. In this work, thermoplastics used in a particular additive manufacturing process - the fused filament fabrication (FFF) – are investigated. Traction and compression tests are performed using two numerical tools, different yield criterions and three variations of the Newton-Raphson method for the elasto-plastic incremental-iterative process. The stress-strain curves are compared with experimental data provided in the literature. The numerical tools used are the Finite Element Method (FEM) and the Radial Point Interpolation Method (RPIM), which is a meshless method [1]. In order to discretize the problem domain, meshless methods only require an unstructured nodal distribution. The numerical integration of the Galerkin weak form is performed using a background integration mesh and the nodal connectivity is enforced by the overlap of influence-domains defined in each integration point. In the end, a comparison study is performed between the results obtained using meshless methods and the finite element method.

REFERENCES

[1] Belinha, J.: Meshless Methods in Biomechanics - Bone Tissue Remodelling Analysis. Lecture Notes in Computational Vision and Biomechanics 16, Tavares, João Manuel R.S., Jorge, Renato Natal Eds., Springer Netherlands (2014).

ACKNOWLEDGMENTS

The authors truly acknowledge the funding provided by Ministério da Ciência, Tecnologia e Ensino Superior – Fundação para a Ciência e a Tecnologia (Portugal), under grants: SFRH/BPD/111020/2015 and SFRH/BD/121019/2016, and by project funding MIT-EXPL/ISF/0084/2017 and UID/EMS/50022/2013 (funding provided by the inter-institutional projects from LAETA). Additionally, the authors gratefully acknowledge the funding of Project NORTE-01-0145-FEDER-000022 – SciTech – Science and Technology for Competitive and Sustainable Industries, co-financed by Programa Operacional Regional do Norte (NORTE2020), through Fundo Europeu de Desenvolvimento Regional (FEDER).

Miscellaneous Topics

(Posters Session)

Fatigue Behaviour of Cold-Formed Rail Profiles for Racking Structures: a Numerical Simulation Perspective

A. Martins[a*], V. Gomes[a], A.M.P. de Jesus[a,b], A. Santos[a,b], J.A.F.O. Correia[a,b,c], A.A. Fernandes[a,b]

[a]*Faculty of Engineering, University of Porto, Porto, Portugal*
[b]*INEGI, University of Porto, Campus FEUP, Portugal*
[c]*CONSTRUCT, Faculty of Engineering, University of Porto, Campus FEUP, Portugal*
**Corresponding author: up201303013@fe.up.pt*

Keywords: Cold forming; Residual stresses; Fatigue; External cyclic loads; Rail profiles.

ABSTRACT

Cold roll forming is a continuous process aiming a progressive bending of metals using stations with rotating rolls without changing material thickness [1]. Racking systems used today in logistic industries are normally made of thin-walled cold formed steel members. Cold roll forming processes introduce residual stresses in steel components and when combined with service loading stresses (e.g. due to the passage of shuttles in racking systems), these stresses may change the resulting stress range or average, affecting fatigue life of these components. FASTCOLD project purpose is to develop fatigue design rules for cold formed steel members. Design rules already exist for hot-rolled steel details in EN1993-1-9 [2]. However, for cold formed steel sections, they are missing on a European level (EN1993-1-9: Design of steel structures - Part 1-9: Fatigue does not present fatigue design rules or classification of cold-formed thin-walled details) [2]. Due to the lack of these fatigue design rules for cold rolled formed steel members, this paper aims at analysing the stresses induced by roll forming and the influence of external cyclic loads on fatigue life of these profiles.

A parametric study of a U-channel profile with nine simulations was conducted to determine and analyse the influence of several parameters on the final shape of cold roll formed steel profiles, such as the number of forming stations, the ratio radius/thickness, the distance between stations, the material properties, the friction between the rolls and the strip and the number of elements used across the thickness of the strip. More importantly, an evaluation of residual stresses distribution across the thickness and along the surface of the strip width was performed. The development and design of the simulation models (specification of machine parameters, rolls design, flower patter, mesh definition, etc.) and the numerical simulation were performed using COPRA® FEA RF finite element software. Furthermore, a roll forming numerical simulation was also performed for a Z-section profile, in order to analyse the three-dimensional effects of this manufacturing process in this structure, as well as the residual stresses generated. Afterwards, a local stress-based approach was used to estimate fatigue life of these components when subjected to cyclic loading. The stress range calculated incorporated the stresses after the roll forming process and the stresses induced by external cyclic loading. A similar fatigue analyse was conducted for a Z-section (rail section) profile, used in racking systems. Finally, a comparison of the maximum load that can be applied in both profiles in order to achieve a fatigue endurance limit (according to [2], the limit is established for 5 million cycles) was performed.

Numerical results of this study showed that residual stresses across the thickness of both profiles displayed some differences in stress distribution from the theoretical solution of press-braked profiles [3], due to the existence of three-dimensional effects that cannot be neglected (the bending occurs gradually, which can lead to defects such as edge waviness, bow and twist, depending on the design of the process and rolls). Fig. 1 revels the smaller differences between the theoretical solution and the through the thickness residual stresses distribution of the Z-section profile.

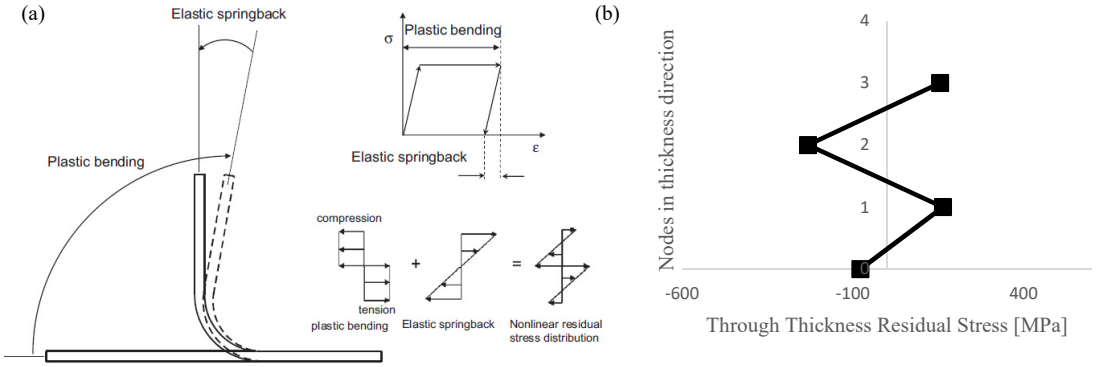

Fig. 1. Nonlinear through the thickness residual stress distribution in corner regions of thin sheets: (a) theoretical solution [3]; (b) numerical results for the Z-section profile.

Regarding fatigue analysis of these components, bending regions represent the critical areas where fatigue cracks tend to nucleate. For the U-channel profile, the inner bend surface presented a tensile state, after the roll forming process. After the application of external cyclic loads, these tensile stresses increased their magnitude, which represents a detrimental situation for fatigue life. Afterwards, stress range in the critical node for the three loads used (2 kN, 4.5 kN and 9 kN) was determined. A stress relaxation after the first cycle was observed, especially for higher loads. The second cycle showed no variations of the maximum and minimum stresses, proving an elastic behaviour of the material. For this reason, a stress-based approach was used to estimate fatigue life. For an external load of 9 kN, the estimated number of cycles until failure was 540 (low cycle fatigue). Stress based approaches are not suitable for low cycle fatigue, leading to the conclusion that an isotropic hardening rule might not be adequate to simulate roll forming profiles subjected to cyclic loading, since the Bauschinger effect is not reproduced. Instead, a kinematic hardening rule might be more suitable. A similar analysis was conducted for the Z-section profile, where the cyclic load was applied in the top and bottom surfaces of the large flange. The results for this last profile led to the same conclusions reached for U-channel profile. Finally, concerning fatigue endurance limit of these profiles, results showed higher values for the U-channel profile (3.5 kN) then for the Z-section profile (2.8 kN and 3.3 KN for the model where the load was applied in the top and bottom surfaces of the flange, respectively). Higher values were expected for the Z-section profile, since this profile was designed to present higher stiffness, due to the presence of small flanges in the both lateral ends of the structure. These results can be explain by the differences in the meshes used for both simulation models or the differences in the process and roll design in the cold roll forming process. Moreover, the load applied in the U-channel profile is located approximately in the middle of the flange, while the load applied in the Z-section profile is located further away from the bend region, leading to higher stresses and decreasing the maximum load that can be applied.

REFERENCES

[1] Halmos, G.T.: Roll Forming Handbook. Journal of Chemical Information and Modelling 53 (2013).
[2] EN 1993-1-9: Eurocode 3: Design of Steel Structures - Part 1-9: Fatigue. European Committee for Standardization (CEN) 7 (2005).
[3] Moen, C.D., Igusa, T., Schafer, B.W.: Prediction of Residual Stresses and Strains in Cold-Formed Steel Members. Thin-Walled Structures 46(11), 1274–89 (2008).

ACKNOWLEDGMENTS

The authors express their gratitude to the FASTCOLD RFCS European Project, the SciTech-Science and Technology for Competitive and Sustainable Industries, R&D project NORTE-01-0145-FEDER-000022 co-financed by Programme Operational Regional do Norte ("NORTE2020") through Fundo Europeu de Desenvolvimento Regional (FEDER) and the Portuguese Science Foundation (FCT) through the post-doctoral grant SFRH/BPD/107825/2015 for their collaboration, financial and technical support during this research work. In addition, data M is acknowledged for providing the software used in this research.

Static and Fatigue Behaviour of Bolted Joints Made of Thin Plates

V.M.G. Gomes[a*], M. Rodrigues[b], M. Figueiredo[a], J.A.F.O Correia[a,b,c], A.A. Fernandes[a,b], A.M.P. de Jesus[a,b]

[a] *Faculty of Engineering, University of Porto, Portugal*
[b] *INEGI, University of Porto, Portugal*
[c] *CONSTRUCT, University of Porto, Portugal*
** Corresponding author: vtgomes@fe.up.pt*

Keywords: Rack structures; Bolted joints; Monotonic behaviour; Friction; Fatigue life.

ABSTRACT

This paper presents a study about the slip, static and fatigue behaviour of bolted joints, exploring the use of thin plates, the effect of the preload levels, and the effect of different surface coatings of cold-formed steel members used for rack structures in logistic warehouses. This study investigated two structural steel grades, namely the S355MC without coating (usually called "black steel"), and the S350GD provided with zinc coating. S350GD grade was also provided with paint cover made of a HEMPEL HEMPADUR 15553 plus HEMPEL HEMPATEX 56360 applied over the primary zinc coating. Slip tests were performed in accordance the EN 1090 [1] standard to evaluate the joint slip factors for the three surface treatments and similar materials mentioned before. According to EN 1090 standard, M16 bolts were used, and the applied clamping torque was the correspondent to 70% of the ultimate stress. LVDTs were applied to measure the relative displacement and detect the sliding forces. Table 1 shows the slip factors obtained for the surface finishes tested.

Table 1. Slip factors obtained from the slip tests according to EN 1090 [1].

	Uncoated, "black steel"	Zinc coated	Zinc coated + painted
Slip factors	0.28	0.31	0.14

Besides the slip tests, the static monotonic tests were also investigated for surface finishes mentioned before. Monotonic static tests were performed in two geometries with 1+1 and 4+4 bolts, with 2 and 3 mm thick plates, and two bolt preload levels. The clamping torques applied on M16 bolts were 25%×70% and 70% of the ultimate strength of the bolts. Numerical simulations were created using ANSYS finite element software. From numerical models and besides the load-displacement curves, the failure modes and their respective equivalent plastic strain were simulated as illustrated in Fig. 1. Fig. 2 shows the behaviour curves of bolted joints. From this comparison, there was a maximum difference of 11% in ultimate loads.

Lastly, preliminary fatigue tests were performed with snug tight and preloaded M16 bolts. Posteriorly, M12 bolts were tested and analysed statistically in accordance the ASTM standard [2]. Fig. 3 presents the average S-N curve and their respective confidence intervals based in two and three standard deviations. Fig. 3 shows that there is a great difference between the provided curve by EN 1993-1-3 Eurocode 3 [3] and the average S-N curve obtained by experimental data and also shows that the increase preload is beneficial for fatigue life. Actual S-N curves in EC3, for non-preloaded bolted joints, is not safe for the tested bolted joints.

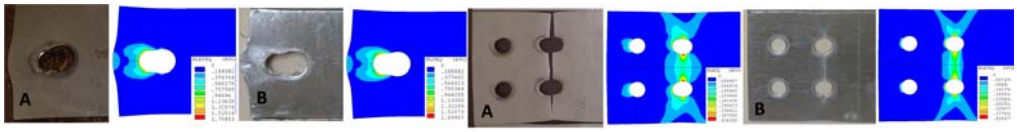

Fig. 1. Experimental vs numerical (equivalent plastic strain fields in ultimate load) failure modes: left, 1+1 bolted joint; right, 4+4 bolted joint. Steel grades: A-S355MC, B-S350GD.

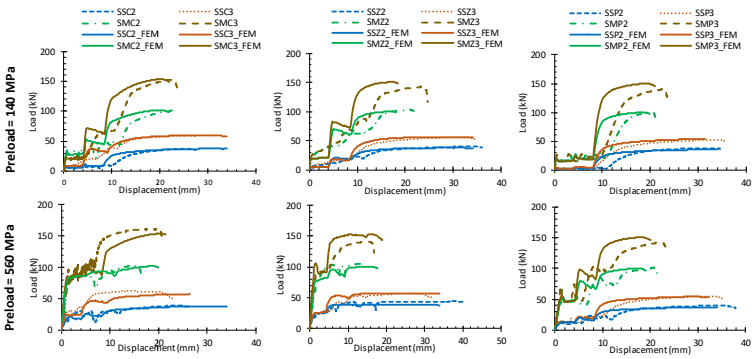

Fig. 2. Experimental vs. numerical monotonic load-displacement curves.

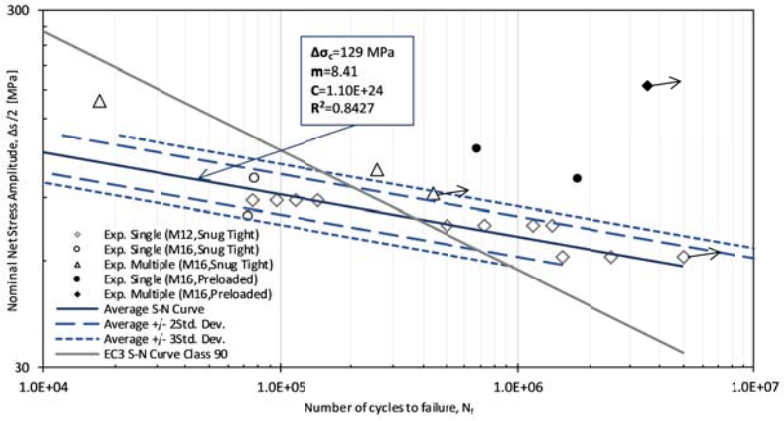

Fig. 3. Average S-N curve in according to ASTM standard [2] from experimental data of snug tight M12 bolts. Comparison with EC3 [3] S-N Curve with Class 90 and other geometries and preloaded joints.

REFERENCES

[1] CEN, EN 1090-2: Execution of steel structures and aluminium structures – Part 2: Technical requirements for steel structures. (2008) Article title. Journal 2(5), 99–110 (2016).
[2] ASTM: Standard Practice for Statistical Analysis of Linear or Linearized Stress-Life (S-N) and Strain-Life (ε-N) Fatigue Data. Annual Book of ASTM Standards, 1–7 (2012).
[3] CEN, EN 1993-1-3-Eurocode 3: Design of Steel structures – part 1-9: Fatigue (2005).

ACKNOWLEDGMENTS

The authors express their gratitude to the FASTCOLD RFCS European Project. The SciTech (Science and Technology for Competitive and Sustainable Industries) R&D project NORTE-01-0145-FEDER-000022 co-financed by Programme Operational Regional do Norte ("NORTE2020") through Fundo Europeu de Desenvolvimento Regional (FEDER) and the Portuguese Science Foundation (FCT) through the post-doctoral grant SFRH/BPD/107825/2015 are also acknowledged for their financial.

The Influence of Short-Time Low-Temperature Thermal Treatments on the Fatigue Performances of a Large-Deformed Austenitic Steel Doped With Nitrogen

G. Mussot-Hoinard[a*], P. Charbonnier[a], P. Laheurte[a]

[a]*Université de Lorraine - Metz-LEM3 - UMR 7239 - 7 rue Félix Savart- BP 15082- 57073 Metz Cedex03, France*
**Corresponding author: genevieve.mussot@univ-lorraine.fr*

Keywords: Austenitic steel; Nickel-free; High-nitrogen; Microstructure; Mechanical properties; Fatigue.

ABSTRACT

This study is in the framework of product development of very high strength and good ductility Cr-Mn-Mo-N steels using ribbons in spring form. The nominal chemical composition of the nitrogen-containing austenitic steel is given in Table 1. Nitrogen and manganese are nickel substituting elements. This austenitic steel with 0.46 %wt. of nickel and over 0.4 %wt. of nitrogen is defined as a nickel-free high-nitrogen steel [1,2,3].

Table 1. Nominal composition of the alloy

Weight %	Cr	Mn	Mo	Si	N	Ni	C	V	P	Nb	S	Al
	16.49	12.50	3.25	0.84	0.82	0.46	0.07	0.03	0.017	0.011	0.007	0.001

The as-received material is a ribbon of a 0.12mm thickness with a large true deformation rate calculated at 248%, corresponding to the adding of a 226% multi-pass cold-drawing rational strain and a 42% cold-rolling rational strain, according respectively to Eq. (1) and Eq. (2). Φ is the diameter of a wire and e the thickness of the ribbon.

$$\varepsilon_{\text{rational (cold-drawing)}} = 2\ln(\Phi_2/\Phi_1) \quad (1)$$

$$\varepsilon_{\text{rational (cold-rolling)}} = 2\ln(e/\Phi) \quad (2)$$

In order to optimize the mechanical resistance of the raw material, thermal treatments were proceeded on the ribbon. For this study, the temperature range of 425°C to 500°C under air was explored during 10min short-times. The increase of Re and Rm parameters is well observed on the tensile performances (Fig. 1a) of the material (Zwick testing machine). The fracture facies of the raw material shows a ductile behaviour (Fig. 1b1) with cupules occurring at small oxides inclusions [4], while the thermal treated specimens let show a brittle behaviour that raise with increasing temperature (Fig.1b2, 1b3).

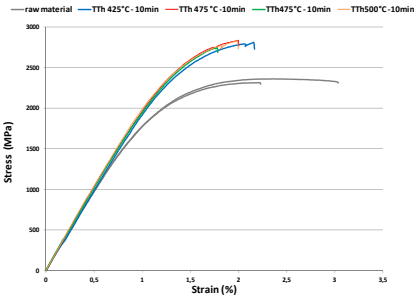

a)

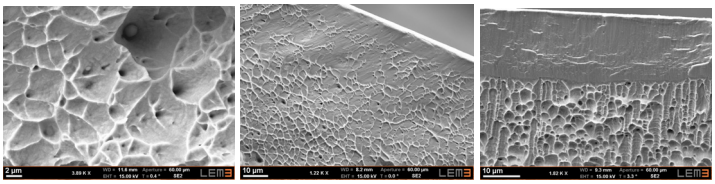

b1) raw material b2) TTh 450°C – 10 min b3) TTh 475°C – 10 min

Fig. 1. a) Tensile performances of the ribbon and b) example of fracture facies, for the raw material and with 10 min short-time thermal treatments (Zeiss).

Fatigue tests, using an automated servo-hydraulic MTS testing machine equipped with a 0.25kN force transducer, were conducted at room temperature and under a bending mode that is more suitable to the behaviour of springs. Fatigue tests were only undertaken at 3% strain amplitude according to Eq. (3).

$$\varepsilon = 6\, e\, u / L^2 \qquad (3)$$

Taking into account the L distant between the supports, a pre-compressive displacement u of 1 mm was applied as to simulate the in situ pre-stress supported by the spring. Using a sinusoidal profile (Fig. 1a) at a frequency of 5Hz, mechanical strain cycles were then purchased onto the specimen by an additional compressive displacement of 1mm such as to obtain the required 3% strain amplitude.
The fatigue limit was set at 3000 cycles. Fatigue life results show clearly a thermal dependence (Fig. 1a) of the material. The fatigue performance of the raw material reaches and exceeds the 3000 cycles while the short-time thermal treatment specimens failed before. However, the best results were obtained by the 10min - 425°C specimen that failed reproducibly around 2000 cycles. Fatigue lines were observed on the tensile surface of the broken specimen and the break in thickness seems to be relatively brittle. Moreover, the 10 min - 450°C, 475°C and 500°C treated specimens were respectively characterized by very scattered lower lifetime results.

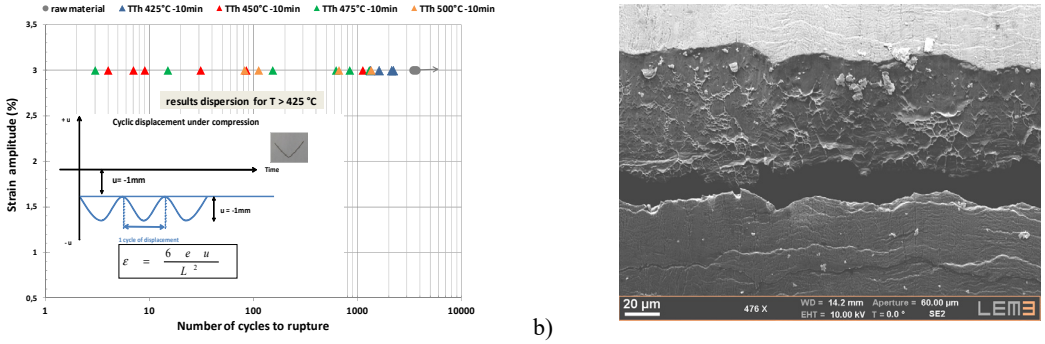

a) b)

Fig. 2. a) Fatigue performances of the ribbon for the raw material and with 10 min short-time thermal treatments and b), the 10min-425°C specimen failure (Zeiss)

In conclusion, a weakness dependence of the Cr-Mn-Mo-N steel to the short-time low-temperature heat treatments was observed in fatigue. This result could probably be explained by the interaction of the structural hardening mechanisms involved during the heating, the working hardening during fatigue and the inclusions distribution on the part of the sample submitted to the maximum stress. This part is the subject of work in progress.

REFERENCES

[1] Koch, S., Buchner, R., Tikhovski, I., Brauer, H., Runiewiewicz. A., Dudzinski, W., Fisher, A.: Mechanical, chemical and tribological properties of the nickel-free high-nitrogen steel. Materialwiss. Werkst. 33, 705-715 (2002).
[2] Yang, K., Ren, Y.: Nickel-free austenitic stainless steels for medical applications. Sci. Technol. Adv. Mater. 11, 13pp, 014105 (2010).
[3] Talha, M., Behera, C.K., Sinha, O.P.: A review on nickel-free nitrogen containing austenitic stainless steels for biomedical applications. Mater. Sci. Eng. C 33(7), 3563-3575 (2013).
[4] Zhang, L., Thomas, B.G.: State of the art in the control inclusions during steel ingot casting. Met. Mat. Trans. B 37, 733-761 (2006).

Strength Analysis of Tramway Bogie Frame

Vaclav Kraus[a], Miloslav Kepka jr.[a], Miloslav Kepka[a*], Daniel Doubrava[b]

[a] *RTI – Regional Technological Institute, University of West Bohemia, Czech Republic*
[b] *R&D, SKODA TRANSPORTATION, Czech Republic*
**Corresponding author: kepkam@rti.zcu.cz*

Keywords: Tram bogie frame; Strength analysis; Tests of railway vehicles.

ABSTRACT

This paper aims to describe the designing of the powered bogie frame of a tramway with respect to the structure's strength. At the ŠKODA TRANSPORTATION company, great emphasis is placed on the design process, as well as on testing and test runs [1, 2]. At the development stage, the R&D Department at ŠKODA TRANSPORTATION works together with external specialist facilities, such as the RTI – Regional Technological Institute, a research centre affiliated with the Faculty of Mechanical Engineering of the University of West Bohemia. The outcome of this cooperation was the design of a modern tramway bogie. The bogie frame consists of castings and weldments, as shown in Fig. 1.

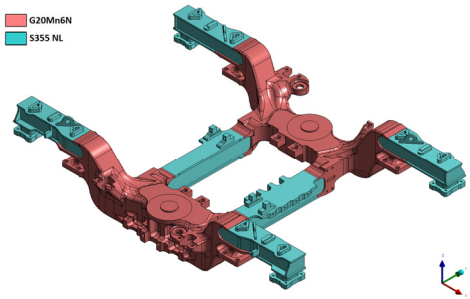

Fig. 1. Tramway bogie frame and identification of its materials.

At the design stage, FE calculations of the bogie frame are performed. They involve load magnitudes, which are typically based on requirements set out in standards, such as [3]. Fatigue strength of a welded frame under dynamic load is limited primarily by the weld joints. This is the reason why their analysis receives major attention. To demonstrate fatigue strength, the endurance limit approach and/or the cumulative damage approach can be used. In the design process, endurance limit is demonstrated by means of nominal stress analysis. Guidelines for such evaluation can be found, for instance, in [4, 5]. A schematic representation of the evaluation procedure is shown in Fig. 2. The entire procedure is examined and documented in detail in the full paper. Once the frame has been designed and manufactured, it is fatigue-tested. This test is outside the scope of this paper but descriptions of bogie frame testing can be found in [6]. Prototypes of new tramways undergo static and on-track strength demonstration tests. Using these tests, stresses in critical locations of the frame are identified under real-world operating conditions and the lifetime of the frame is assessed. In this design step, fatigue strength is demonstrated using the endurance limit approach and/or the cumulative damage approach. At research center RTI, fatigue life is determined from measured data with the aid of the nCode GlyphWorks software. The software offers target life calculations by which under-designed and over-designed locations of the structure can be

identified, because they evaluate by how much the load on a particular measured location should be reduced or, by contrast, could still be increased while matching the specified lifetime.

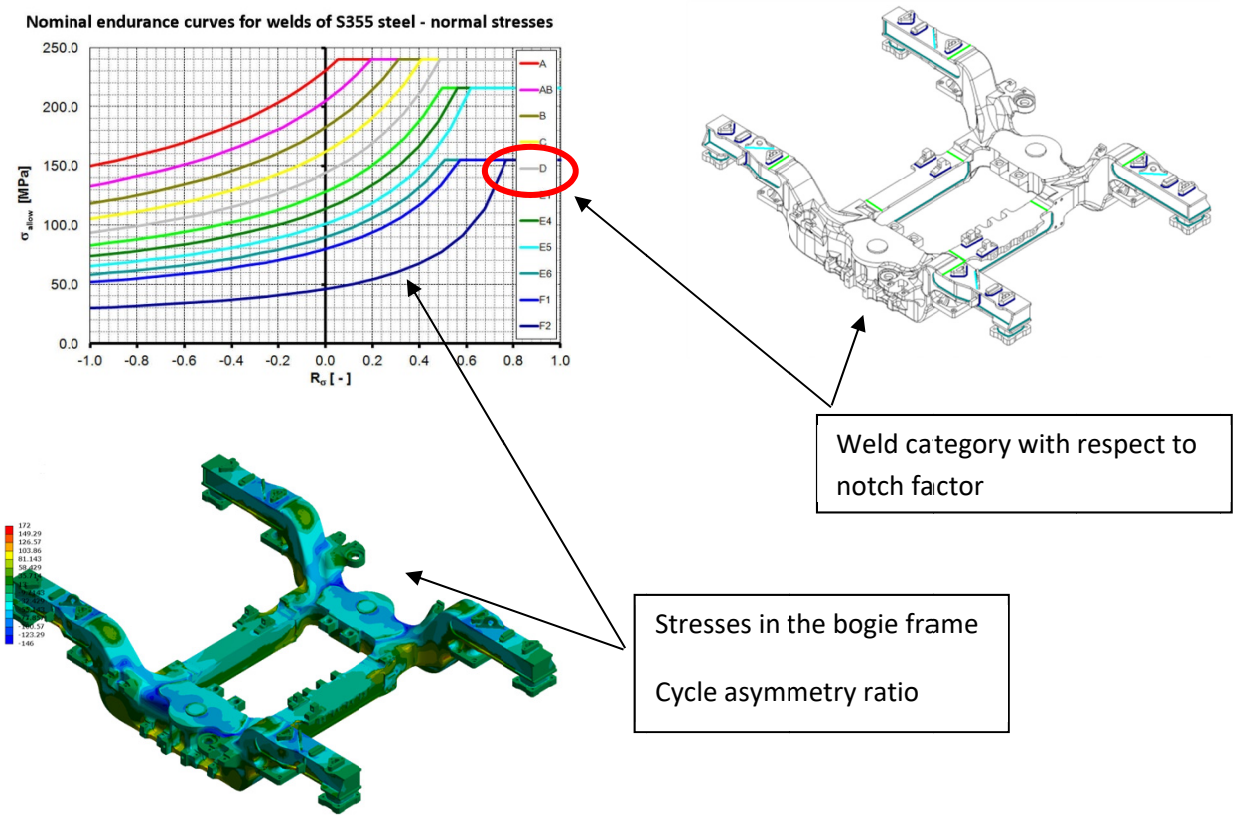

Fig. 2. Schematic representation of fatigue evaluation of welds.

REFERENCES

[1] Kraus, V., Doubrava, D.: Strength analysis of the powered bogie frame of 30T tram, Skoda Transportation research report, 2014 (in Czech).

[2] Kraus, V., Cuchy, P., Drasky, T.: On-track strength demonstration test of powered bogie of 30T tram, Skoda Transportation research report, 2015 (in Czech).

[3] CSN EN 13749, Railway applications – Wheelsets and bogies – Method of specifying the structural requirements of bogie frames, CNI, July 2005 (in Czech).

[4] FKM-Richtlinie; Rechnerischer Festigkeitsnachweis für Maschinenbauteile aus Stahl, Eisenguss- und Aluminiumwerkstoffen; 6. Auflage 2012.

[5] DVS1612, Gestaltung und Dauerfestigkeitsbewertung von Schweißverbindungen an Stählen im Schienenfahrzeugbau, DVS-Verlag GmbH, August 2014.

[6] Kepka, M., Chvojan, J.: Remarks to testing of strength and fatigue life of rail vehicle structures. In Proceeding of the 6th International Conference on Mechanics and Materials in Design. Avintes: LusoImpress S.A., 83-84 (2015).

ACKNOWLEDGMENTS

The present contribution has been prepared under project LO1502 Development of the Regional Technological Institute under the auspices of the National Sustainability Programme I of the Ministry of Education of the Czech Republic aimed to support research, experimental development and innovation.

Fatigue Behaviour Investigation of Stabilization Construction of Posterior Lumbar Spine Pedicle Screw: Finite Element Analysis

M. Bendoukha[a*], M. Mosbah[a]

[a] *Mechnical Engineering Department, Abdelhamid Ibn Badis University of Mostaganem, Algeria*
**Corresponding author: Mohamed.bendoukha@univ-mosta.dz*

Keywords: Posterior; Lumbar; Spine; Fatigue; Finite Element Method.

ABSTRACT

This study aimed to analyse the fatigue life of the posterior lumbar spine fusion structure, finite element analysis was used to investigate the fatigue behaviour of the lumbar spine stabilization system. This system is already being used in orthopaedic surgery. We study the fatigue, deformation and safety factors. It was observed that the simulation results are in good agreement with experimental cases. To obtain a more realistic simulation, boundary conditions were applied according to standards specified in the ASTM Standard F1717-04. Two three-dimensional Models of the stabilization structure with two bars and four bars were built by the commercial 3D software, Solid Works 2013, and imported into ANSYS software for static analysis. The maximum and minimum stresses of risk nodes under different loads and moments were obtained. The fatigue life was then calculated using the relevant mathematical formula of S-N curve and Goodman curve. It was found that the stress in the middle of the crossbeam between the two bars is larger than the surroundings and is liable to suffer from fatigue. Three different types of materials were selected during analysis. Two materials where Ti-6Al-4V and 316L. Minimum fatigue cycles, critical fatigue areas, stresses and safety factor values have been identified. The results obtained from the finite element analysis showed that this system were safe enough in terms of fatigue life. As a result of fatigue analysis, and found to be successful. The current study has also demonstrated that analysing spinal implants with the finite element method (FEM) can be applied with confidence to support standard fatigue testing and used as an alternative. Further studies can expand the simulations to clinical relevance due to complex physical relevance.

Four different loading methods were applied for calculation after grid generation: pair of compressive loads, a pair of tensile loads, a pair of bending moments and a single lateral load were added to UHMWPE holding blocks respectively. Some results of the calculated stress clouds compression and tensile loading types, safety factor, biaxial indication, life, damage. We showed that higher stress is distributed in the connection area of the beam and bar when the structure is loaded with compressive force, tensile force and lateral force. When the structure is loaded with bending moment, higher stress locates in the area of the middle of the beam.

Table 1. Mechanical properties of materials used in analysis.

Material	Elastic Modulus (GPa)	Poisson's Ratio	Yield Strength (MPa)	Ultimate Strength (MPa)
Ti-6Al-4V [11]	113.8	0.33	880	950
Stainless Steel (316L) [10,11]	195.0	0.30	170	480

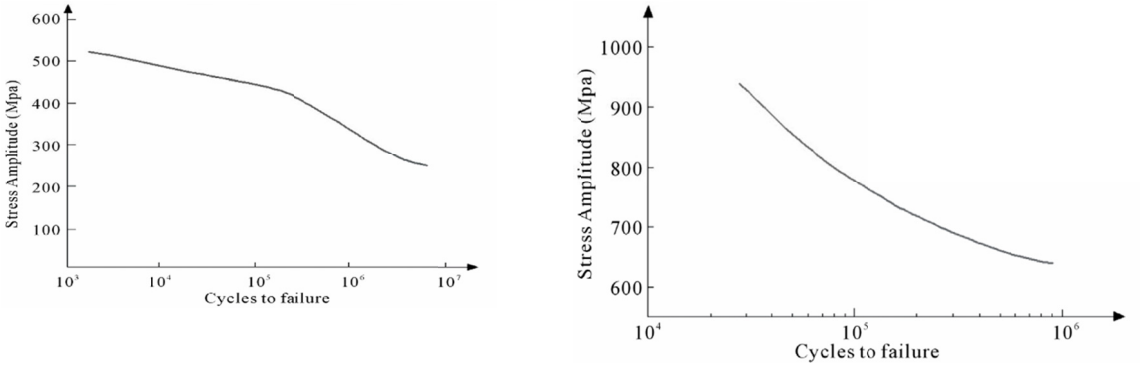

Fig. 1. S-N curves used for 316L (left) and Ti6Al4V (right).

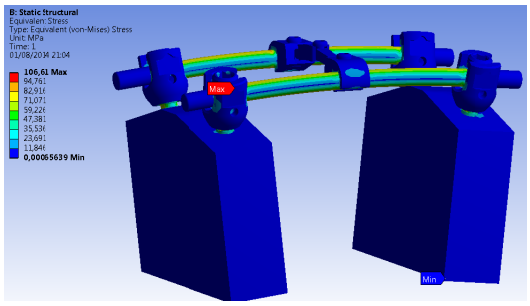

Fig. 2. Stress field for lateral load of 100N.

REFERENCES

[1] Wagnac, E., Michardière, D., Garo, A., Arnoux, P.J., Mac-Thiong, J.M., Aubin, C.E.: Biomechanical Analysis of Pedicle Screw Placement: A Feasibility Study Studies in Health Technology and Informatics 158, 167-171 (2009).
[2] Wang, Y., Jin, A.M., Fang, G.F.: Three-Dimensional Finite Element Analysis of the Lumbar Pedicle Screw Instrumentation. Journal of Clinical Rehabilitative Tissue Engineering Research 12(48), 9439-9442 (2008).
[3] Christensen, F.B., Nielsen, B.K., Hansen, E.S., Pilgaard, S., Bunger, C.E.: Anterior Lumbar Intercorporal Spondylodesis. Radiological and Functional Therapeutic Results, Ugeskrift for Laeger 156(37), 5285-5289 (1994).
[4] Angevine, P.D., Dickman, C.A., Mc Cormick, P.C.: Lumbar Fusion with and Without Pedicle Screw Fixation: Comments on a Prospective, Randomized Study. Spine 32(13), 1466-1471 (2007).
[5] Sagomonyants, K.B., Jarman-Smith, M.L., Devine, J.N., Aronow, M.S., Gronowicz, G.A.: The in Vitro Response of Human Osteoblasts to Polyetheretherketone (PEEK) Substrates Compared to Commercially Pure Titanium. Biomaterials 29 (11), 1563-1572 (2008).

Fatigue Behaviour of AISI 304 Steel Strengthened With Composite Coating

M. Duda[a*], J. Pach[b], D. Pyka[a], G. Lesiuk[a]

[a] *Faculty of Mechanical Engineering, Department of Mechanics, Materials Science and Engineering, Wrocław University of Science and Technology, Smoluchowskiego 25, 50-370 Wrocław, Poland*
[b] *Faculty of Mechanical Enginering, Department of Foundry, Polymers and Automation, Wrocław University of Science and Technology, Smoluchowskiego 25, 50-370 Wrocław, Poland*
**Corresponding author: monika.duda@pwr.edu.pl*

Keywords: Composite coating; Fatigue behaviour; Pull-off strength.

ABSTRACT

Improving materials fatigue strength is an engineering challenge in both strength of materials and material science. Its importance grows as pressure on improving efficiency and decreasing costs is getting higher. In this paper, authors present an influence of composite coating on AISI 304 sheets fatigue behaviour. Surface strengthening is an efficient method of improving fatigue crack growth resistance of the material and was investigated in papers [1, 2]. Improving fatigue resistance of the material is an issue of multidisciplinary importance as it can be applied in both civil and mechanical engineering to both newly designed and already existing structures [1, 3]. In this paper, have been proposed and investigated various coatings based on EP, PUA and composites of EP and PUA matrix. Types of coatings are presented in the Table 1.

Additionally to the fatigue resistance there were investigated the average thickness of the coating and its' pull-off strength. Obtained results were compared and related to the fatigue resistance of the samples. Proposed coatings are alternative to widely investigated CFRP patches.

Table 1. Types of coating

Coating	EP	EP + PUA
	EP + glass fabric	EP + glass fabric + PUA
	EP + hemp fibre	EP + hemp fibre + PUA

REFERENCES

[1] Lesiuk, G., Katkowski, M., Duda, M., Królicka, A., Correia, J.A.F.O., De Jesus, A.M.P., Rabiega, J.: Improvement of the fatigue crack growth resistance in long term operated steel strengthened with CFRP patches, 2nd International Conference on Structural Integrity, ICSI 2017, 4-7 September 2017, Funchal, Madeira, Portugal.
[2] Ai-Saadi, N.T.K., Mohammed, A., Al-Mahaidi, L.: Fatigue performance of near-surface mounted CFRP strips embedded in concrete girders using cementitious adhesive made with graphene oxide. Construction and Building Materials 148, 632-647 (2017).
[3] Tabrizi, S., Kazem, H., Rizkalla, S., Kobayashi, A.: New small-diameter CFRP material for flexural strengthening of steel bridge girders. Construction and Building Materials 95, 748-756 (2015).

Fatigue Wave Loads Estimation Using Morison Formula for an Offshore Jacket-Type Platform

António Mourão[a*], J.A.F.O. Correia[a], J. Barbosa[a,b], J.M. Castro[a], C. Rebelo[c], M. Correia[d], N. Fantuzzi[e], R. Calçada[a]

[a] *Faculty of Engineering, University of Porto, Portugal*
[b] *Technology Centre, Federal University of Rio Grande do Norte, Natal, Brazil*
[c] *Faculty of Science and Technology, University of Coimbra, Portugal*
[d] *Senior Structural Engineer, Force Technology, Norway*
[e] *Department of Civil, Chemical, Environmental and Materials Engineering, University of Bologna, Italy*
**Corresponding author: up201306134@fe.up.pt*

Keywords: Fatigue; Offshore platform; Wave loads; Wave theory; Morison formula.

ABSTRACT

Regardless of the structure resistance to static loads, marine structures such as jacket-type offshore platforms are subjected to cyclic environmental loads that, even though inferior to the static tensile stress, result in fatigue cumulative damage by shortening the service life of the platform.

Environmental loads have demonstrated to be of significant importance towards fatigue damage accumulation for offshore platforms. Among which, wave loads have shown to be the most conditioning ones, especially when the majority of the structure is submerged such as in the present case.

In order to carry out the wave loads acting on the structure, a scan in terms of wave measurements (in the form of wave data scatter diagram) must be made according to the platform geographical location. This procedure must respect the interval imposed by the Norsok standard [1] expressed by Eq. (1) that relates wave length, λ and wave height H_s to the wave period, resulting in the simplified wave measurements in Table 1.

$$15H_s < \lambda < 25H_s \tag{1}$$

During service life, offshore structures are subjected to a significant number of loads, some of which are of non-linear nature [2], with this in mind an overview into several wave theories both linear and non-linear is proposed. As it is well-known, environmental loads depend on wave characteristics and may fall into different ranges of applicability, as displayed in Fig. 1.

In accordance with the wave measurement presented in Table 1, Stokes 2nd order wave theory would be sufficient, however Stokes 5th order is used in parallel with Airy's wave theory for both finite and infinite water depth providing a more complete and accurate overview of wave particle kinematics.

Morison load formula applied to fixed structures was estimated according to the DNV-GL recommended practice [4]. These loads can be obtained for each water depth level as a function of time and geometric characteristics (see Fig. 2).

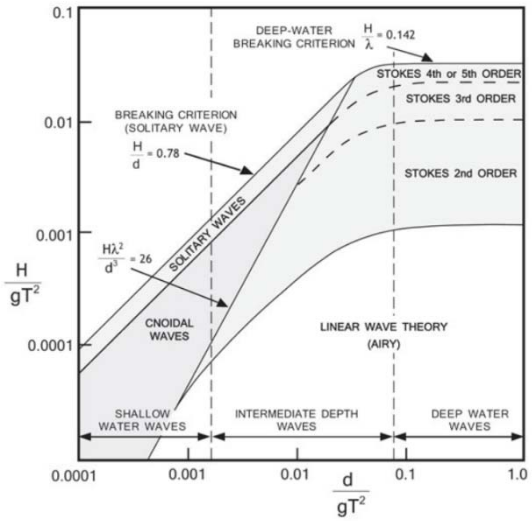

Fig. 1. Wave theories range of applicability [3].

Table 1. Wave measurements for a generic direction of wave loading.

Wave number	Wave height, H_s [m]	Wave period [s]
1	1	3.58
2	3	6.2
3	4.5	7.6
4	5.5	8.4
5	6.5	9.13
6	7.5	9.81
7	9	10.74
8	14	13.4

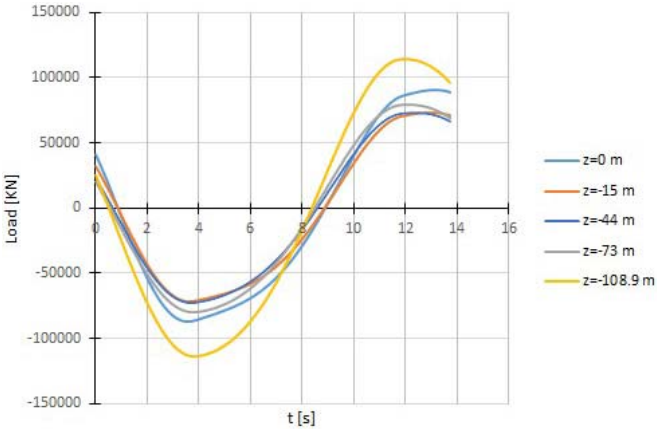

Fig. 2. Load values for each water depth according to Stokes 5th order wave theory.

REFERENCES

[1] N-003: Actions and Action Effects, Rev, vol. 1, Norsok Standard (2017).
[2] Faltinsen, O.: Sea loads on ships and offshore structures. Cambridge University Press (1993).
[3] https://www.flow3d.com/modeling-capabilities/waves/, last accessed 2018/7/25.
[4] Det Norske Veritas: Environmental conditions and environmental loads. Recommend Practice DNV-RP-C205 (2014).

Multiaxial Fatigue Life Estimation of Bolted and Welded Onshore Wind Turbine Transition Piece

Mohammad Reza Shah Mohammadi[a,*], Muhammad Farhan[b], António Mourão[c], Carlos Rebelo[a], José António Correia[c]

[a] *ISISE, Department of Civil Engineering, University of Coimbra, P-3004 516, Coimbra, Portugal.*
[b] *Department of Civil Engineering, University of Petras, Petras, Greece.*
[c] *INEGI, Faculty of Engineering, University of Porto, Porto, Portugal.*

**Corresponding author: mrsm@uc.pt*

Keywords: Wind Turbine; Multiaxial fatigue, Wind Turbine, Transition piece; Steel Structures.

ABSTRACT

Recently, new lattice and hybrid lattice-tubular supporting structures are introduced in order to increase the wind turbine power capacity by increasing the tower height[1]. The wind turbine tower is subjected to highly dynamic loading and therefore prone to fatigue damage. One of the promising concepts is the hybrid lattice-tubular supporting structure for the wind turbine height between 120 m to 220 m. hybrid supporting structure consists of lattice structure, tubular tower and a transition piece which is employed as connection between the lattice and the tubular tower[2]. The transition piece is one crucial part to be designed for the whole lifetime of the wind turbine operation. The transition piece must transfer all the loads from the upper tubular tower to the lattice structure and consequently the ground. Moreover, it should withstand all ultimate limit state loading and the fatigue loads. Past researches have been conducted on onshore and offshore wind turbine transition piece to design and investigate the fatigue behavior[3]–[6]. The fatigue behavior of a wind turbine structure can take advantage of the probabilistic methods for fatigue analysis, which can treat the uncertainties is more rigorous way and provide more comprehensive results. In this research, two welded and bolted modular transition pieces are introduced. The fatigue life time of welded solution with normal and high strength steel grades are investigated using Brown-Miller method. Then, the high strength steel solution with welded and bolted connection are compared. The results show, the normal grade solution is preferable in the welded solutions. However, the bolted solution can be considered for a transition piece fabricated with high strength steel. The fatigue life time for both welded and bolted transition pieces are listed in Table 1 and Table 2. For the case study using S355 fatigue results of the transition piece reveals that if the wind is equal to 12m/s constantly over the service life it can sustain up to 60 years while transition piece using S690 steel can sustain up to 15 years. Moreover, the most loaded element, where a potential crack initiation may happen is shown in Fig. 1 for both welded case studies. The service time of the bolted transition piece using S690 is a bit less than the welded transition piece using S355 as the maximum stress is higher in the model. Moreover, it shows an improvement in fatigue behaviour of the design using the high strength steel material by changing the design mind set from the welded to the bolted connection. Fig.1-c shows the detail view of the stress distribution and the damage in the bolted connection.

In conclusion, design of transition piece concept was proposed with the application of multiaxial fatigue situation. The high strength steel concept with welding connection led to smaller dimensions; however, an increase of the thickness is required to have the standard 25 years' life time. Moreover, the outcome of the investigation shows that switching from the welding connection to bolted connections leads to better fatigue behaver of the high strength steel material.

Table 1. The life time results for the welded transition piece.

Normal Strain with SWT correction		
	Transition Piece using S355	Transition Piece using S690
Worst Life- in Years	60.45	15
Largest (+ or -) SMAX	407.591 MPa	737.408MPa
Largest Damage	1.887E-6	3.541E-5

Table 2. The life time results for the bolted transition piece.

Normal Strain with SWT correction	
	Transition Piece using S690
Worst Life- in Years	50.02
Largest (+ or -) SMAX	475.1 MPa
Largest Damage	2.62E-6

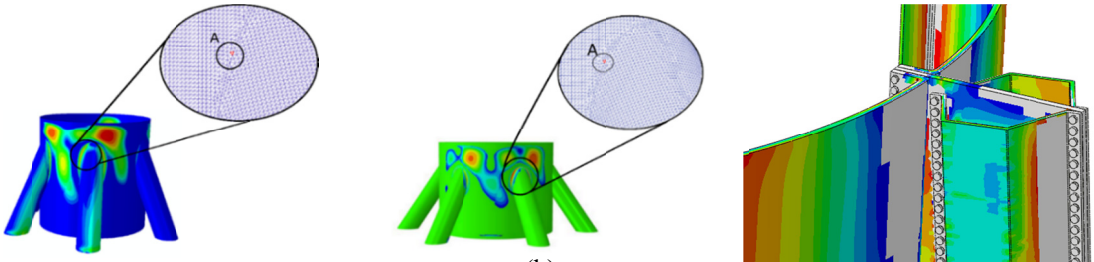

(a) (b) (c)

Fig. 1. (a) welded S355, (b) welded S690, (c) bolted S690 transition pieces.

REFERENCES

[1] Jovašević, S., Shah Mohammadi, M.R., Rebelo, C., Pavlović, M., Veljković, M.: New Lattice-Tubular Tower for Onshore WEC – Part 1: Structural Optimization. *Procedia Eng.* 199, 3236–3241 (2017).

[2] Mohammadi, M.R.S., Farhan, M., Rebelo, C., Veljković, M.: Preliminary transition piece design for an onshore wind turbine. *ce/papers* 1(2–3), 4400–4409 (2017).

[3] Lee, Y.S., González, J. A., Lee, J.H., Il Kim, Y., Park, K.C., Han, S.: Structural topology optimization of the transition piece for an offshore wind turbine with jacket foundation. *Renew. Energy* 85, 1214–1225 (2016).

[4] Lee, Y.S., Choi, B.L., Lee, J.H., Kim, S.Y., Han, S.: Reliability-based design optimization of monopile transition piece for offshore wind turbine system. *Renew. Energy* 71, 729–741 (2014).

[5] Shah Mohammadi, M. R., Farhan, M., Rebelo, C., Veljković, M.: Preliminary Transition Piece Design for an Onshore Wind Turbine. in *EuroSteel* (2017).

[6] Geodome LTD, "Development of Jackets and Transition Pieces for Wind-Turbine Installations," 2015. [Online]. Available: http://www.geodome.co.uk/www.geodome.co.uk/applications/off-shore.html.

ACKNOWLEDGMENTS

The authors acknowledge with thanks the support of the European Commission's Framework Programs "Horizon 2020" program through the Marie Skłodowska-Curie Innovative Training Networks (ITN) "AEOLUS4FUTURE – Efficient harvesting of the wind energy" (H2020-MSCA-ITN-2014: Grant agreement no. 643167) and RFCS – Research Fund for Coal and Steel program through the Grant Agreement RFSR-CT-2015-00021-SHOWTIME. This work was also financed by FEDER - COMPETE and by national funds within the scope of the projects POCI-01-0145-FEDER-007633 and CENTRO-01-0145-FEDER-000006.

Fatigue Analysis of a Concrete Chimney Under Wind Loads

Hermes Carvalho[a*], Victor Roberto Verga Mendes[a], Sebastião Salvador Real Pereira[a], José António Fonseca de Oliveira Correia[b]

[a] *Structural Engineering Department, Federal University of Minas Gerais, Brazil*
[b] *Faculty of Engineering, University of Porto, Portugal*
**Corresponding author: hermes@dees.ufmg.br*

Keywords: Chimney subjected to wind loads; Fatigue life evaluation; Nonlinear dynamic analysis; Fluid-structure interaction; Aerodynamic damping.

ABSTRACT

Usually, the analysis of structures under wind loading is performed using an equivalent static analysis, where the influence of floating response is taken into account by the gust factor. This methodology can be used in case of rigid structures for not presenting a considerable dynamic response [1]. More flexible structures, in particular those lightly damped, may show an important resonant response and their dynamic properties must be considered in the analysis [2]. For the analysis of fatigue life is necessary to know the history of the load as well as the total response of the structure to these loads. The aim of this paper is to present fatigue life evaluation through dynamic analysis of concrete chimney under wind loading considering the geometric nonlinearity, the vibration caused by the kinetic energy of wind gusts and the aerodynamic damping due to the relative movement between this structure and the wind. The formulation proposed is applied on real structure (180-meter-high concrete chimney).

A numerical procedure in ANSYS [3] was developed for dynamic analysis with variable wind forces in time and space. Superimposed on the structural damping, aerodynamic damping was considered directly in determining the dynamic wind pressures, through the use of relative velocities between the structure and the wind, according to Eq. 1.

$$q_{wind} = \frac{1}{2}\rho \ V_R^2 \tag{1}$$

$$V_R = (V(t) - V_{str}) \tag{2}$$

Where q_{wind} is wind dynamic pressure; ρ is air density; V_R is relative speed between wind and structure, in the node considered; $V(t)$ is wind speed; V_{str} is structure speed, in wind direction, in the considered node.

Wind velocity can be expressed as a time function composed of a mean and a floating component. In the proposed procedure, the mean plot is obtained from the ABNT NBR 6123: 1988 [4] and the floating plot is determined by statistical parameters such as: probability distribution, power spectrum and cross correlation functions.

Fig. 1 shows the temporal evolution of the displacements, velocities and accelerations of the top node of the chimney, and the support reactions of the base node of the 180 meter-high structure with a wind velocity equal to 32m/s. Table 1 shows the maximum values for each temporal evolution.

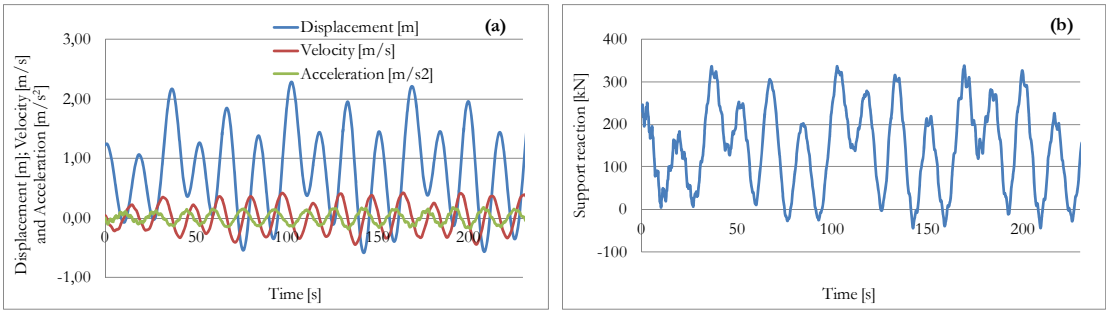

Fig. 1. Temporal evolution of displacement, velocity, acceleration (a) and support reaction (b).

Table 1. Maximum values of displacement, velocity, acceleration, support reaction and bending moment.

Variable	Max. Value
Displacement[m]	2.29
Velocity [m/s]	0.42
Acceleration [m/s2]	0.17
Horizontal Reaction Fx [kN]	347.52
Bending Moment Mz [kN.m]	57850.58

From the time history of the efforts in the structure base, obtained through the dynamic analysis, it was possible verify the fatigue of the reinforcement according to ABNT NBR 6118:2014 [5]. It should be noted that in some cases of high stiffness structures such concrete chimneys with large diameters, the reinforcement design is determine by serviceability limit state (fatigue).

REFERENCES

[1] Simiu, E., Scanlan, R.H.: Wind Effects on Structures: An Introduction to Wind Engineering, 2.ed. New York: John Wiley and Sons (1986).
[2] Hirsh, G., Bachman, H.: Wind induced vibrations. Vibration Problems in Structures. Zurich: Institut fur Baustatik und Konstruktion/Birkhauser Verlag Basel (1995).
[3] ANSYS-12.1. Release 1.0 Documentation for Ansys. Canonsburg, United States (2009).
[4] Associação Brasileira de Normas Técnicas – ABNT. NBR 6123: Forças devidas ao Vento em Edificações. Rio de Janeiro (1988).
[5] Associação Brasileira de Normas Técnicas – ABNT. NBR 6118: Projeto de Estruturas de Concreto. Rio de Janeiro (2014).

Evaluation of Mean Stress Effects Based on Artificial Neural Network Applied to the High-Cycle Fatigue Data of the P355NL1 Steel

Joelton F. Barbosa[a,b,c*], J.A.F.O. Correia[b], R.C.S.F. Júnior[a], G. Lesiuk[d], Shun-Peng Zhu[f], A.M.P. De Jesus[b], R.A.B. Calçada[b]

[a]*Mechanical Engineering Department,* Federal University of Rio Grande do Norte, Natal, Brazil
[b]*Mechanical Engineering Department,* Faculty of Engineering, University of Porto, Porto, Portugal
[c]*Engineering Department,* Federal Rural University of the Semi-Arid Region, Mossoró, Brazil
[d]*Faculty of Mechanical Engineering,* Wrocław University of Science and Technology, Wrocław, Poland
[f]*School of Mechanical and Electrical Engineering*, University of Electronic Science and Technology of China, Chengdu, China
**Corresponding author: joeltonfb@gmail.com*

Keywords: Mean stress; Haigh diagram; High cycle fatigue; Life prediction; Stress ratio.

ABSTRACT

The effect of mean stress plays an important role in fatigue life prediction, its influence significantly changes the fatigue behaviour of high cycle, directly decreasing the value of the fatigue limit with the increase of the mean tension. This can be explained by the observation that the positive mean tension increases the opening of the crack and accelerates the accumulation of fatigue damages. Formulating the effects of mean stresses over the useful life of the material is important so that designers can dimension components and structures that meet performance and safety criteria at the end of their useful life. The construction of the Haigh diagram allows to understand the effect of the increase mean tension in the gradual reduction of the amplitude of maximum axial tension that the material can support without failures. There are many empirical formulations in the literature that use both physical and mathematical precepts. However, there is no precise unified method that is able to represent in a general empirical way, the effect of the mean stress on the high cycle fatigue of the predominantly loaded in the traction region, in metals. The purpose of this work is to develop a methodology to formulate and validate the construction of the Haigh diagram, based on artificial neural networks. Able to generalize an estimate of the safe region of high cycle operation as a function of the mean stress and the maximum stress amplitude in the region of predominance of traction loading, with only two S-N curves. The methodology is based on a quantitative analysis of experimental fatigue data of P355NL1 steel, which are used in pressure vessel designs. The data of fatigue tests provided are for the fatigue ratio R = {-1, -0.5, 0}. A multilayer perceptron network has been trained with backpropagation algorithm, its architecture consists of two input neurons (σ_a, N) and one output neuron (σ_m). Has been used a single hidden layer with 2 to 30 neurons, all with sigmoid activation function and a linear function in the output neuron. The results show that the training of the network with only two curves S-N, R=-0.5 and R=0, managed to obtain good approximations of the high cycle experimental data. Thus, it is concluded that this formulation of the Haigh diagram using artificial neural networks can aid the engineering design in the design of the fatigue resistance limit and provide the safe operating region visualization with only two S-N curves.

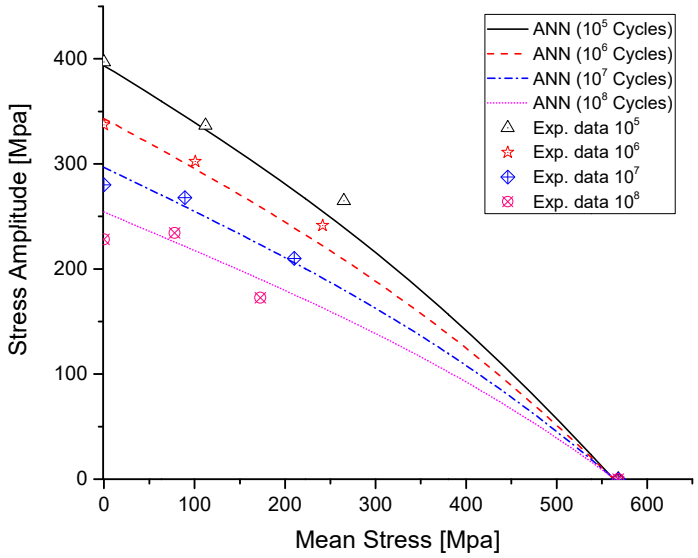

Fig. 1. Haigh diagram defining safe and failure regions in terms of amplitude stress versus mean stresses in the steel P355NL1, by ANN, artificial neural network.

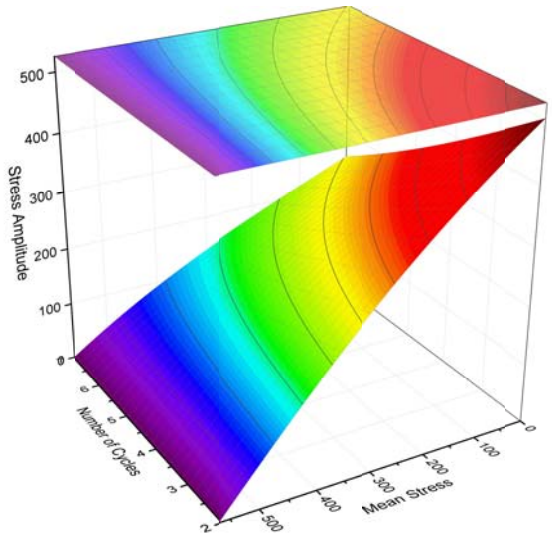

Fig. 2. Safe operating region for P355NL steel as a function of mean stress, amplitude stress and number of cycles.

REFERENCES

[1] Júnior, R.C.S.F., Neto, A.D.D., Aquino, E.M.F.: Building of constant life diagrams of fatigue using artificial neural networks. International Journal of Fatigue 27(7), 746-751 (2005).
[2] De Jesus, A.M.P., Ribeiro, A.S., Fernandes, A.A.: Low and high cycle fatigue and cyclic elasto-plastic behavior of the P355NL1 steel. Journal of Pressure Vessel Technology 128(3), 298-304 (2006).
[3] Lu, S., Su, Y., Yang, M., Li, Y.: A modified walker model dealing with mean stress effect in fatigue life prediction for aeroengine disks. Mathematical Problems in Engineering 2018, ID 5148278, (2018).
[4] Zhu, S.-P., Lei, Q., Huang, H.-Z., Yang, Y.-J., Peng, W.: Mean stress effect correction in strain energy-based fatigue life prediction of metals. International Journal of Damage Mechanics 26(8), 1219-1241 (2017).

ACKNOWLEDGMENTS

The authors gratefully acknowledge the financial support for this research work provided by the Brazilian Science Foundation's CAPES. The authors also acknowledge the Portuguese Science Foundation (FCT) for the financial support through the postdoctoral grant SFRH/BPD/107825/2015.

Magnetic Response During Fatigue Crack Growth Process

R. Mech[a*], G. Lesiuk[a], J.A.F.O. Correia[b], A.M.P. de Jesus[b]

[a] *Department of Mechanics, Material Science and Engineering, Wrocław University of Science and Technology, Smoluchowskiego 25, 50-370 Wrocław, Poland*
[b] *INEGI/Faculty of Engineering, University of Porto, Rua Dr. Roberto Frias, 4200-465 Porto, Portugal*
**Corresponding author: rafal.mech@pwr.edu.pl*

Keywords: Crack propagation; Fatigue; Magnetic signals; Notches; AISI 304 steel; Mild steel.

ABSTRACT

This paper presents the results of the fatigue crack propagation obtained for AISI 304 steel (0.04%C, 1.1%Mn, 0.41%Si, 0.0437%P, 0.0044%S, 18.16%Cr, 8%Ni, 0.0335%Mo, 0.1%V, 0.32%Cu) for specimen presented in Fig. 1. Additionally, the FCGR test was performed for structural low carbon mild steel (from existing long term operated structural members) using CT specimens (performed in accordance with ASTM E647 [1]). All experiments were performed using constant amplitude load procedure (R=0.1). For both type of steels, the kinetic fatigue fracture diagrams were constructed.

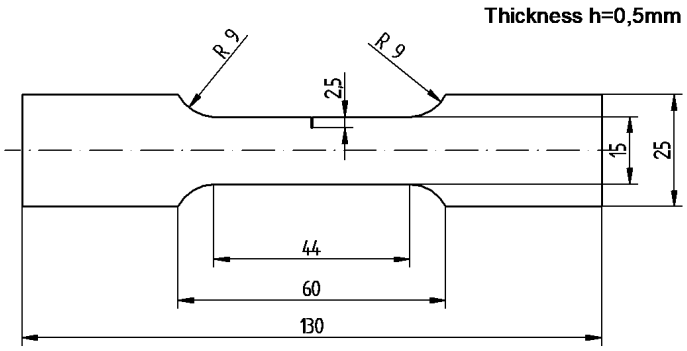

Fig. 1. Shape and dimensions of specimen used in experiment.

During typical fatigue crack growth rate test, the magnetic signals were registered in order to estimate the changes in magnetic response during fatigue crack growth process. The main idea of measurement system consist in use of magnetostrictive composite layer in order to identify changes of magnetic field around this layer during the experiment. Additionally a 3D magnetic field probe was applied (consisted of 3 Hall's sensors), which was placed next to the sample during the experiment and allowed to received information about changes in magnetic field around the crack. It is believed that this method might be a base for a new approach to the evaluation of the fatigue crack growth rate.

REFERENCES

[1] ASTM E647-15e1, Standard Test Method for Measurement of Fatigue Crack Growth Rates, ASTM International, West Conshohocken, PA (2015).

Mixed Mode Fracture of “Engineered Stone” Composite Materials

G. Lesiuk[a*], M. Cieciura[a], M. Smolnicki[a], J.A.F.O. Correia[b], A.M.P. de Jesus[b]

[a] *Department of Mechanics, Material Science and Engineering, Wrocław University of Science and Technology, Smoluchowskiego 25, 50-370 Wrocław, Poland*
[b] *INEGI/Faculty of Engineering, University of Porto, Rua Dr. Roberto Frias, 4200-465 Porto, Portugal*
**Corresponding author: Grzegorz.Lesiuk@pwr.edu.pl*

Keywords: Composite materials; Mixed mode fracture; Fracture toughness; Crack paths; SIF calculation.

ABSTRACT

Composite material “Engineered Stone” is an interesting alternative for classical stone materials in kitchen sink industry. However, based on the literature data, there is a lack of the basic fracture properties of this material under complex load state. In presented paper, the SCB (Semi Circular Bend) specimens were extracted from new series of kitchen sinks in order to estimate fracture properties under mixed mode loading conditions. From microscopic point of view, investigated composite material is based on crushed natural stones, quartz in polyester resin matrix.

In order to investigate mechanical properties and fracture tests several experiments were performed in order to better understanding the typical fracture behaviour of components made from “Engineered Stone”. Typical mechanical damage of kitchen sink is presented in Fig. 1.

Fig. 1. Typical damaged kitchen sink; origin of crack is indicated by arrow with marked sections for microscopic analysis.

For fracture test the SCB specimens were involved (Fig. 2a) with different notch inclination angle (Fig. 2b). The main dimensions of SCB specimen were following: R=37.5 mm, thickness t=12.5 mm, s/R=0.8, a/R=0.45. Fracture toughness of the material was estimated for pure mode I (SENB specimen)

and mixed mode state. Based on the experimental results the estimated K_{IC} value (from SENB specimen, sharp notch prepared by diamond saw) was equal K_{IC}=1.74MPa√m.

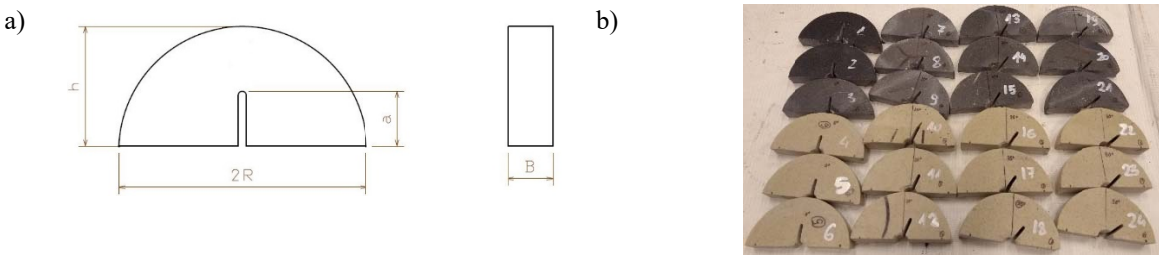

Fig. 2. Mixed mode load test: a) SCB specimen; b) general view on the tested specimens.

The stress intensity factors were calculated using general solutions of SIFs presented by Kuruppu et al. [1]:

$$K_I = Y_I \frac{P_{max}\sqrt{\pi a}}{2RB} \tag{1}$$

$$K_{II} = Y_{II} \frac{P_{max}\sqrt{\pi a}}{2RB} \tag{2}$$

Where: P – applied force, a – crack length, R – specimen radius, B – specimen thickness. Y_I, Y_{II} – non-dimensional function were determined numerically (FEM, Abaqus) for applied span/radius rate and normalized crack length a/R=0.45. The obtained results are presented in Fig. 3.

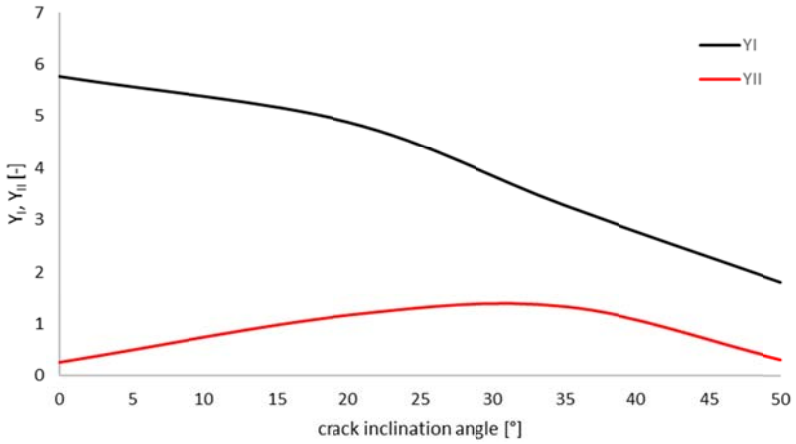

Fig. 3. Geometric factor Y_I, Y_{II} as a function of crack inclination angle.

REFERENCES

[1] Kuruppu, M.D., Obara, Y., Ayatollahi, M.R., Chong, K.P., Funatsu, T.: ISRM Suggested Method for Determining the Mode I Static Fracture Toughness Using Semi-Circular Bend Specimen. Rock Mechanics and Rock Engineering 47(1), 267-274 (2014).

ACKNOWLEDGMENTS

The experimental works have been supported by the Wroclaw University of Science and Technology – project no 401/0029/17.

A Stress Intensity Factor Study for a Pressure Vessel CT Specimen Using Finite Element Method

P. Raposo[a,b], B. Farahani[b], J.A.F.O. Correia[a,b*], J. Belinha[c,b], A.M.P. de Jesus[b], R.N. Jorge[b], R.A.B. Calçada[a]

[a]*Civil Engineering, FEUP, Portugal*
[b]*INEGI, FEUP, Portugal*
[c]*ISEP, Portugal*
**Corresponding author: jacorreia@fe.up.pt*

Keywords: Compact Tension Specimens; Stress intensity Factors; FEM; Pressure vessel steel.

ABSTRACT

This study aims to determine the mode I Stress Intensity Factor, K_I, for a steel alloy specimen extracted from a pressure vessel, so-called P355NL. The geometric and mechanical properties are derived from Compact Tension, CT, specimens available in the relevant literature. The theoretical value of K_I is evaluated through the formulation reported in ASTM E 647-15 for the geometric properties used in the previous study. Numerically, to solve the CT specimen problem, a Finite Element code software, ABAQUS© is used. Therefore, obtained numerical results are then compared to the theoretical ones, leading to assess the numerical analyses' performance. In this study, distinct crack lengths are considered as; a = {8, 9, …, 20 mm}. This study needs experimental campaigns in order to obtain the mechanical properties of the materials and extensive numerical studies, calibrated and compared with the experimental/reference values. Hence, a pre-cracked CT specimen made of a mild steel from a pressure vessel P355NL1 was used in this study. Fig. 1 presents the CT specimen with the recommended dimensions and in Fig. 2, the load application scheme is demonstrated. It was considered that $\Delta P = P_{max} - P_{min} = 1634.1\ N$ and $R = P_{min}/P_{max} = 0$. Table 1 reports the geometric dimensions of the CT specimen considered in this study. The ΔK values were computed relying on the foregoing theoretical equation and also they have been obtained by the FEM formulation analysed in ABAQUS© as can be seen on Table 3. Moreover, Fig. 3 demonstrates the von Mises stress and the vertical displacement variation on the fractured CT specimen if a = 14 mm.

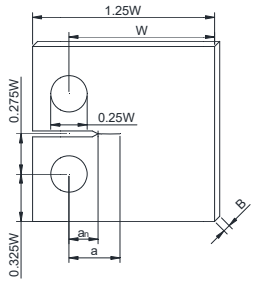

Fig. 1. Recommended dimensions for CT specimens according to the test standard.

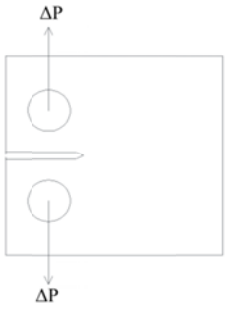

Fig. 2. Schematic view of the fatigue test condition.

This work addresses the calculation of the mode I stress intensity factor, K, through the theoretical expression proposed by ASTM E 647, and by numerical approaches using the Finite Element Methods (FEM). For the proposed CT specimen, several crack lengths were simulated The FEM model was solved

using the standard FEM based code software ABAQUS© allowing to directly obtain K, assuming the strain energy release rate criterion in the presence of integral contours. Comparing the calculated theoretical value based on ASTM E647 standard with numerical results, a good agreement between the values was reached. Overall, the numerical methods are a reliable and robust source of results, leading to accurate predictions of the behaviour of materials/components/structures, which with adequate calibration can lead to the reduction of experimental tests, which have very high associated costs.

Table 1. Mechanical properties of the steel.

Material	$E(MPa)$	v	$f_y\ (MPa)$	$f_u\ (MPa)$
P355NL	205200	0.275	418.06	568.11

Table 2. CT specimen; K_I obtained for each method and the respective error.

a (mm)	ΔK_{ASTM} (MPa.m$^{0.5}$)	ΔK_{FEM} (MPa.m$^{0.5}$)	Error (%)
8	255.429	241.456	5.470
9	274.430	289.687	5.560
10	294.117	305.519	3.877
11	314.473	322.558	2.571
12	335.699	340.256	1.357
13	358.031	359.996	0.549
14	381.746	379.195	0.668
15	407.176	402.532	1.140
16	434.711	426.434	1.904
17	464.820	470.597	1.243
18	498.069	502.037	0.797
19	535.141	539.793	0.869
20	576.873	584.069	1.247

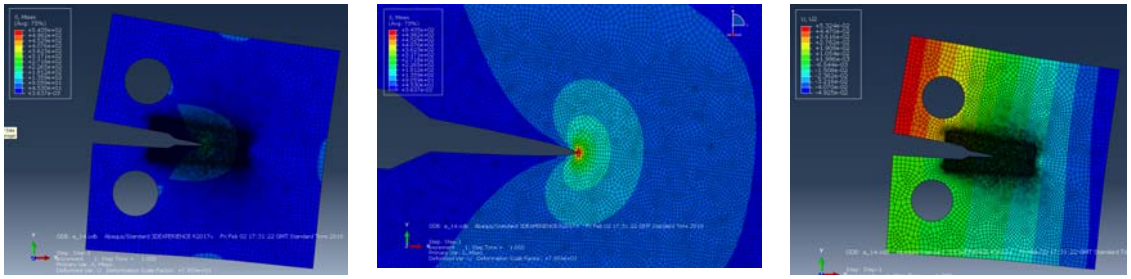

von Mises stress | von Mises stress at the crack tip | vertical displacement, U_2

Fig. 3. CT specimen with a crack of $a = 14\ mm$, FEM ABAQUS.

ACKNOWLEDGMENTS

The authors acknowledge the Portuguese Science Foundation (FCT) for the financial support through the doctoral grants PD/BD/135257/2017 and PD/BD/114095/2015 and postdoctoral grant SFRH/BPD/107825/2015. The authors gratefully acknowledge the funding of SciTech: Science and Technology for Competitive and Sustainable Industries, R&D project co-financed by Operational North Regional Program (NORTE2020), through European Fund of Regional Development (FEDER).

Correlation Between the Pivot Node Concept and Fatigue Crack Closure

J. Garcia-Manrique[a*], D. Camas[a], A. Gonzalez-Herrera[a]

[a] *Departamento de Ingeniería Civil, de Materiales y Fabricación, Universidad de Málaga, Spain*
**Corresponding author: josegmo@uma.es*

Keywords: Finite element analysis; Crack growth; Fatigue crack closure; Stress intensity factor (SIF); Pivot node.

ABSTRACT

The study of fatigue crack growth has been commonly done by means of bi-dimensional models and assuming a homogeneous behaviour through the thickness. According to the specimen thickness, a state of plane stress or plane strain is presumed. However, recently, it has been shown that thickness effects influence considerably the crack tip behaviour. Tri-dimensional studies present a higher computational cost but the current computational capabilities have triggered their use. These works have revealed a series of effects along the thickness with a strong influence on the crack front growth: plastic zone size, crack closure or stress intensity factor distribution [1-6].

One of the experimental evidences that can be explained as a direct consequence of these effects is the curvature of the crack. It is observed that when the crack advance, the crack front changes adopting a curved shape, growing faster at the interior than at the exterior. Two mechanisms can explain this effect: the first one is related to the crack closure effect near the surface, it would imply a smaller effective ΔK close to the surface, and therefore a slower crack growth rate. The second one, related to the plastic zone size decrement observed in a small region close to the surface, is due to ΔK being smaller near the surface than in the interior. Both mechanisms are difficult to evaluate separately. A series of works were devoted to study these effects.

A research line has been focused in the analysis of the stress intensity factor distribution along the thickness [4-6]. These works evaluate the finite element model (FEM) of an Al 2024-T35 compact tension specimen with no plastic wake effect introduced, according to the methodology developed by the authors. The three-dimensional behaviour in the vicinity of the crack front is simulated through numerical analysis with ANSYS code and J-integral method is used to determinate the curves of K evolution along the thickness. The main finding of these studies is that the distribution of K is not homogeneous; it presents a variable profile through the thickness. The overall values for the whole model accurately agree with the nominal K applied.

The K profiles along the thickness are characterized by a series of parameters that allow us to analyse the distribution of K in terms of the expected K_{nom} against variations of geometrical (thickness) and external (applied load) factors. We can observe three different zones limited by two characteristic points, one which separates the results according to whether they are higher or lower than K_{nom} (denoted Do) or the point (called Da) corresponding to a distributed load state similar to the middle plane of the specimen. Results for different thicknesses (b = 3-9 mm) and loads applied (K_{nom} = 9-30 MPa·m$^{1/2}$) were studied. For all these cases the abrupt drop in the results was maintained in an area close to the outside of the specimen.

One of the most relevant finding was the identification of a point at a certain distance of the external surface where the value obtained of K was constant regardless the load applied. This point was called

pivot node and presents advantages for the correlation of numerical and experimental studies. The significance of this finding is that the SIF remains independent of the load range. This suggests the hypothesis that differences found on K at the interior or the exterior of this pivot node would lead to differences on crack growth rates that will shape the curvature of the crack, however the overall crack growth rate would be dominated by the K_{nom} defined at this point.

Another important issue was that when evaluating the influence of the thickness, the position of the pivot node is related with the absolute distance to the surface instead to an equivalent dimensionless distance for each thickness. The position of the pivot node was in the range 0.36-41 mm from the surface, for all the thicknesses and load levels studied.

As the dependence of the binomial maximum load - thickness disappears in this narrow region of the thickness; this becomes an ideal zone to correlate results (experimental or numerical). It was observed that these results agreed with previous experimental results where numerical crack closure prediction was validated with experimental crack growth data [1].

Crack opening and closure values, obtained for 3D finite element model with constant amplitude load, were evaluated along the thickness and used to evaluate their correlation with different experimental crack growth data with different R. The correlation coefficients were used to identify the position of the thickness for maximum correlation. When the results were plotted in terms of the absolute distance to the exterior, it was found that the maximum values were present in the same area, ranging from 0.2 to 0.4, coincident with the region of the specimen correspondent to the pivot node.

The present paper looks into the relation between fatigue crack closure estimation and the significance of the pivot node concept. The previous correlation was made in terms of a constant K_{nom}. In the present work, K values necessaries to obtain ΔK_{eff} are updated according to the SIF distribution along the thickness obtained with the fracture simulations (without plastic wake). Correlations confirm the previous conclusion regarding the significance of the pivot node position.

REFERENCES

[1] Gonzalez-Herrera, A., Zapatero, J.: Tri-dimensional numerical modeling of plasticity induced crack closure. Eng Fract Mech 75, 4513–4528 (2008).
[2] Camas, D., Garcia-Manrique, J., Gonzalez-Herrera, A.: Numerical study of the thickness transition in bi-dimensional specimen cracks. Int J Fatigue 33, 921-928 (2011).
[3] Camas, D., Garcia-Manrique, J., Gonzalez-Herrera, A.: Crack front curvature: Influence and effects on the crack tip fields in bi-dimensional specimens. Int J Fatigue 44, 41-50 (2012).
[4] Garcia-Manrique, J., Camas, D., Lopez-Crespo, P., Gonzalez-Herrera, A.: Stress intensity factor analysis of through thickness effects. Int J Fatigue 46, 58-66 (2013).
[5] Garcia-Manrique, J., Camas, D., Gonzalez-Herrera, A.: Study of the stress intensity factor analysis through thickness: Methodological aspects. Fatigue Fract. Eng. Mater. Struct. 40, 1295-1308. (2017).
[6] Garcia-Manrique, J., Camas-Peña D., Lopez-Martinez J., Gonzalez-Herrera A.: Analysis of the stress intensity factor along the thickness: The concept of pivot node on straight crack fronts. Fatigue Fract Eng Mater Struct. 41(4), 869-880 (2017).

Simultaneous Use of Cable and Sacrificial Piles for Reduction of Local Scour around Group of Piers Bridge

Shaghayegh Yaghoubi[a*], Vahid Javidi Vahdati[b], J.A.F.O. Correia[c], T. Ferradosa[c], A. de Jesus[c], F. Taveira Pinto[c], R. Calçada[c]

[a] *Maritime Department, Amirkabir University of Technology, Tehran, Iran*
[b] *Shahrod University, Semnan, Iran*
[c] *Faculty of Engineering, University of Porto, Portugal*
**Corresponding author: sh.yaqoubi@aut.ac.ir*

Keywords: Local scour; Cable; Sacrificial piles; Group of piers; Scour reduction.

ABSTRACT

In this study, the simultaneous application of sacrificial piles and cable was experimentally examined as a pier scour countermeasure. The experiments were conducted for single pier and group of two and three piers under clear water conditions. Simultaneous use of sacrificial piles and cable has high efficiency in reducing the scour depth at single pier and group of two piers. Around60% of scour depth was reduced at single pier and in group of two piers it was observed to be 46% and 12% at front and rear piers, respectively. In group of three piers, the sacrificial piles with triangular configuration were able to decrease the scour depth considerably with a value of 69% reduction at first pier. However, the cable has a negative effect on reduction of scour depth at group of three piers. This research highlights that combination of cable and sacrificial piles is a suitable method to decrease the local scour at single and group of two piers while sacrificial piles can be highly recommended for group of three piers.

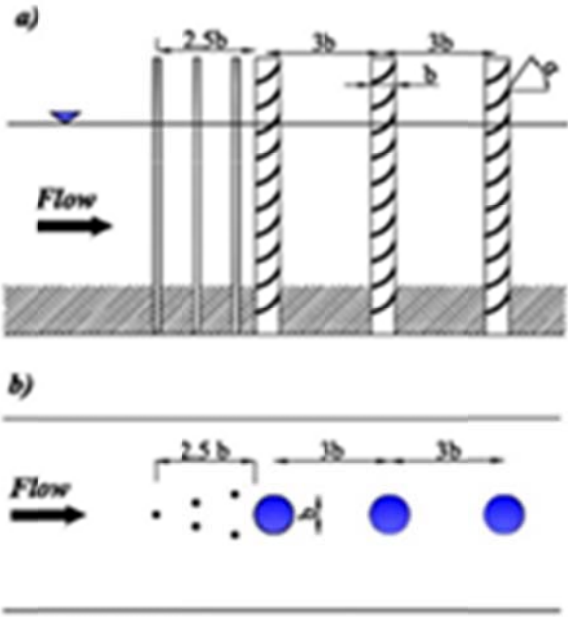

Fig. 1. Simultaneous use of sacrificial piles and cable: a) aide view; b) plan view.

REFERENCES

Ataie-Ashtiani, B., Beheshti, A.A.: Experimental investigation of clear-water local scour at pile groups. Journal of Hydraulic Engineering 132, 1100-1104 (2006).
Chabert, J., Engeldinger, P.: Etude des affouillementsautour des piles de ponts. Serie A, Laboratoire National d'Hydraulique, Chatou, France (1956)(in French).
Chang, F.F.M., Karim, M.: An experimental study of reducing scour around bridge piers using piles. Report, South Dakota Department of Highways, Pierre, SD, USA (1972).
Chiew, Y.: Scour Protection at Bridge Piers. Journal of Hydraulic Engineering 118, 1260-1269 (1992).

ACKNOWLEDGMENTS

Special thanks are given to Ataie Dr. Reza Rashmekarim, Shahrod University, Semnan, Iran, for his professional guidance and valuable discussion in the research process. The authors also acknowledge the Portuguese Science Foundation (FCT) for the financial support through the postdoctoral grant SFRH/BPD/107825/2015 and gratefully acknowledge the funding of SciTech – Science and Technology for Competitive and Sustainable Industries (NORTE-01-0145- FEDER-000022), R&D project cofinanced by Programa Operacional Regional do Norte (NORTE2020) through Fundo Europeu de Desenvolvimento Regional (FEDER).

Effects of Different Loads in a Brittle Plate with 4 Notches, Screws and Rivets with Central Notch through LAMMPS Software

Shaghayegh Yaghoubi[a*], J.A.F.O. Correia[b], T. Ferradosa[b], A. de Jesus[b], F. Taveira Pinto[b], R. Calçada[b]

[a] *Maritime Department, Amirkabir University of Technology, Tehran, Iran*
[c] *Faculty of Engineering, University of Porto, Portugal*
**Corresponding author: sh.yaqoubi@aut.ac.ir*

Keywords: Peridynamic theory; LAMMPS software; Brittle plate; Notches; Modelling.

ABSTRACT

The peridynamic is similar to formulated non-territorial theory by Konin. Despite of continuum mechanics, the peridynamic theory is reformulation of motion equations based on integration and deferential integration equations in solid mechanics. This feature provides the direct usage of peridynamic equations for modelling discontinuities, cracks and development of damage in different points of material. In fact, the damage is part of peridynamic rules and fundamental model. Peridynamic theory with continues concept is developed in finite distance. This theory is presented according to internal forces of materials that material points apply force each other directly from finite distance, while the classic theory of solid mechanics is based on continuous distribution of mass for a material. Although some advanced concepts in fracture mechanics have been developed in classical continuum mechanics during recent decades, the prediction of crack initiation and its growth in materials is still a major challenge. The main difficulty is because of the mathematical formulation, which assumes that a body remains continuous as it deforms. In fact, the classical theory is formulated using spatial partial differential equations, and these spatial derivatives are undefined at discontinuities. To overcome this problem, peridynamic theory (PD) could be used to improve the analysis of cracked structures. Basically, the peridynamic theory is a reformulation of the equation of motion in solid mechanics that is better suited for modelling bodies with discontinuities, such as cracks. The theory uses spatial integral equations that can be applied to a discontinuity. The present study uses this approach to study the effects of different loads in a brittle plate with 4 notches, screws and rivets with central notch through LAMMPS software.

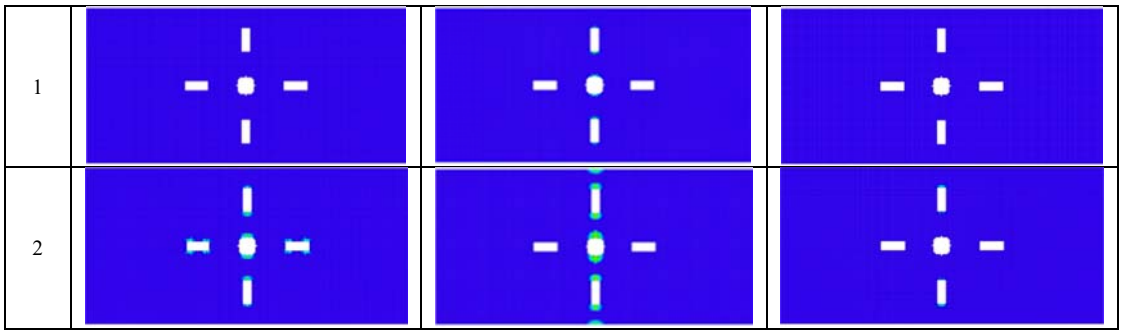

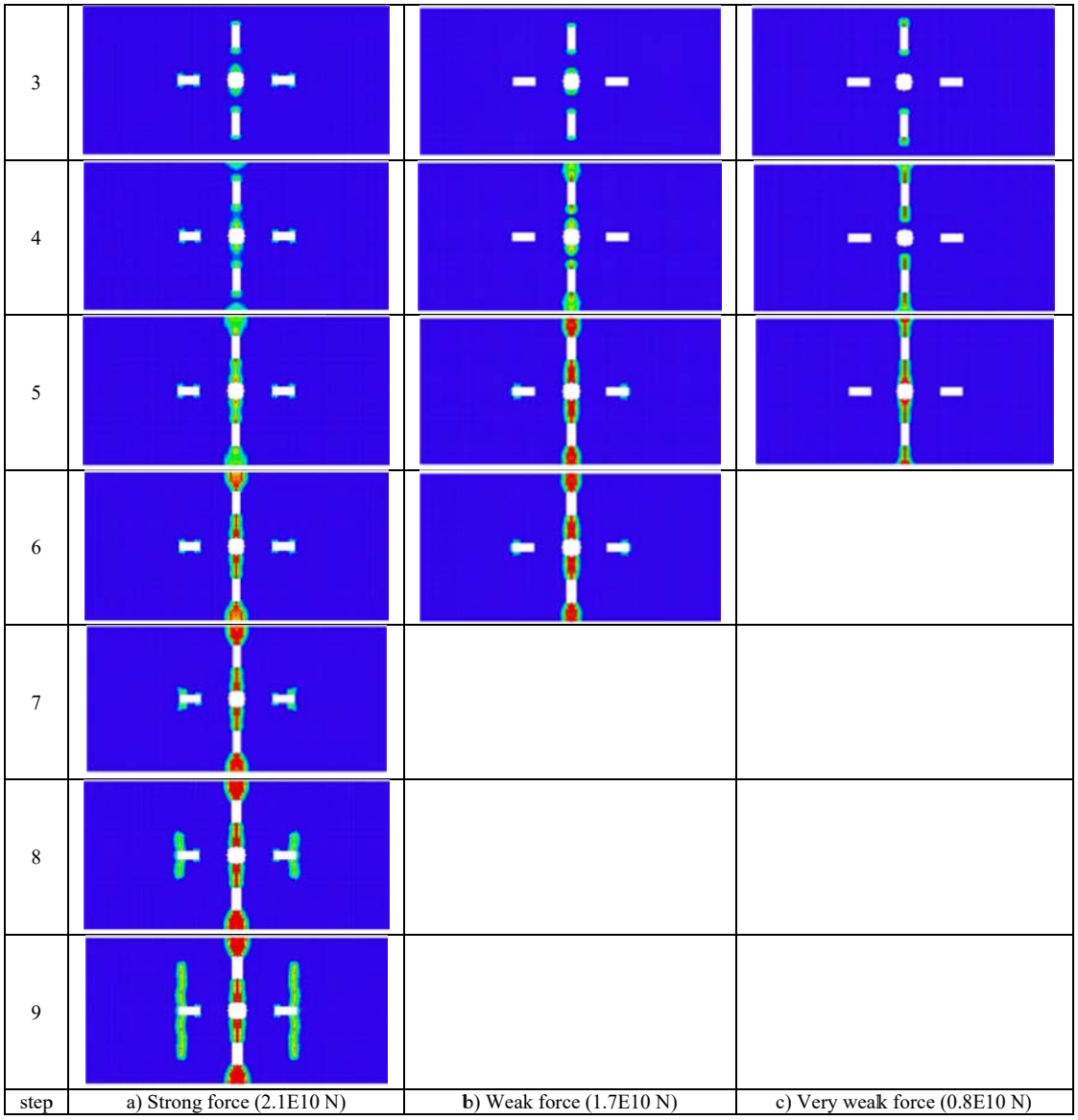

Fig. 1**.** Effects of different loads in a brittle plate with 4 notches, screws and rivets with central notch.

REFERENCES

Hou, L.Y., Zhang, D.R., Zhang, X.X.: Interaction between thermal cracking and steam reforming reactions of aviation kerosene. Fuel Processing Technology 167, 655-662 (2017).

Yuan, H., Zhang, W., Castelluccio, G.M., Kim, J., Liu, Y.: Microstructure-sensitive estimation of small fatigue crack growth in bridge steel welds. International Journal of Fatigue 112, 183-197 (2018).

Choudhury, B., Chandrasekaran, M.: Investigation on welding characteristics of aerospace materials–A review. Materials Today: Proceedings 4(8), 7519-7526 (2017).

Velu, M.: A Short Review on Fracture and Fatigue Crack Growth in Welded Joints. Materials Today: Proceedings 5(5), 11364-11370 (2018).

Wanhill, R.J.H., Byrnes, R.T., Smith, C.L.: Stress corrosion cracking (SCC) in aerospace vehicles. Stress Corrosion Cracking: Theory and Practice. Woodhead Publishing Series in Metals and Surface Engineering, 608-650 (2011).

Mishra, R.K., Thomas, J., Srinivasan, K., Nandi, V., Bhatt, R.R.: Failure analysis of an un- cooled turbine blade in an aero gas turbine engine. Engineering Failure Analysis, 79, 836-844 (2017).

The Structural Analysis of Dental Restorations Based On Advanced Discretization Techniques

Farid Mehri Sofiani[a*], Behzad V. Farahani[a,b], J. Belinha[b,c]

[a] *FEUP, Faculty of Engineering, University of Porto, Dr. Roberto Frias Street, 4200-465, Porto, Portugal.*
[b] *INEGI, Institute of Science and Innovation in Mechanical and Industrial Engineering, Dr. Roberto Frias Street, 400, 4200-465, Porto, Portugal.*
[c] *ISEP, Mechanical Engineering Department, School of Engineering, Polytechnic of Porto, Rua Dr. António Bernardino de Almeida, 431, 4249-015 Porto, Portugal.*
**Corresponding author: up201600432@fe.up.pt*

Keywords: Meshless methods; FEM; Fracture strength; Dental restorations; Ultrathin veneers.

ABSTRACT

This study aims to evaluate the structural response of metallic and ceramic dental restorations. In the last few years several biomaterials were developed to increase the structural resistance and durability of dental restorations. In order to gauge the structural response of some of those materials, approximated geometric models were constructed and analysed using advanced discretization techniques, such as the Finite Element Method (FEM) and Radial Point Interpolation Meshless methods (RPIMs). For many years, FEM was the chosen numerical method for structural analysis, however the use of complex geometries or the generation of highly distorted elements causes low quality shape functions, which affects directly the performance of the FEM. Therefore, in order to suppress this need, in last twenty years the scientific community has witness the birth and development of several meshless methods, which are numerical methods more flexible and equally accurate. Two meshless methods are used in this project: the Radial Point Interpolation Method (RPIM) and the Natural Neighbour RPIM (NNRPIM). Although being a recent numerical method, the NNRPIM has already been extended to many engineering fields. The model of the maxillary bone and existent teeth were obtained from available anonymised computational axial tomography images (CAT scan) and the restored tooth (and all the supporting structures) were built in a CAD software. In the end, the relevant variable fields (displacement/stress/strain fields) were obtained with the three numerical techniques and comparisons are made.

REFERENCES

[1] Belinha, J.: Meshless Methods in Biomechanics: Bone Tissue Remodelling Analysis, Vol. 16. Springer Netherlands (2014).
[2] Farahani, B.V., Belinha, J., Andrade Pires, F.M., Ferreira, A.J.M., Moreira, P.M.G.P.: Extending a radial point interpolation meshless method to non-local constitutive damage models. Theor. Appl. Fract. Mech. 85(A), 84–98 (2016).
[3] Farahani, B.V., Belinha, J., Pires, F.M.A., Ferreira, A.J.M., Moreira, P.M.G.P.: A meshless approach to non-local damage modelling of concrete. Eng. Anal. Bound. Elem. 79, 62–74 (2017).
[4] Egbert, J.S., Johnson, A.C., Tantbirojn, D., Versluis, A.: Fracture strength of ultrathin occlusal veneer restorations made from CAD/CAM composite or hybrid ceramic materials. Oral Science International 12(2), 53-58 (2015).
[5] Zhang, Y., Mai, Z.-S., Barani, A., Bush, M., Lawn, B.: Fracture-resistant monolithic dental crowns. Dent. Mater. 32, 442-449 (2016).

ACKNOWLEDGMENTS

The authors acknowledge the funding by Ministério da Educação e Ciência, Fundação para a Ciência e a Tecnologia (FCT-Portugal), under grants PD/BD/114095/2015 and SFRH/BPD/111020/2015 and by project funding MIT-EXPL/ISF/0084/2017. Additionally, the authors gratefully acknowledge the funding of Project NORTE-01-0145-FEDER-000022 – SciTech – Science and Technology for Competitive and Sustainable Industries, co-financed by Programa Operacional Regional do Norte (NORTE2020), through Fundo Europeu de Desenvolvimento Regional (FEDER).

Effect of LPBF Processing Parameters on 316L Stainless Steel: Tensile Properties, Microstructure and Machinability

Tiago C. Leça[a,b*], Rui L. Neto[a,b], Jorge L. Alves[a,b], A.M.P de Jesus[a,b], João P. Pereira[b]

[a]*Faculty of Engineering of University of Porto, Porto, Portugal*
[b]*INEGI, University of Porto, Porto, Portugal*
**Corresponding author: tiagocarvalholeca@gmail.com*

Keywords: Porosity; Ductility; Machinability; LPBF; Additive manufacturing.

ABSTRACT

Metal additive manufacturing (AM) is a process where 3D parts are progressively created by adding thin layers of materials guided by a digital model. It became a popular method to produce complex structural shapes that would be difficult or impossible to fabricate through conventional processes. Metal AM has a great potential in optimizing topologically structural components that represent several economic advantages for industries such as aeronautical. Laser Powder Bed Fusion is an AM process that uses laser(s) as heat source. Currently, it is possible to build components faster by using multi lasers in LPBF machines. This allows higher production rates of components. For the production of large components, lasers work simultaneously through different scan fields on parts being processed. Post-machinability has been a need of the additively produced parts since the surface roughness, dimensional and geometric tolerances of *as fabricated* parts are insufficient for a large number of applications.

This work consisted on an experimental study aiming to determine defects relation with a defined set of LPBF processing parameters, on 316L stainless steel. More specifically, this study evaluated the influence of those processing parameters (Table 1) on tensile properties, dimensional accuracy, machinability and microstructure. Three cylindrical samples were produced for each set of parameters and then subjected to a stress relief heat treatment. Dimensional distortions/deviations of samples were measured, through 3D scanning, before and after heat treatment and compared to original STL file. Samples were then submitted to machining tests to determine differences between AM samples and conventionally produced samples. The metallic powder served as feedstock was also analysed. Tensile specimens were created and tested to evaluate mechanical properties dependence on processing parameters. Surface roughness was investigated on the *as-fabricated* condition and after machining. Metallographic samples were also produced to evaluate porosity levels and to understand solidification features. Fracture of tensile specimens was investigated in order to determine possible causes. Some samples were CT scanned for porosity measurements comparison.

Table 1. Different processes parameters of which effect was investigated on samples (2 x 2 x 2 x 3 repetitions).

Scan Strategy	Hatch Spacing	Scan Fields
Stripes	80 µm	1
Chess	100 µm	2

It was observed that samples with high values of *hatch spacing* had higher porosity. Samples fabricated with two scan fields had more porosity concentrated near the interface. Tensile specimens with higher porosity levels showed fragile rupture with low values of elongation. No significant changes were seen in the ultimate strength values according to porosity content, but elongation was strongly affected. Some sets of samples have been found to meet minimum tensile properties specified in materials standards (ASTM A276) regardless the reduced porosity values. Tensile curves and properties for the specified sets of samples are shown in Fig.1 and Table 2.

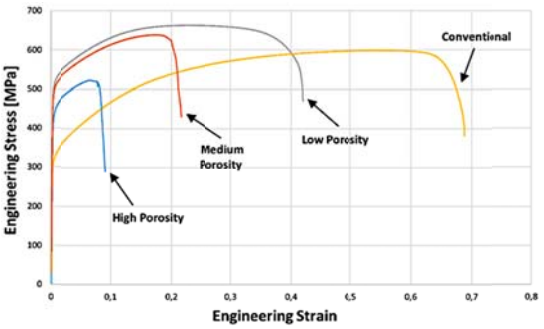

Fig. 1. Tensile curves of individual samples.

Table 2. Results of tensile tests for sets of samples.

Samples	Yield Strength [MPa]	Tensile Strength [MPa]	Elongation %
AM low-porosity	495.3	654.2	37.7
AM medium-porosity	460.0	609.7	17.3
AM high-porosity	432.1	534.6	8.2
Conventional	343.3	595.3	66.5
ASTM A276*	310	620	30

*properties tabled for cold-finished 316L

To evaluate machinability properties of different LPBF samples, dry external cylindrical turning was performed with fixed cutting parameters for all tensile specimens (cutting speed = 30 m/min, depth of cut = 0.5 mm and feed = 0.1 mm/rot, rotation speed = 900 rpm). Load spectra were measured on tool. Results showed that samples with higher content of porosity have a more scattered load spectrum due to the unloading of the tool when passing through a void and to the instant impact of starting to cut again, contrary to what happens to conventional material which is less scattered. Average cutting forces are presented in Fig.2 and representative load spectra are shown in Fig.3.

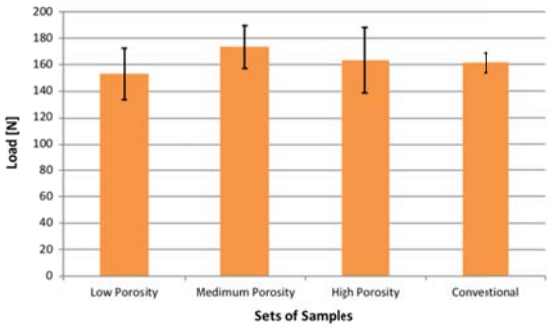

Fig. 2. Mean cutting forces referred to set of samples.

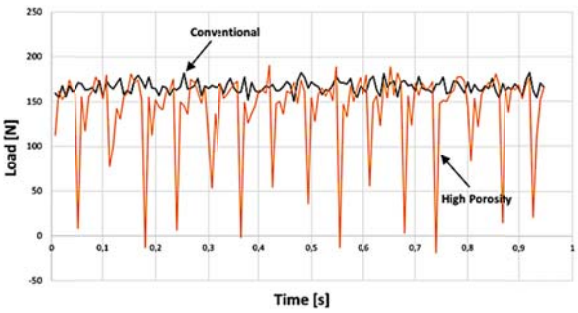

Fig. 3. Representative cutting loads spectra.

Metallographic samples were prepared to analyse the microstructure of the deposited 316L material. It was observed through electrochemically etching the overlap of solidified melt-pools. Melt-pools boundaries of a low porosity sample are clearly identifiable in Fig.4. The distances between consecutive melt-pools were consistent with pre-defined process parameters. Fracture surfaces of samples were investigated to understand rupture cause. Fig.5 shows SEM image of ductile rupture of a low porosity sample.

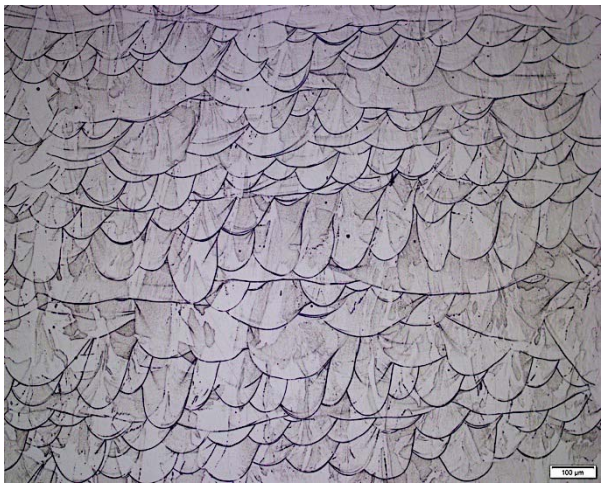

Fig. 4. Microstructure of 316L LPBF sample.

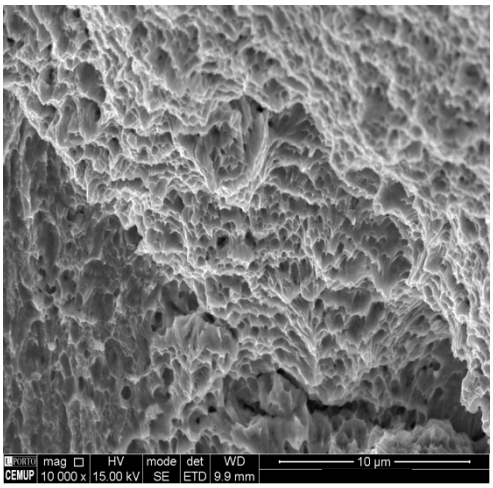

Fig. 5. Ductile fracture of low porosity content.

In short, LPBF samples with high values of porosity have an accentuated decrease on elongation properties. Porosity seems to have a minor effect on strength of 316L deposited material. Machining spectrums present more scatter on cutting forces measurements on AM samples when compared to conventional material. Microstructures of 316 L deposited material revealed some inter-layer porosity and it was seen consistency with the trajectory parameters. It was also concluded that brittle rupture is associated with higher levels or porosity on samples. Samples with higher values of hatch spacing presented higher content of porosity and two scan fields samples presented defects on fields transition zone and on nearby regions. Scan strategy showed a less substantial effect on porosity.

ACKNOWLEDGMENTS

To the completion of this study it was essential INEGI's and DEMec contribute with the processed materials and for supporting all experimental means.

List of authors

Sponsors

Gold Sponsor

JAF0C

PROJETOS

Other Sponsors

Organization